I. THE STRUCTURE AND PROPERTIES OF CLOSED CIRCULAR DUPLEX DNA

II. CHEMICALLY INTERACTING SYSTEMS AT EQUILIBRIUM IN A BUOYANT DENSITY GRADIENT

Thesis by

William Robert Bauer

In Partial Fulfillment of the Requirements

For the Degree of

Doctor of Philosophy

California Institute of Technology

Pasadena, California

1968

(Submitted December 15, 1967)

This thesis is dedicated

to my parents,

in appreciation of their

encouragement and assistance.

ACKNOWLEDGMENTS

I am especially grateful to Jerry Vinograd, under whose direction I have worked both as an undergraduate and as a graduate student. His great enthusiasm for research has been contagious, and he has been a constant source of intellectual stimulation and encouragement.

I should like to thank Physics I for convincing me that I should not be a nuclear physicist, and my first chemistry instructor, Norman Davidson, for stimulating my initial interest in chemistry.

The financial assistance of the National Science Foundation has been greatly appreciated.

Finally, I would like to thank my colleagues in the sub-basement of Church Laboratory who have provided helpful discussions as well as amusing moments. In particular, thanks are due to Dr. Roger Radloff for his ability to separate the probable from the merely possible. Miss Rebecca Kent has provided invaluable advice and assistance in the preparation of the manuscripts upon which this thesis is based.

ABSTRACT

I. The binding of the intercalating dye ethidium bromide to closed circular SV 40 DNA causes an unwinding of the duplex structure and a simultaneous and quantitatively equivalent unwinding of the superhelices. The buoyant densities and sedimentation velocities of both intact (I) and singly nicked (II) SV 40 DNAs were measured as a function of free dye concentration. The buoyant density data were used to determine the binding isotherms over a dye concentration range extending from 0 to 600 μg/ml in 5.8 M CsCl. At high dye concentrations all of the binding sites in II, but not in I, are saturated. At free dye concentrations less than 5.4 μg/ml, I has a greater affinity for dye than II. At a critical amount of dye bound I and II have equal affinities, and at higher dye concentration I has a lower affinity than II. The number of superhelical turns, τ, present in I is calculated at each dye concentration using Fuller and Waring's (1964) estimate of the angle of duplex unwinding per intercalation. The results reveal that SV 40 DNA I contains about -13 superhelical turns in concentrated salt solutions.

The free energy of superhelix formation is calculated as a function of τ from a consideration of the effect of the superhelical turns upon the binding isotherm of ethidium bromide to SV 40 DNA I. The value of the free energy is about 100 kcal/mole DNA in the native molecule. The free energy estimates are used to calculate the pitch and radius of the superhelix as a function of the number

of superhelical turns. The pitch and radius of the native I superhelix are 430 Å and 135 Å, respectively.

A buoyant density method for the isolation and detection of closed circular DNA is described. The method is based upon the reduced binding of the intercalating dye, ethidium bromide, by closed circular DNA. In an application of this method it is found that HeLa cells contain in addition to closed circular mitochondrial DNA of mean length 4.81 microns, a heterogeneous group of smaller DNA molecules which vary in size from 0.2 to 3.5 microns and a paucidisperse group of multiples of the mitochondrial length.

II. The general theory is presented for the sedimentation equilibrium of a macromolecule in a concentrated binary solvent in the presence of an additional reacting small molecule. Equations are derived for the calculation of the buoyant density of the complex and for the determination of the binding isotherm of the reagent to the macrospecies. The standard buoyant density, a thermodynamic function, is defined and the density gradients which characterize the four component system are derived. The theory is applied to the specific cases of the binding of ethidium bromide to SV 40 DNA and of the binding of mercury and silver to DNA.

TABLE OF CONTENTS

Part I

THE STRUCTURE AND PROPERTIES OF CLOSED CIRCULAR DUPLEX DNA

CHAPTER I

The Interaction of Closed Circular DNA with Intercalative Dyes. I. The Superhelix Density of SV 40 DNA in the Presence and Absence of Dye

by William Bauer and Jerome Vinograd

This chapter has been accepted for publication by the Journal of Molecular Biology

INTRODUCTION

Covalently closed circular duplex DNA is widely distributed in nature. The rapidly growing list of such DNAs now includes the DNAs from the tumor viruses: polyoma (Weil & Vinograd, 1963; Dulbecco & Vogt, 1963), SV 40, rabbit and human papilloma (Crawford & Black, 1964; Crawford, 1964, 1965); bacteriophage DNAs: the intracellular forms of ϕx 174 (Kleinschmidt, Burton & Sinsheimer, 1963), M13 (Play, Preuss & Hofschneider, 1966), Lambda (Young & Sinsheimer, 1964; Bode & Kaiser, 1965) and P22 (Rhoades & Thomas, 1967); the colicinogenic factor E_1, a bacterial plasmid (Roth & Helinski, 1967); and the mitochondrial DNAs from sheep heart (Kroon, Borst, Van Bruggen & Ruttenburg, 1966), beef heart, mouse and chicken liver (Borst & Ruttenburg, 1966), human leukocytes (Clayton & Vinograd, 1967), HeLa cells (Radloff, Bauer & Vinograd, 1967), and unfertilized sea urchin eggs (Pikó, Tyler & Vinograd, 1967). An understanding of the biological significance of the closure requires a detailed knowledge of the structure and special chemical properties of these molecules. The present study is concerned with the effects of intercalating dyes upon the properties of closed circular SV 40 DNA. An estimate is made of the number of superhelical turns present in this molecule. In Part II of this series (Bauer & Vinograd, 1967a) the free energy of superhelix formation is calculated.

Vinograd, Lebowitz, Radloff, Watson & Laipis (1965) proposed that closed circular duplex DNAs contain superhelical turns

which the chemical forces in the Watson-Crick structure maintain in the molecule. These superhelical turns cannot be removed without simultaneously changing the average pitch (base pairs/turn) of the duplex, a requirement which follows from topological considerations alone. The superhelix winding number, τ, describes the number of turns that the duplex makes about the axis of the superhelix. The topological winding number, α, is defined as the number of complete revolutions made by one strand about the duplex axis, when the axis is constrained to lie in a plane. The duplex winding number, β, is the number of complete revolutions made by one strand about the duplex axis in the unconstrained molecule. In the Watson-Crick structure, β is taken to be numerically equal to one-tenth the number of base pairs and designated as β_0. The three winding numbers are linearly related (Vinograd & Lebowitz, 1966), and may be connected by the simple equation

$$\tau = \alpha - \beta. \qquad (1)$$

Glaubiger & Hearst (1967) have recently presented an analytical proof of equation (1). The superhelix density, σ, an intensive quantity equal to the number of superhelical turns per ten base pairs, is defined by the equation

$$\sigma \equiv \frac{\tau}{\beta^0} \qquad (2)$$

where β^0 is a normalizing factor equal to one-tenth the number of base pairs in the molecule.

By convention, right-handed duplex turns are taken to be positive and the quantities α and β_0 are positive in native DNA. The relationship between the handedness of the superhelical turns and the sign of τ depends upon whether or not the turns are interwound. The sign convention for non-interwound superhelical turns, as in the toroidal molecule (Vinograd & Lebowitz, 1966), is the same as for duplex turns--right-handed turns are considered to be positive. The sign convention is reversed for interwound superhelical turns, as in the twisted molecules. Here left-handed turns are considered to be positive. The reversal of handedness upon interwinding is the result of a 90° rotation of the viewing axis, as illustrated in Fig. 1. The superhelical turns are right-handed and τ is negative in the interwound superhelical form (the twisted form) of native SV 40 DNA.

The interwound form of the superhelix contains two complete superhelical turns for every full revolution of the duplex about the superhelical axis; the toroidal form contains one superhelical turn for every full revolution. If an interwound superhelix containing τ superhelical turns is projected onto a plane, the resulting projection will contain $|\tau|$ crossover points and $|\tau| + 1$ loops.

The superhelix density, σ, is altered by any change in the environmental conditions or by chemical reactions which cause a change in the average pitch of the duplex helix. Alterations in the average pitch of the duplex helix may be induced, for example, by acid, alkali, temperature, low ionic strength, nonaqueous solvents, uv irradiation, and by the binding of intercalating dyes. The subject

FIG. 1. Sections of the two possible first order superhelical models for closed circular DNA. Either of these models, or a combination of them, formally represents the closed circular molecule which contains negative superhelices, $\tau < 0$.
(a) A section of the toroidal model shown about its superhelical axis, X. The winding is left-handed about this axis.
(b) A section of the interwound model shown twisted about its superhelical axis, Y. The winding is right-handed about this axis, but remains left-handed if viewed about the axis X. Both models contain the correct number of duplex turns per superhelical turn in native SV 40 DNA.

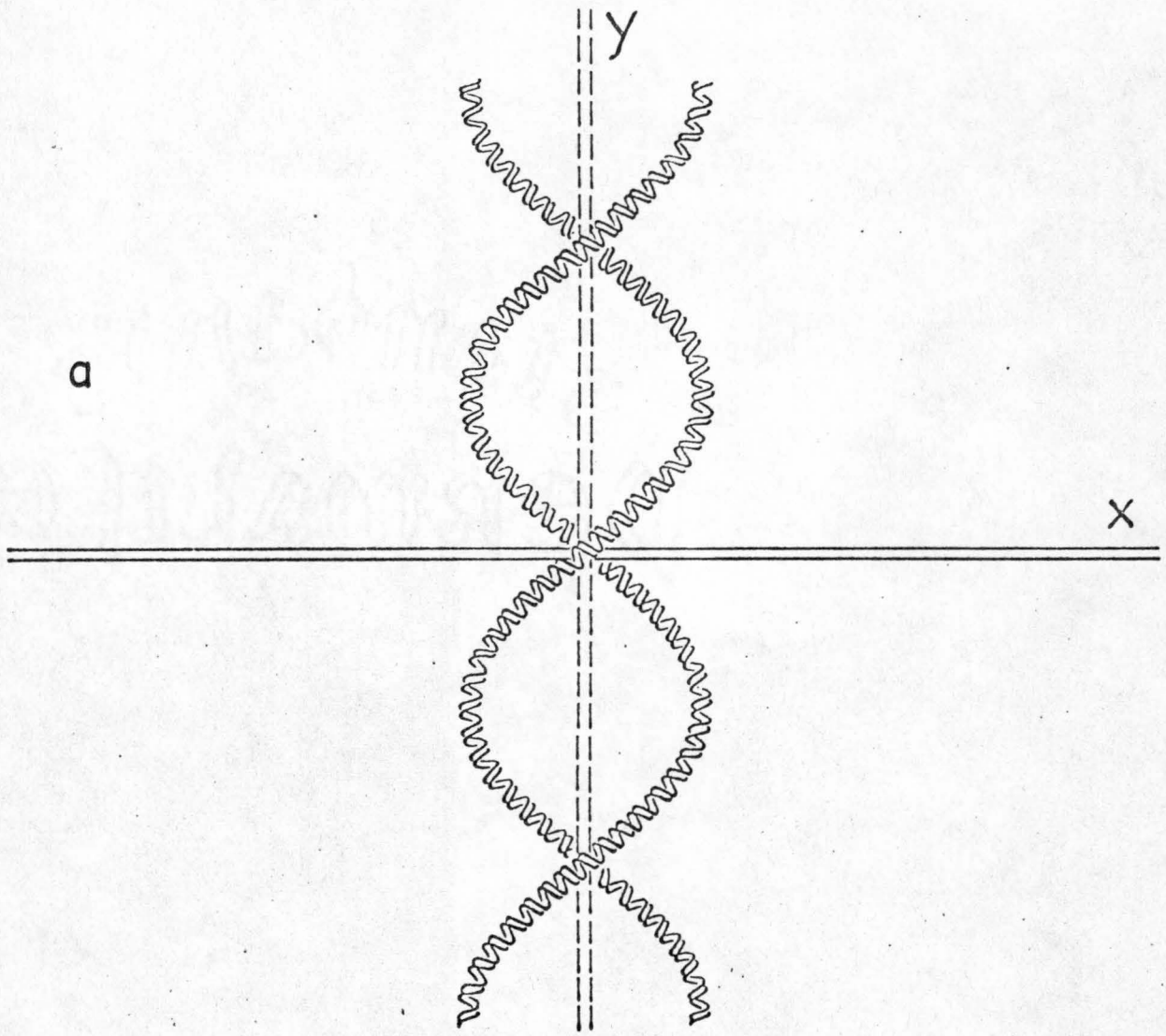
y
a
x

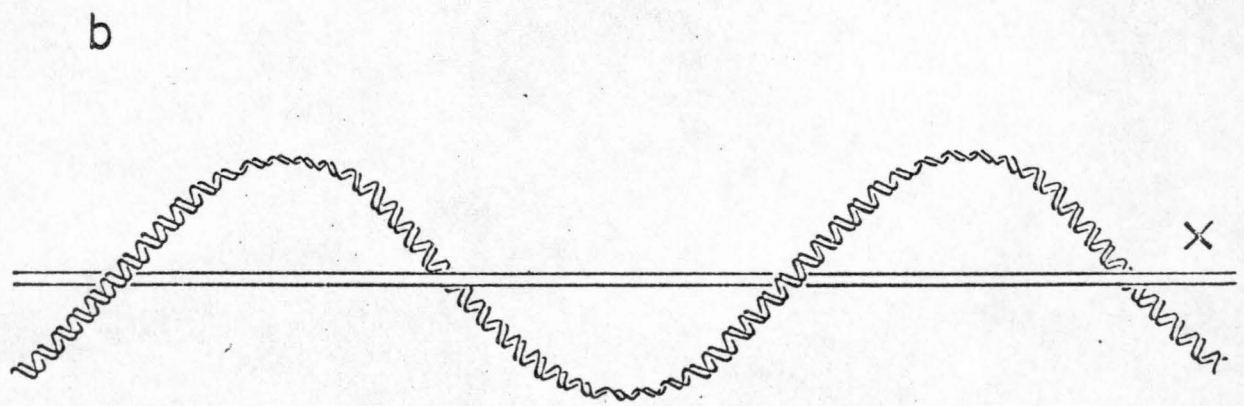
b
x

of the present paper is the effect of dye binding upon the superhelix density σ. In this study we have also determined the number of superhelical turns in native SV 40 DNA in the absence of dye.

The interaction of the aminoacridines (Lerman, 1961; Neville & Davies, 1966) and of ethidium bromide (Le Pecq, 1965; Waring, 1965) with DNA has been studied extensively, and it has been concluded that these dyes are capable of intercalative binding between DNA base pairs. Fuller & Waring (1964) concluded from model building studies that the intercalation of an ethidium bromide molecule unwinds the duplex by 12°. The relationship between τ, the number of superhelical turns, ν, the number of moles of dye bound per mole of nucleotide, and ϕ, the angle of unwinding in radians per bound dye molecule, is

$$\tau = \tau_0 + (\frac{\phi}{2\pi}) \cdot (10\beta_0) \cdot 2\nu, \tag{3}$$

where τ_0 is the number of superhelical turns in the absence of dye. The corresponding relation expressed in terms of the superhelix density is

$$\sigma = \sigma_0 + \frac{10\phi}{\pi} \nu. \tag{4a}$$

where σ_0 is the superhelix density in the absence of dye.

For $\phi = \pi/15$

$$\sigma = \sigma_0 + 0.67\nu. \tag{4b}$$

At a critical value of ν, $\nu = \nu_c$, the superhelical turns disappear

totally and $\sigma_0 = -0.67\nu_c$. At values of $\nu > \nu_c$, σ becomes positive and superhelices of opposite handedness are formed.

Intercalation of increasing amounts of dye thus causes a continuous and reversible change in the superhelix density, Fig. 2. The two states characterized by $\sigma = 0$, and $\nu = \nu_c$ may be achieved either irreversibly by the introduction of a single strand scission and subsequent intercalation of ν_c dye molecules per nucleotide, (a) → (d) → (e), or reversibly by the intercalation of ν_c dye molecules per nucleotide in the intact molecule, (a) ⇌ (b). The two states (b) and (e) can be interconverted by the reversible cleavage of a phosphodiester bond. Such a reaction can proceed without a change in the superhelix density or in the amount of dye bound.

The compact molecule I has been shown (Vinograd, Lebowitz & Watson, 1967) to convert spontaneously to the relaxed molecule II upon introducing one single-strand scission or nick. This result demonstrates that the superhelical molecule has a greater free energy than either the nicked molecule or the corresponding closed circular duplex with σ equal to zero. Both entropic and enthalpic effects contribute to the higher free energy. The superhelical molecule is a more ordered form than a closed molecule having $\sigma = 0$. The duplex in the superhelix is also subjected to additional bending and torsional stresses. On the other hand, the superhelical molecule is more stable at room temperature and at neutral pH than the partially denatured form brought to the state $\sigma = 0$ by the melting of $10\tau_0$ base pairs.

FIG. 2. Representation of the effects of the binding of ethidium bromide to SV 40 DNA I and II. The upper part of the diagram presents three stages in the reversible binding of dye to SV 40 DNA I. (a) This represents the dye-free molecule with fourteen superhelical turns, $\tau_0 = -14$. The addition of 420 molecules of ethidium bromide completely unwinds the superhelical turns to form the relaxed molecule, (b). The addition of a further 720 dye molecules, which occurs at a free dye concentration of 100 μg/ml, leads to the formation of a positive superhelical molecule, $\tau = 24$, shown in (c).

The lower part of the diagram shows three stages in the reversible binding of dye to SV 40 DNA II, which remains relaxed throughout. (e) This represents the relaxed, nicked molecule with the same number of dye molecules bound as to the relaxed, intact molecule in (b). The arrows joining (b) and (e) indicate that the nick may be introduced or repaired without change of the 420 molecules of ethidium bromide bound. The nicked molecule is nearly saturated, as shown in (f), with 1860 molecules of ethidium bromide bound. Introduction of a single strand scission into I in the presence of a high dye concentration results in an irreversible unwinding of the superhelix accompanied by an approximately 65% increase of the amount of dye bound. In this diagram each block, ■, represents 30 molecules of dye. All of the dye molecules are

not shown in (c). The number of dye molecules in (b), (d), (e), and (f) represent experimental values determined in this study.

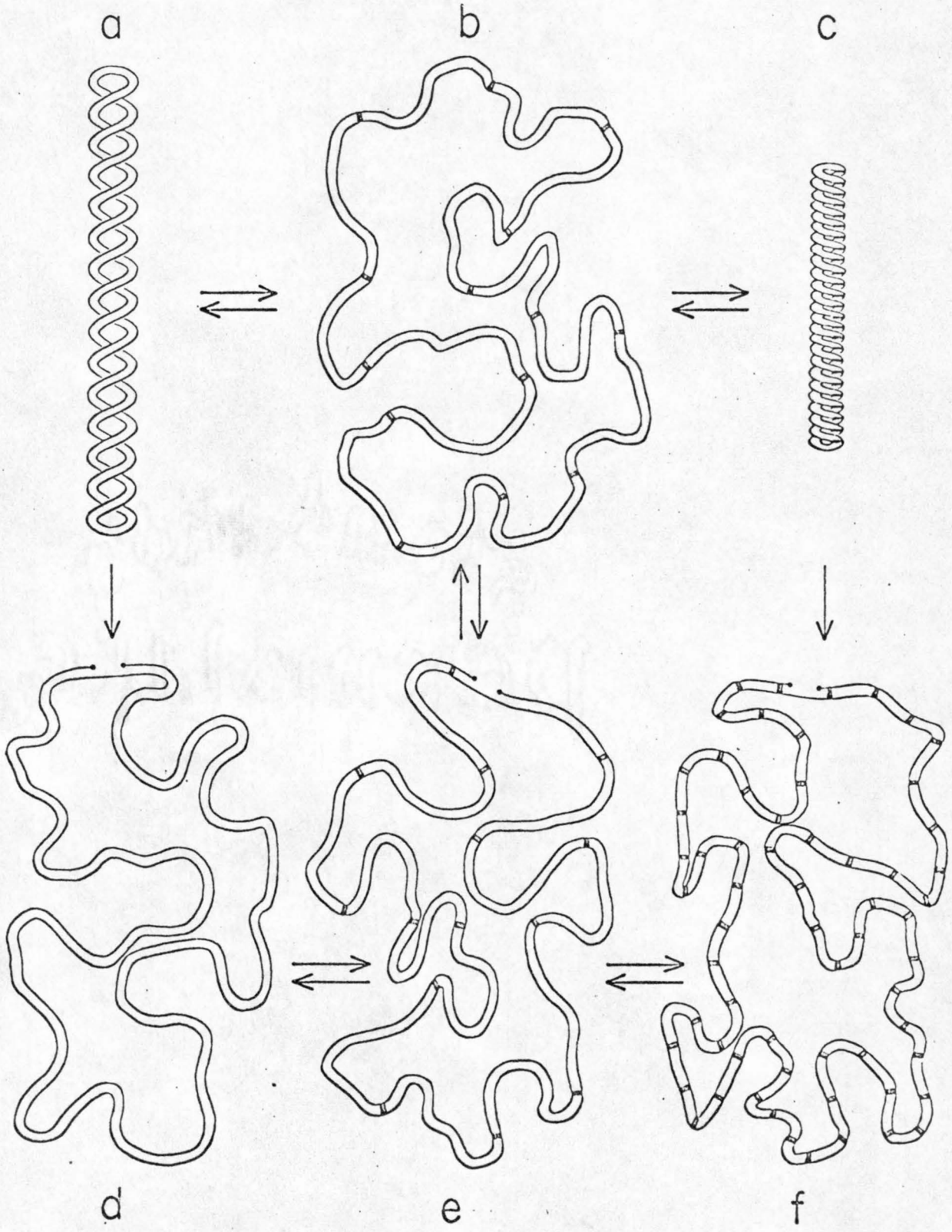
a
b
c
d
e
f

Any physical property sensitive to the amount of dye bound may, in theory, be used to determine σ_0 from ν_c in a comparative study of the binding of dye to the nicked and intact forms of closed circular DNA. Since σ_0 is small compared to unity, physical properties measurably affected by the binding of small amounts of dye must be employed. Two such properties, sedimentation velocity and buoyant density, were used in the present study, in which the effects of the binding of ethidium bromide (3,8-diamino-6-phenyl-5-ethyl-phenanthridinium bromide), Fig. 3, were investigated.

Ethidium bromide and 9-aminoacridine have similar effects on the sedimentation velocity of SV 40 DNA. The sedimentation coefficient of the nicked form decreased only slightly with increasing dye concentration, while s for the intact material first decreased by about 25%, and then became identical with s for the nicked material. With further dye addition the sedimentation coefficient of the intact form again increased to a value nearly equal to that of the dye-free closed circular species. Closed circular SV 40 DNA contains -16.0 ± 3.5 superhelical turns as calculated from the amount of dye bound at the minimum of the sedimentation velocity curve. While this manuscript was in preparation, Crawford & Waring (1967) reported similar sedimentation velocity results with ethidium bromide and polyoma DNA.

Closed circular SV 40 DNA displayed a greater affinity for dye than did the nicked form in buoyant density experiments in the presence of low concentrations of ethidium bromide. The order of

FIG. 3. Structure of ethidium bromide.

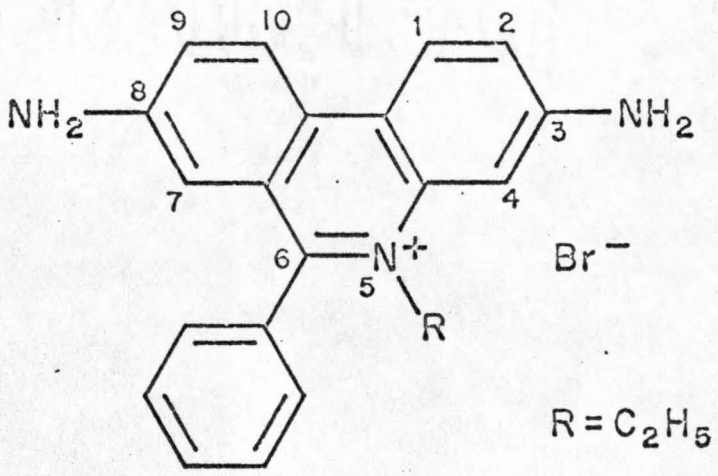

ETHIDIUM BROMIDE

affinities was reversed at high dye concentrations. Closed circular SV 40 DNA contains -12.7 ± 1.5 superhelical turns, as calculated from the buoyant density at the crossover point and from the relations between the amount of dye bound and the buoyant density of the DNA-dye complex.

The uptake of dye by the closed circular form at dye concentrations in excess of 100 μg/ml was approximately 65% as large as the uptake by the nicked form. This latter observation has formed the basis for the development of a convenient procedure for the isolation and detection of closed circular DNA in the preparative ultracentrifuge (Radloff, Bauer & Vinograd, 1967). The free energy of superhelix formation can be estimated from an analysis of the dye binding isotherms for SV 40 DNA I and II. This analysis is given in Part II (Bauer & Vinograd, 1967a).

Using another method to determine superhelix density, Vinograd, Lebowitz & Watson (1967) found that a very similar closed circular DNA from polyoma virus contained -15 ± 1 superhelical turns. This conclusion was reached from an analysis of the results of a buoyant density titration over the range of pH in which the alkali induced helix coil transition occurs.

MATERIALS AND METHODS

(a) Source of materials

Optical grade CsCl from the Harshaw Chemical Co., Cleveland, Ohio, and ethidium bromide from Boots Pure Drug Co., Ltd., Nottingham, England, were used without further purification. The 9-aminoacridine was obtained as a purified preparation from Dr. R. L. Peterson. Tris(hydroxymethyl)aminomethane · HCl buffer was prepared from "Trizma Base", reagent grade, obtained from the Sigma Chemical Co.

(b) Source of DNAs

Crab dAT from C. Antennarius sperm was isolated by the Cs_2SO_4, $HgCl_2$ method (Davidson, Widholm, Nandi, Jensen, Olivera & Wang, 1965). This DNA contains about 3% guanine-cytosine, and has a buoyant density at 25° of 1.669_5 g/ml. Closed circular SV 40 DNA was prepared by phenol extraction of SV 40 virus isolated from a lysate of infected green monkey cells grown in tissue culture. The nicked SV 40 II DNA was obtained from a purified sample of SV 40 I that had been allowed to stand for several months at -20°. The single strand scissions were presumably due to the action of trace amounts of reducing agents. The SV 40 I DNA was isolated from the leading band of a sucrose gradient, 5-20% sucrose, 0.1 M NaCl, 0.005 M EDTA, 0.05 M phosphate pH 7.5, 16 hours, 23 K rpm in an SW 25.1 rotor at 15°. The DNAs were analyzed at frequent intervals

by analytical band velocity sedimentation in neutral 2.8 M CsCl, (Vinograd, Bruner, Kent & Weigle, 1963).

(c) Analytical ultracentrifugation

A Spinco Model E ultracentrifuge equipped with an electronic speed control, photoelectronic scanner, and multiplexer was used. The buoyant density experiments were performed at 25° in a 4 or 6 cell rotor with double sector cells and a double sector offset counterbalance. The sedimentation velocity experiments, completed before the installation of the multiplexer, were performed at 20° in a 2 cell rotor with a rotary alternator. Centerpieces with optical path lengths of 2 and 4 mm were fabricated from commercial 12 mm charcoal-filled Epon centerpieces.

The rotor speed, measured with a Berkely Model 5510 EPUT meter connected to Gate A of the scanner, was found to be constant to within ± 0.03% during each velocity experiment. The odometer readings were used to calculate the average rotor speeds in the buoyant density experiments.

The RTIC unit was used for temperature measurement and control. The rotor thermistors were calibrated with an NBS thermometer. A Beckman monochromator and a PEK xenon-mercury lamp were used. The lamp emission maximum at 265.4 mμ was used in most of the experiments. At high dye concentrations, wavelengths between 335 and 521 mμ were used. The monochromator exit slit was set at 2.0 mm.

The time required to reach equilibrium in the buoyant density experiments with DNA and dye was found to be greater than in the absence of dye. In order to estimate the equilibrium time, successive scans were made of buoyant SV 40 DNA in various ethidium bromide concentrations at intervals of 12 hours for five days. It was found that band positions attained equilibrium after 24 hours, but that the band width decreased until about 36 hours had elapsed. All buoyant density scans were made after a minimum of 36 hours at speed.

Boundary sedimentation velocity experiments were performed with mixtures of SV 40 DNA I and II containing known amounts of ethidium bromide or 9-aminoacridine. At the conclusion of each experiment the analytical cells were allowed to stand overnight at 4° to resuspend the DNA-dye complex. A further aliquot of dye at a concentration of 200 μg/ml was added to the solution sector with a 10 μl Hamilton syringe. The cell contents were mixed briefly with a Vortex mixer.

Six such experimental series were performed, with two different mixtures of SV 40 DNA I and II. The mixtures contained 25% and 75% I, and were selected so as to eliminate ambiguities in the identifications of components. The total DNA concentration was 20 μg/ml. During the sedimentation the free dye concentration was observed to remain uniform throughout the cell. At the salt concentrations employed, $(1 - \bar{v}_4\rho)$, the buoyancy term associated with the bound dye, is essentially zero. In the foregoing term $\bar{v}_4$ is the partial specific volume of the dye chloride, and ρ is the density of

the solution. The sedimentation coefficient measured in such a reacting system refers unambiguously to the DNA-dye complex characteristic of the free dye concentration present in the cell.

(d) Recording and analysis of results

Although the Offner recorder supplied with the Spinco scanner is adequate for distance measurements, the maximum pen excursion in the concentration dimension, 7 cm, is inadequate for precise measurements. The limitation was overcome by incorporating a model 135A Moseley x-y recorder with a maximum pen excursion of 18 cm in the ordinate direction. The expanded scale was particularly useful for the computer evaluations of the buoyant density experiments. In later experiments, a model 7001 AM Moseley x-y recorder with a maximum pen excursion of 25 cm was used. The traces were measured with a K & E ruler and the ordinates were converted to absorbance units with the stairsteps calibration marks, which had been previously calibrated with known ethidium bromide solutions. The spectra of seven known ethidium bromide solutions in CsCl, ρ^0 = 1.65 g/ml, were determined with a Cary Model 15 recording spectrophotometer. A reciprocal extinction coefficient of 24.8 μg/ml per unit absorbance at 265.4 mμ was calculated. The molar extinction coefficient at 490 mμ agreed within 4% with the published value (Le Pecq, 1965). The extinction coefficient at 265 mμ is valid in CsCl solutions of ρ = 1.5-1.7 gm/ml, the solvent in which the buoyant density experiments were performed. The spectrum of

ethidium bromide was observed to shift slightly to higher wavelengths in the presence of CsCl. A plot of pen excursion vs the nominal stairstep value is presented in Fig. 4 in which it is seen that the pen response is nonlinear in the upper regions. Fig. 5 shows the optical density measured with the scanner, corrected with the stairsteps calibration and corrected for the effect of the optical path, plotted against the optical density measured spectrophotometrically. This plot is very nearly linear over the entire optical density range. The three curves present data for ethidium bromide at 265.4 mμ, and for calf thymus DNA at 265.4 and 280 mμ. All measurements were done in 5.8 M CsCl.

A small offset of about 0.025 OD may be observed in Fig. 5. This offset was observed in an experiment with aliquots of the same CsCl solution, $\rho = 1.65$, in both sectors of a double sector cell, and was subtracted from the data obtained experimentally. All analytical ultracentrifuge experiments were performed with a scanner suppression setting of zero. The suppression system significantly distorted the calibration curves such as are shown in Figs. 4 and 5.

The densities of the CsCl solutions were calculated from refractive index measurements, using the equation given by Ifft, Voet & Vinograd (1961). The refractive index change due to the Tris-HCl buffer, 0.0003, was subtracted from the measured value. No refractive index effect was found for the ethidium bromide at 300 μg/ml.

FIG. 4. Pen excursion vs calibration settings obtained with the photoelectric scanning accessory supplied by Beckman Instruments, Inc. and a parallel Moseley 135A x-y recorder. The separate curves ○, ●, △, ▲ are plotted from data obtained at 36, 20, 1, and 10 hr. after the beginning of an experiment in which scanner and light source were left on continuously.

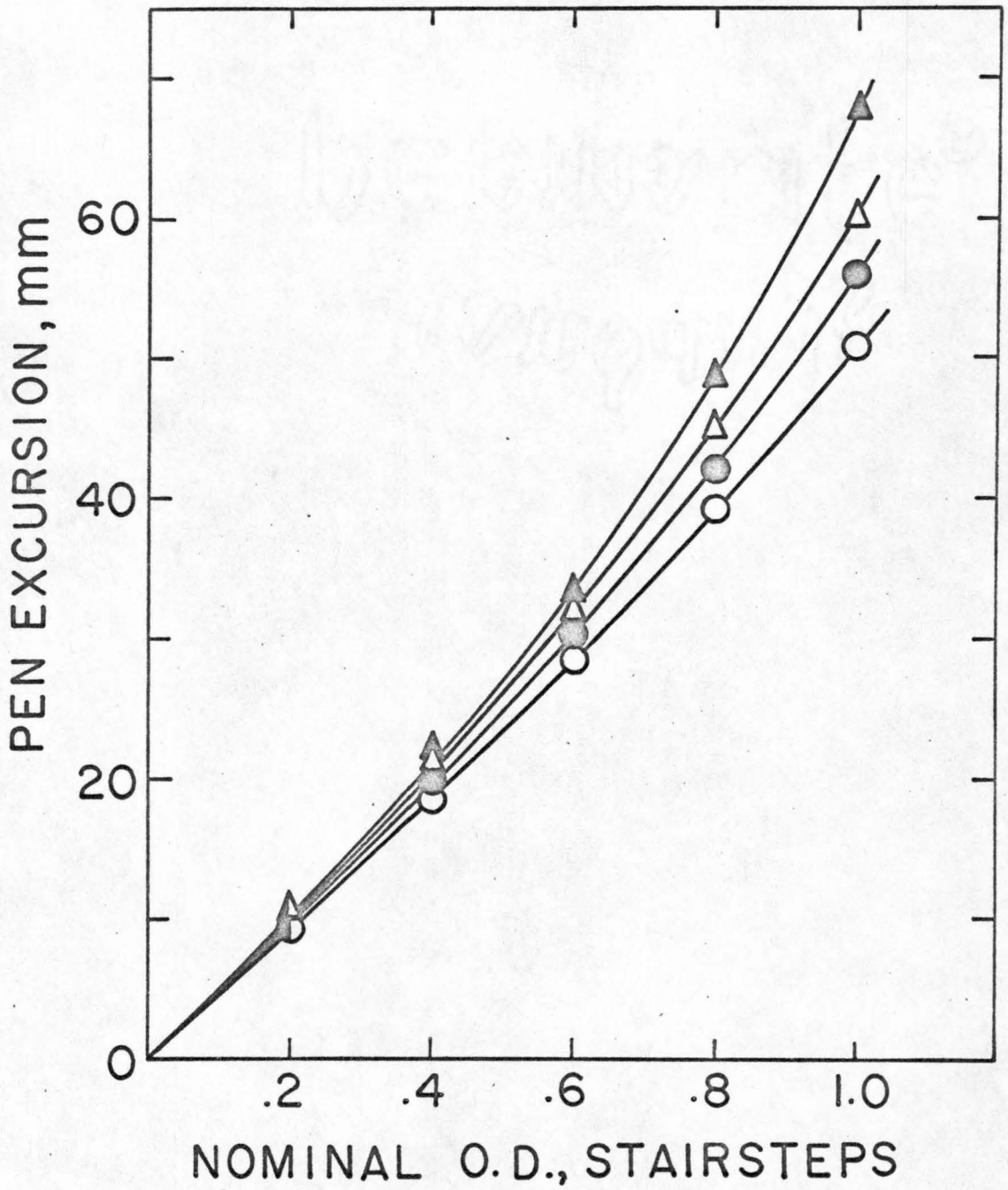
PEN EXCURSION, mm
0
20
40
60
.2
.4
.6
.8
1.0
NOMINAL O.D., STAIRSTEPS

FIG. 5. Calibration curves for conversion to optical density of absorbance measured with the photoelectric scanner. The optical densities in the cells at 44 K rpm calculated from the scanner records are plotted against the optical densities of the solutions measured with a Cary 15 recording spectrophotometer. ○. Calf thymus DNA in CsCl, ρ° = 1.65 g/ml, at 265.4 mμ. ●. Ethidium bromide in CsCl, ρ° = 1.65 g/ml, at 265.4 mμ. □. Calf thymus DNA in CsCl, ρ° = 1.65 g/ml, at 280 mμ. The lines for ethidium bromide and for DNA at 280 mμ have been offset by 0.2 and 0.4 units respectively.

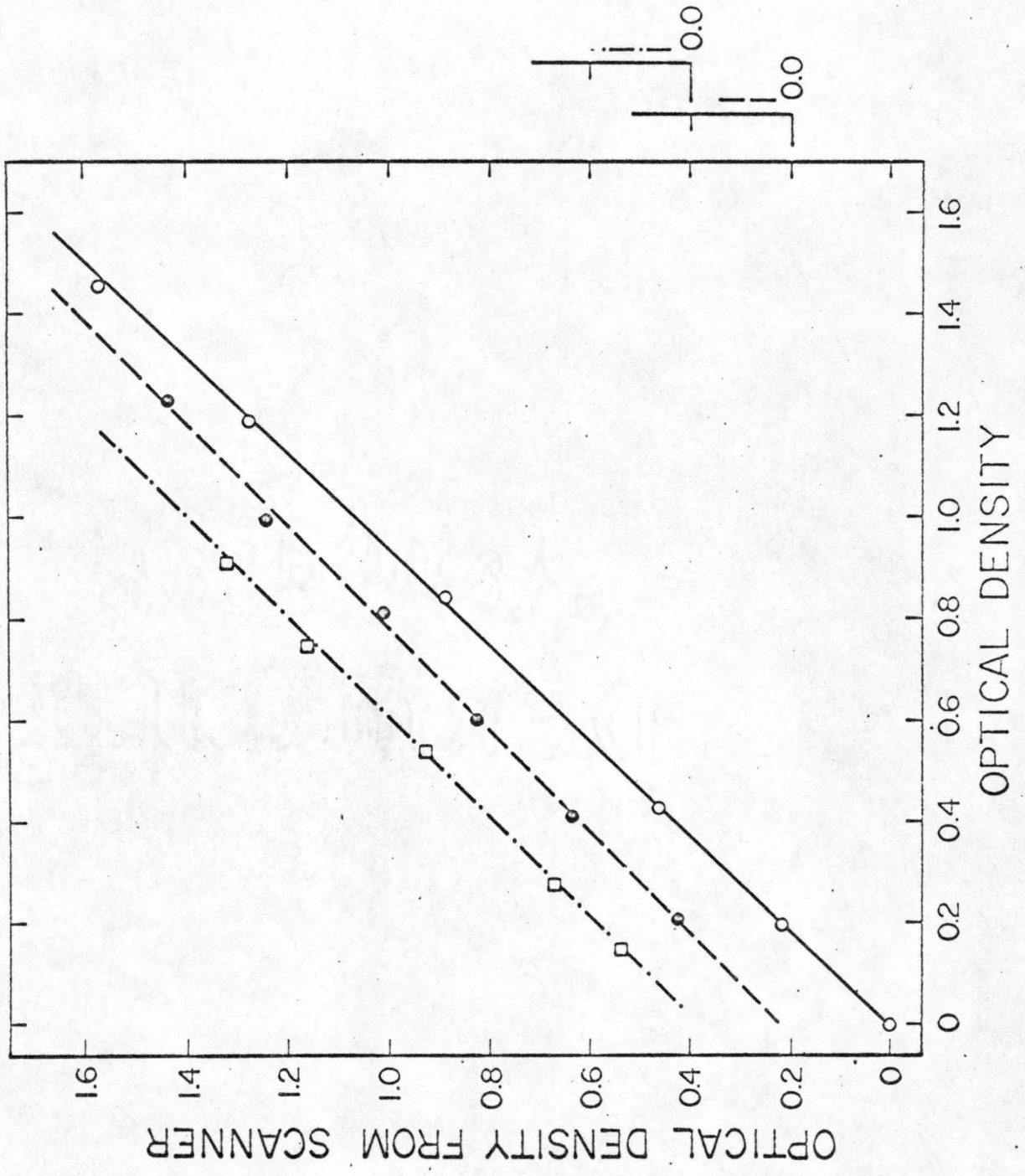
0.0
0.0
OPTICAL DENSITY
0
0.2
0.4
0.6
0.8
1.0
1.2
1.4
1.6
OPTICAL DENSITY FROM SCANNER
0
0.2
0.4
0.6
0.8
1.0
1.2
1.4
1.6

(e) Use of the computer

An IBM 7040/7094 computing system was used to calculate the results of both the sedimentation velocity and the buoyant density experiments. The sedimentation coefficients were calculated from a least squares fit to a straight line. The results were plotted for visual inspection with a Calcomp plotter. The 95% confidence limit was calculated for each sedimentation coefficient with the Student's T distribution.

The experimental results from the scanner in buoyant density experiments were obtained in the form of plots of uncorrected pen excursion vs density. In order to evaluate the positions of maximum polymer concentration, it was necessary to correct for two effects which distorted the band profiles: the uneven distribution of the dye in the cell and, in some cases, the partial overlap of the bands. The principal data conversion procedures were:

1. The pen excursion and distance measurements were converted to real concentrations and actual distances from the center of rotation.

2. A generalized least squares polynomial fitting procedure was used to obtain an empirical equation to describe the free dye distribution. Regions of the cell occupied by DNA bands were ignored in the curve fitting procedure. Figures 6a and 7a show typical tracings obtained with the Moseley x-y recorder of bands of SV 40 I and II at equilibrium in a buoyant CsCl solution containing ethidium bromide. The bands in Fig. 6, at an initial ethidium

bromide concentration of 10 μg/ml, are partially overlapped. In Fig. 7, obtained in an experiment with an initial ethidium bromide concentration of 15 μg/ml, the two bands are essentially completely separated. Figures 6b and 7b present computer-generated plots of the experimental measurements corrected for the nonlinear effects of the scanner. In addition, these figures contain a plot of the dye distribution calculated from the polynomial fit.

3. The absorbance due to dye was then subtracted in order to obtain the net absorbance of the DNA-dye complex. The resulting set of data points was fitted to Gaussian curves with Stone's (1962) least squares procedure. Representative results are shown in Figs. 6c and 7c. The solid lines represent the computed Gaussians; the data points include the corrections both for scanner nonlinearity and for dye absorbance.

FIG. 6. Experimental and computer records of two overlapping bands of SV 40 DNA at equilibrium in CsCl containing ethidium bromide. The values on the abscissa are distances in real space from the center of rotation. The initial concentrations of ethidium bromide, DNA and CsCl were 10.0 μg/ml, 2.5 μg/ml, and 1.654 g/ml respectively in the experiment performed at 43,723 rpm, 25.0°, 36 hrs.

a. Record obtained with Moseley 135A x-y recorder. The "stair-steps" calibration marks in absorbance units are on the right-hand side of the diagram. The pips at the bottom of the liquid column correspond to the two menisci at the FC-43 fluorocarbon interfaces.

b. Results of computer fitting procedures for the concentration distributions of the free dye and the DNA-dye complex. The data taken from the record in the DNA free regions in the tracing in Fig. 6a were fitted to a cubic polynomial. The interpolated free dye absorbances were subtracted from the absorbance profile of the DNA-dye complex. The resulting data for the DNA-dye complex were fitted to two Gaussians as described in the text. The free dye absorbance distribution was added to these curves in order to examine the quality of the fit to the input data points. The lines in this figure present the calculated curves and the symbols, the measured data points.

c. The optical density distribution of the DNA-dye complex after subtraction of the interpolated free dye optical density. The lines present the separate Gaussian curves for the two components, and the points present the measured data after subtraction of the contribution of the free dye.

a

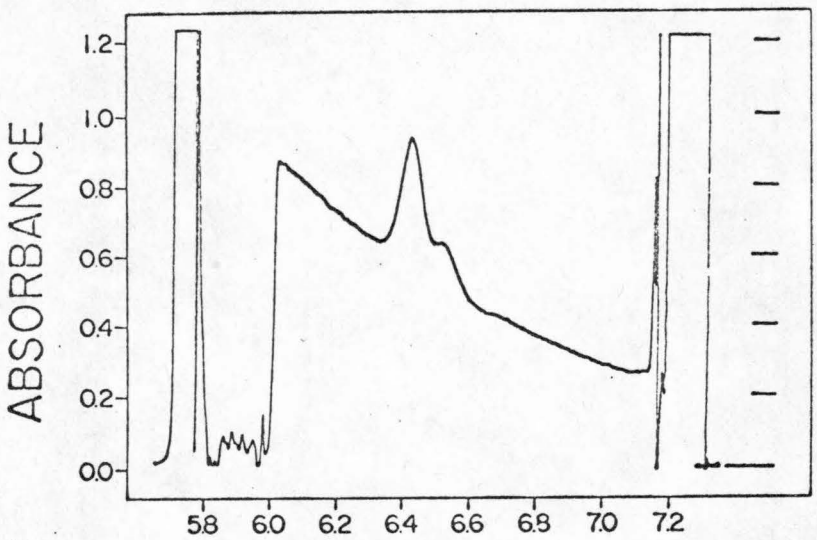
ABSORBANCE
1.2
1.0
0.8
0.6
0.4
0.2
0.0
5.8
6.0
6.2
6.4
6.6
6.8
7.0
7.2

b

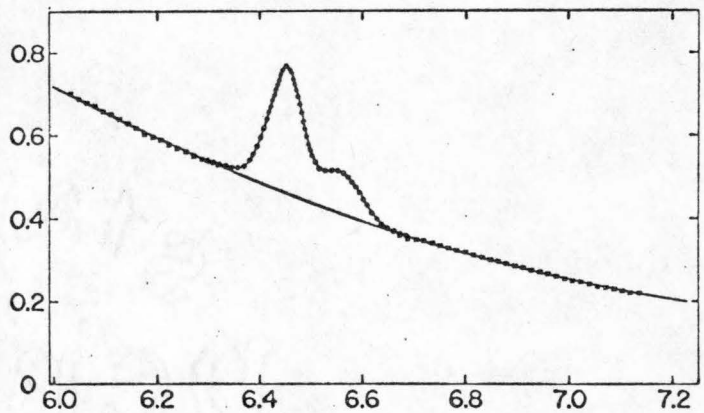
0.8
0.6
0.4
0.2
0
6.0
6.2
6.4
6.6
6.8
7.0
7.2

c

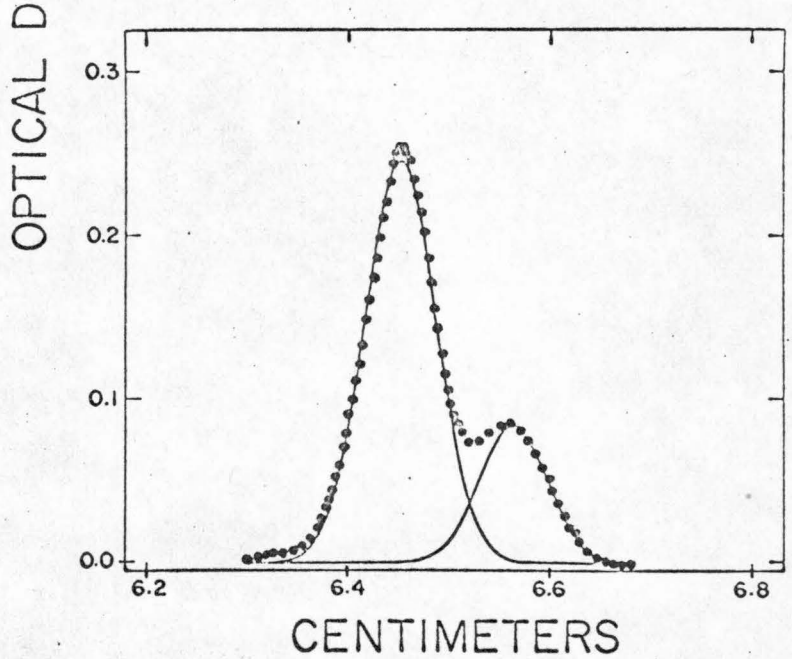
OPTICAL DENSITY
0.3
0.2
0.1
0.0
6.2
6.4
6.6
6.8
CENTIMETERS

FIG. 7. Experimental and computer records of two nonoverlapping bands of SV 40 DNA at equilibrium in CsCl containing ethidium bromide. The initial concentrations of ethidium bromide, DNA and CsCl were 15.0 μg/ml, 2.5 μg/ml, and 1.649 g/ml respectively. The experiment was performed at 43,723 rpm, 25.0°, 36 hrs. For further explanation refer to Fig. 6.

a

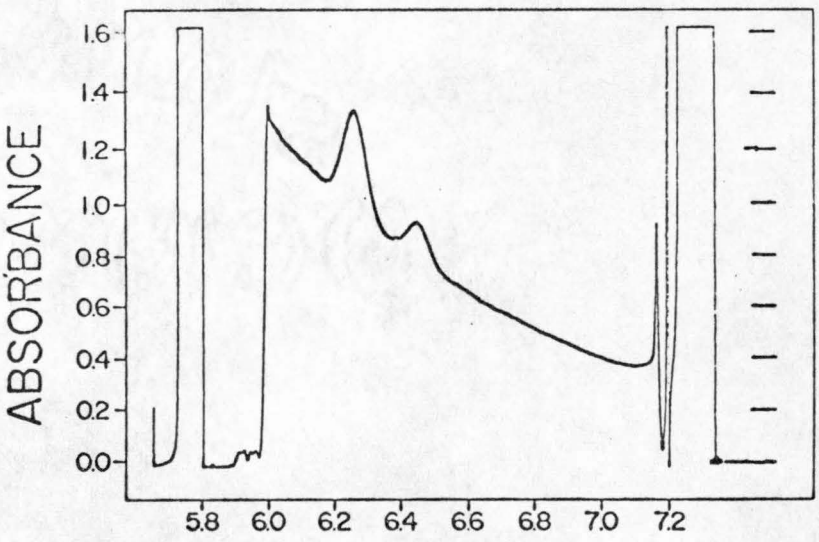
ABSORBANCE
1.6
1.4
1.2
1.0
0.8
0.6
0.4
0.2
0.0
5.8
6.0
6.2
6.4
6.6
6.8
7.0
7.2

b

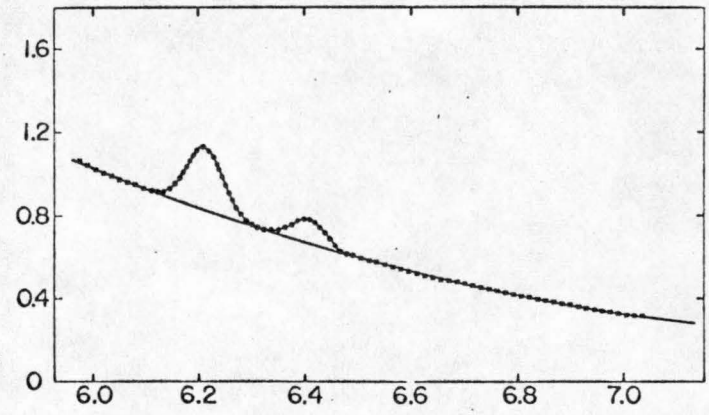
1.6
1.2
0.8
0.4
0
6.0
6.2
6.4
6.6
6.8
7.0

c

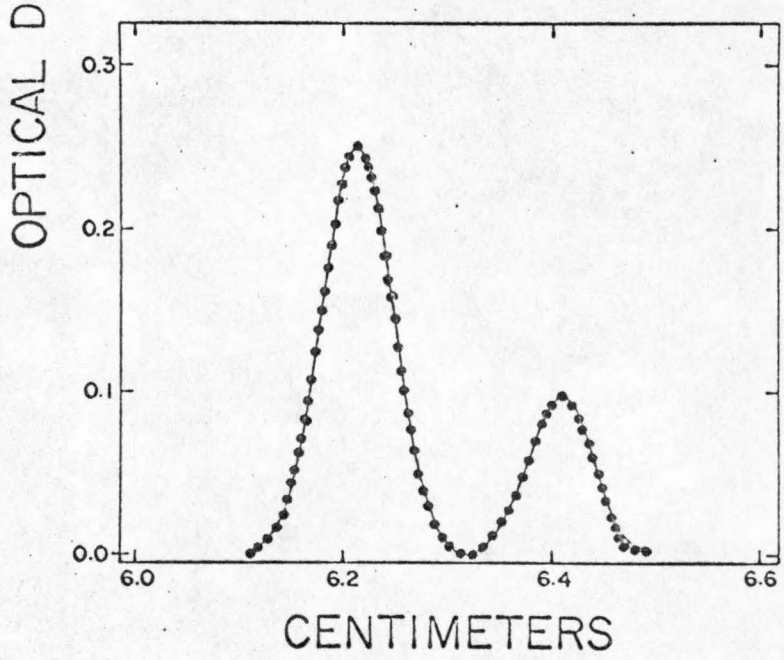
OPTICAL DENSITY
0.3
0.2
0.1
0.0
6.0
6.2
6.4
6.6
CENTIMETERS

RESULTS

(a) Sedimentation velocity experiments

Figure 8 shows the effect of addition of ethidium bromide upon the sedimentation coefficient of the closed and nicked circular components of SV 40 DNA. The results are plotted as a function of ν_{II}, the mole ratio of bound dye to nucleotide in II. The latter quantity was calculated from the measured free dye concentration centripetal to the slow boundary according to the equation of Scatchard (1949)

$$\nu = \frac{\nu_m kc}{1 + kc} \tag{5}$$

where k is the association constant, ν_m the maximum mole ratio of bound dye to nucleotide, and c the free dye concentration in moles/liter. For this calculation the estimates $k = 1.0 \times 10^5$ ℓ/M and $\nu_m = 0.20$ were taken from the data of Le Pecq (1965) for linear DNA.

The sedimentation coefficient of component II decreases approximately linearly over the range studied with a slope of about 0.5 S, a behavior similar to that previously reported for linear DNA (Le Pecq, 1965). The change in the sedimentation coefficient of component I is strikingly different. The sedimentation coefficient first decreases in the region $0.0 \leq \nu_{II} \leq 0.04$, followed by a region in which only one boundary could be distinguished experimentally. As the free dye concentration is increased beyond this dip region, the sedimentation coefficient of component I rises with increasing

FIG. 8. Sedimentation velocity of SV 40 DNA in 1.0 M NaCl in various concentrations of ethidium bromide. The symbols ○ and ● refer to results from resolved boundaries of intact SV 40 I and nicked SV 40 II, respectively. The weight average sedimentation coefficients from nonresolved boundaries are indicated by the symbol ◑. The error bars on the data points represent the 95% confidence limits in the sedimentation coefficients. When not shown the error was smaller than ± 0.155. The sedimentation coefficients are presented as a function of ν_{II} calculated with Eq. (5) as described in the text. The dye concentrations used ranged from 0.0 to 12.0 μg/ml. The total DNA concentration was approximately 20 μg/ml and the ratio of I/II was either 0.5 or 2.0 in the six series of experiments performed. In the experiment at ν = 0.045 the initial concentrations of I, II, total dye and free dye were 7.0, 13.0, 4.3, 3.2 μg/ml respectively. The experiments were performed at 44 K rpm and at 20°. The measured sedimentation coefficients were corrected for the effects of NaCl on the viscosity and density of the solution.

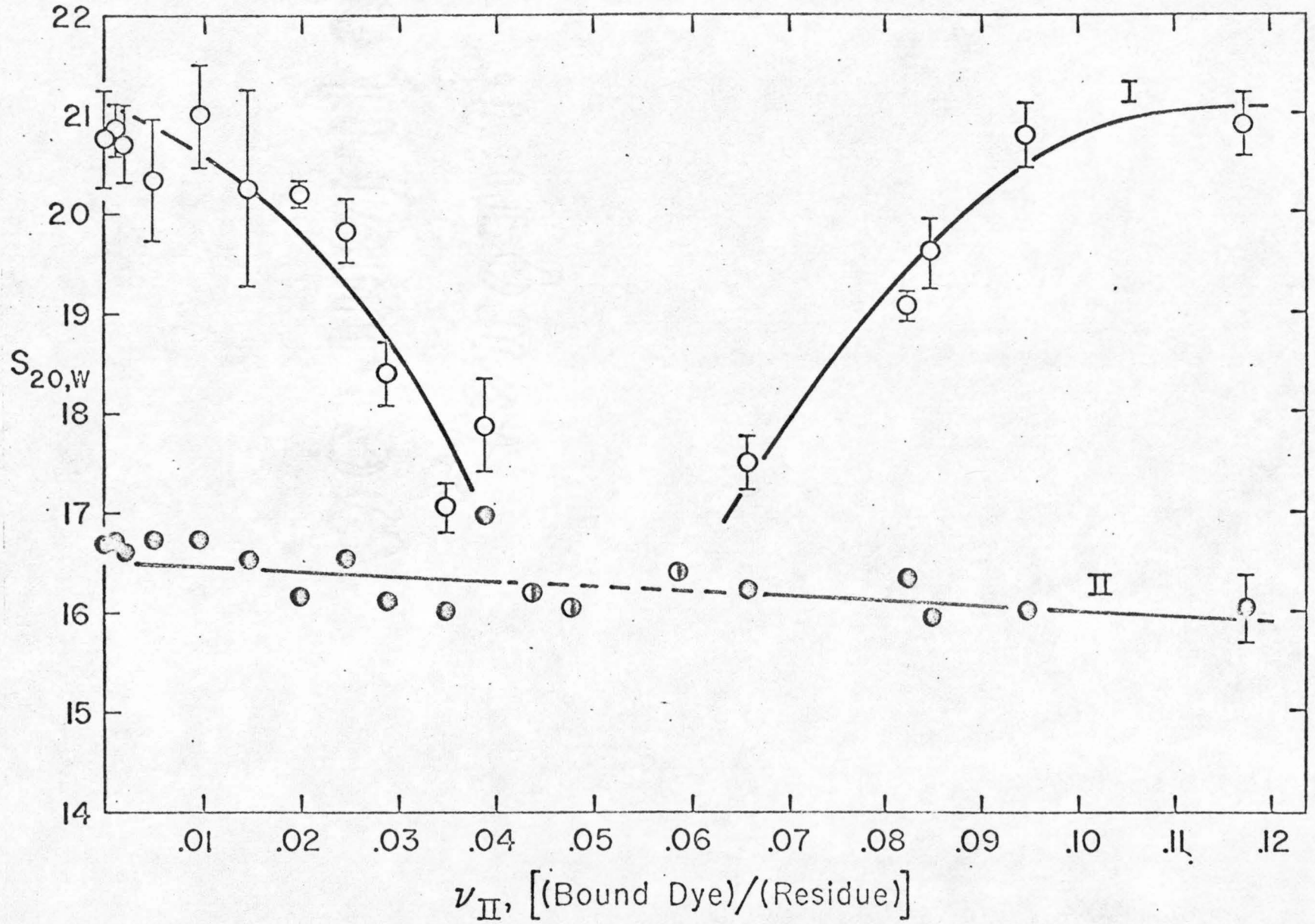
22
21
20
19
18
17
16
15
14
$S_{20,w}$
I
II
.01
.02
.03
.04
.05
.06
.07
.08
.09
.10
.11
.12
ν_{II}, [(Bound Dye)/(Residue)]

dye concentration, until the ratio s_I/s_{II} approaches a value nearly equal to the sedimentation coefficient ratio in the absence of dye. The midpoint of the dip region corresponds to the critical amount of dye bound and $\nu_I = \nu_c = \nu_{II}$. In Appendix I it is shown that

$$\frac{s_I(\nu)}{s_{II}(\nu)} = \frac{f_{II}(\nu)[1 + K\nu_I]}{f_I(\nu)[1 + K\nu_{II}]}$$

where f is the frictional coefficient and

$$K = \frac{[1 - \bar{v}_{4,h}\rho]M_3}{[1 - \bar{v}_{3,h}\rho]M_4}$$

where $\bar{v}_{4,h}$ and $\bar{v}_{3,h}$ are the partial specific volumes of the preferentially hydrated dye and DNA, ρ is the density of the solution, and M_3 and M_4 are the anhydrous molecular weights of the average DNA nucleotide and of the dye respectively. At $\nu = \nu_c$ the ratio of sedimentation coefficients is unity and, since component I is now a fully relaxed circle, $f_I(\nu_c) = f_{II}(\nu_c)$.

Equation (6) then requires that $\nu_I = \nu_{II}$ at the midpoint of the dip. Taking $\nu_c = 0.05 \pm 0.01$, we calculate that the initial superhelix density $\sigma_0 = -0.033 \pm 0.007$ and that the initial number of superhelical turns $\tau_0 = -16.0 \pm 3.5$.

The results for the binding of 9-aminoacridine are shown in Fig. 9. Here the sedimentation coefficients of components I and II are plotted as a function of the initial total dye/nucleotide ratio, r_f.

FIG. 9. Sedimentation velocity of SV 40 DNA at an ionic strength of 0.028 M (0.01 M NaCl, 0.001 M sodium phosphate, pH 7.0) containing various concentrations of 9-aminoacridine. For explanation of symbols refer to Fig. 8. The sedimentation coefficients are plotted as a function of the ratio of the total dye concentration to the total nucleotide concentration. At $r_f = 0.075$ the initial concentrations of I, II, total dye, and free dye were 10.0, 11.0, 1.0, 0.8 μg/ml respectively.

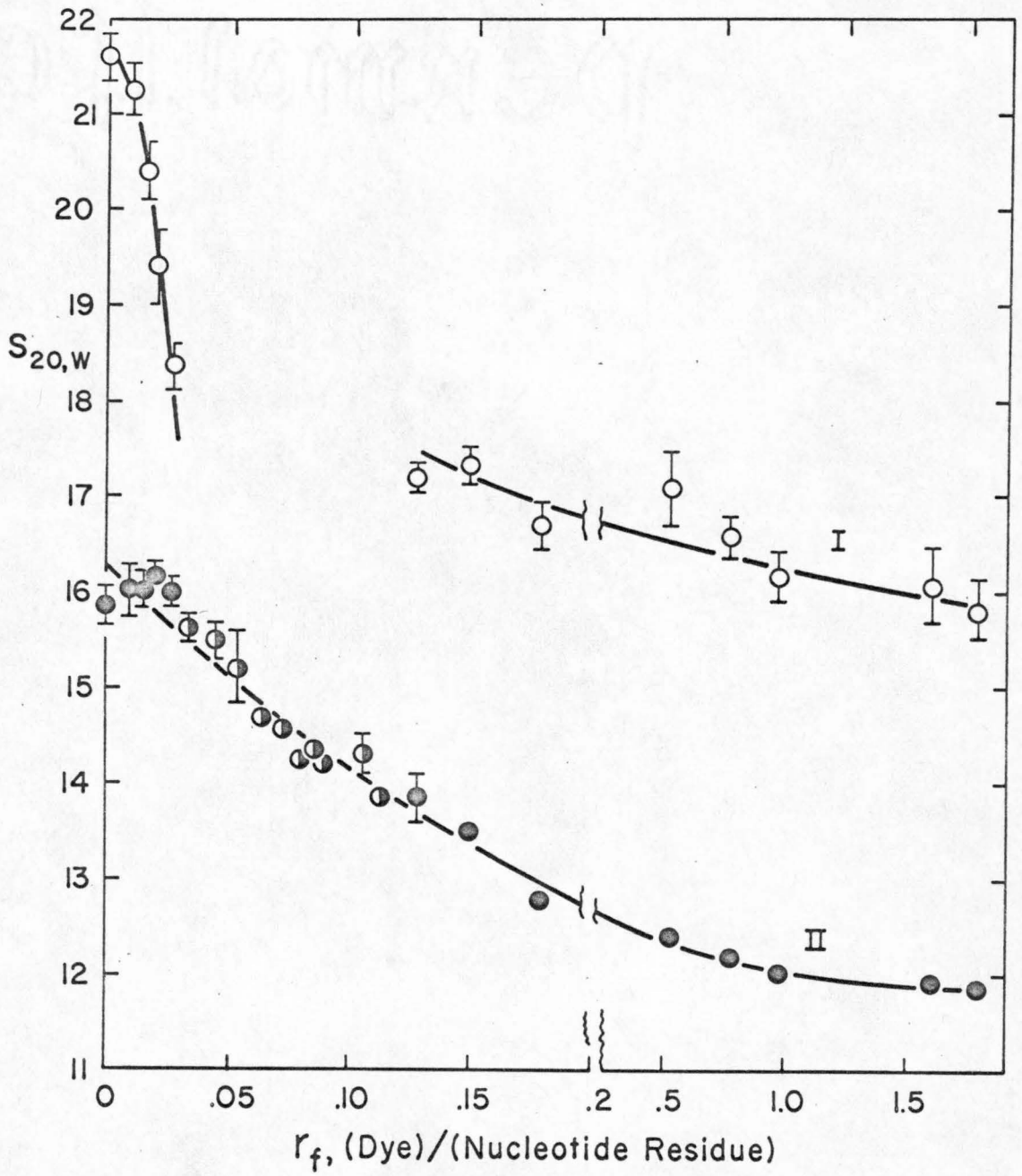
22
21
20
19
18
17
16
15
14
13
12
11
$S_{20,w}$
I
II
0
.05
.10
.15
.2
.5
1.0
1.5
r_f, (Dye)/(Nucleotide Residue)

The reduction in sedimentation coefficient of SV 40 DNA II, which is greater than in the case of ethidium bromide addition, is similar to that reported for linear DNA (Lerman, 1961). The sedimentation behavior of the closed circular DNA as a function of the 9-aminoacridine concentration is qualitatively similar to that shown in Fig. 8 for ethidium bromide. In the region $0.03 \leq r_f \leq 0.12$ only one boundary was observed. It has been calculated with Yew & Davidson's estimate of the association constant for strong binding, $k = 1.6 \times 10^5$ ℓ/M, and $\nu_m = 0.2$ at an ionic strength of 0.02 M, that the midpoint of this region corresponds to $\nu_c = 0.043 \pm 0.02$. If we now assume that the angle of unwinding of the helix per molecule of 9-aminoacridine intercalated is the same as for ethidium bromide, we calculate that $\sigma_0 = -0.029 \pm 0.015$ and that $\tau_0 = -14 \pm 7$. These results bracket the more precise values calculated from the ethidium bromide sedimentation velocity studies.

Although the sedimentation velocity experiments provide data for the estimation of ν_c, and thus of σ_0 and τ_0, it is not possible to calculate either ν_I or $\sigma(\nu_I)$ at other than the critical amount of dye bound. The sedimentation velocity results do indicate, however, the qualitative behavior of σ as a function of ν_I. The addition of small amounts of dye causes a reduction in the sedimentation coefficient and an unwinding of the superhelical turns until $\sigma = 0$ at $\nu = \nu_c$. Further dye addition results in the introduction of positive superhelical turns as required by equation (4). The sedimentation coefficient increases at first rapidly and then slowly, until an apparent

plateau in the ratio s_I/s_{II} is reached at a value approximately equal to that in the absence of dye. This result suggests that a practical upper limit is reached in the number of positive superhelical turns which can be introduced by dye addition. An alternative interpretation is that the upper plateau merely represents an insensitivity of the sedimentation coefficient to the introduction of more than a certain number of superhelical turns. As is shown below, this ambiguity does not arise in the interpretation of the buoyant density results, which show that the superhelix density continues to increase upon dye binding at high dye concentrations.

(b) Buoyant density experiments at low ethidium concentrations

Purified DNA I and II were used in this series of experiments. Frequent analyses of the intact closed circular DNA by analytical band velocity sedimentation showed that spontaneous conversion of I to II was less than 5% over the period of the experiments. Native crab dAT was used as a buoyant density marker. Since the crab dAT reacts with ethidium bromide, it was necessary to calibrate its buoyant density as a function of dye concentration at band center. Figure 10 presents the results of this calibration. The experimental points are the buoyant densities measured by the absolute method (Vinograd & Hearst, 1962) and the solid line represents the quadratic least squares fit to the data. The equation of best fit is

$$\rho = 1.6696 - 0.005624\, c_0 + 0.000081\, c_0^2 \qquad (7)$$

FIG. 10. The buoyant density of crab dAT in CsCl containing ethidium bromide. The buoyant densities were evaluated from the distance between the band and the CsCl isoconcentration position using the buoyant density gradient and Eq. (40a) in Vinograd & Hearst (1962). The free dye concentrations at band center, c_0, were obtained by interpolating the dye concentrations measured on the scanner records in the DNA-free regions of the cell. The solid line is the best least squares quadratic fit to the experimental data, as discussed in the text.

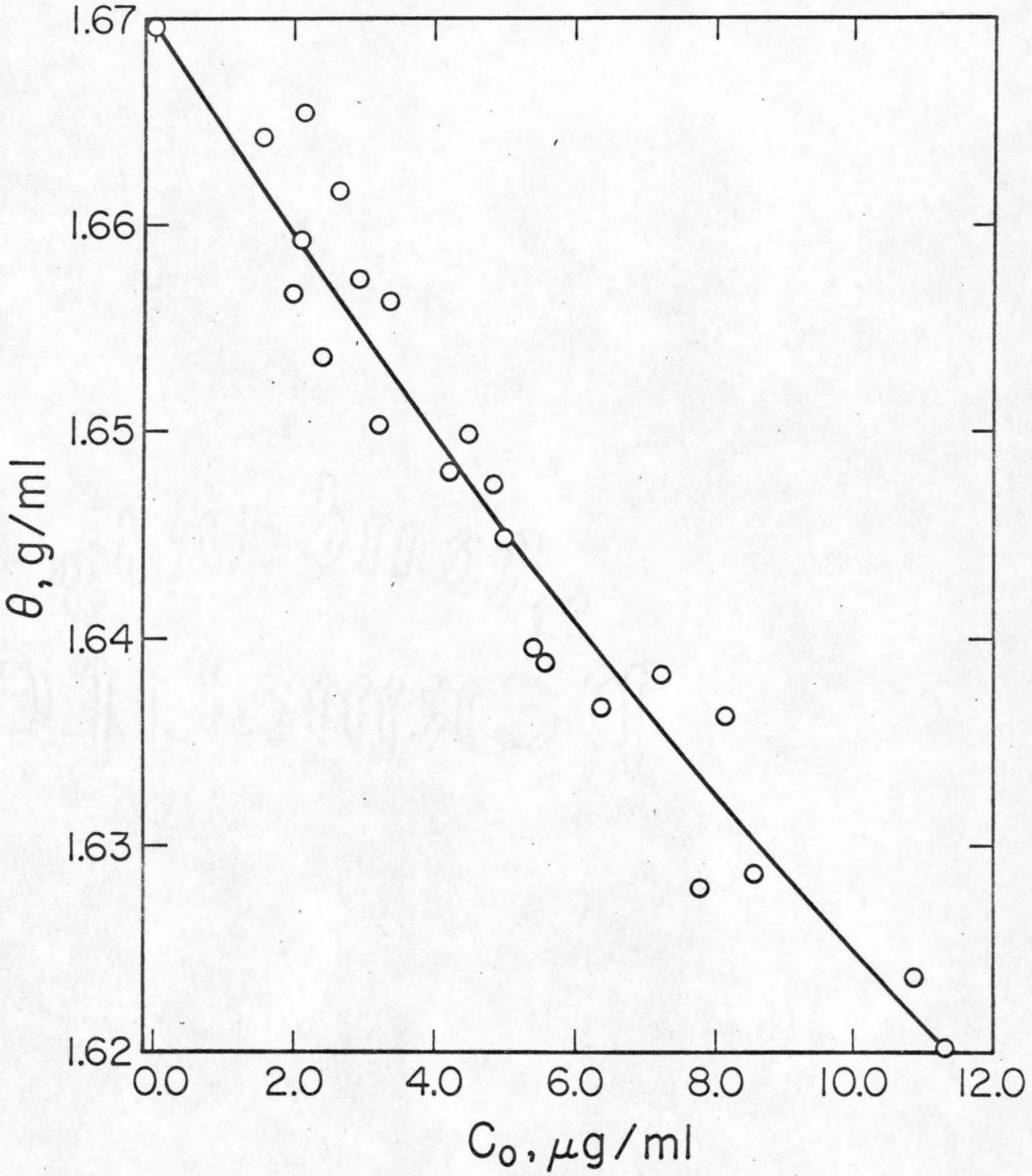
1.67
1.66
1.65
1.64
1.63
1.62
θ, g/ml
0.0
2.0
4.0
6.0
8.0
10.0
12.0
C₀, μg/ml

where c_0 is the free dye concentration in μg/ml ethidium bromide at band center. The value for the buoyant density in the absence of dye, θ_0, is the mean of several measurements; it was assigned a weight equal to ten times the weight of the other data points.

It is a result of the thermodynamic theory for a four component system at buoyant equilibrium (Bauer & Vinograd, 1967b), that the buoyant density of the complex between a macromolecule, water and a non-preferentially hydrated fourth component is given by

$$\theta = \frac{1 + \Gamma' + \nu'}{\bar{v}_3 + \Gamma' \bar{v}_1 + \nu' \bar{v}_4} \qquad (8)$$

where Γ' is the preferential solvation of the DNA at band center by water in g/g DNA; $\nu' = (M_4/M_3)\nu$, where M_4 and M_3 are the dye and average nucleotide residue molecular weights; $\bar{v}_1$ is the partial specific volume of water, $\bar{v}_3$ is the anhydrous partial specific volume of CsDNA; and $\bar{v}_4$ is the anhydrous partial specific volume of the fourth component--in this case ethidium chloride. The quantity $\bar{v}_4$ was determined as described in Appendix II and was found to be equal to 1.02 ± 0.03 ml/g. The value $\bar{v}_3 = 0.479$ ml/g (Hearst, 1962) for CsDNA was used.

Figure 11 presents the buoyant densities of I and II as a function of the free dye concentration at band center. Table 1 lists the conditions for the experiments. At low dye concentrations the closed circular component initially has a greater affinity for dye than does the nicked circular DNA. The affinity then decreases with

FIG. 11. The buoyant density of SV 40 DNA I, ○, and II, ●, in CsCl containing low concentrations of ethidium bromide. The buoyant densities were evaluated from the distance between the SV 40 band and a marker band of crab dAT. The free dye concentrations were calculated as described in the legend to Fig. 10.

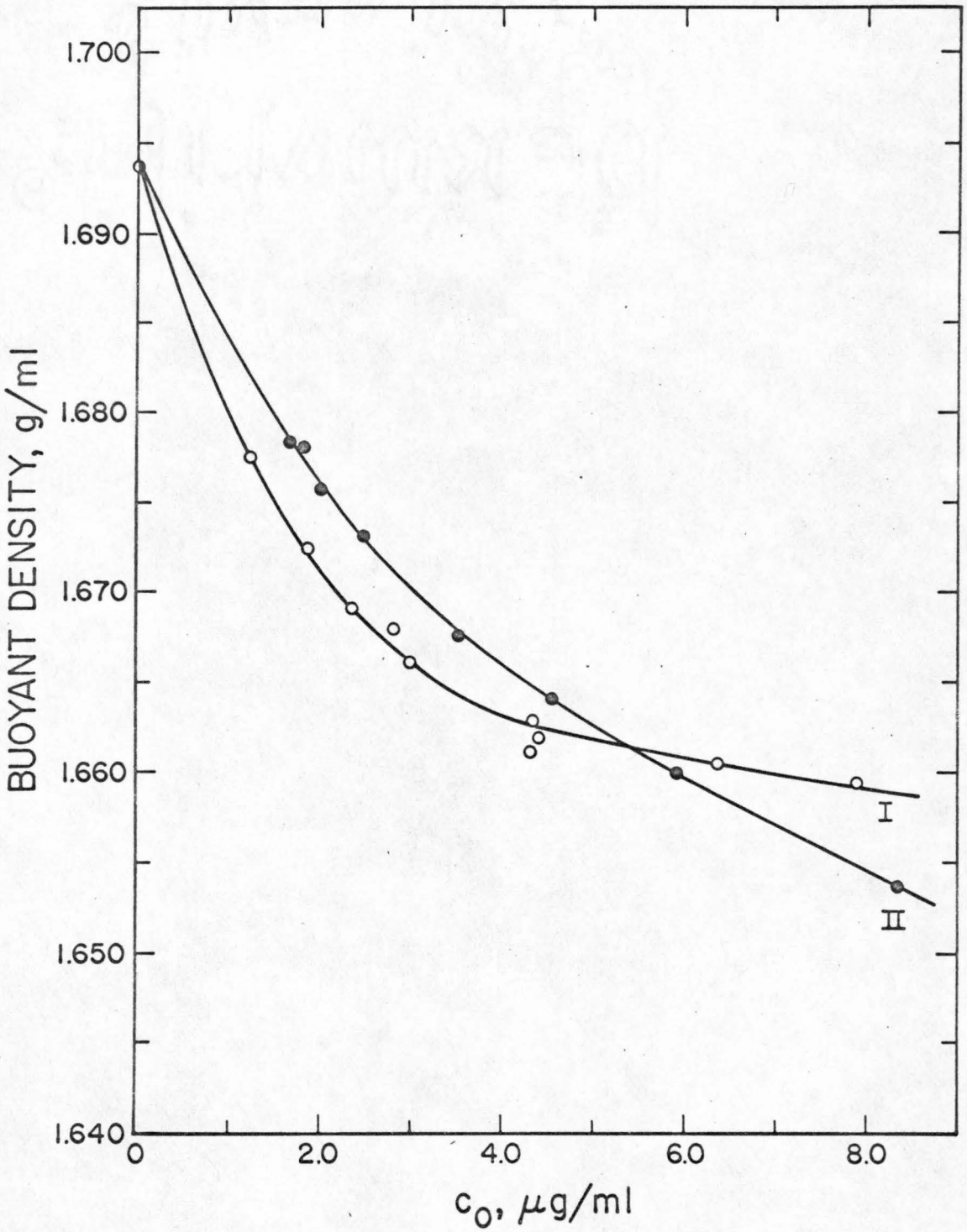
1.700
1.690
1.680
1.670
1.660
1.650
1.640
BUOYANT DENSITY, g/ml
0
2.0
4.0
6.0
8.0
c_0, μg/ml
I
II

increasing dye concentration until, after ν_c dye molecules are bound, the affinity of I for dye becomes smaller than the affinity of II. The buoyant density curves cross at a value of $\theta_c = 1.661_5$ g/ml. The buoyant density shift, $\Delta\theta = \theta_0 - \theta_c$, corresponds according to Eq. (9) to a critical value of dye bound, $\nu_c = 0.039_0 \pm 0.004$. We then calculate with Eq. (4), that $\sigma_0 = -0.026_4 \pm 0.003$ and $\tau_0 = -12.7 \pm 1.5$. These more precise results are in agreement with the estimates from the sedimentation velocity experiments.

(c) Buoyant density experiments at high ethidium concentrations

Figure 12 presents absolute buoyant densities as a function of dye concentration at band center, c_0, for both components I and II. The experimental conditions are presented in Table 1. A marker DNA was not used because the density shifts were relatively large over this dye concentration range. Previously separated components were not used in these experiments, since the differential dye affinity was great enough to cause physical separation of I from II in the analytical cell. The two components were completely resolved at a free dye concentration greater than about 20 μg/ml. The dashed lines in Fig. 12 connect the buoyant densities of the pairs of components present in the same analytical centrifuge cell. The maximum observed separation between the closed and nicked circular SV 40 DNA components present in the same cell was about 50 μg/ml. The maximum difference in buoyant density at constant dye concentration is 40 mg/ml at a free dye concentration in excess of 100 μg/ml. The greater

FIG. 12. The buoyant density of SV 40 DNA I, ○, and II, ●, in CsCl containing ethidium bromide. The buoyant densities and the free dye concentrations at band center were evaluated as described in the legend to Fig. 10. The dashed lines connect the points obtained in a single cell.

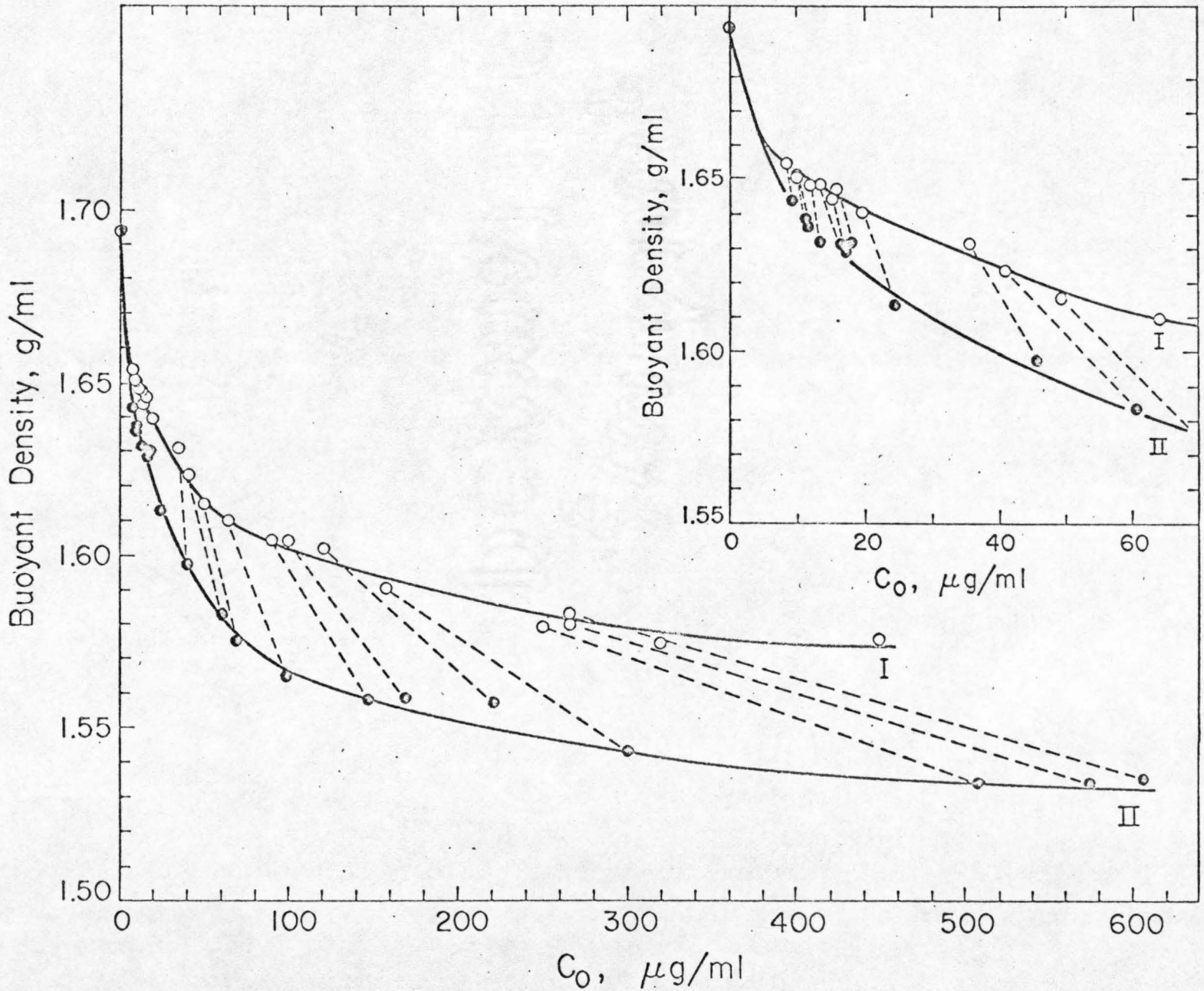
Buoyant Density, g/ml
1.70
1.65
1.60
1.55
1.50
0
100
200
300
400
500
600
C_0, μg/ml
I
II
Buoyant Density, g/ml
1.65
1.60
1.55
0
20
40
60
C_0, μg/ml
I
II

TABLE I

Experimental conditions for the buoyant density determinations presented in Figs. 11 and 12

Initial dye concentration c° (μg/ml)	Free dye concentration, band center c_o (μg/ml) I	Free dye concentration, band center c_o (μg/ml) II	Initial DNA concentration[a] (μg/ml)	Solution density (g/ml)	Centerpiece thickness (mm)	Wave length (mμ)
0.0 - 2.5	0.0 - 3.5	0.0 - 4.2	1.5[b]	1.700	12.0	265.4
2.3 - 6.5	1.8 - 6.3	3.0 - 8.7	1.5[b]	1.650	12.0	265.4
10	9.5	11.5	1.5	1.615	12.0	265.4
30	20.0	24.5	1.5	1.610	12.0	265.4
50	41.0	60.0	4.0	1.610	4.0	265.4
80	63.2	98.0	7.0	1.600	2.0	265.4
125	99.0	169.0	7.0	1.604	2.0	487 - 521[c]
200	158.0	300.0	7.0	1.594	2.0	487 - 521[c]
300	250.0	507.0	7.0	1.598	2.0	487 - 521[c]
400	267.0	580.0	7.0	1.592	2.0	487 - 521[c]

[a] Mixtures containing equal amounts of I and II were used unless otherwise noted.
[b] Separate experiments done with purified samples of I and II, crab dAT as a marker.
[c] Wavelengths used for the free and bound dye, respectively.

physical separation between I and II in a cell containing ethidium bromide at concentrations below saturation is due to the extensive redistribution of the dye, Figs. 6, 7. The separations in buoyant CsCl containing ethidium bromide, Fig. 12, may be reproduced in the preparative ultracentrifuge, and provide a method for the detection and isolation of closed circular DNA (Radloff, Bauer & Vinograd, 1967).

(d) Calculation of the amount of dye bound from the buoyant density of the DNA-dye complex

In order to calculate the moles dye bound per nucleotide, ν, equation (8) is rearranged and combined with the relationships $\nu = \nu'(M_3/M_4)$, $\theta_0 = (1 + \Gamma_0')/(\bar{v}_3 + \Gamma_0'\bar{v}_1)$, and $\Gamma' = \Gamma_0' + \Delta\Gamma'$, where the subscript zero refers to the quantities evaluated in buoyant density experiments in the absence of dye.

$$\nu = \left(\frac{M_3}{M_4}\right)\left[(1 + \Gamma_0')(\Delta\theta/\theta_0) - \Delta\Gamma'(\bar{v}_1\theta - 1)\right]/(\bar{v}_4\theta - 1) \qquad (9)$$

In Eq. (9) $\Delta\theta = \theta_0 - \theta$. The preferential solvation by water may be computed from the density of the solution at band center. Equation (9) may be rewritten

$$\nu = \frac{a\Delta\theta - b(\bar{v}_1\theta - 1)\Delta\Gamma'}{(\bar{v}_4\theta - 1)} \qquad (10)$$

In Eq. (10) $a = (M_3/M_4)(1 + \Gamma_0')/\theta_0 = 0.9259$ ml/g and $b = (M_3/M_4) =$

= 1.232 ml/g, where M_3 = 430 for the average Cs nucleotide residue, M_4 = 349 for ethidium chloride, and $\theta_0 = 1.693_7$ g/ml for SV 40 DNA. The buoyant density, θ_0, was measured in several experiments in which crab dAT ($\theta_0 = 1.669_6$ g/ml) and M. lysodeikticus ($\theta_0 = 1.726_5$) DNAs were present as markers. No difference was observed between the buoyant densities of SV 40 DNA I and II.

Figure 13 presents a plot of ν as a function of the buoyant density decrement for SV 40 DNA. The solid curve was calculated with equation (10). The results of Appendix III were used to derive the best least squares polynomial to describe the relationship between $\Delta\Gamma'(\theta)$ and θ.

$$\Delta\Gamma'(\theta) = 0.04092 - 0.7282\eta + 4.592\eta^2 - 16.08\eta^3 + 20.56\eta^4, \quad \text{(11a)}$$

$$\Delta\Gamma' = \Delta\Gamma'(\theta) - \Delta\Gamma'(\theta_0) \quad \text{(11b)}$$

where $\eta = \theta - 1.5$. Equations (11a, b) may be used to calculate $\Delta\Gamma'$ for any DNA for which the slopes of a plot of θ vs a_w are similar to that for T4 DNA. Figure 17 shows a plot of Eq. (11a) over the density range 1.5-1.73 g/ml for a DNA with θ_0 = 1.6. This polynomial, together with Eq. (11b), may be used in place of Eq. (III-6) to obtain $\Delta\Gamma'$ in Eq. (9). Equations (4) and (9), together with the measured value of θ_0 and the calculated value of Γ_0', Eq. (III-6a) may be used to calculate ν from $\Delta\theta$ for any other DNA. The dashed curve in Fig. 13 was calculated with Eq. (10), and $\Delta\Gamma' = 0$. Setting $\Delta\Gamma'$ equal to zero neglects changes in the preferential hydration which occurs as the band is shifted into more dilute salt solutions

FIG. 13. The moles of ethidium bound to SV 40 DNA as a function of the buoyant density decrement. The solid curve takes into account changes in preferential hydration which occur as the band is shifted into more dilute salt solutions upon binding dye. The dashed curve was calculated without taking this effect into account.

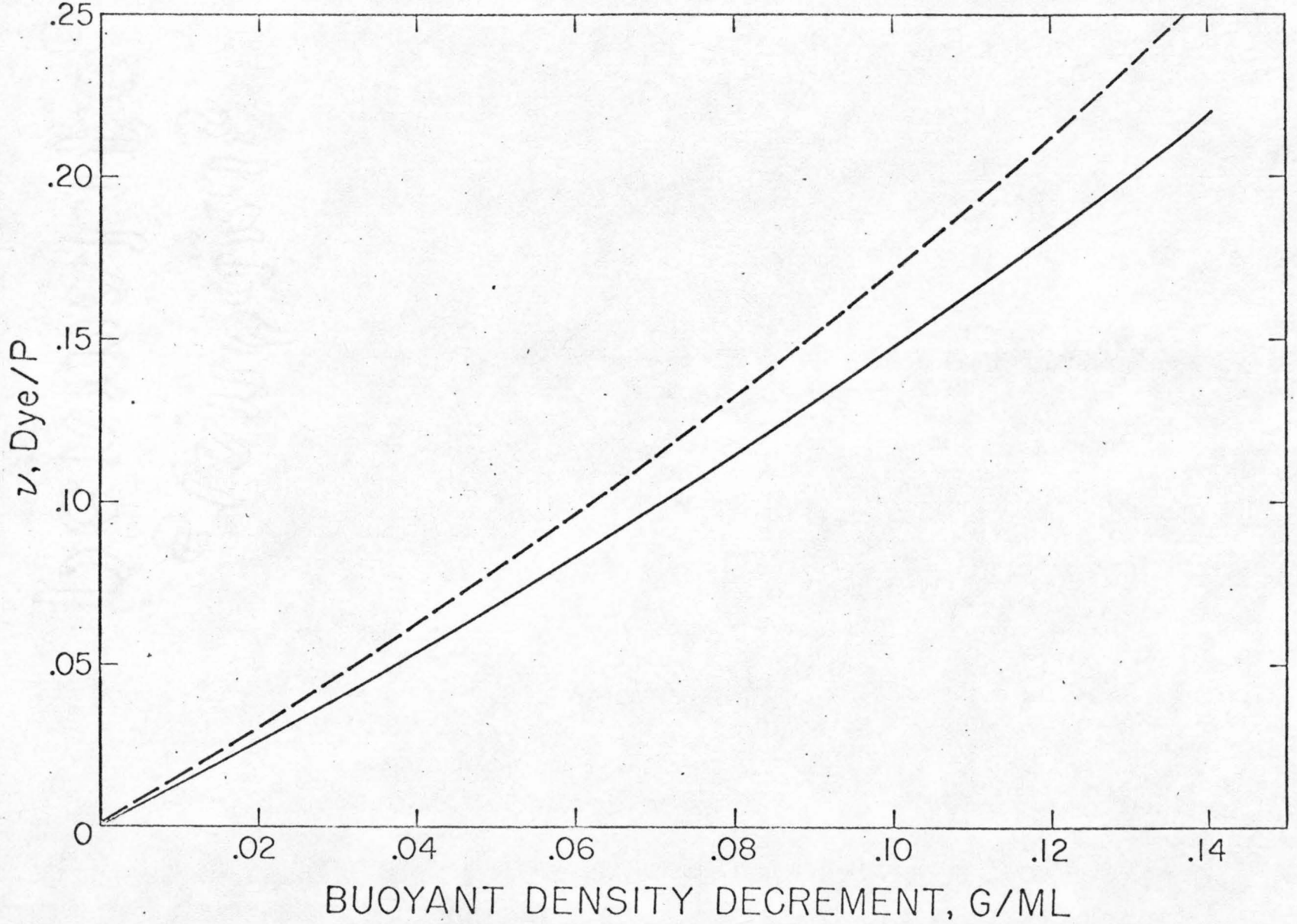
.25
.20
.15
.10
.05
0
ν, Dye/P
.02
.04
.06
.08
.10
.12
.14
BUOYANT DENSITY DECREMENT, G/ML

upon binding dye.

Equations (3), (9), and (10) were also used to calculate ν and τ as a function of the free dye concentration at band center. The binding isotherm obtained from the results of the buoyant density experiments are presented in Fig. 14a for both I and II at low dye concentration. Figures 14b and 14c present the binding data for I and II respectively over the dye concentration range, 0 to 600 μg/ml. The curve for I appears to level off within the range of dye concentrations studied at a value of $\nu = 0.15$, whereas the curve for II approaches an asymptote at $\nu = 0.22$. An analysis of the binding data for SV DNA II according to the method of Scatchard, presented in Part II, shows that two types of binding sites are involved. The intercalative binding extends up to $\nu = 0.20$, as found previously by Le Pecq & Paoletti (1967) and by Waring (1965). At higher dye levels, the effect of the binding at a second site is observed. The total binding proceeds until $\nu = 0.22$. At 0.04 M salt, Waring (1965) observed secondary binding of ethidium bromide up to a value of $\nu = 1.0$. The data of Waring (1965) and of Le Pecq & Paoletti (1967) show a reduction of secondary binding with increasing salt concentration up to 1.0 M and 2.5 M respectively. The results of Waring in 3×10^{-4} M $MgCl_2$ show secondary binding which begins at $\nu \approx 0.18$. The secondary binding does not appear to cause unwinding of the duplex helix, as indicated by the constancy of the difference $\nu_{II} - \nu_I$ in the high dye region, Fig. 15. If the amount of secondary binding obtained for SV 40 DNA II is subtracted from the maximum value of ν for SV 40 DNA I, the

saturation value of ν_I for intercalative binding may be estimated as 0.13 moles dye per mole nucleotide.

FIG. 14. The moles of ethidium bound per phosphate in SV 40 DNA as a function of free dye concentration at band center, c_0. The values for ν, the dye bound per residue, were calculated with Eq. (9) from the data shown in Figs. 11 and 12. The values for ν, the dye bound per residue, were calculated with Eq. (9) from the data shown in Figs. 11 and 12. The values for τ were calculated with Eq. (3). The dashed line represents the maximum number of binding sites per residue. Except for the effect of pressure on the binding constant, these curves may be regarded as representing simple binding isotherms. The data for both I and II at low dye concentration are shown in (a). The complete data for SV 40 I are presented in (b). The data for II are presented in (c), together with the curve for I. The binding by I at low dye concentrations is higher than the binding by II. Above the crossover point, represented by $\tau = 0$, $\nu_0 = 0.0390$, and $c_0 = 5.4$ μg/ml, the affinity of II for the ethidium is greater than that of I, a consequence of the positive free energy of superhelix formation as discussed in Part II of this series.

D
0.05
0.04
0.03
0.02
0.01
0.00
ν, MOLES DYE/MOLE RESIDUE
2
0
-2
-4
-6
-8
-10
-12
τ, SUPERHELICES/DNA
0.01
0.00
-0.05
-0.10
-0.15
-0.20
-0.25
σ, SUPERHELICES/10 BASE PAIRS
0
2.0
4.0
6.0
8.0
c_o, μg/ml

c_o, mM/l
0.0
0.2
0.4
0.6
0.8
1.0
1.2
1.4
0.20
0.15
0.10
0.05
0.00
q
ν, MOLES DYE/MOLE RESIDUE
0
100
200
300
400
500
c_o, μg/ml
40
30
20
10
0
-10
τ, SUPERHELICES/DNA
0.08
0.06
0.04
0.02
0
-0.02
σ, SUPERHELICES/10 BASE PAIRS

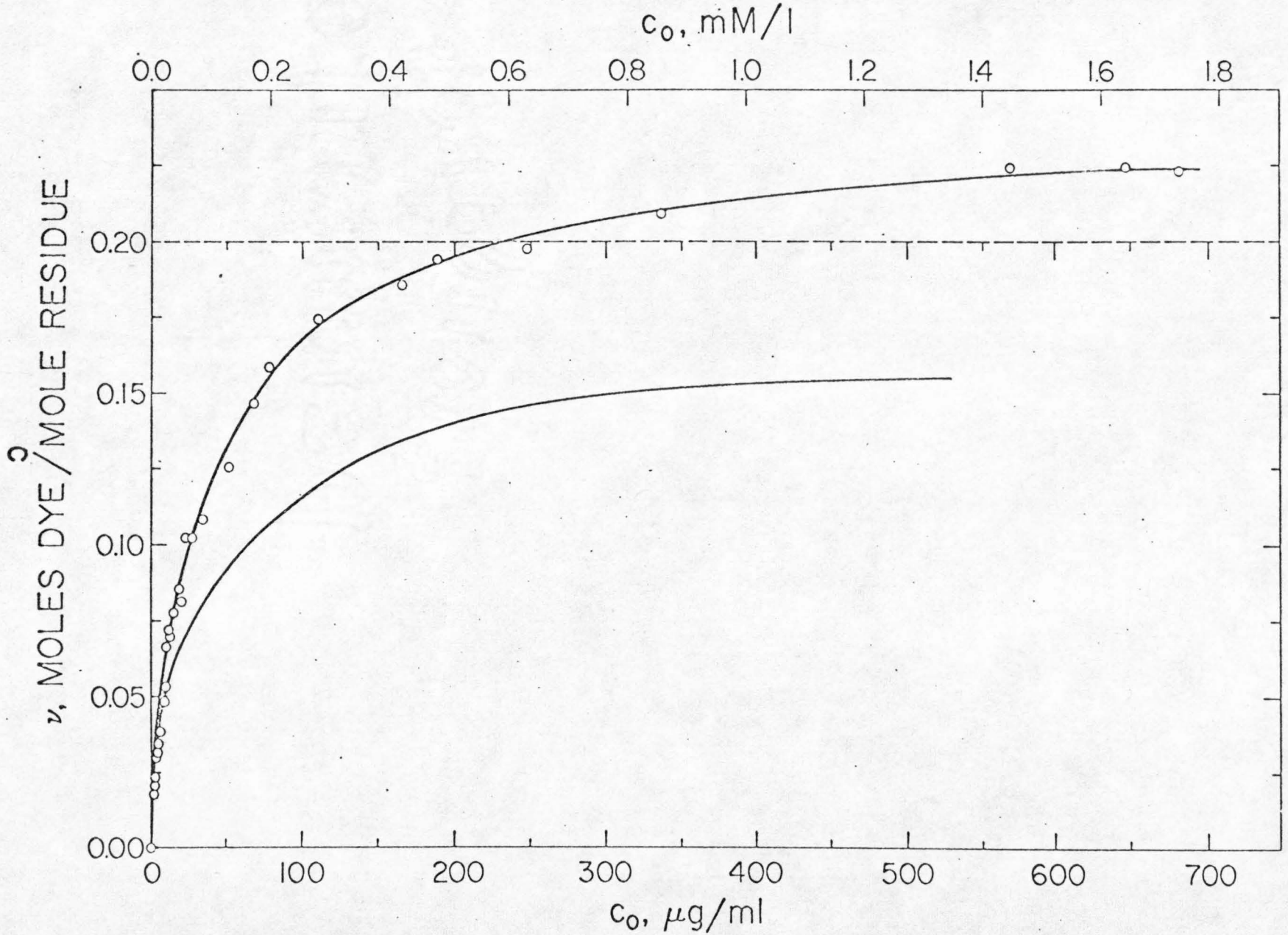
c_0, mM/l
0.0
0.2
0.4
0.6
0.8
1.0
1.2
1.4
1.6
1.8
ν, MOLES DYE/MOLE RESIDUE
0.00
0.05
0.10
0.15
0.20
0
100
200
300
400
500
600
700
c_0, μg/ml

FIG. 15. The effect of the presence of superhelices on the binding of ethidium chloride to SV 40 DNA. The curves present the difference in the amount of dye bound, $\nu_I - \nu_{II}$ taken from Fig. 14, as a function of the free dye concentration.

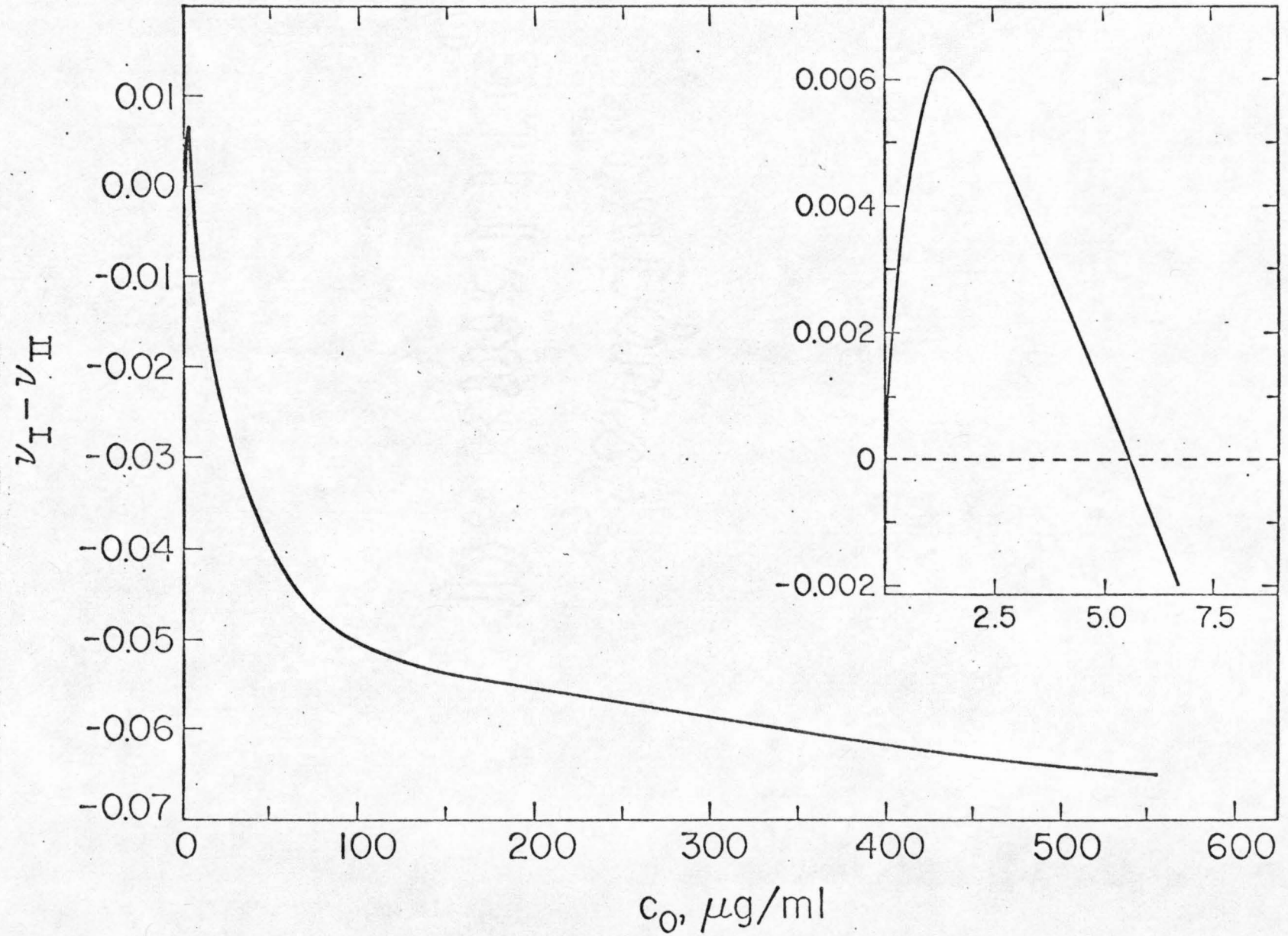
0.01
0.00
-0.01
-0.02
-0.03
-0.04
-0.05
-0.06
-0.07
$\nu_I - \nu_{II}$
0
100
200
300
400
500
600
c_0, μg/ml
0.006
0.004
0.002
0
-0.002
2.5
5.0
7.5

DISCUSSION

The experiments with ethidium bromide described in this study have provided two essentially independent estimates of the superhelix density of native SV 40 DNA in concentrated salt solutions. From the sedimentation velocity data, we have calculated that $\tau_0 = -16.0 \pm 3.5$, and that $\sigma_0 = -0.033 \pm 0.007$. The result obtained by the buoyant density method was $\tau_0 = -12.7 \pm 1.5$, and $\sigma_0 = -0.026_4 \pm 0.003$. In both the sedimentation velocity and the buoyant density methods it is assumed that the angle of unwinding of the duplex helix per intercalated dye molecule is 12°, and that this angle is independent both of the amount of dye bound and of the solution environment of the DNA molecule. Fuller & Waring (1964), in their model building studies, could not rigorously exclude the possible value of 36° for the unwinding angle, as proposed earlier by Lerman (1964) for the acridines, nor did they give an estimate of the uncertainty in the 12° value. The superhelix density of polyoma DNA as determined in an alkaline buoyant density titration (Vinograd, Lebowitz, and Watson, 1967) is indistinguishable from the value obtained here for SV 40 DNA. These two DNAs are contained in closely related viruses and appear to have similar molecular weights and sedimentation velocity properties. The above agreement in the superhelix densities suggests that the 12° value is not seriously in error. Crawford and Waring (1967) also used the 12° unwinding angle to estimate the superhelix density of polyoma DNA from the position of the minimum in a plot of

the sedimentation velocity vs ethidium bromide concentration. Unfortunately, their results, τ_0 = -10 to -15, or σ_0 = -0.021 to -0.032, are not accurate enough for a test of Fuller and Waring's (1964) value of the unwinding angle ϕ. The results for τ_0 and σ_0 for SV 40 DNA calculated in this work may be subject to revision by a multiplicative constant in the event that a more accurate and different value of the unwinding angle is determined. The binding isotherms are, however, unaffected by the magnitude of the unwinding angle.

While the results of these experiments are most simply interpreted in terms of an unwinding caused by intercalation of dye between the base pairs, they would be adequately explained by any binding mechanism that caused unwinding of the duplex.

In this application of the buoyant density method to a chemically reacting system it has been demonstrated that the buoyant density shift is a direct measure of the extent of the reaction. The method is thermodynamic in nature and is comparable to dialysis equilibrium, but with the distinct advantage that much smaller amounts of material are required. The buoyant density decrement is a direct measure of the amount of dye bound, in contrast to all spectroscopic methods, which depend upon the detailed electronic interactions that occur. Except at very low dye concentrations, the closed circular DNA is automatically separated from all other DNAs as well as from other macromolecular components capable of binding dye. The method has a further advantage if the absorption spectrum of the

complex is suitably different from that of the DNA and if the extinction coefficient of the complex is sufficiently large. The distribution of the bound dye over a band can then be separately measured as described in Appendix II, and an estimate may be made of the bound dye per nucleotide at band center independently of the buoyant density shift.

Kirsten, Kirsten & Szybalski (1966) have pointed out that many dyes and antibiotics, including ethidium bromide, lower the buoyant density of linear DNA. The quantitative aspects of this work are unclear however, because of a failure to take into account both the extensive redistribution of dye at equilibrium and, at low dye concentrations, the reduction of the free dye concentration by the binding reaction.

The effects of changes in preferential hydration of the DNA-dye complex due to the water activity and pressure terms have been considered in detail, and have been shown to account for 12-15% of the buoyant density shift. The buoyant effect of the binding of dye molecules to the DNA thus accounts for 85-88% of the observed buoyant density shift. The total shift includes the escalating effect caused by the additional hydration that occurs when the band moves to regions of lower salt concentration and lower pressures. It should be pointed out that the present treatment does not take into account the possibility of changes in the net hydration of DNA as a consequence of dye binding at constant water activity and constant pressure. It will be shown in Part II of this series that the number of sites available for

intercalative dye binding in SV 40 DNA II calculated from the buoyant shift is in agreement with the value determined for linear DNA by a fluorescence study (Le Pecq & Paoletti, 1967). We therefore conclude that the above interaction term is small.

The sedimentation velocity results are most readily interpreted in terms of a continuous unwinding of the duplex with increasing total dye concentration, with an accompanying change in the superhelix density from negative, through zero, to positive values. However, it was not possible from the sedimentation velocity results alone to exclude that the unwinding of the duplex which occurs at the early stages of the binding reaction is essentially reversed during the later stages, and that the sign of the superhelix density always remains negative. In such an event the minimum in the sedimentation velocity-dye curve would not be a meaningful measure of the superhelix density in the absence of dye. The restriction in the dye binding at high dye concentration, observed in the buoyant density experiments, make this interpretation untenable.

The superhelix density of naturally occurring closed circular DNA is of intrinsic interest in the theory of the translational and rotational frictional coefficients of superhelical DNA. Shortly after the discovery of this type of DNA, Bloomfield (1966) considered the hydrodynamic behavior of a model consisting of adhering flexible loops of beads of equal size, according to the basic equations developed by Kirkwood (1954). From the ratio of the sedimentation coefficients, s_I/s_{II}, Bloomfield estimated that $\tau_0 = 2$ for SV 40 DNA I.

Kurata (1966), with an essentially similar approach, took into account the stiffness term expressed by the constant parameter in the equation of Hearst & Stockmayer (1962) for the relations between sedimentation coefficient and molecular weight for linear DNA. He estimated that τ_0 is in the range of 5-9. More recently Gray (1967) used the Kirkwood (1954) equation to calculate the sedimentation coefficient of a rigid superhelix. A set of results was obtained in which the pairs of superhelix density and superhelix pitch (or superhelix diameter) were consistent with the experimental ratio s_I/s_{II}. For polyoma DNA and $\tau_0 = -16$ his results yield a superhelix diameter of 300 Å. It will be shown in Part II that the superhelix diameter for a similar model can be estimated from the free energy of superhelix formation.

The results presented here for the effects of known and variable superhelix densities on the sedimentation coefficient will provide further data for the testing of the applicability of theoretical treatments of this conformation. Figure 16 clearly shows that the dependence of the sedimentation coefficient upon the superhelix density is not linear. At low values of τ, between $\tau = -3$ and $\tau = +3$, the sedimentation coefficient changes rapidly and approximately symmetrically with the absolute value of τ. At higher absolute values of τ, the sedimentation coefficient changes much more slowly with τ, and s becomes an insensitive index of the superhelix density. The recently reported (Kroon, Borst, Van Bruggen & Ruttenburg, 1966) ratio for s_I/s_{II} in 1 M NaCl of 1.44 for sheep heart

FIG. 16. The dependence of the sedimentation coefficient of SV 40 DNA I on ν_I, the moles of ethidium chloride bound per mole nucleotic residue. The values of ν were obtained by a procedure described in the text. The upper abscissa shows τ, the number of superhelical turns per molecule, and σ, the superhelix density, as calculated with Eqs. (3) and (4).

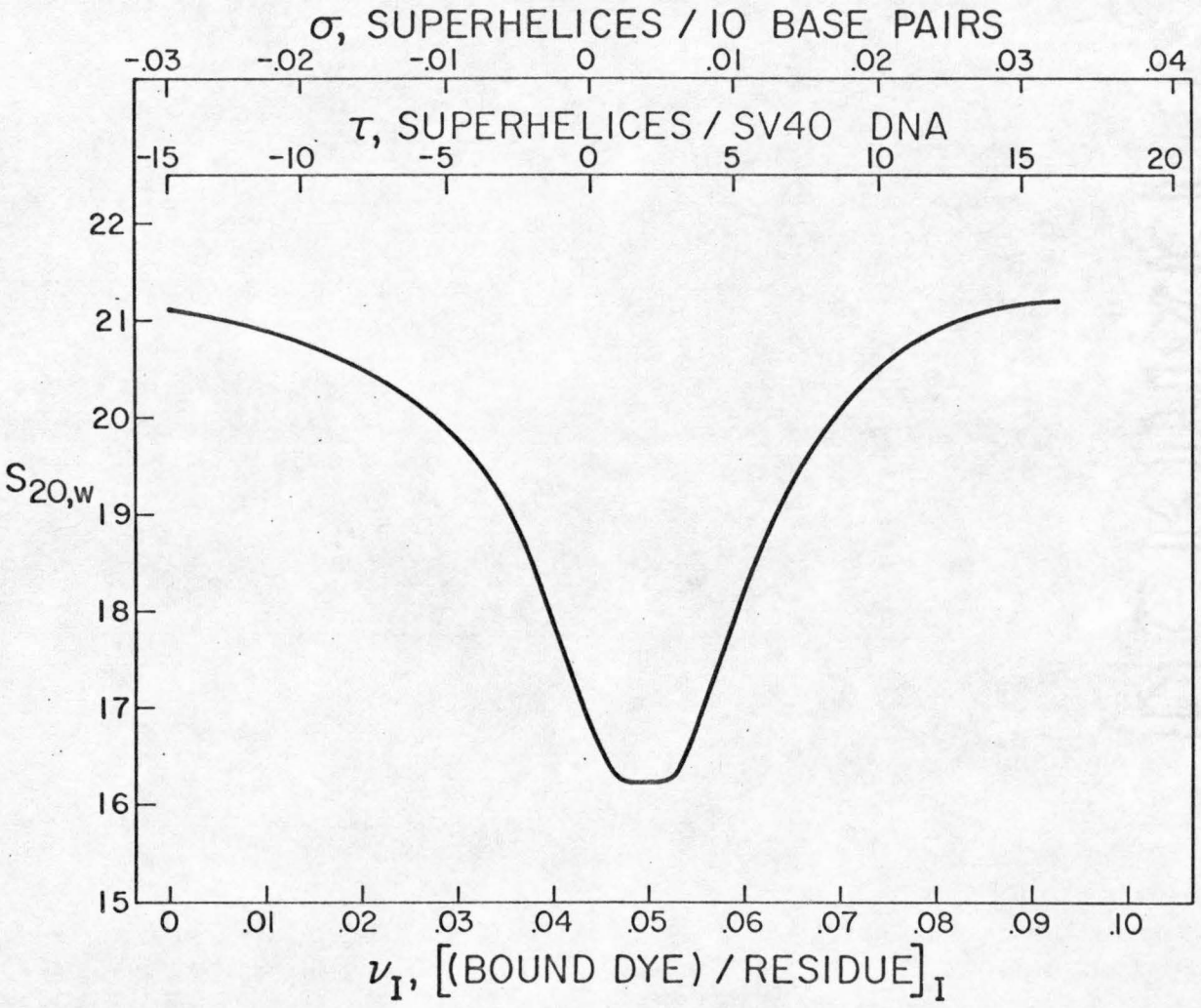
σ, SUPERHELICES / 10 BASE PAIRS
-.03
-.02
-.01
0
.01
.02
.03
.04
τ, SUPERHELICES / SV40 DNA
-15
-10
-5
0
5
10
15
20
22
21
20
19
18
17
16
15
S20,w
0
.01
.02
.03
.04
.05
.06
.07
.08
.09
.10
νI, [(BOUND DYE) / RESIDUE]I

mitochondrial DNA indicates that this closed circular DNA has a higher superhelix density than the viral DNA's, which have ratios of sedimentation coefficients, s_I/s_{II}, similar to that of SV 40 DNA.

Figure 16 was derived by combining the data read from the smoothed curves presented in Figs. 8 and 14a, c. Figure 8 contains the relationship between s_I and ν_{II} in 1 M NaCl, whereas Fig. 14b contains the relationship between ν_{II} and ν_I at a constant dye concentration in 5.4-5.6 M CsCl. In combining these relationships to obtain s_I as a function of ν_I, we have assumed that the free energy of superhelix formation is the same in both salt solutions. For this calculation it is not necessary to make any assumptions concerning the value of the intrinsic binding constant.

The curve for SV 40 DNA I in Fig. 16, together with the curve for SV 40 DNA II in Fig. 8, illustrates the sedimentation velocity behavior of these two forms of the molecule as a function of the amount of dye bound to each. The nicked form exhibits only a small decrease in sedimentation coefficient when ethidium chloride is bound. Lerman (1961) has suggested that the comparable behavior seen upon the addition of intercalating dyes, such as the aminoacridines, to linear DNA is due to an extension of the duplex helix. It should be pointed out, however, that changes in the sedimentation coefficient upon binding of dye may also arise from changes in the effective mass of the sedimenting species, from changes in the frictional coefficient per unit length and from changes in the stiffness of the molecule. The stiffness may be expected to affect the radius

of gyration of the coiled conformation of the molecule. It is because we expect that this latter factor may be large that we avoid normalizing the curve presented in Fig. 16 by the corresponding curve for s_{II} vs ν_{II} in Fig. 8.

We thank L. Wenzel and J. Edens for their assistance in the growth of the SV 40 virus and R. Kent for her assistance in the preparation of the manuscript. The research has been supported in part by Grants HE 03394 from the National Health Institute, CA 08014 from the National Cancer Institute, the United States Public Health Service, and by a fellowship from the National Science Foundation.

This is contribution 3561 from the Department of Chemistry of the California Institute of Technology.

APPENDIX I

Derivation of equation (6)

The sedimentation coefficient of the preferentially hydrated DNA-dye complex may be expressed in terms of the molecular weight, partial specific volume and translational frictional coefficient of the macromolecular complex by the well-known equation

$$s = M_s(1 - \bar{v}_s\rho) / Nf_s \quad . \tag{I-1}$$

The molecular weight and partial specific volume of the hydrated DNA-dye complex may be written with the assumption of additive volumes,

$$M_s = M_{3,h}(1 + \nu') \tag{I-2}$$

and

$$\bar{v}_s = \frac{\bar{v}_{3,h} + \nu' \bar{v}_{4,h}}{1 + \nu'} \quad , \tag{I-3}$$

where $M_{3,h}$ and $\bar{v}_{3,h}$ are the molecular weight and partial specific volume of the hydrated DNA in the absence of dye, $\bar{v}_{4,h}$ is the partial specific volume of the hydrated dye, and ν' is the grams hydrated dye per gram DNA.

Equation (I-1) may be rewritten

$$s = s_0 \frac{f_{s,0}}{f_s} (1 + K\nu) \tag{I-4}$$

where $f_{s,0}$ and s_0 are the translational frictional coefficient and sedimentation coefficient of the hydrated DNA in the absence of dye, and the constant

$$K = \left(\frac{1 - \bar{v}_{4,h}\rho}{1 - \bar{v}_{3,h}\rho}\right)\left(\frac{M_{3,h}}{M_{4,h}}\right) \quad .$$

The desired result is obtained from Eq. (1-4) written for components I and II,

$$\frac{s_I(\nu)}{s_{II}(\nu)} = \frac{f_{II,s}(\nu)}{f_{I,s}(\nu)} \quad \frac{(1 + K\nu_I)}{(1 + K\nu_{II})} \quad , \qquad \text{(I-5)}$$

where $\nu = \nu'(M_3/M_4)$.

APPENDIX II

The partial specific volume of ethidium chloride bound to DNA

The buoyant density of a complex formed by a macromolecule, water, and one additional small molecular weight species is given by Eq. (8)

$$\theta = \frac{1 + \Gamma' + \nu'}{\bar{v}_3 + \Gamma' \bar{v}_1 + \nu' \bar{v}_4} \quad . \tag{II-1}$$

In the system CsDNA, water, and ethidium chloride, Γ' is the preferential hydration of the DNA in grams water per gram DNA, ν' is the grams dye bound per gram DNA, and $\bar{v}_1$, $\bar{v}_3$, and $\bar{v}_4$ are the partial specific volumes of water, CsDNA, and bound ethidium chloride respectively.

If a mixture of SV 40 DNAs I and II is equilibrated with a solution of CsCl and ethidium chloride in the presence of a centrifugal field, the two components will in general form buoyant bands of DNA-dye complex at different positions in the analytical cell and with binding ratios at band center given by

$$\nu'_I = c_{bI}/p_I \tag{II-2a}$$

$$\nu'_{II} = c_{bII}/p_{II}, \tag{II-2b}$$

where c_b is the concentration of bound dye at band center in μg/ml, p

is the DNA nucleotide concentration at band center in μg/ml, and $p_t \equiv p_I + p_{II}$. Equation (II-1) may be written for each component separately and rearranged to give

$$p_i = \frac{c_{bi}(\theta_i \bar{v}_4 - 1)}{(b_i - a_i)}, \quad i = I, II \qquad \text{(II-3)}$$

where $a_i = \theta_i(\bar{v}_3 + \Gamma_i' \bar{v}_1)$ and $b_i = 1 + \Gamma_i'$.

Equation (II-3) may be written for each of the SV 40 DNA components I and II, with the further substitutions $g_i = c_{bi}/p_t$ and $h_i = a_i - b_i$, and the resulting equations added and solved for $\bar{v}_4$.

$$\bar{v}_4 = \frac{h_I h_{II} + g_I h_{II} + g_{II} h_I}{g_I h_I \theta_I + g_{II} h_{II} \theta_{II}} \qquad \text{(II-4)}$$

Equation (II-4) may be used to determine $\bar{v}_4$ for the bound ethidium chloride in an experiment in which the bound dye and DNA nucleotide concentrations are separately measured at band center.

The results of experiments to determine $\bar{v}_4$ with Eq. (II-4) are summarized in Table II. The concentrations c_{bI} and c_{bII} of dye bound to the two components at band center were measured at 521 mμ, the absorption maximum for bound dye, and converted to concentrations in μg/ml with the extinction coefficient of 106 μg/ml/OD obtained from the data of Le Pecq (1965). The buoyant densities, θ_I and θ_{II}, were obtained from the measured free dye concentrations at band center and from Fig. 12.

TABLE II

The determination of the partial specific volume of ethidium chloride bound to DNA

Initial dye c° (μg/ml)	Free dye[a] c_o (μg/ml)		Bound dye[a] c_b (μg/ml)		DNA[a] p_o (μg/ml)	
	I	II	I	II	I	II
30	24.70	34.79	5.80	4.54	31.09	103.7
40	34.73	51.62	7.39	6.29	34.52	112.9
90	39.02	61.54	11.81	11.77	73.40	240.5
50	40.33	65.54	7.36	5.67	38.06	119.3
60	50.14	81.81	7.68	8.34	34.82	113.1
70	57.85	94.05	7.48	7.19	35.17	108.9
110	71.15	116.6	15.09	16.15	67.34	208.4

continued ...

TABLE II continued

Preferential hydration[a,b] Γ' (g/g)		Buoyant density[c] θ (g/ml)		Partial specific volume $\bar{v}_4$ (ml/g)
I	II	I	II	
0.2812	0.2868	1.6357	1.6037	0.986
0.2827	0.2902	1.6762	1.5886	0.981
0.2833	0.2918	1.6227	1.5817	1.104
0.2835	0.2920	1.6218	1.5812	1.046
0.2845	0.2945	1.6156	1.5720	0.996
0.2852	0.2957	1.6124	1.5680	1.025
0.2859	0.2972	1.6082	1.5628	1.010
				$\bar{v}_4 = 1.02 \pm 0.03$(S.D.)

[a]Refers to band center

[b]Calculated with Eq. (11)

[c]Taken from Fig. 12

In order to estimate the total DNA concentration at band center, the photoelectric scanner was first calibrated at 265.4 mμ and at 280 mμ with known solutions of calf thymus DNA in the presence of CsCl of density 1.65 g/ml. Figure 5 shows these calibration curves. A least squares straight line was fitted to the data, with the result that

$$OD^{265.4} = 1.10\, A^{265.4}/\ell - 0.020 \qquad \text{(II-5a)}$$

$$OD^{280} = 1.068\, A^{280}/\ell - 0.015 \qquad \text{(II-5b)}$$

where ℓ is the cell thickness in cm and A is the absorbance.

Aliquots of the stock solution of SV 40 DNA, a mixture of I and II, were then assayed for total DNA concentration by measurement of the total mass in a buoyant band obtained from a known volume of the DNA stock. Knowledge of the total mass of DNA present in an analytical cell during an experiment in the presence of dye was assured by adding weighed aliquots of the stock DNA solution.

In order to estimate the DNA concentrations at band center in the presence of dye, it is assumed that the amount of dye bound per DNA phosphate, ν, changes only slightly over a band. This assumption is valid both at low dye concentrations, where the gradient of dye concentration is small, and at high dye concentrations, where the change of ν with c is small. The observed profile of bound dye concentration over a buoyant band is then proportional to the DNA concentration, with a proportionally constant given by

$$\lambda_i = m_i/\phi \Delta r \Sigma A_j r_j , \quad i = 1, II \qquad (II-6)$$

where m is the mass of DNA, ϕ the sector angle of 2.5°, Δr the radial increment used in the numerical integration, and A_j, the absorbance at the radial position r_j. The fraction of the total DNA mass present as SV 40 DNA I and II was estimated by a band sedimentation velocity experiment, and Eq. (II-6) was used to calculate

$$p_t = \lambda_I A_I + \lambda_{II} A_{II} . \qquad (II-7)$$

Since the weighting factors λ_I and λ_{II} are in general of comparable magnitude, error introduced by incorrect estimation of the distribution of the total DNA mass between I and II will affect the result only slightly.

Table II presents the results of several sets of experiments which were used with Eq. (II-4) and the other relationships developed in this Appendix to calculate values of $\bar{v}_4$. The final result is that $\bar{v}_4 = 1.02 \pm 0.03$. It is to be emphasized that this value of the partial specific volume of ethidium chloride refers to the bound dye, in which the molecule lies largely in a hydrophobic environment.

APPENDIX III

Preferential hydration of Cs DNA-dye complex as a function of solution density in concentrated CsCl solutions

The preferential hydration at band center of a DNA-dye complex at equilibrium in the ultracentrifuge is a function of the buoyant density of the DNA, and of the free dye concentration, the water activity, and the pressure at band center.

$$\Gamma'(\theta_0, C_{4,0}, A_{w,0}, P_0) = \Gamma_0'(\theta_0) + \Delta\Gamma'(C_{4,0}, A_{w,0}, P_0) \qquad \text{(III-1)}$$

In Eq. (III-1) Γ_0' and θ_0 are the buoyant density and preferential hydration of the DNA in the absence of dye. The subscript zero otherwise refers to band center. Differentiating Eq. (III-1),

$$d\Gamma' = \left(\frac{\partial \Gamma'}{\partial a_{w,0}}\right)_{c_{4,0},P_0} da_{w,0} + \left(\frac{\partial \Gamma'}{\partial P_0}\right)_{a_{w,0},c_{4,0}} dP_0 + \left(\frac{\partial \Gamma'}{\partial c_{4,0}}\right)_{a_{w,0},P_0} dc_{4,0} \qquad \text{(III-2)}$$

We assume that the binding of dye does not change the preferential hydration of the DNA at constant $a_{w,0}$ and P_0 and write

$$\frac{d\Gamma'}{d\theta} = \left(\frac{\partial \Gamma'}{\partial a_{w,0}}\right)_{P_0,c_{4,0}} \frac{da_{w,0}}{d\theta} + \left(\frac{\partial \Gamma'}{\partial P_0}\right)_{a_{w,0},c_{4,0}} \frac{dP_0}{d\theta} \; . \qquad \text{(III-3)}$$

The partial differential quantities of Eq. (III-3) may be expressed in terms of changes in the buoyant density. Differentiating Eq. (9) at

constant $c_{4,o}$, $\bar{v}_1$, $\bar{v}_3$, and $\bar{v}_4$ with respect to $a_{w,o}$ and P_o, we obtain

$$\left(\frac{\partial \Gamma'}{\partial a_{w,o}}\right)_{c_{4,o},P_o} = \frac{(\bar{v}_3 - \bar{v}_1)}{(\bar{v}_1\theta - 1)^2} \left(\frac{\partial \theta}{\partial a_{w,o}}\right)_{c_{4,o},P_o} \qquad \text{(III-4a)}$$

$$\left(\frac{\partial \Gamma'}{\partial P_o}\right)_{c_{4,o}\ a_{w,o}} = \frac{(\bar{v}_3 - \bar{v}_1)}{(v_1\theta - 1)^2} \cdot \left(\frac{\partial \theta}{\partial P_o}\right)_{c_{4,o}\ a_{w,o}}. \qquad \text{(III-4b)}$$

We assume that the changes in buoyant density with pressure and water activity are independent of dye concentration, and replace the partial derivatives in θ in Eq. (III-4) by the corresponding quantities in θ_o. The change in the net hydration with solution density at band center is obtained by combining Eqs. (III-3) and (III-4).

$$\frac{d\Gamma'}{d\theta} = \frac{(\bar{v}_3 - \bar{v}_1)}{(\bar{v}_1\theta - 1)^2} \left[\left(\frac{\partial \theta_o}{\partial a_{w,o}}\right)_{P_o} \frac{da_{w,o}}{d\theta} + \left(\frac{\partial \theta_o}{\partial P_o}\right)_{a_{w,o}} \frac{dP_o}{d\theta}\right]_{c_{4,o}=0} \qquad \text{(III-5)}$$

Upon integrating from θ_o to θ, we obtain the result

$$\Gamma' = \Gamma_o' + (\bar{v}_3 - \bar{v}_1) \int_{\theta}^{\theta_o} (\bar{v}_1\theta - 1)^{-2} \left[\left(\frac{\partial \theta_o}{\partial a_{w,o}}\right)_{P_o} \frac{da_{w,o}}{d\theta} + \left(\frac{\partial \theta_o}{\partial P_o}\right)_{a_{w,o}} \frac{dP_o}{d\theta}\right]_{c_{4,o}=0} d\theta \qquad \text{(III-6)}$$

The constant Γ_0' was calculated for SV 40 DNA in CsCl from the equation

$$\theta_0 = \frac{1 + \Gamma_0'}{\bar{v}_3 + \Gamma_0' \bar{v}_1} \quad . \qquad \text{(III-7)}$$

In this equation $\bar{v}_3$ was taken to be 0.47_9 ml/g for Cs DNA (Hearst, 1962), and $\bar{v}_1$ was estimated to be unity. The measured value of $\theta_0 = 1.693_7$ g/ml for SV 40 DNA I and II then allows the calculation of $\Gamma_0' = 0.272$ g H_2O/g Cs DNA.

In order to evaluate the integral in Eq. (III-6) it is necessary to estimate the partial and total differentials which appear in the integral as a function of solution density at band center. The partial differential $(\partial\theta_0/\partial a_{w,o})_{P_0}$ and the total differential $da_{w,o}/d\theta$ were determined over the density range 1.3 - 1.8 by a least square polynomial fit to the data given by Hearst & Vinograd (1961).

Let

$$\delta = \theta - 1.3 \quad , \qquad \text{(III-8a)}$$

and

$$\alpha = a_{w,0} - 0.69 \quad . \qquad \text{(III-8b)}$$

The results may be expressed by the polynomials

$$\alpha = 0.23653043 - 0.4124158\delta + 0.1315234\delta^2 - 0.3329120\delta^3 + 0.1278416\delta^4 \qquad \text{(III-9)}$$

$$(\partial\theta_0/\partial a_{w,o})_{P_0} = 0.19608976 - 40.114488\alpha + 678.9384\alpha^2 - 4228.361\alpha^3 + 7652.710\alpha^4 \qquad \text{(III-10)}$$

and

$$\frac{da_{w,o}}{d\theta} = -0.41241587 + 0.26304692\delta - 0.99873624\delta^2 + 0.51136676\delta^3 \qquad \text{(III-11)}$$

The only available measurement of the effect of pressure on buoyant density has been made by Hearst, Ifft & Vinograd (1961) on T_4 DNA in CsCl. We use their value and assume that changes in the pressure dependence of buoyant density with solution density are neglibile.

$$\left(\frac{\partial \theta_o}{\partial P_o}\right)_{a_{w,o}} = -3.91 \times 10^{-11} \text{ cgs} \qquad \text{(III-12)}$$

The pressure dependence of solution density at band center is given by

$$\frac{dP_o}{d\theta} = \rho\beta(\rho) \qquad \text{(III-13)}$$

where $\beta(\rho)$ is defined by Ifft, Voet & Vinograd (1961) as

$$\beta(\rho) = \frac{d\ell n a_{w,o}}{d\rho} \quad \frac{RT}{(1 - \bar{v}_2\rho)M_2} \qquad \text{(III-14)}$$

where M_2 and $\bar{v}_2$ are the molecular weight and partial specific volume of CsCl. This quantity was re-evaluated with a least squares polynomial fit to the data of Ifft, Voet & Vinograd (1961) and is given by

$$\beta(\rho) \times 10^9 = 1.5514549 - 2.91017170 + 10.9669106\delta^2$$
$$- 29.1101148\delta^3 + 52.6071334\delta^4$$
$$- 49.8646536\delta^5 + 18.3008697\delta^6 \qquad \text{(III-15)}$$

The Eqs. (III-9) - (III-13) and (III-15) were combined with (III-6) to evaluate Γ' and ν' as a function of buoyant density. The integration was performed with an IBM 7040-7094 computer using Simpson's rule. The results of the integration of Eq. (III-6) over the density range 1.50 - 1.73, for a DNA of $\theta_0 = 1.6$, were fitted to a least squares quadratic polynomial in the quantity $\eta = \theta - 1.50$.

$$\Delta\Gamma' = 0.2974 - 0.7282\eta + 4.592\eta^2 - 16.08\eta^3 + 20.56\eta^4. \qquad \text{(III-16)}$$

Figure 17 shows the results of the polynomial fit. Equation (III-16) or Fig. 17 may be used to calculate Γ' for any DNA over the density range chosen, as explained in the legend to Fig. 17.

FIG. 17. The preferential hydration of a CsDNA-dye complex as a function of the CsCl concentration, as indicated by the measured buoyant density. The calculations are based on solutions of Eq. (III-6) for a DNA with $\theta_0 = 1.6$, and the line is the best least squares quadratic polynomial fit as given by Eq. (III-16). For a DNA with any other initial buoyant density, θ_0, the curve will be shifted vertically by an amount corresponding to the difference in the amount of preferential solvation in the absence of dye, Γ_0'. The net shift in preferential hydration for another DNA is $\Delta\Gamma'(\theta) - \Delta\Gamma'(\theta_0)$, where $\Delta\Gamma'(\theta)$ is the value of $\Delta\Gamma'$ read from this plot at θ, and $\Delta\Gamma'(\theta_0)$ is the corresponding quantity at $\theta = \theta_0$.

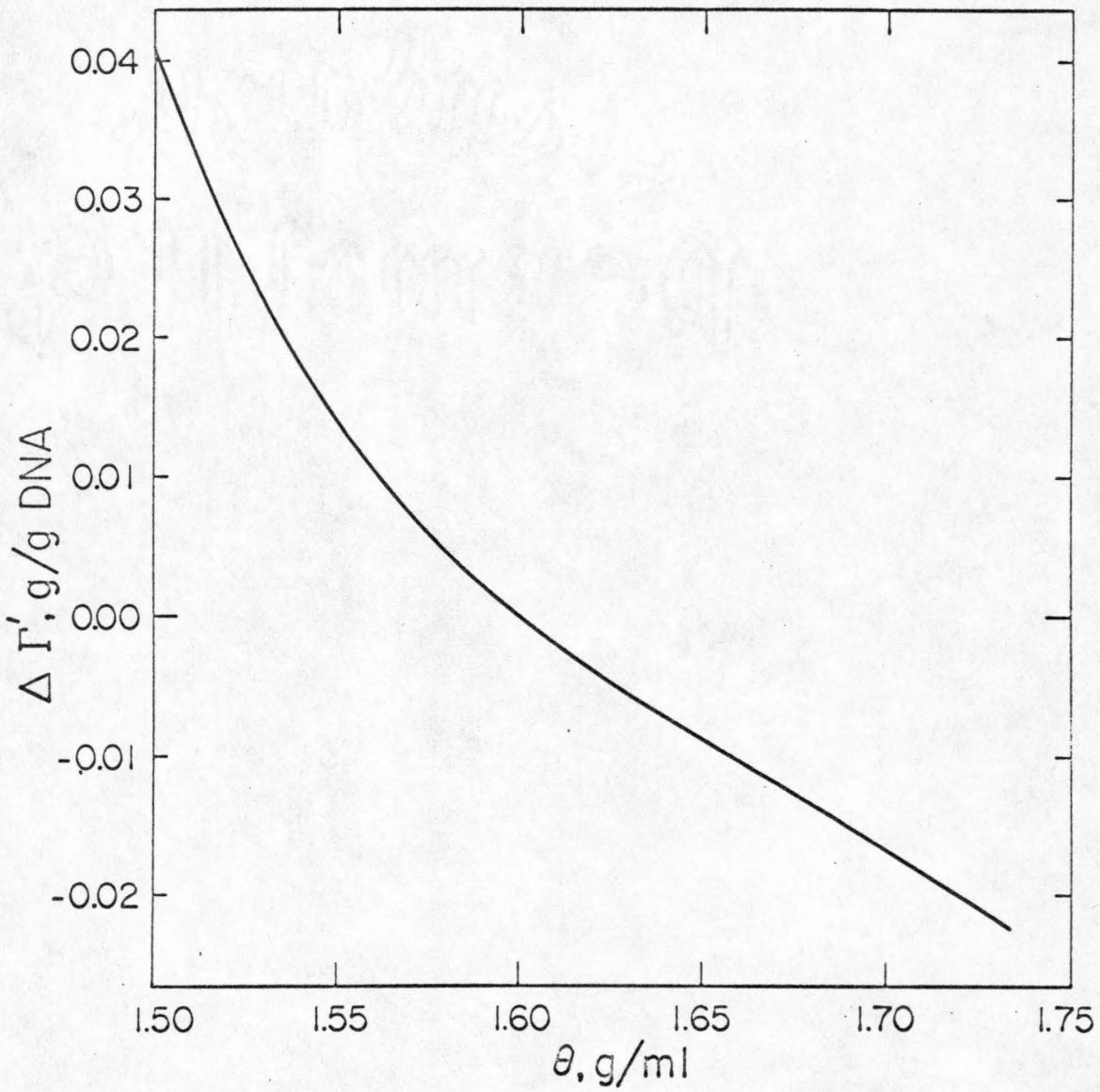
0.04
0.03
0.02
0.01
0.00
-0.01
-0.02
Δ Γ', g/g DNA
1.50
1.55
1.60
1.65
1.70
1.75
θ, g/ml

REFERENCES

Bauer, W. R. & Vinograd, J. (1967ab). Manuscripts in preparation.

Bloomfield, V. A. (1966). Proc. Nat. Acad. Sci., 55, 717.

Bode, V. C. & Kaiser, A. D. (1965). J. Mol. Biol., 14, 399.

Borst, P. & Ruttenburg, G. J. C. M. (1966). Biochim. biophys. Acta, 114, 645.

Clayton, D. A. & Vinograd, J. (1967). Unpublished.

Crawford, L. V. (1964). J. Mol. Biol., 8, 489.

Crawford, L. V. (1965). J. Mol. Biol., 13, 362.

Crawford, L. V. & Black, P. H. (1964). Virology, 24, 388.

Crawford, L. V. & Waring, M. J. (1967). J. Mol. Biol., 25, 23.

Davidson, N. D., Widholm, J. M., Nandi, U. S., Jensen, R. H., Olivera, B. M. & Wang, J. C. (1965). Proc. Nat. Acad. Sci., 53, 111.

Dulbecco, R. & Vogt, M. (1963). Proc. Nat. Acad. Sci., 50, 236.

Fuller, W. & Waring, M. J. (1964). Berichte der Bunsengesellschaft, 68, 805.

Glaubiger, D. & Hearst, J. E. (1967). Biopolymers, in press.

Gray, H. B. (1967). Biopolymers, in press.

Hearst, J. E. (1962), J. Mol. Biol., 4, 415.

Hearst, J. E., Ifft, J. B. & Vinograd, J. (1961). Proc. Nat. Acad. Sci., 47, 1015.

Hearst, J. E. & Stockmayer, W. H. (1962). J. Chem. Phys., 37, 1425.

Hearst, J. E. & Vinograd, J. (1961). Proc. Nat. Acad. Sci., 47, 1005.

Ifft, J. B., Voet, D. E. & Vinograd, J. (1961). J. Phys. Chem., 65, 1138.

Kirkwood, J. (1954). J. Polymer Sci., 12, 1.

Kirsten, W., Kirsten, H. & Szybalski, W. (1966). Biochemistry, 5, 236.

Kleinschmidt, A. K., Burton, A. & Sinsheimer, R. L. (1963). Science, 142, 1961.

Kroon, A. M., Borst, P., Van Bruggen, E. F. J. & Ruttenburg, G. J. C. M. (1966). Proc. Nat. Acad. Sci., 56, 1836.

Kurata, M. (1966). Bull. Inst. Chem. Rois. Kyoto, 44, 150.

Le Pecq, J.-B. (1965). Thesis, Faculté des Sciences, Paris.

Le Pecq, J.-B. & Paoletti, C. (1967). J. Mol. Biol., 27, 87.

Lerman, L. S. (1961). J. Mol. Biol., 3, 18.

Lerman, L. S. (1964). J. Cell. Comp. Physiol., 64: Sup. 1, 1.

Neville, D. M. & Davies, D. R. (1966). J. Mol. Biol., 17, 57.

Pikó, L., Tyler, A. & Vinograd, J. (1967). Biol. Bull., 132, 68.

Play, D. S., Preuss, A. & Hofschneider, P. H. (1966). J. Mol. Biol., 21, 485.

Radloff, R., Bauer, W. R. & Vinograd, J. (1967). Proc. Nat. Acad. Sci., 57, 1514.

Rhoades, M. & Thomas, C. A. (1967). Private communication.

Roth, T. & Helinski, D. (1967). Proc. Nat. Acad. Sci., in press.

Scatchard, G. (1949). Ann. N.Y. Acad. Sci., 51, 660.

Stone, H. (1962). J. Optical Soc. Am., 52, 998.

Vinograd, J., Bruner, R., Kent, R. & Weigel, J. (1963). Proc. Nat. Acad. Sci., 49, 902.

Vinograd, J. & Hearst, J. E. (1962). In Fortschritte der Chemie Organischer Naturstoffe, ed. L. Zechmeister, vol. XX, p. 372. Vienna: Springer-Verlag.

Vinograd, J. & Lebowitz, J. (1966). J. Gen. Physiol., 49, 103, and Macromolecular Metabolism, p. 103. Boston: Little, Brown & Co.

Vinograd, J., Lebowitz, J., Radloff, R. & Laipis, P. (1965). Proc. Nat. Acad. Sci., 53, 1104.

Vinograd, J., Lebowitz, J. & Watson, R. (1967). J. Mol. Biol., in press.

Waring, M. J. (1965). J. Mol. Biol., 13, 269.

Weil, R. & Vinograd, J. (1963). Proc. Nat. Acad. Sci., 50, 730.

Yew, F. F. & Davidson, N. D., private communication.

Young, E. T., II & Sinsheimer, R. L. (1964). J. Mol. Biol., 10, 562.

CHAPTER II

The Interaction of Closed Circular DNA with Intercalative Dyes. II. The Free Energy of Superhelix Formation in SV 40 DNA

1. Introduction

The binding of intercalating dyes to closed circular DNA may be used to change the superhelix density of the DNA by known amounts. The relation between σ, the number of superhelical turns per ten base pairs, and ν, the moles dye bound per mole nucleotide residue, was shown in Part I of this series (Bauer and Vinograd, 1967) to be given by the equation

$$\sigma = \sigma_0 + \left(\frac{\phi}{18}\right) \nu \, . \qquad (1)$$

In this equation ϕ represents the angle of unwinding of the duplex upon the intercalation of each dye molecule and σ_0 the superhelix density in the absence of dye.

The binding isotherms in concentrated CsCl solutions for the binding of the dye ethidium bromide to closed circular (I) and nicked circular (II) SV 40 DNA have been determined by a buoyant density method, as described in Part I. Fuller and Waring (1964) have estimated by an examination of molecular models that the angle of unwinding, ϕ, is equal to 12° for the intercalation of ethidium bromide into duplex DNA. With the use of this value, equation (1) becomes

$$\sigma = \sigma_0 + 0.67 \, \nu \, . \qquad (2)$$

The number of superhelical turns, τ, in SV 40 DNA, which contains 4800 base pairs (Crawford and Black, 1964), is given by the expression

$$\tau = \tau_0 + 320\ \nu\ , \qquad (3)$$

where τ_0 is equal to the number of superhelical turns present in native SV 40 DNA I in the absence of dye.

The binding isotherms given in Fig. 14 of Part I also describe the dependence of the number of superhelical turns in SV 40 DNA I upon the free dye concentration. The quantities τ and ν are linearly related, as is shown in equation (3). The affinity of I for dye depends upon both the number and the sign of the superhelical turns present in the molecule. At dye concentrations below 5.4 μg/ml, τ is negative and the affinity of I for dye is greater than that of II. At the critical dye concentration of 5.4 μg/ml, SV 40 DNA's I and II have the same affinity for ethidium bromide, and all superhelical turns have been removed from I. It was calculated that $\tau_0 = -12.7 \pm 1.5$ superhelical turns, based upon the measured value of ν_c, the amount of dye bound per nucleotide at the critical point. At higher dye concentrations τ becomes positive and the dye binding affinity of SV 40 DNA I is lower than that of SV 40 DNA II.

These results are interpreted to mean that the introduction of superhelical turns into the closed circular duplex is accompanied by a positive free energy change which lowers the net chemical free energy available for the binding of dye at a given dye concentration and results in a net reduction of the binding affinity. The binding of the intercalating dye to the native SV 40 DNA I molecule may take place only with a concomitant reduction in the absolute value of the

number of superhelical turns. In this event the removal of superhelical turns introduces a negative free energy contribution to the binding reaction and the affinity for dye is increased. The free energy of formation of superhelical turns in the closed circular DNA may be accounted for by an enthalpic term associated with the bending of the duplex and by an entropic term associated with the more highly ordered conformation of the superhelical molecule.

It is shown in the present paper that the binding data for SV 40 DNA II in the region below $\nu = 0.18$ can be satisfactorily represented by the relationship derived by Scatchard (1949) for the independent binding of small molecules to one class of sites on a polymer. The binding data for SV 40 DNA I can be represented by a similar relation modified to include a perturbation due to the free energy of superhelix formation. The free energy is calculated as a function of the number of superhelical turns over the range $\tau = -13$ to $\tau = +45$. The free energy of superhelix formation of the native molecule in the absence of dye is calculated to be 100 kcal per mole of DNA or 21 cal per mole base pair. The free energy per superhelical turn is calculated to be 7.7 kcal per mole DNA.

If it is assumed that the enthalpy of superhelix formation is approximately equal to the free energy, the superhelix pitch of the native molecule may be estimated with the value of the Young's modulus for duplex DNA estimated by J. J. Hermans from data obtained by Cohen and Eisenberg (1966). We calculate that for native

SV 40 DNA I in the absence of dye the superhelix pitch is 430 Å and the superhelix radius is 135 Å.

2. Results

a. Calculation of the Free Energy of Superhelix Formation

The binding of a small molecule to a polymer may be represented by a linear equation (Scatchard, 1949) containing the intrinsic association constant, k, and the maximum available number of sites per residue, ν_m, provided that the binding does not show cooperativity and that the binding sites are equivalent and independent.

$$\frac{\nu}{c} = k\nu_m - k\nu \; . \qquad (4)$$

In equation (4), c is the free dye concentration at a given value of ν, the moles of reagent bound per mole of binding site.

In Part I of this series the binding of ethidium bromide to SV 40 DNA I and II was determined by measuring the buoyant density decrease which results from dye binding. The binding isotherms have been plotted according to equation (4) for SV 40 DNA II in Fig. 1. The straight line represents the best least squares fit through the points below $\nu = 0.20$. Primary or intercalative binding with a maximum site ratio of $\nu_m = 0.20$ is clearly indicated. Some secondary binding is also apparent to a value of $\nu = 0.22$ as measured by the buoyant density method. The method is comparable to equilibrium dialysis and does not depend upon the detailed electronic interactions

Figure 1

The quotient ν/c plotted as a function of the binding ratio, ν, in moles/moles nucleotide for the binding of ethidium bromide to SV 40 DNA II in 5.8 M CsCl. The free dye concentration, c, is expressed in moles/liter. The experimental data were obtained as described in Part I (Bauer and Vinograd, 1967), and the solid line represents a least squares linear fit to the data points. The solid circles represent values which probably include significant amounts of secondary binding, and these were not included in the curve fitting.

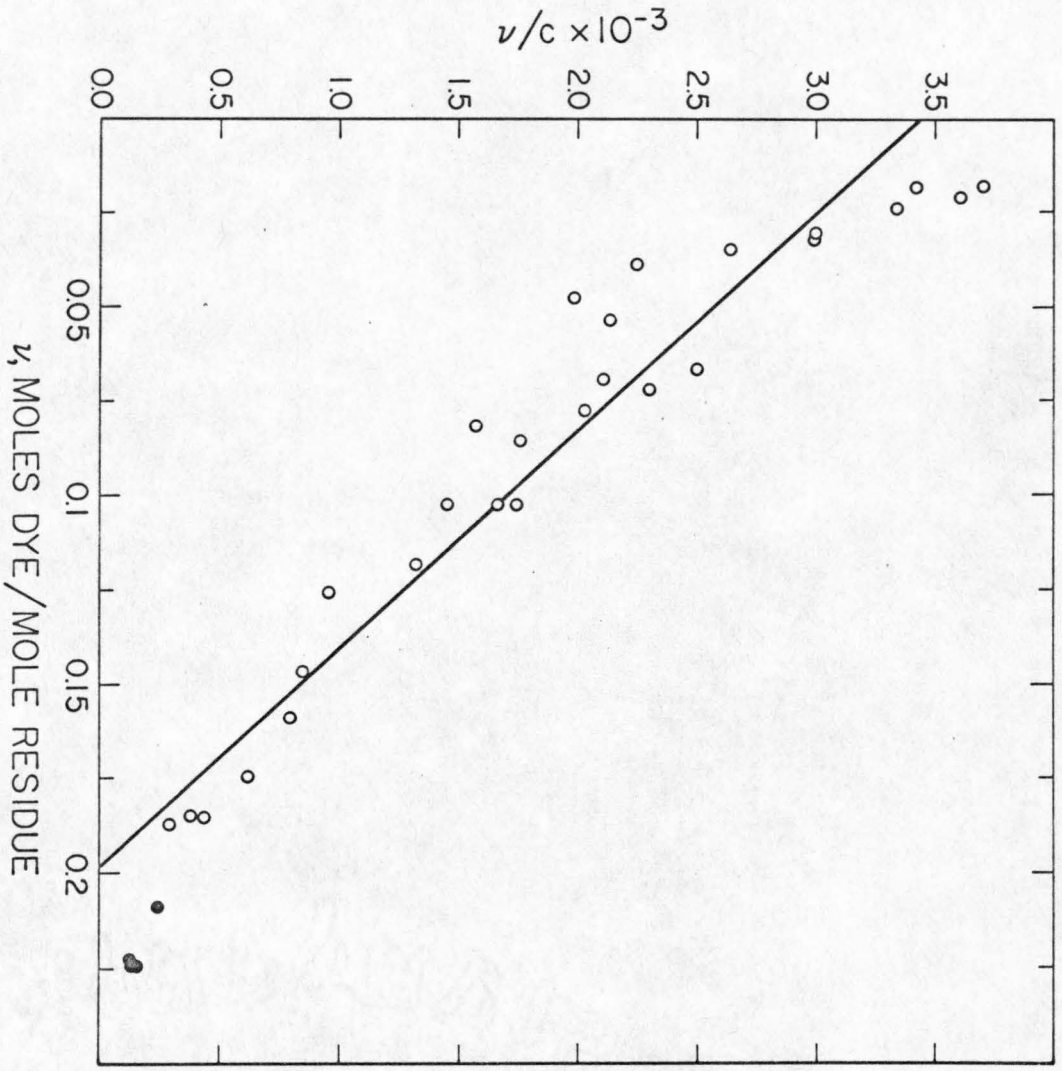
$\nu/c \times 10^{-3}$
0.0
0.5
1.0
1.5
2.0
2.5
3.0
3.5
0.05
0.1
0.15
0.2
ν, MOLES DYE/MOLE RESIDUE

which characterize spectroscopic methods.

Figure 2 presents the results of a Scatchard plot for the binding of ethidium bromide to SV 40 DNA I. The binding to the closed circular molecule shows marked deviation from linearity over the entire isotherm, as well as an apparent reduction in the maximum number of available sites. Since the linear binding behavior of this dye to SV 40 DNA II indicates that the binding is not intrinsically cooperative, the non-linear binding curve to SV 40 DNA I suggests that the binding affinity of the sites in the closed circular molecule depends upon the binding ratio, ν. This alteration in the binding affinity with increasing ν may be expressed in terms of a change in the net free energy of the binding reaction, in a manner similar to that proposed by Scatchard (1949) for the titration of ovalbumin.

The reaction of ethidium bromide (E) and DNA (P_0) to form the complex (PE_y) may be written

$$P_0 + yE \rightleftharpoons PE_y \,, \tag{5}$$

where y is the number of dye molecules bound per DNA molecule. If we assume equal initial reaction probabilities at each of y_m reaction sites, the net free energy for the reaction is

$$\frac{\Delta G_y}{RT} = \ell n \left[\frac{c_y}{(P_0)c^y} \right] + \ell n \left[\frac{y!(y_m - y)!}{y_m!} \right] - y\ell nk + U(y) \tag{6}$$

where $y = p_0 \nu$, $y_m = p_0 \nu_m$ and p_0 is the number of nucleotides per DNA molecule. In the case of SV 40 DNA, $\nu_m = 0.2$, $p_0 = 9600$ and $y_m = 1920$. The quantity U(y) represents the dimensionless free energy

Figure 2

The quotient ν/c plotted as a function of ν for the binding of ethidium bromide to SV 40 DNA I in 5.8 M CsCl. The data points were obtained as described in Part I.

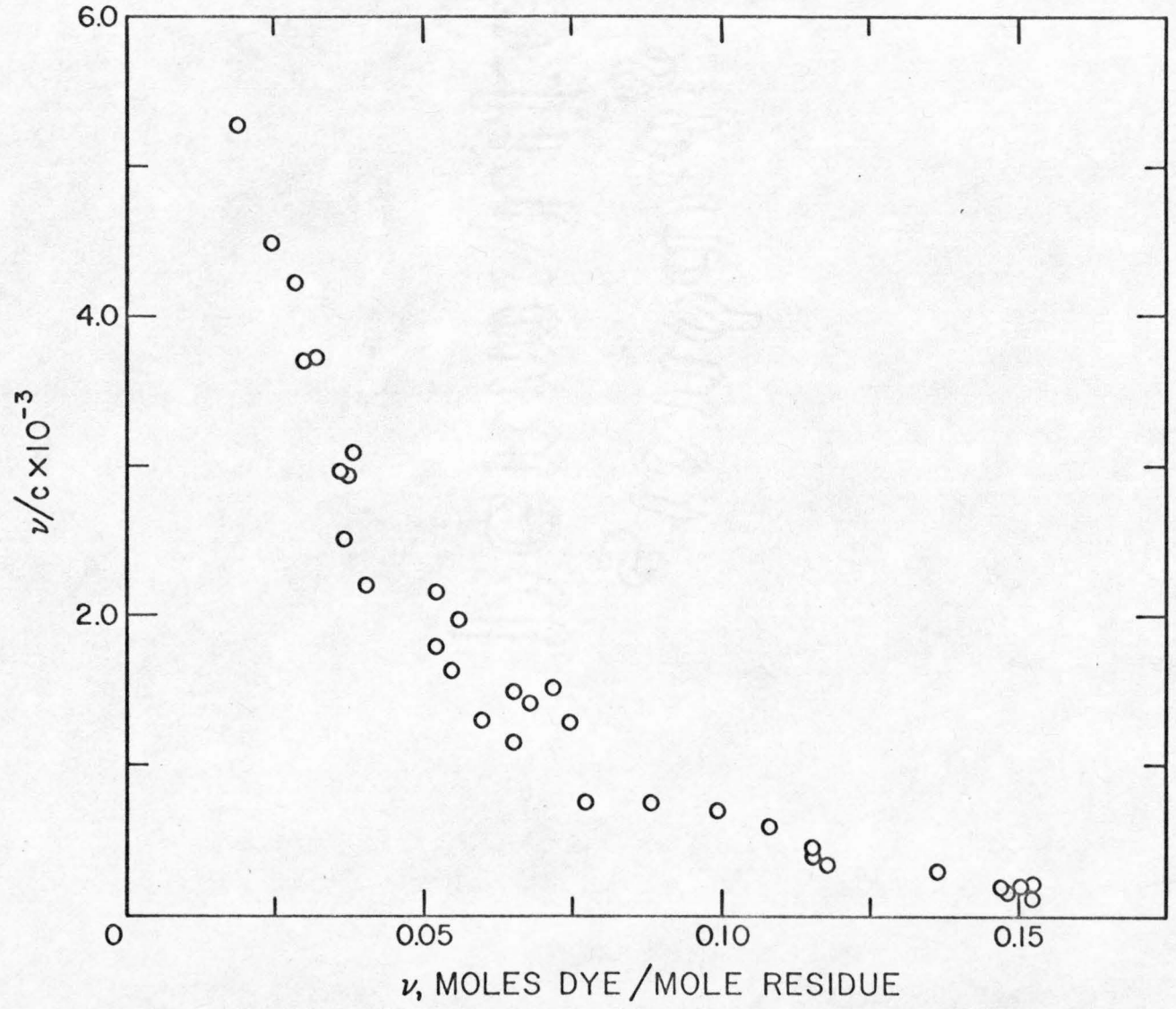
6.0
4.0
2.0
0
0.05
0.10
0.15
$\nu/c \times 10^{-3}$
ν, MOLES DYE / MOLE RESIDUE

term associated with the superhelical turns as specified below, and U(y) = 0 in the case of SV 40 DNA II. The average association, $\bar{y}$, may be shown (Scatchard, 1949; Katchalsky and Gillis, 1949) to be given by

$$\bar{y} = \frac{\sum_{y=0}^{y_m} \frac{y_m!}{y!(y_m - y)!} (kc)^y e^{-U(y)} y}{\sum_{y=0}^{y_m} \frac{y_m!}{y!(y_m - y)!} (kc)^y e^{-U(y)}} . \qquad (7)$$

For the case U(y) = 0, equation (7) may be shown (Scatchard, 1949) to lead to the relationship for binding to independent sites, equation (4).

For SV 40 DNA I, the ratio between c_y and c_{y-1} may be obtained from equation (6), by setting $\Delta G_y = \Delta G_{y-1} = 0$ at equilibrium.

$$\frac{c_y}{c_{y-1}} = \frac{y_m + 1 - y}{y} kc \exp\left\{ - \left[U(y) - U(y-1) \right] \right\} \qquad (8)$$

The sums in both the numerator and denominator of equation (7) have a pronounced maximum at the same value of y (Katchalsky and Spitnik, 1947), and it can be shown that the existence of this common maximum is unaffected by U(y) for a system with a large value of y_m (Scatchard, 1949). The maximum is determined by equating the quantities c_y and c_{y-1}. From equation (8) and the observation that $y_m \gg 1$,

$$kc = \frac{\bar{y}}{y_m - \bar{y}} \exp \left[\langle U(y) - U(y-1) \rangle \right] , \qquad (9)$$

where $\langle U(y) - U(y-1) \rangle$ is the average increase in superhelix energy upon the addition of one dye molecule at the maximum, $y = \bar{y}$. This is the general form of the binding equation which is appropriate for the present use.

The net free energy of the reaction for the binding of ethidium to SV 40 DNA I, may be written as a Taylor series in the number of superhelical turns, τ. The quantity τ is proportional to $\bar{y} - \bar{y}_0$, where $\bar{y}_0$ is the number of moles dye bound per mole DNA when the number of superhelical turns $\tau = 0$.

$$U(\bar{y}) = \sum_{i=0}^{\infty} w_i (\bar{y} - \bar{y}_0)^i \qquad (10)$$

It was shown in Part I (Bauer and Vinograd, 1967) that $\bar{y}_0 = 380$ for SV 40 DNA I.

The first two terms in equation (10), for i=0 and i=1, must be equal to zero because of the boundary conditions $U(\bar{y} = \bar{y}_0) = 0$ and $U(\bar{y} \neq \bar{y}_0) > 0$. In order to estimate the free energy of superhelix formation, the next two higher terms of the series are selected and the energy function is assigned the form

$$U(\bar{y}) = w_2 (\bar{y} - \bar{y}_0)^2 + w_3 (\bar{y} - \bar{y}_0)^3 \qquad (11a)$$

$$U(\bar{y} - 1) = w_2 (\bar{y} - \bar{y}_0 - 1)^2 + w_3 (\bar{y} - \bar{y}_0 - 1)^3 . \qquad (11b)$$

Equation (9) can now be written

$$kc = \frac{\bar{y}}{y_m - \bar{y}} \exp\left\{\left[2w_2\left(\frac{y_m + 1}{y_m}\right) - 3w_3\left(\frac{y_m + 1}{y_m}\right)\right](\bar{y} - \bar{y}_0)\right.$$

$$\left. + \left[3w_3\left(\frac{y_m + 1}{y_m}\right)^2 (\bar{y} - \bar{y}_0)^2\right]\right\} \exp(w_3 - w_2) \qquad (12)$$

or

$$k'c = \frac{\bar{y}}{y_m - \bar{y}} \exp\left[\frac{a}{p_0}(\bar{y} - \bar{y}_0) + \frac{b}{p_0^2}(\bar{y} - \bar{y}_0)^2\right] \qquad (13)$$

where the apparent binding constant, k′, is defined as

$$k' = k \exp(w_2 - w_3). \qquad (14a)$$

The coefficients a and b are related to w_2 and w_3 by

$$w_2 = \frac{1}{2p_0}\left(\frac{y_m}{y_m + 1}\right)\left[a + \frac{b}{p_0}\left(\frac{y_m}{y_m + 1}\right)\right] \qquad (14b)$$

and

$$w_3 = \frac{b}{3p_0^2}\left(\frac{y_m}{y_m + 1}\right)^2 . \qquad (14c)$$

Two independent methods were employed to estimate the coefficients a and b in equation (13). In the logarithmic expansion method, equation (13) is rewritten in the form

$$\ell n(\bar{y}/c) = \ell n\, k' + \ell n(y_m - \bar{y}_0) + \ell n\left(1 - \frac{\bar{y} - \bar{y}_0}{y_m - \bar{y}_0}\right) - \frac{a}{p_0}(\bar{y} - \bar{y}_0)$$

$$- \frac{b}{p_0^2}(\bar{y} - \bar{y}_0)^2 \qquad (15)$$

and the approximation is made that

$$\ell n\left\{1 - \left(\frac{\bar{y} - \bar{y}_0}{y_m - \bar{y}_0}\right)\right\} = -\left(\frac{\bar{y} - \bar{y}_0}{y_m - \bar{y}_0}\right) - \frac{1}{2}\left(\frac{\bar{y} - \bar{y}_0}{y_m - \bar{y}_0}\right)^2 - \frac{1}{3}\left(\frac{\bar{y} - \bar{y}_0}{y_m - \bar{y}_0}\right)^3 - \cdots (16)$$

Equation (15) may then be written in the form

$$\ell n(\bar{y}/c) = \sum_{i=0}^{\infty} \alpha_i (y - y_0)^i , \qquad (17)$$

where the first three coefficients are given by

$$\alpha_0 = \ell n\, k' + \ell n(y_m - \bar{y}_0) \qquad (18a)$$

$$-\alpha_1 = \frac{a}{p_0} + (y_m - \bar{y}_0)^{-1} \qquad (18b)$$

$$-\alpha_2 = \frac{b}{p_0^2} + \tfrac{1}{2}(y_m - \bar{y}_0)^{-2} \qquad (18c)$$

The values of the three coefficients α_0, α, and α_2 were calculated by a least squares quadratic fit to a plot of $\ell n(\bar{y}/c)$ versus $(\bar{y} - \bar{y}_0)$. The results of this fit are shown in Fig. 3(a) for SV 40 DNA I and, as a check on the method, for SV 40 DNA II in Fig. 3(b). The coefficients for both components are listed in Table I, as well as the coefficients w_2 and w_3 for the free energy, equation (10), and the calculated value of the intrinsic binding constant, k. For this calculation it was assumed that $y_m = 1960$ for SV40 DNA I. The second method, described below, does not require that this value be assumed in advance.

In the second method of estimation of the free energy

Figure 3

The logarithmic method for the determination of the free energy coefficients, a and b. The logarithm of the ratio $\bar{y}/c$ is plotted as a function of $\bar{y} - \bar{y}_0$ for (a) SV 40 DNA I and (b) SV 40 DNA II. The solid line represents the best least squares quadratic polynomial fit to the data points. The quantity $\bar{y}$ is the average binding ratio in moles ethidium per mole CsDNA, and $\bar{y}_0$ is the value of the binding ratio at $\tau = 0$.

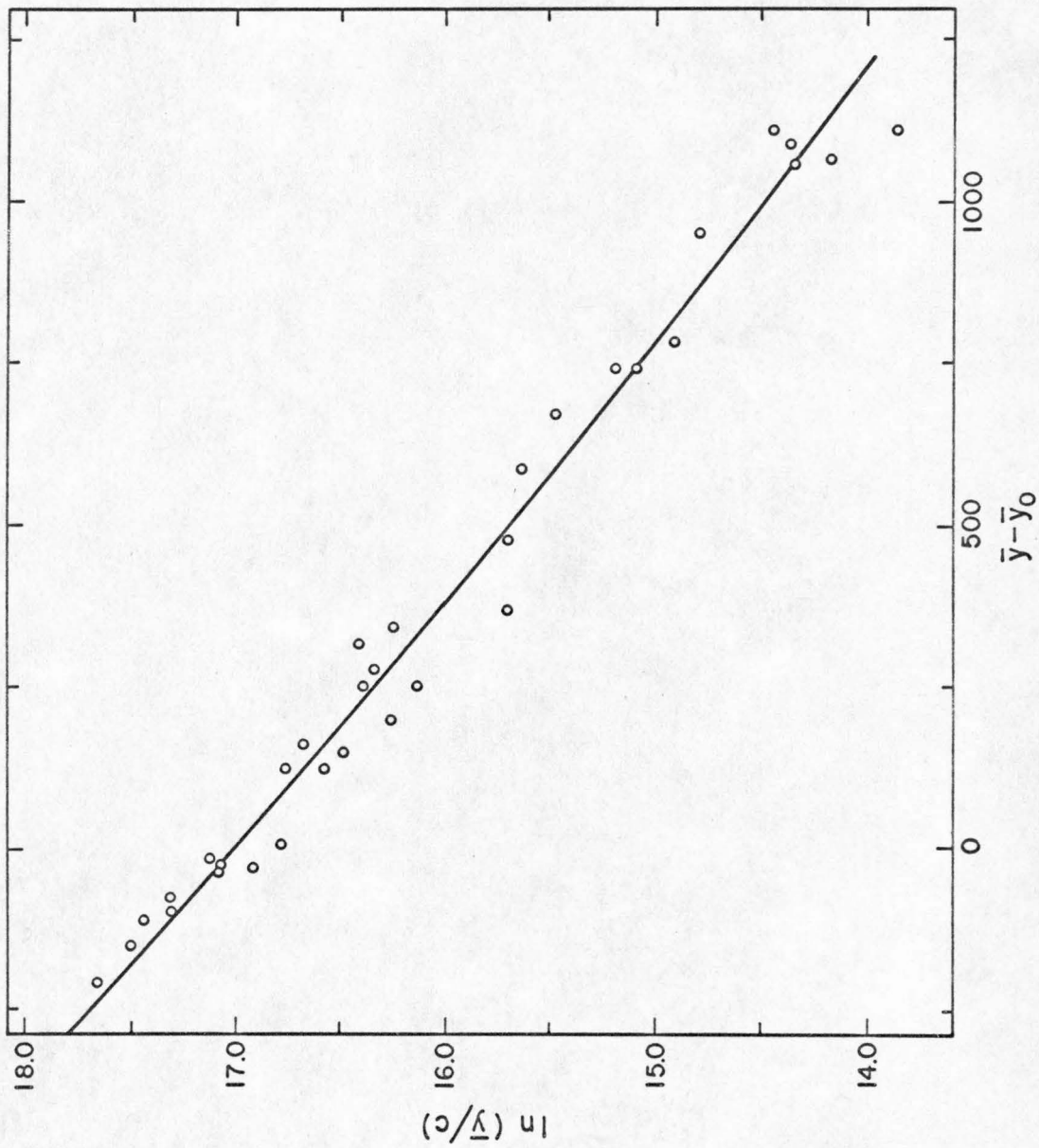

D

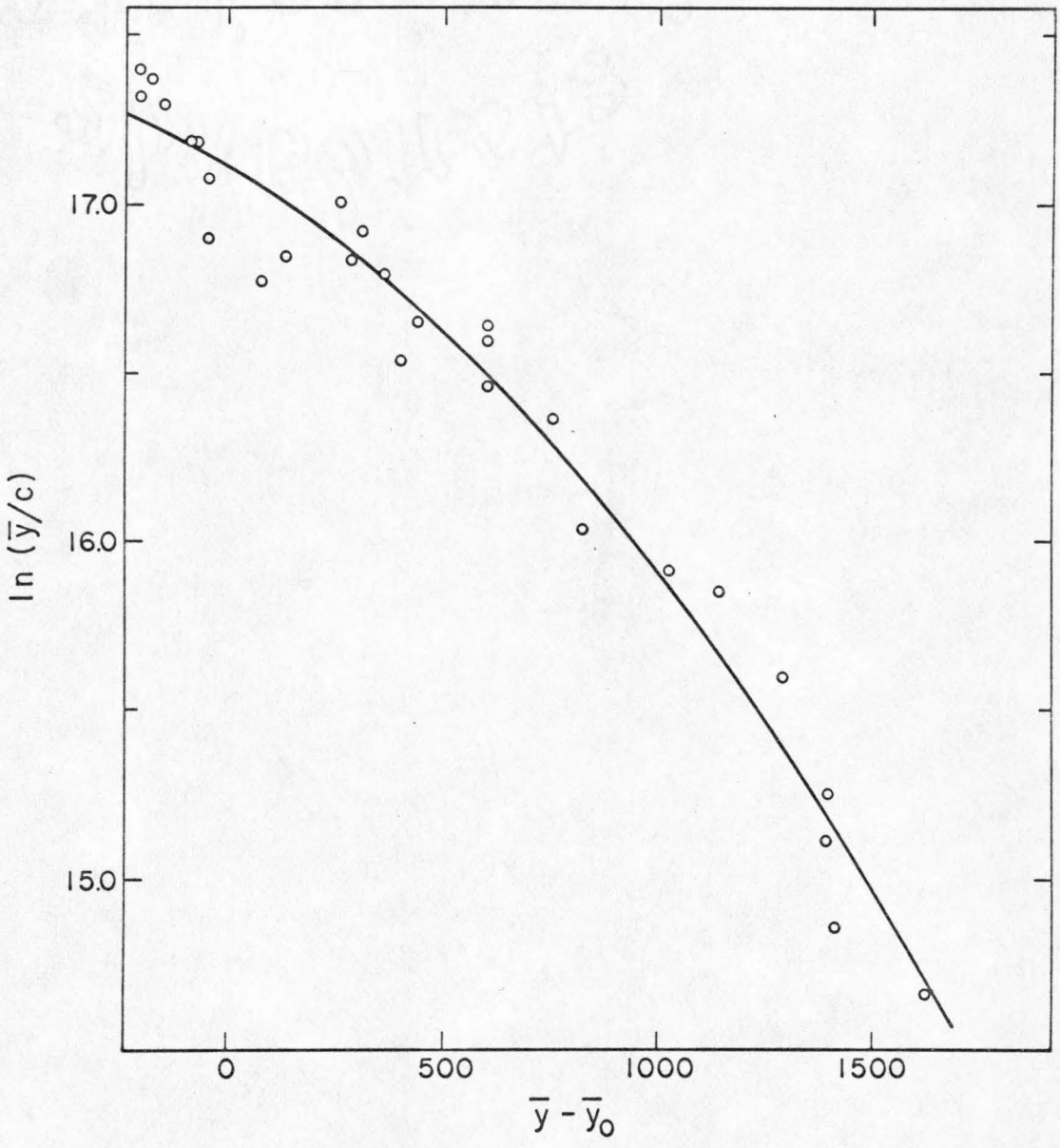

b

TABLE I

Calculated Free Energy Coefficients

Coefficient	Logarithmic method		Trial-and-error method, DNA I
	DNA I	DNA II	
α_0	17.0889	17.0962	–
$p_0\alpha_1$	-25.8841	-7.0097	–
$p_0^2\alpha_2$	16.6113	-41.1330	–
a	19.7	0.87	23
b	-40	22	-110
w_2	1.03×10^{3}	4.5×10^{-5}	1.2×10^{-3}
w_3	-1.4×10^{-7}	8×10^{-8}	-3.5×10^{-7}
W_1	0.92	0.04	1.08
W_2	-0.005	0.002	-0.01
ν_m	0.2 †	0.2 †	0.19
k	1.73×10^{4}	1.74×10^{4}	1.9×10^{4}

† The value $\nu_m = 0.2$ was assumed in the logarithmic method.

parameters, the coefficients a and b in equation (13) were systematically varied by means of a computer generated trial and error procedure. After each trial the least squares standard deviation between the resulting curve and the input data points was calculated, given by S.E. $= \{\Sigma[(y/c)_{calc} - (y/c)]^2\}^{\frac{1}{2}}$. Figure 4(a) presents a plot of the normalized relative standard error of fit as a function of b for various values of a. In Fig. 4(b) the relative standard error at the minimum of each curve is plotted as a function of coefficient a. At the minimum standard deviation the values a = 23 and b = -110 were obtained. These results may be compared with the estimates with the logarithmic method, Table I. The two methods yield the same results to within 15% for a, and a factor of 2 for b. The trial and error method resulted in the estimates $k = 1.9 \times 10^4$ ℓ/M and $\nu_m = 0.19$, in substantial agreement with the values calculated for SV 40 DNA II. Figure 4 (a, b) shows that the minimum in the standard error curve is relatively sharp for coefficient a and relatively shallow for coefficient b. The maximum site ratio, ν_m, was calculated for various displacements from the minimum position of the curve in Fig. 4(b). Unrealistically high values of $\nu_m > 0.22$ were obtained for $a > 25$, reaching $\nu_m = 1.0$ at a = 27.5 and becoming negative for $a > 28.5$. At values of $a < 18$ the calculated values of ν_m are all unrealistically low, decreasing from $\nu_m = 0.165$ at a = 18. Values of $\nu_m \approx 0.2$ are obtained only in the immediate region of the minimum in the standard error curve, Fig. 4(b). This result is consistent with the assumption that SV 40 DNA I contains the same

Figure 4

The trial and error method for the determination of the free energy coefficients, a and b. (a) The relative standard deviation is plotted as a function of the second coefficient, b, for selected values of the first coefficient, a. The minimum of each curve is indicated by an arrow. (b) The relative standard deviation at the minima of the curves in (a) is plotted as a function of the first energy coefficient, a. The joint minimum occurs at the values a = 23 and b = -110. For further explanation refer to the text.

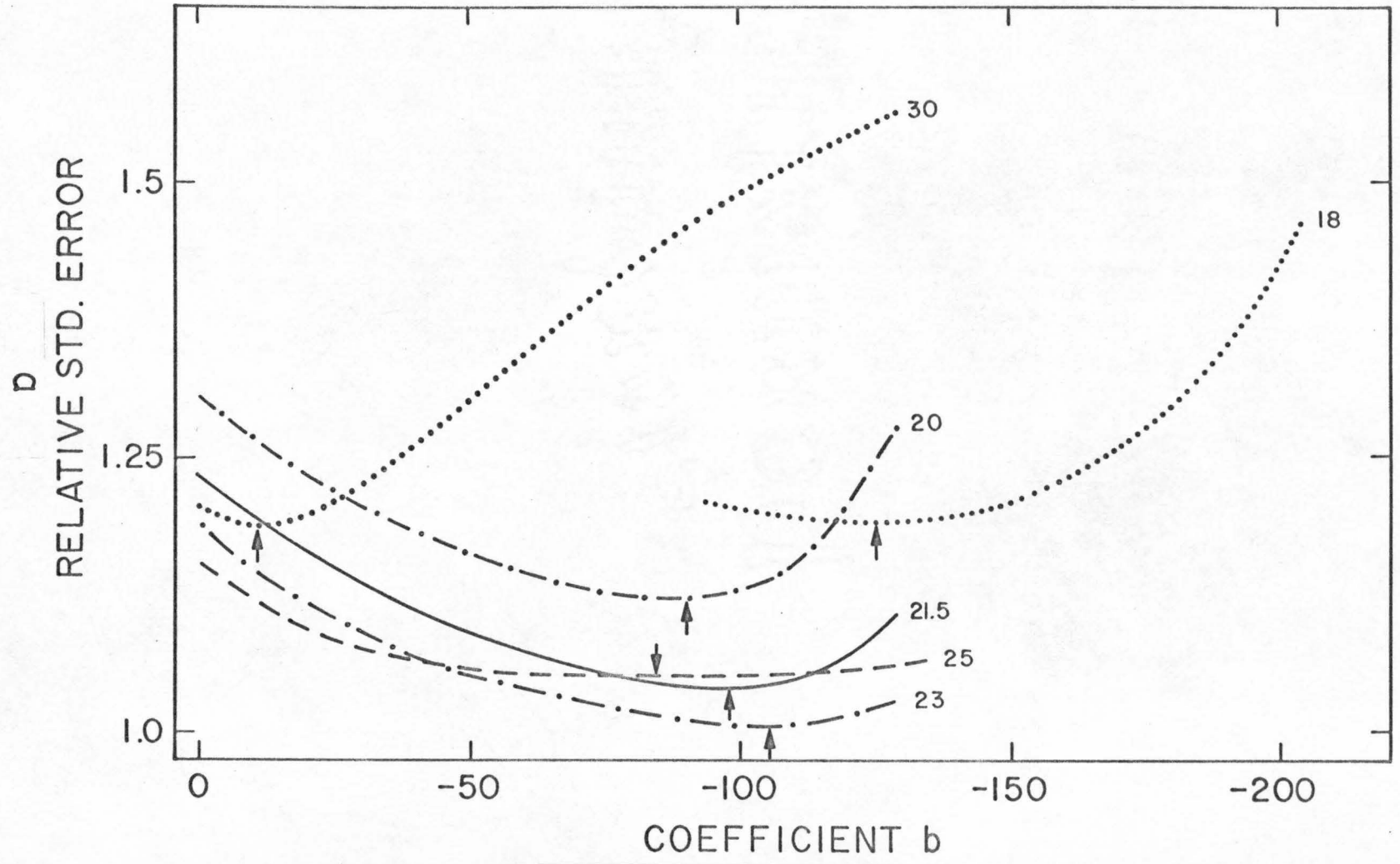
D
RELATIVE STD. ERROR
1.5
1.25
1.0
0
-50
-100
-150
-200
COEFFICIENT b
30
18
20
21.5
25
23

q

number of available binding sites as does SV 40 DNA II. Similar conclusions follow from a consideration of the value of the association constant calculated for various values of a. Since the trial and error method is highly sensitive to data scatter, the results are expected to be much less precise than those obtained with the logarithmic method. The agreement of the calculated binding constant and of the number of binding sites using the two methods, however, tends to confirm the validity of the series approximation used in the logarithmic method.

The modified Scatchard equation for SV 40 DNA I, equation (13), may be recast in terms of the variables ν and ν_m,

$$(\nu/c)' \equiv (\nu/c) \exp \left\{ -\left[a(\nu - \nu_0) + b(\nu - \nu_0)^2 \right] \right\} = k(\nu_m - \nu). \qquad (19a)$$

A plot of $(\nu/c)'$ versus ν, together with the best least squares fit to the corrected experimental points, is presented in Fig. 5(a). The intrinsic binding constant k is equal to the negative slope of this line and has the value 1.73×10^4 ℓ/M, in good agreement with the value $k = 1.74 \times 10^4$ ℓ/M for SV 40 DNA II calculated from the data in Fig. 1 with equation (4). The value of the intercept at $(\nu/c)' = 0$, $\nu_m = 0.20$, indicates that the series expansion used in the logarithmic method is sufficiently accurate in the analysis. The linearity of the corrected binding curve in Fig. 5(a) indicates that the truncated power series, equation (11a), is adequate to represent the free energy of superhelix formation and to explain the complex character of the binding curve of dye to closed circular SV 40 DNA.

Figure 5

(a) The binding data for SV 40 DNA I and ethidium bromide plotted according to equation (19a). The quantity $(\nu/c)'$ represents the behavior of the quotient ν/c for SV 40 DNA I in the absence of perturbations of the binding isotherm due to the presence of the superhelical turns, and the straight line is the best least squares fit to the corrected data points. This curve should be compared with Fig. 1 for the binding of ethidium bromide to SV 40 DNA II. (b) The experimental data for the binding of ethidium bromide to SV 40 DNA I are plotted as in Fig. 2. The solid curve was calculated from equation (19b) with the free energy coefficients calculated by the logarithmic method and given in Table I.

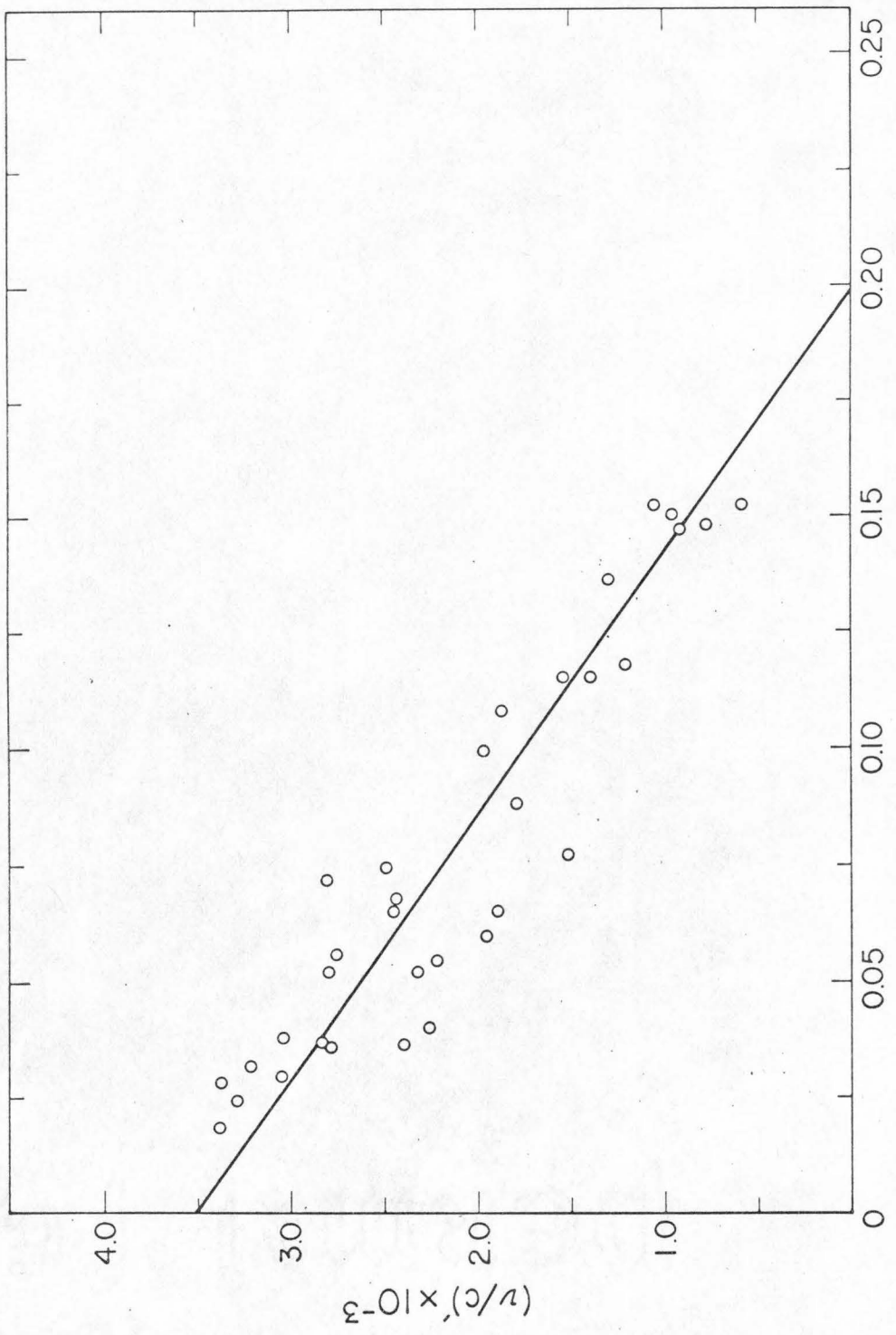
4.0
3.0
2.0
1.0
0
0.05
0.10
0.15
0.20
0.25
$(\nu/c)' \times 10^{-3}$
ν, MOLES DYE/MOLE RESIDUE

a

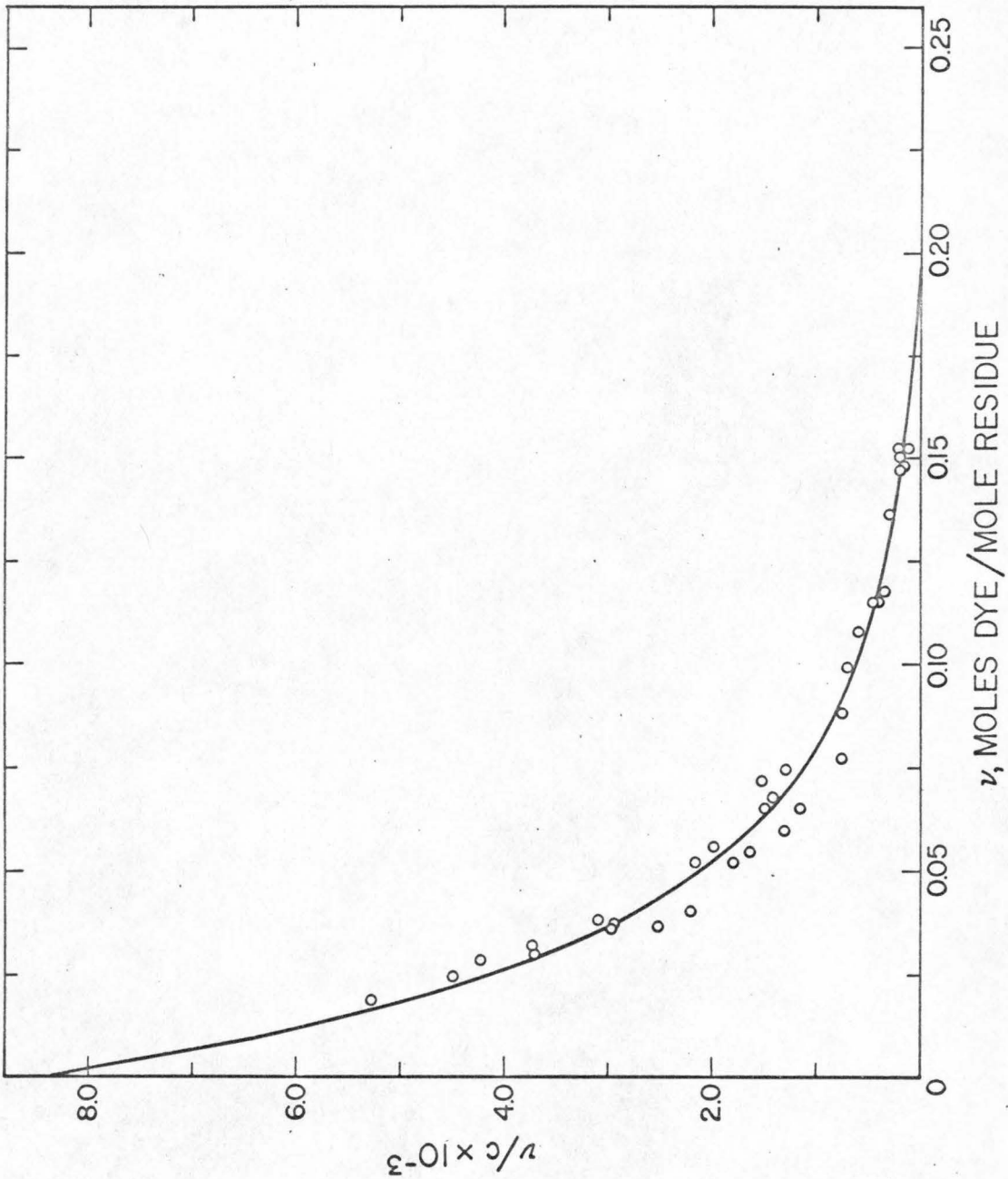

b

Figure 5(b) presents the experimental values of ν/c versus ν for SV 40 DNA I. The solid line in this figure represents a plot of the right side of the equation

$$\nu/c = k(\nu_m - \nu) \exp [\ a(\nu - \nu_0) + b(\nu - \nu_0)^2\ ] , \tag{19b}$$

versus ν. Figure 5(b) demonstrates that the calculated free energy coefficients may be used to obtain a satisfactory representation of the experimental binding data for SV 40 DNA I.

Values for the free energy coefficients in terms of τ are also given in Table I. They were calculated with the relationships

$$\tau = \frac{\bar{y} - \bar{y}_0}{30} , \tag{20a}$$

$$W_1 = 900\, w_2 \tag{20b}$$

and

$$W_2 = 27 \times 10^3\, w_3 . \tag{20c}$$

The free energy of superhelix formation in units of RT is then given by

$$\frac{\Delta G_\tau}{RT} = 0.92\tau^2 - 0.005\tau^3. \tag{21}$$

A plot of ΔG_τ versus τ is given in Fig. 6(a). The free energy curve is approximately parabolic, except for the distortion introduced by the cubic term in equation (21). The free energy of the superhelix is greater in negative than in positive superhelices at the same

Figure 6

(a) The free energy of superhelix formation as a function of the number of superhelical turns, τ, for SV 40 DNA I.

(b) The free energy of superhelix formation per turn as a function of τ for SV 40 DNA I.

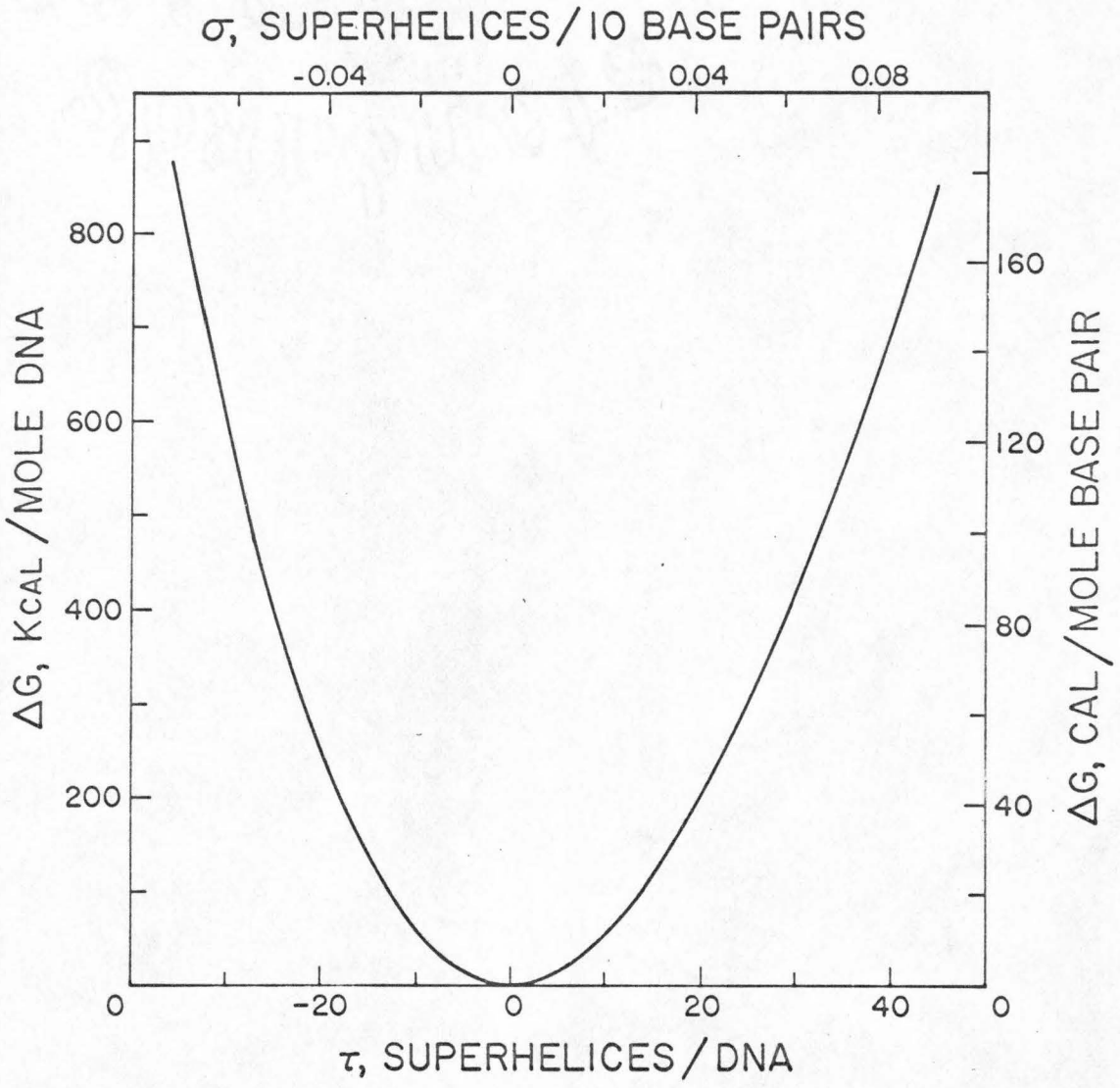
σ, SUPERHELICES / 10 BASE PAIRS
-0.04
0
0.04
0.08
800
600
400
200
0
ΔG, KCAL / MOLE DNA
160
120
80
40
0
ΔG, CAL / MOLE BASE PAIR
-20
0
20
40
τ, SUPERHELICES / DNA

a

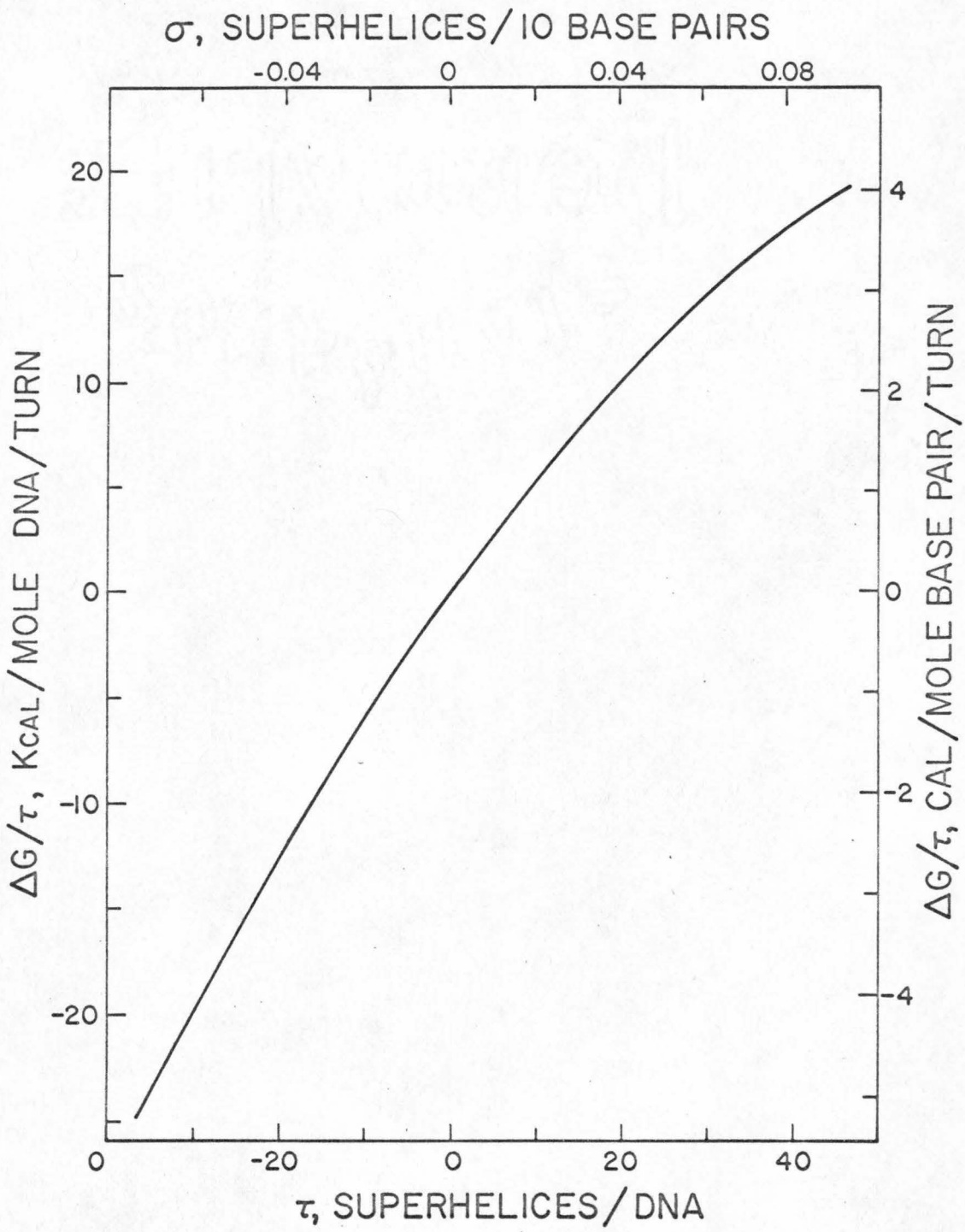
σ, SUPERHELICES/10 BASE PAIRS
-0.04
0
0.04
0.08
20
10
0
-10
-20
4
2
0
-2
-4
ΔG/τ, KCAL/MOLE DNA/TURN
ΔG/τ, CAL/MOLE BASE PAIR/TURN
0
-20
0
20
40
τ, SUPERHELICES/DNA

b

absolute value of τ. This result, for DNA molecules containing variable amounts of dye, and therefore of varying lengths, is discussed in greater detail below.

At a value of $\tau_0 = -13$, characteristic of the native DNA I molecule in the absence of dye, $\Delta G_0 = 100$ kcal/mole DNA, or 21 cal/mole base pair. This energy is available to do work in any process which involves a reduction in the number of superhelical turns. This may be done either reversibly by introducing local or generalized unwinding of the duplex, or irreversibly by introducing a single strand scission and a physical swivel to serve as the site for rotation required for the unwinding.

Figure 6(b) presents a plot of the free energy of superhelix formation per turn, $\Delta G_\tau/\tau$, as a function of the number of superhelical turns. It has been assumed for this calculation that the free energy is distributed uniformly over all the superhelical turns, and end effects have been neglected. The free energy per turn increases approximately linearly with the number of turns in the superhelix.

b. The Pitch and Radius of the Superhelix

A regular superhelix of a given contour length may be specified by designating the type of structure, interwound or toroidal; the number of superhelical turns; and either the pitch or the superhelix radius.

Representative scale models of the two structural types for SV 40 DNA are presented in Fig. 7(a) for the interwound form and in Fig. 7(b) for the toroidal form. The models were constructed of aluminum wire with $\tau_0 = -14$ superhelical turns. The interwound models are figures of constant radius of curvature, except for the neglect of end effects. The radius of curvature in these models increases from right to left.

There is at the present time no direct experimental evidence available to distinguish between the two possible structural models for closed circular DNA in solution. A torsion-free but bent interwound superhelix can be formed in order to accommodate the winding up of a closed duplex, as shown in Fig. 1 of Vinograd, Lebowitz, and Watson (1967). The formation of a toroidal superhelix in response to the unwinding of a closed circular duplex can only be accomplished with the introduction of torsional strain along the duplex. Therefore, it is to be expected that the toroidal molecule is of a higher energy than the interwound form and is less likely to be present in solution. A similar conclusion was reached in a theoretical analysis of the sedimentation velocity of closed circular DNA. Gray (1967) considered the hydrodynamic properties of stiff models of both the interwound and toroidal forms and concluded that only the interwound form was consistent with the experimental data. The models in Fig. 7(a) are constructed for several different possible values of the superhelix pitch. A definite superhelix radius corresponds to each choice of the pitch. Except for end effects, these models may be regarded as

Figure 7

Scale models constructed of aluminum wire for a closed circular DNA with $\tau_0 = -14$. The models are of constant contour length and the construction scale is 500 Å/inch. (a) The interwound form of the superhelix. The models were constructed for selected values of the pitch and superhelix radius, and the pitch decreases from left to right with the following values: I, 875Å; II, 685Å; III, 590Å; IV, 416Å; V, 210Å; VI, 25Å. The unnumbered model at the extreme right represents the SV40 virus. The calculations presented in the text indicate that model IV best represents SV40 DNA I in concentrated CsCl solutions. (b) The toroidal form of the superhelix. The models illustrate both extremes and selected intermediate values of the superhelix pitch and radius. The toroidal molecule is probably a much higher energy form than the interwound molecule, as discussed in the text.

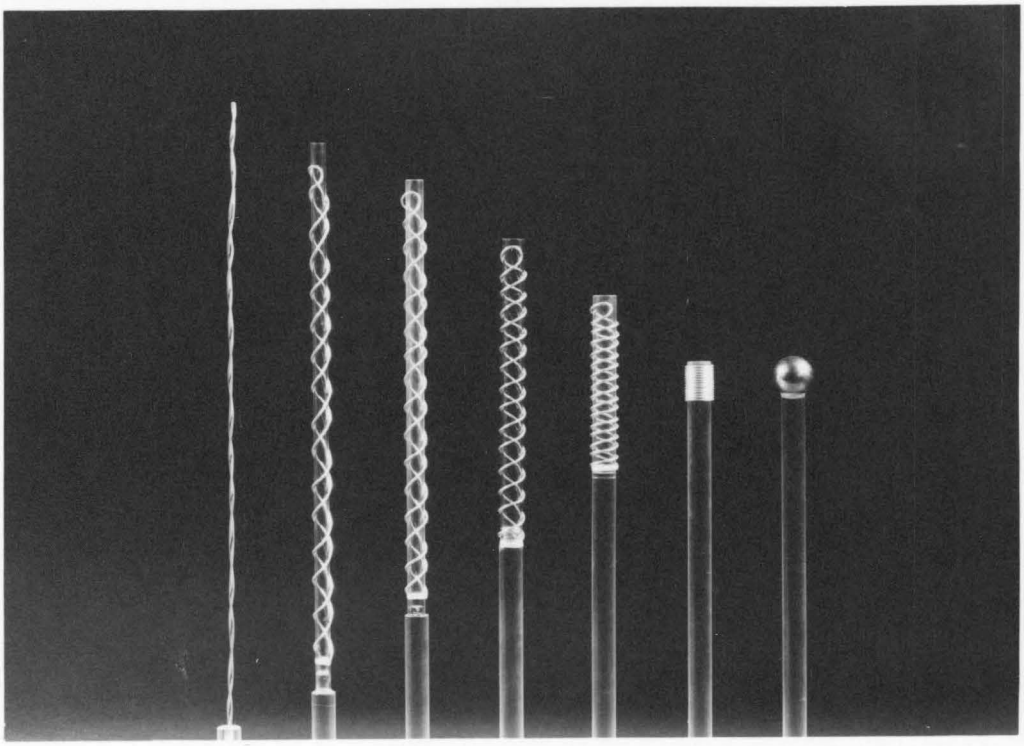

I II III IV V VI

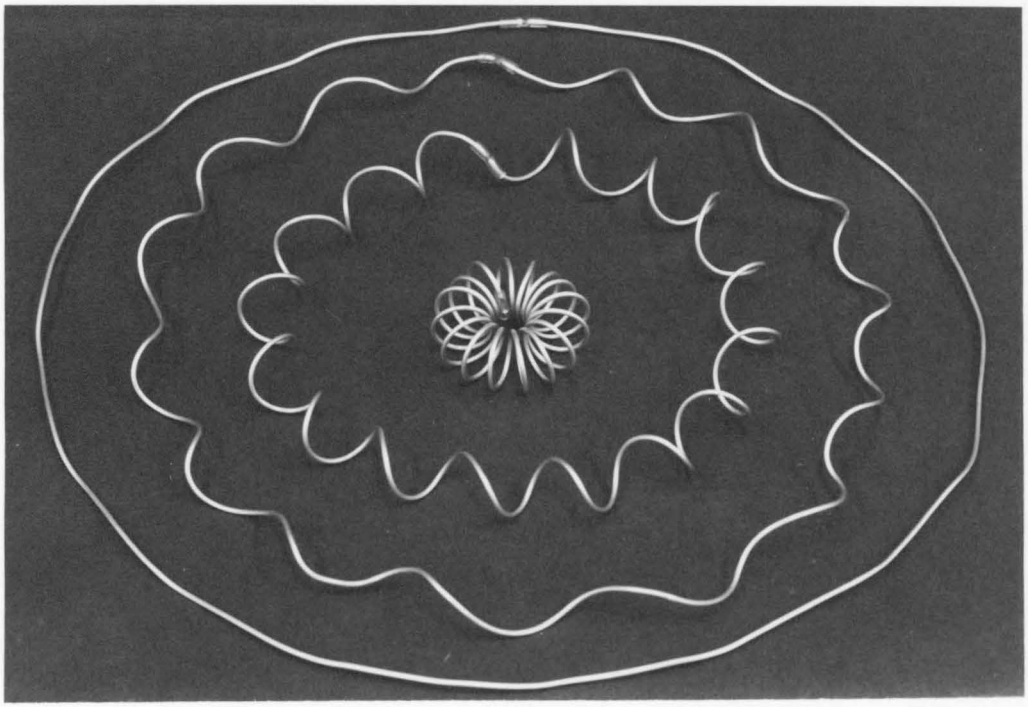

torsion-free isotropic rods which are bent so as to maintain a constant radius of curvature. Since the energy of such a structure is inversely related to the radius of curvature, knowledge of the binding energy may be used to calculate the radius of curvature of the superhelix and to choose among the several forms illustrated in Fig. 7(a).

If a straight rod is bent into a circular arc, the total bending energy, U, is given by:

$$U = \frac{\pi}{8} \frac{Eb^4 s}{R^2} \tag{22}$$

where E is the Young's modulus for the material, b is the radius of the cross section of the rod, s is the contour length, and R is the radius of curvature. For the case of a rod bent into a torsion-free superhelix, as in Fig. 7(a), the radius of curvature is given by

$$R = \frac{4\pi r^2 + p^2}{4\pi^2 r} \tag{23}$$

where $p = 2L/\tau$ is the pitch of the superhelix, L is the length of the interwound superhelix along its center line, τ is the number of interwound superhelical turns, and r is the radius of the superhelix. The contour length of an interwound superhelix is given by

$$s^2 = \tau^2(4\pi^2 r^2 + p^2) \ . \tag{24}$$

The radius of the superhelix is found by combining equations (23) and (24),

$$r = \frac{s^2}{4\pi^2\tau^2 R} \quad . \tag{25}$$

The radius may be expressed in terms of the physical parameters of the rod by combining equations (22) and (25)

$$r = \frac{s^2}{\pi^2\tau^2 b^2}\left(\frac{U}{2\pi sE}\right)^{\frac{1}{2}} \quad . \tag{26}$$

From equations (24) and (26), the corresponding solution for the pitch of the superhelix is

$$p = \frac{s}{\tau}\left[1 - \frac{2sU}{\pi^3\tau^2 b^4 E}\right]^{\frac{1}{2}} \quad . \tag{27}$$

For the case of SV 40 DNA in the presence of ethidium bromide, if it is assumed that the entropy of superhelix formation is very small, the bending energy may be taken to be equal to the free energy of superhelix formation

$$U = \Delta G = kT(W_1\tau^2 + W_2\tau^3) \quad . \tag{28}$$

Equations (26) and (27) then become

$$r = \frac{s^2}{\pi^2 b^2 |\tau|}\left[\frac{kT(W_1 + W_2\tau)}{2\pi sE}\right]^{\frac{1}{2}} \tag{29}$$

and

$$p = \frac{s}{|\tau|}\left[1 - \frac{2skT(W_1 + W_2\tau)}{\pi^3 b^4 E}\right]^{\frac{1}{2}} \quad . \tag{30}$$

In order to calculate numerical values for the radius and pitch of the superhelix, it is necessary to estimate the Young's modulus for DNA. This has been done by J. J. Hermans in Cohen and Eisenberg (1966) from the temperature dependence of the intrinsic viscosity of a DNA of molecular weight 2×10^5 Daltons. The calculated value was $E = 0.5 \times 10^{10}$ dynes/cm^2. Using equation (8) of Cohen and Eisenberg (1966) and their experimental measurement of the ratio of end-to-end distance to contour length of $\langle L \rangle / L_{max} = 0.89$ at 25°, we calculate $E = 0.7 \times 10^{10}$ dyne/cm^2. The value of 9 Å for b, the radius of the DNA molecule, was that used in the above calculation to obtain the Young's modulus from the more directly calculated quantity Eb^4. It is this latter quantity which is significant in the equations presented here.

The free energy of superhelix formation calculated from equation (6) refers to the DNA molecule in the absence of dye, except as discussed at the end of this section. The appropriate value of the DNA contour length, s, will be taken to be that of the native SV 40 DNA molecule. Although no estimate is available for the contour length of SV 40 DNA, Stoeckenius (1963) has estimated that for polyoma DNA, $s = 1.6 \times 10^{-4}$ cm. SV 40 and polyoma DNAs are very similar in molecular weight and neutral sedimentation velocity (Crawford and Black, 1964; Crawford, 1964), and we use the above value as an estimate of s for SV 40 DNA. The length of the DNA extends by approximately 20% at full saturation with ethidium bromide, if it is assumed that there is no accompanying change in the

duplex radius. The other constants of equations (29) and (30) are $k = 1.381 \times 10^{-16}$ ergs/molecule and $T = 298°$ K. For closed circular DNA, equations (29) and (30) may then be written

$$r = \frac{2.16 \times 10^{-5}}{|\tau|} (1 - 0.0057\,\tau)^{\frac{1}{2}} \text{ cm} , \tag{31}$$

and $$p = \frac{1.5 \times 10^{-4}}{|\tau|} [\, 1 - 0.80(1 - 0.0057\,\tau)\,]^{\frac{1}{2}} \text{ cm} . \tag{32}$$

Figure 8(a) presents a plot of the superhelix radius and Fig. 8(b) a plot of the superhelix pitch as a function of the number of superhelical turns, τ. For native SV 40 DNA I, with $\tau_0 = -13$, we calculate the values of 135 Å for the radius and 430 Å for the pitch of the interwound superhelix. The nearest values calculated by Gray (1967), using hydrodynamic considerations, were for polyoma DNA with $\tau_0 = -16$. If we take $s^0_{20,w}$ for this DNA to be 20.3 S (Weil and Vinograd, 1963) the interpolated values for the radius and pitch are r = 146 Å and p = 400 Å. Referring again to Fig. 7(a), model IV with a pitch of 416 Å is indicated as best representing the configuration in solution of a closed circular DNA of molecular weight approximately 3.2×10^6 Daltons. This conclusion follows from both the thermodynamic results presented here and from the hydrodynamic results of Gray (1967).

The calculations of the superhelix radius and pitch presented here have assumed that the stiffness of the DNA molecule is unaffected by the presence of the bound dye. This assumption is supported by the relative insensitivity of the sedimentation coefficient

Figure 8

The results of the calculations of the interwound superhelix dimensions for SV 40 DNA in concentrated CsCl. (a) The radius of the superhelix plotted as a function of the number of superhelical turns, τ. (b) The pitch of the superhelix plotted as a function of τ. For native SV 40 DNA, with $\tau_0 = -13$, the calculations yield the values r = 135 Å and p = 430 Å.

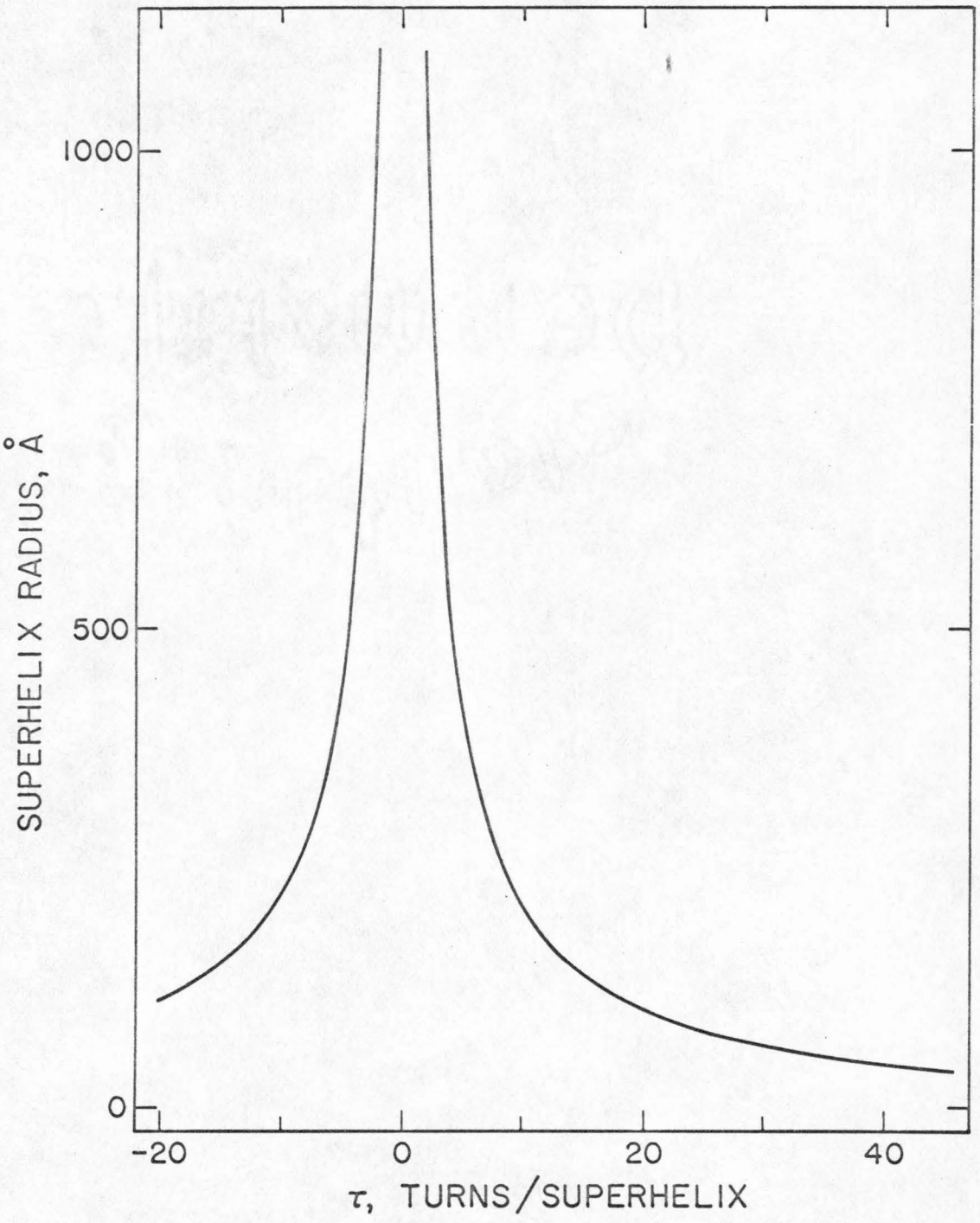

a

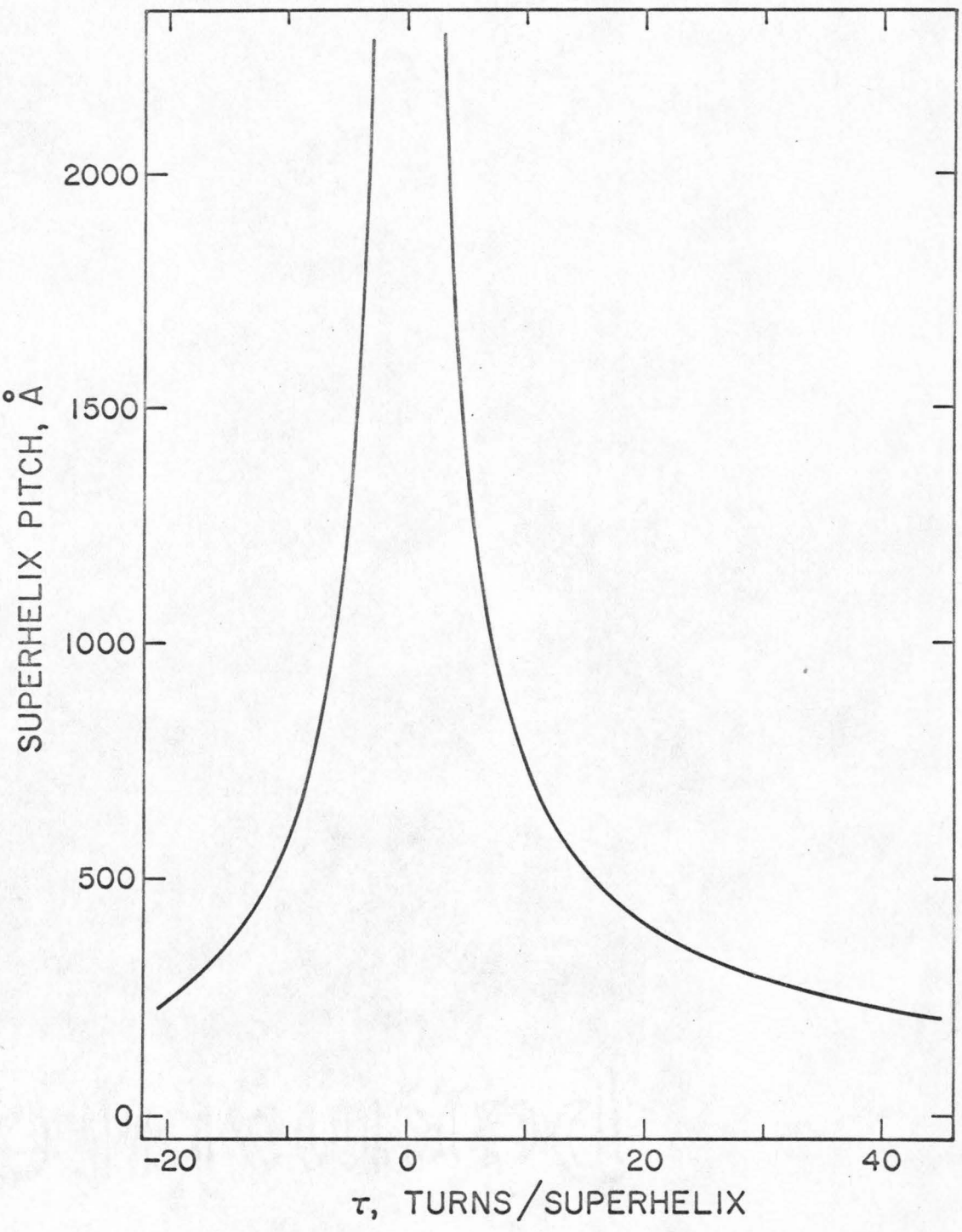
2000
1500
1000
500
0
SUPERHELIX PITCH, Å
-20
0
20
40
τ, TURNS/SUPERHELIX

b

of SV 40 DNA II to the amount of dye bound, as shown in Bauer and Vinograd (1967). Changes in stiffness of the DNA molecule in the presence of dye would be reflected in the Young's modulus. There is at the present time no data available to permit an independent calculation of the magnitude of this effect.

3. Discussion

The calculations presented here have enabled us to estimate the free energy of superhelix formation of SV 40 DNA. These calculations are based upon an analysis of the effects of the superhelical turns upon the binding isotherm with ethidium bromide. The free energy has been calculated as a function of the number of superhelical turns, with the result that $\Delta G_\tau/RT = 0.92\tau^2 - 0.005\tau^3$. The free energy of the molecule increases approximately parabolically with τ. The presence of the cubic term in equation (21) introduces an asymmetry of second order. For a given absolute value of τ, the free energy ΔG_τ is greater for negative than for positive superhelical turns. Although the magnitude of the cubic coefficient W_2 could not be precisely determined, the calculations clearly indicate that the sign of W_2 is negative and that it is small compared to W_1. This asymmetry in the free energy function might be due to a change in the stiffness of the molecule as increasing amounts of dye are bound, a factor which could not be taken into account in the calculations. If this is the case, the negative sign of W_2 requires that the molecule become less rigid as a result of the presence of the intercalated dye. An alternative explanation is that the enthalpy of superhelix formation varies with the

direction in which the duplex is stressed in the bending process. An increase in the number of negative superhelical turns requires overwinding of the duplex, whereas an increase in the number of positive superhelical turns may only be done with a corresponding increase in the duplex underwinding. This explanation implies that the energy required to overwind the duplex is greater than the energy required to underwind the duplex. It should be emphasized that this calculation refers to SV 40 DNA in 5.8 M CsCl at 25°. The free energy difference required to account for this effect may be roughly estimated with the use of equation (21). The difference in free energy due to superhelix formation between two molecules, containing $-\tau$ and $+\tau$ superhelical turns respectively, is

$$\Delta G_{-\tau} - \Delta G_{\tau} = -2\,RTW_2|\tau|^3 . \qquad (33a)$$

At 25° for a DNA containing 4800 base pairs, equation (33a) may be written in numerical form

$$\Delta G_{-\tau} - \Delta G_{\tau} = 1.2 \times 10^{-3}|\tau|^3 \text{ cal/mole base pair.} \qquad (33b)$$

For $|\tau| = 13$ superhelical turns this energy difference is approximately 2.6 cal/mole base pair. It is apparent that very small energy differences are sufficient to give rise to the calculated asymmetry in the free energy function.

The numerical values of the free energy of superhelix formation calculated here are dependent upon the angle of unwinding for

intercalation, ϕ, which was used to calculate the number of superhelical turns in closed circular SV 40 DNA from the ethidium chloride binding isotherm (Bauer and Vinograd, 1967). Fuller and Waring (1964) were able to estimate the value $\phi = 12°$ with the aid of molecular models. A comparison of the value $\tau_0 = -13$, obtained in Part I, with the value $\tau_0 = -15$ for polyoma DNA (Vinograd, Lebowitz, and Watson, 1967), obtained by a method which is independent of ϕ, suggests that the 12° estimate is not unreasonable. Polyoma and SV 40 DNAs are closely similar in molecular weight and sedimentation velocity.

The binding isotherm for the reaction of ethidium bromide with SV 40 DNA I and our estimate of the free energy of superhelix formation were combined for the calculation of the intrinsic association constant and the maximum value of the binding ratio. We calculate that $k = 1.73 \times 10^4$ liters/mole and $\nu_m = 0.20$, in agreement with the results for SV 40 DNA II. This agreement indicates that the differences in the observed binding isotherms for SV 40 DNAs I and II are a result of the additional free energy required for superhelix formation in the closed molecule. As a consequence $\nu_I > \nu_{II}$ at low dye concentrations, where $\tau < 0$, and superhelical turns are removed as binding proceeds. In the high dye concentration region, where $\tau > 0$ and additional superhelical turns are incorporated with the binding of dye, $\nu_{II} > \nu_I$. At the critical point of the isotherm, where $\tau = 0$, $\nu_I = \nu_{II}$ and the binding affinities of DNAs I and II are equal.

The results for SV 40 DNA II, Fig. 1, also indicate the presence of some secondary binding at very high dye concentrations. The binding of ethidium bromide to various linear DNAs has been studied by Waring (1965), who observed the metachromatic effects, and by Le Pecq and Paoletti (1967), using the fluorescence changes which result from binding. Waring (1965) observed a single binding site up to a value of $\nu = 0.18$, but at higher binding ratios departure from linearity was detected. At 0.0001 M salt a complex could be formed up to $\nu_m = 1.0$, and this maximum value of ν was found to decrease with increasing salt. Non-linear or secondary binding was still observed in solutions containing 0.001 M $MgCl_2$. Le Pecq and Paoletti (1967) found that the binding isotherm is linear when plotted according to the method of Scatchard (1949), up to a value of $\nu = 0.16$, the highest binding ratio studied. In both investigations the value of ν_m calculated for the linear or primary site binding was approximately 0.2.

We calculate that the free energy required to introduce the first superhelical turn into the closed molecule is approximately equal to the thermal energy, kT, and that the energy required for two turns is about 4kT. It seems reasonable to assume that these values may also be applied to the nicked circular SV 40 DNA II molecule. The free energy of base stacking in aqueous solution has been estimated by Simpkins and Richards (1967) from an analysis of the titration properties of the dinucleotides. They calculate the value $\Delta G^{\circ}_{st} = -1.0$ kcal/mole, approximately 1.7 kT, at 20° in 0.1 M NaCl for the ApA

dinucleotide. We take this value as an indication of the magnitude of the free energy change which characterizes the rotation of the duplex about a phosphodiester bond scission. The free energy gained from the transition $\tau = \pm 1$ to $\tau = 0$ is less than ΔG_{st}, and the free energy gained from the transition $\tau = \pm 2$ to $\tau = \pm 1$ is approximately twice as large. A population of SV 40 DNA II molecules might therefore be expected to contain significant numbers of molecules with one or two residual superhelical turns, since the energies involved are all of the order of kT.

Because the free energy of superhelix formation is positive, native DNA I is destabilized toward thermal melting compared to DNA II. This relative instability should bring about an early melting of the closed circular molecule. As melting proceeds, with the unpairing of bases in the duplex, the number of superhelical turns decreases and the instability of I relative to II diminishes. The closed circular DNA I should, therefore, experience an early asymmetric melting transition. Such behavior has been observed in the alkaline buoyant density titration of polyoma DNA (Vinograd, Lebowitz, and Watson, 1967).

The calculated values of the free energy of superhelix formation were used to estimate the pitch and diameter of the superhelix as a function of the number of superhelical turns. The values r = 135 Å and p = 430 Å were obtained, and these agree well with the theoretical calculations of Gray (1967) based upon hydrodynamic properties, as discussed above. Our calculated values are nevertheless of a

tentative nature, primarily because of uncertainty in the value of the Young's modulus for this molecule. Moreover, the assumption that the Young's modulus is not a function of the binding ratio ν may be unwarranted. The agreement of our estimates with those of Gray may be taken as an indication that the value of Eb^4 for the product of Young's modulus and the fourth power of the effective radius of the DNA is not greatly in error.

We thank R. Kent for her assistance in the preparation of this manuscript. The research has been supported in part by Grants HE 03394 and CA 08014 from the United States Public Health Service, and by a fellowship from the National Science Foundation.

This is contribution no. from the Department of Chemistry, California Institute of Technology.

REFERENCES

Bauer, W. & Vinograd, J. (1967). J. Mol. Biol., in press.

Cohen, G. & Eisenberg, H. (1966). Biopolymers, 4, 429.

Crawford, L. V. (1964). Virology, 22, 149.

Crawford, L. V. & Black, P. H. (1964). Virology, 24, 388.

Fuller, W. & Waring, M. J. (1964). Berichte der Bunsengesellschaft, 68, 805.

Gray, H. B. (1967). Biopolymers, in press.

Katchalsky, A. & Gillis, J. (1949). Rec. Chim. Trav., 68, 879.

Katchalsky, A. & Spitnik, P. (1947). J. Polymer Sci., 2, 432.

Le Pecq, J.-B. & Paoletti, C. (1967). J. Mol. Biol., 27, 87.

Scatchard, G. (1949). Ann. N. Y. Acad. Sci., 51, 660.

Simpkins, H. & Richards, E. G. (1967). Biochemistry, 6, 2513.

Stoeckenius, W. (1963). Proc. Nat. Acad. Sci., 50, 737.

Vinograd, J., Lebowitz, J. & Watson, R. (1967). J. Mol. Biol., in press.

Waring, M. J. (1965). J. Mol. Biol., 13, 269.

Weil, R. & Vinograd, J. (1963). Proc. Nat. Acad. Sci., 50, 730.

CHAPTER III

A Dye-Buoyant Density Method for the Detection and Isolation of Closed Circular Duplex DNA: The Closed Circular DNA in HeLa Cells

by Roger Radloff, William Bauer, and Jerome Vinograd

This chapter is the reproduction of a published paper which appeared in the Proceedings of the National Academy of Sciences, Vol. 57, pp. 1514-1521 (1967).

Reprinted from the PROCEEDINGS OF THE NATIONAL ACADEMY OF SCIENCES
Vol. 57, No. 5, pp. 1514–1521. May, 1967.

*A DYE-BUOYANT-DENSITY METHOD FOR THE DETECTION AND ISOLATION OF CLOSED CIRCULAR DUPLEX DNA: THE CLOSED CIRCULAR DNA IN HELA CELLS**

BY ROGER RADLOFF, WILLIAM BAUER, AND JEROME VINOGRAD

NORMAN W. CHURCH LABORATORY FOR CHEMICAL BIOLOGY,†
CALIFORNIA INSTITUTE OF TECHNOLOGY, PASADENA

Communicated by James Bonner, March 2, 1967

Covalently closed circular duplex DNA's are now known to be widespread among living organisms. This DNA structure, originally identified in polyoma viral DNA,[1, 2] has been assigned to the mitochondrial DNA's in ox[3] and sheep heart,[4] in mouse and chicken liver,[3] and in unfertilized sea urchin egg.[5] The animal viral DNA's—polyoma, SV40,[6] rabbit[7] and human[8] papilloma—the intracellular forms of the bacterial viral DNA's—ϕX174,[9, 10] lambda,[11, 12] M13,[13] and P22[14]—and a bacterial plasmid DNA, the colicinogenic factor E_2,[15] have all been shown to exist as closed circular duplexes. Other mitochondrial DNA's[16, 17] and a portion of the DNA from boar sperm[18] have been reported to be circular, but as yet have not been shown to be covalently closed.

The physicochemical properties of closed circular DNA differ in several respects from those of linear DNA or of circular DNA containing one or more single-strand scissions.[19] The resistance to denaturation,[2, 20] the sedimentation velocity in neutral and alkaline solution, and the buoyant density in alkaline solution are all enhanced in the closed circular molecules. These three effects are a direct consequence of the topological requirement that the number of interstrand cross-overs must remain constant in the closed molecule.

The principal methods currently used for the detection and the isolation of closed circular DNA are based on the first two general properties. In this communication we describe a method based on the buoyant behavior of closed circular DNA in the presence of intercalating dyes.

The binding of intercalative dyes has recently been shown to cause a partial unwinding of the duplex structure in closed circular DNA.[22–24] In such molecules any unwinding of the duplex causes a change in the number of superhelical turns, so that the total number of turns in the molecule remains constant. A small and critical amount of dye-binding reduces the number of superhelical turns to zero. Further dye-binding results in the formation of superhelices of the opposite sign or handedness. The creation of these new superhelices introduces mechanical stresses into the duplex and a more ordered conformation into the molecule. These effects increase the free energy of formation of the DNA-dye complex. The maximum amount of dye that can be bound by the closed molecule is therefore *smaller* than by the linear or nicked circular molecule. Correspondingly, since the buoyant density of the DNA-dye complex[23, 25] is inversely related to the amount of dye bound, the buoyant density of the closed circular DNA-dye complex at saturation is *greater* than that of the linear or nicked circular DNA-dye complex.[23] Bauer and Vinograd have shown that the above effect results in a buoyant density difference of approximately 0.04 gm/ml in CsCl containing saturating amounts of ethidium bromide, an intercalating dye extensively studied by Waring[26] and Le Pecq.[27]

The method has been tested with known mixtures of nicked and closed circular viral DNA's, and has been used to isolate closed circular DNA from the mitochondrial fraction of HeLa cells and from extracts of whole HeLa cells.

Materials and Methods.—Preparation of HeLa cell extracts: HeLa S3 cells were grown on Petri dishes in Eagle's medium containing 10% calf serum. H^3-thymidine, 18 c/mmole, was obtained from the New England Nuclear Corporation. Ten μc per ml of medium were added to each plate 20 hr before the cells were harvested. After washing with isotonic buffer and decanting, the cells were treated by the method described by Hirt[28] for the separation of polyoma DNA from nuclear DNA. Approximately 2 ml of 0.6% sodium dodecylsulphate (SDS), in 0.01 *M* ethylenediaminetetraacetate (EDTA), 0.01 *M* tris, pH 8, were added to the plates. After 30 min at room temperature, the viscous extracts were gently scraped from the plates with a rubber policeman and transferred with a widemouth pipet to a centrifuge tube. Either 5 *M* NaCl or 7 *M* CsCl was then added with gentle mixing to a final salt concentration of 1 *M*. The resulting solution was cooled to 4° and centrifuged for 15 min at 17,000 × *g* in a Servall preparative ultracentrifuge. The supernatant solution was dialyzed at 4° overnight against two changes of 0.01 *M* EDTA, 0.01 *M* tris, pH 8 buffer in order to remove H^3-thymidine. The mitochondria from HeLa cells were isolated by differential centrifugation of an homogenate followed by banding in a sucrose gradient.

Preparation of viral DNA: Polyoma viral DNA was prepared as described previously.[19] The intracellular lambda DNA was kindly supplied by John Kiger and E. T. Young, II, of the Biology Division.

Chemicals: The ethidium bromide was obtained as a gift from Boots Pure Drug Co., Ltd., Nottingham, England. Harshaw optical grade cesium was used. The SDS was obtained from Matheson Company. All other chemicals were of reagent grade.

Preparative ultracentrifugation: The experiments were performed in SW50 rotors in a Beckman Spinco model L preparative ultracentrifuge at 20°C. The CsCl solutions, in either cellulose nitrate or polyallomer tubes, were overlaid with light mineral oil. After centrifugation, the tubes were fractionated with a drop-collection unit obtained from Buchler Instruments. The drops were collected in small vials or on Whatman glass-fiber GF/A filters. The dried filters were immersed in 10 ml of toluene-PPO-POPOP, and the samples were counted in a Packard Tri-Carb scintillation counter.

Electron microscopy: Specimens for electron microscopy were prepared by the method of Kleinschmidt and Zahn[29] and were examined in a Phillips EM200 electron microscope. All electron micrographs were made at a magnification of ×5054. The magnification factor was checked with a grating replica. Cytochrome *c* was obtained from the California Biochemical Corporation.

Fluorescence: Prior to drop collection, the centrifuge tubes were examined in a darkened room with 365 mμ light from a Mineral Light Lamp or preferably from a "Transilluminator" supplied by Ultraviolet Products, Inc., San Gabriel, California. The tubes were photographed on Polaroid type-146L film through a "contrast filter" from Ultraviolet Products, Inc. The fluorescence measurements were performed with a double-monochromator apparatus constructed in this laboratory by W. Galley and N. Davidson. The instrument was calibrated with solutions of ethidium bromide (5×10^{-3} to 1.0 μg/ml) in calf thymus DNA, 20 μg/ml, 1 *M* CsCl. The intensity of fluorescence was measured at 590 mμ with an exciting wavelength of 548 mμ.[30]

Results.—Selection of initial dye concentration, cesium chloride concentration, and centrifugation variables: The conditions for the experiments in the swinging-bucket rotor in the model L ultracentrifuge were selected with the object of obtaining separations similar to those obtained at equilibrium within a reasonable period of time. At equilibrium, the separation between components is approximately constant at initial dye concentrations between 50 and 100 μg/ml.[23] At these dye levels the buoyant densities are between 1.57 and 1.62 gm/ml. Figure 1 presents the dye and density distributions in CsCl solutions centrifuged for 24 and 48 hours. The initial dye concentration in both cases was found at a distance from the meniscus corresponding to four-tenths the length of the liquid column. In

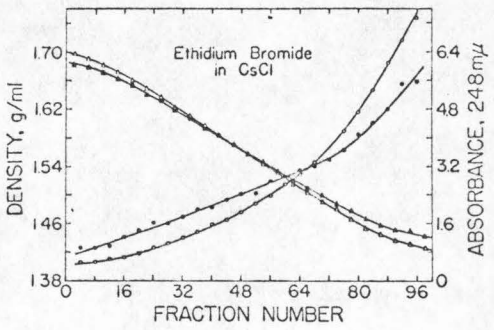

FIG. 1.—Density and dye distributions in CsCl density gradient columns, 3.00 ml 1.550 gm/ml CsCl, 100 μg/ml ethidium bromide, 24 (●, ▲) and 48 (○, △) hr at 43 krpm in a SW50 rotor at 20°.

this region of the cell, the time dependence of the dye concentration is minimal, and the constant density gradient is equal to approximately 0.10 gm/cm⁴.

Results with purified mixtures of nicked and closed circular DNA: Figure 2 presents the results obtained with 1.5 μg of tritiated polyoma DNA. Substantially complete resolution was obtained with this DNA which has a molecular weight of three million daltons. Since the fractional amount of closed circular material corresponded to the fraction obtained in analytical sedimentation velocity analyses,[21] it is concluded that single-strand scissions did not occur during the course of the experiments. An experiment in which the DNA was contained in a thin lamella at the top of the liquid column was performed to test the effect of the initial DNA distribution. The results were substantially the same as those obtained when the DNA was uniformly distributed in the CsCl solution.

The results obtained with a mixture of approximately 60 μg of covalently closed and nicked circular lambda DNA, mol wt = 3×10^7, are presented in Figure 3.

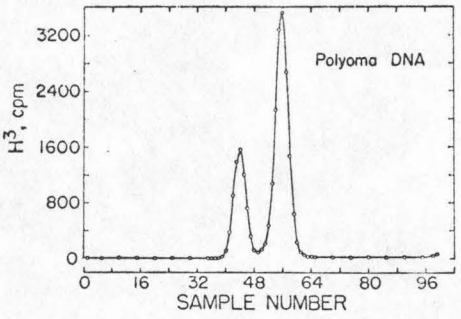

FIG. 2.—A mixture of purified polyoma DNA I and II 1.5 μg in buoyant CsCl, 3.00 ml 1.566 gm/ml CsCl, 100 μg/ml ethidium bromide, 24 hr at 43 krpm, 20°. The band maxima were separated by 12 fractions (four 7.5-μl drops per fraction). The buoyant densities of I and II are 1.588 and 1.553 gm/ml, respectively. The sample contains 30% I as indicated above compared with 32% by analytical band centrifugation.[21]

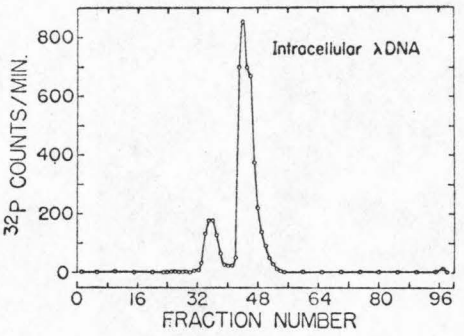

FIG. 3.—A mixture of purified intracellular lambda DNA I and II, 3.00 ml 1.55 gm/ml CsCl, 100 μg/ml ethidium bromide, 24 hr at 43 krpm, 20°. The centroids are separated by 9.5 fractions and 0.31 ml. Component I accounts for 16% of the total counts.

In this experiment, the nicked circular DNA formed a band of relatively high viscosity that may have distorted and broadened the light band during drop collection. An experiment to determine the effect of ethidium bromide on the protoplast assay for lambda DNA[32] was performed in collaboration with J. Kiger and E. T. Young, II. It was found that linear lambda had a normal titer when diluted

by a factor of 1000 from a solution containing ethidium bromide and CsCl at the concentrations which occur at band center.

Detection of DNA by absorbance, fluorescence, and scintillation counting: The data in Figures 2 and 3 were obtained by scintillation counting of dried filter papers containing dye, cesium chloride, and labeled DNA. To examine the effect of the presence of the dye upon counting efficiency, a series of sixteen 50-μl samples of H^3-thymidine in a 1.55 gm/ml CsCl solution containing ethidium bromide in concentrations varying from 0 to 286 μg/ml were counted. The relative counting efficiency decreased linearly with a least-squares slope of 8.6×10^{-4} ml/μg. The dye gradient thus caused a difference of 1 per cent in relative counting efficiency between the two bands in Figure 2, while the dye depressed the relative counting efficiency by 8 per cent.

Red bands containing about 5 μg of DNA can be observed visually in the centrifuge tube. If an adequate amount of DNA is present, the fractionated gradient may be assayed spectrophotometrically at 260 mμ. At saturation, the increase in absorbance caused by dye-binding is about 40 per cent with linear DNA and about 20 per cent with closed circular DNA.

The photograph in Figure 4 shows the fluorescent emission from two DNA bands. The fluorescence from DNA in amounts as low as 0.5 μg per band are detectable visually. Since the separation between the two bands corresponds reliably to 0.30–0.36 ml, it was possible to use the fluorescent, less dense band as a marker to locate closed circular DNA present in amounts below the limit of detectability by spectroscopic or radioactive procedures. The method is thus especially suitable for examining nonradioactive preparations from tissues of higher animals.

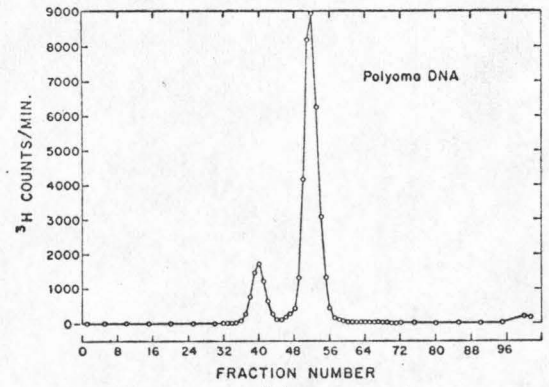

(a)

(b)

FIG. 4.—A mixture of purified polyoma DNA I and II, 3.00 ml, 1.558 gm/ml CsCl, 100 μg/ml ethidium bromide, 48 hr at 43 krpm, 20°. (*a*) The band maxima are separated by 12 fractions and 0.36 ml. The calculated buoyant densities are 1.592 and 1.556 gm/ml. (*b*) A photograph of the centrifuge tube prior to drop collection. The tube contains a total of 4 μg of DNA, and 0.64 μg of component I.

Removal of ethidium bromide from DNA solutions: It is often desirable to remove the dye quantitatively from a DNA sample. This was accomplished in a single passage of 1.0 ml of polyoma I DNA (40 μg/ml DNA, 100 μg/ml dye, 1 *M* CsCl) through a 0.8 × 4.5-cm column of analytical grade Dowex-50 resin. The fractions containing DNA were consolidated and were found to contain less than 1×10^{-2} μg dye in a fluorometric analysis.

Isolation of closed circular DNA from H^3-thymidine-labeled HeLa cells: Hela cell monolayers in Petri dishes containing 10^7 cells were treated with SDS by the pro-

cedure described by Hirt.[28] The results obtained when the extract was purposely sheared and when the shear was minimized (Figs. 5*a* and *b*) show that the relative amount of material in the light band was decreased when shear was minimized. The dense band in Figure 5*a* is clearly contaminated by material from the light band and reprocessing the dense band in a second CsCl-dye gradient would be necessary to obtain resolved bands.

Electron-microscope examination of the circular DNA in the dense band of HeLa cell extracts: Examination of electron micrographs of specimens prepared from fractions 33–36 in the dense band of HeLa cell extracts (Fig. 5*c*) showed less than 0.1

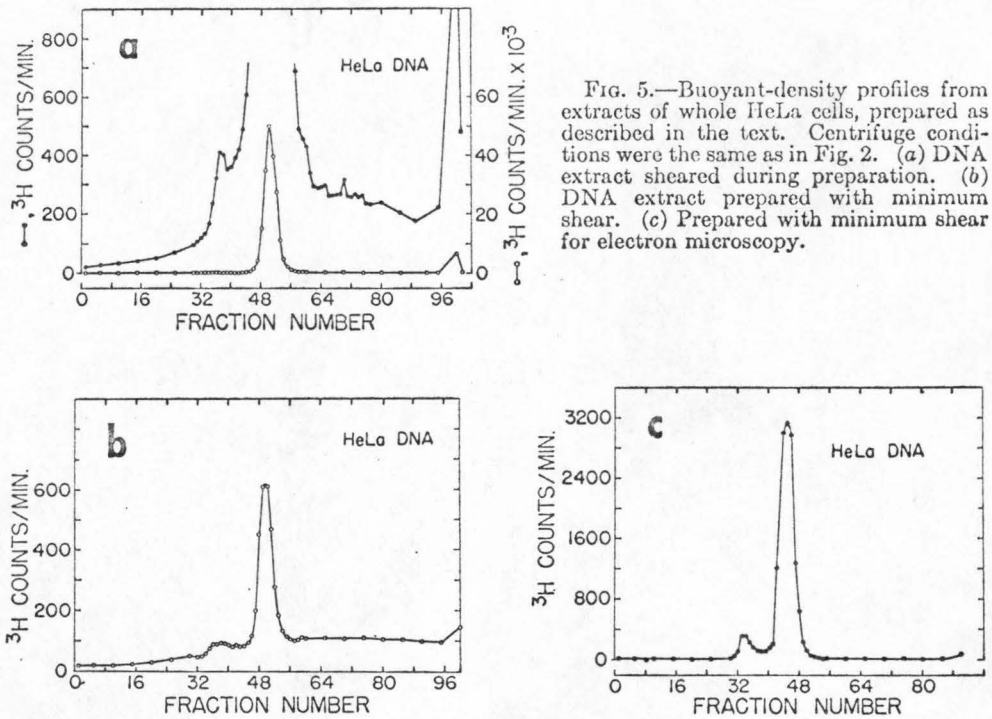

FIG. 5.—Buoyant-density profiles from extracts of whole HeLa cells, prepared as described in the text. Centrifuge conditions were the same as in Fig. 2. (*a*) DNA extract sheared during preparation. (*b*) DNA extract prepared with minimum shear. (*c*) Prepared with minimum shear for electron microscopy.

per cent of distinguishably linear DNA. The light band contained long linear DNA. The dense band contained an array of circles in three size groups: a homogeneous group of molecules with a mean length of 4.81 ± SE 0.24 microns; a heterogeneous population with lengths from 0.2 to 3.5 microns; and a paucidisperse set 2–4 times the length of the DNA in the homogeneous group. Figure 6 presents micrographs selected to illustrate the three size classes, and Figure 7 shows the frequency distribution among the first two groups. A survey of several hundred molecules on sparsely populated specimen grids revealed that the frequencies of the small and the large size classes were each about one-tenth the frequency of the homogeneous size class. In the large size class, the dimers were observed more frequently than the trimers or tetramers. The DNA from mitochondria isolated from HeLa cells consisted principally of molecules in the homogeneous size group. We conclude, therefore, that the homogeneous size class in Figure 7 is of mito

chondrial origin. Small circular DNA's were not observed in significant amounts in the preparation of DNA from the isolated mitochondria.

Discussion.—The method described in this paper has proved to be a simple and direct procedure for obtaining closed circular DNA from extracts of whole cells and cell fractions. The method employs chemically mild conditions; single-strand scissions are not introduced by interaction with the dye, nor is there any permanent rearrangement of the DNA structure. All the steps of the separation

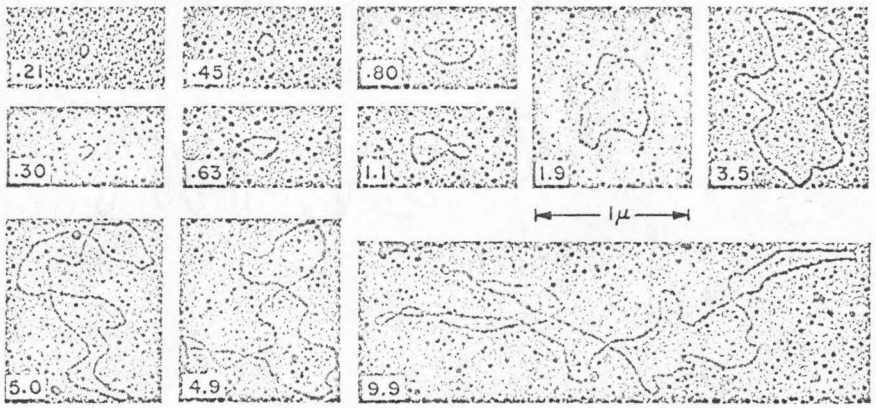

FIG. 6.—Electron micrographs of circular DNA from HeLa cells. Fractions 33–36 from the dense band in Fig. 5*c* were pooled and used in the specimen preparations. The top photographs present selected molecules of the small size range. The number in each insert gives the length in microns of the molecule. The first two molecules in the second row are of mitochondrial size; the third is twice the mitochondrial length.

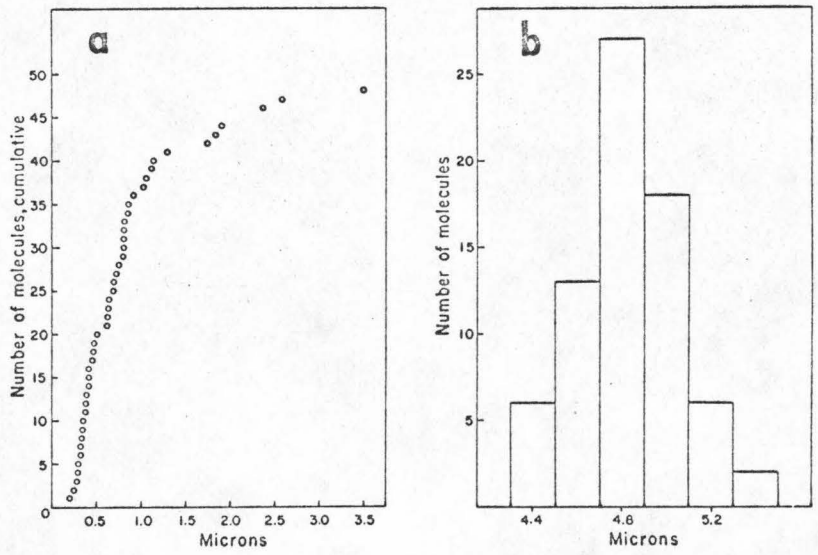

FIG. 7.—Frequency distribution of lengths of circular DNA isolated from the HeLa cell band referred to in the legend for Fig. 6. (*a*) A cumulative frequency distribution of lengths of molecules in the submitochondrial size class. (*b*) A histogram of the distribution of lengths of molecules in the mitochondrial size class.

are carried out at room temperature, or below, and at neutral pH. In the experiments performed so far, the maximum amount of DNA introduced in a single tube was 125 μg of polyoma DNA.

It has become clear, in the course of this initial study of the closed circular DNA in malignant human cells, that a portion of the mitochondrial DNA in HeLa cells is in the form of closed duplexes. These circular molecules are similar in form, size, and homogeneity to the mitochondrial DNA's from invertebrate and vertebrate species previously investigated.[3-5, 16, 17]

The heterogeneous group of small molecules, 0.2–3.5 microns, are to be compared with the size range, 0.5–16.8 microns, reported by Hotta and Bassel[18] to be present in preparations of unfractionated boar sperm DNA. The conclusion that the small circles, seen in our electron micrographs, represent DNA molecules rests on three observations. (1) The small circles were found at the same level in a CsCl-dye gradient as were the closed circular mitochondrial DNA molecules. (2) The grain pattern of the shadowed metal on the small circles viewed at a magnification of 1×10^5 was indistinguishable from the pattern on mitochondrial DNA molecules in the same field. (3) The small circles were seen only very infrequently in DNA preparations from isolated HeLa cell mitochondria. It is thus unlikely that the small circles arise from an artifact in the electron-microscope procedure. A more definitive characterization of these small DNA molecules, which can code for only 200–3500 amino acid residues, requires the preparation of larger quantities of material. The frequency of occurrence of the small molecules in the SDS extracts we have studied does not necessarily represent the frequency of occurrence in the HeLa cell. It is emphasized here that the dye-buoyant method segregates only *closed* circular duplexes. Molecules that contain even one single-strand scission, for whatever reason, find their way to the less dense band and, in whole cell extracts, intermingle with the large excess of linear DNA.

The larger-size circles, which were also seen at a frequency of about 10 per cent relative to mitochondrial DNA in the dense band, are clearly multiples of the mitochondrial length. The mean lengths from measurements of 43 double-length circles and a smaller number of larger multiples were 9.56 ± 0.42, 14.1 ± 0.4, and 19.8 ± 1.1 microns. We have so far not found a fully extended large circle. Nor have we found, in the several large circles which contain infrequent crossovers, any one which could not have arisen from a pairing of two or more mitochondrial molecules. An investigation of the significance of these multiple-size circles in HeLa DNA is in progress. Nass[17] has reported measurements of multiple lengths of mitochondrial molecules liberated from mitochondria by osmotic shock during specimen preparation. She attributed the multiples to the superposition of DNA molecules which originated from single mitochondria.

Summary.—A buoyant-density method for the isolation and detection of closed circular DNA is described. The method is based on the reduced binding of the intercalating dye, ethidium bromide, by closed circular DNA. In an application of this method we have found that HeLa cells contain, in addition to closed circular mitochondrial DNA of mean length, 4.81 microns, a heterogeneous group of smaller DNA molecules which vary in size from 0.2 to 3.5 microns and a paucidisperse group of multiples of the mitochondrial length.

Note added in proof: That double-length closed mitochondrial DNA molecules do occur has been shown by D. Clayton in this laboratory with preparations from leucocytes obtained from the blood of a donor with chronic granulocytic leukemia. Circular DNA molecules free of cross-overs and of twice the mitochondrial length were observed in electron micrographs.

It is a pleasure to thank J. Huberman for providing us with the labeled HeLa cells; J. Kiger and E. T. Young, II, for their gift of closed circular lambda DNA and for allowing us to quote their unpublished analysis; G. Attardi for advice and assistance in the preparation of HeLa mitochondria; L. Wenzel and J. Eden for their assistance in the culture of the polyoma virus; R. Watson for his several technical contributions; and R. Kent for assistance in the preparation of the manuscript.

* This work was supported in part by grants HE 03394 and CA 08014 from the U.S. Public Health Service and by fellowships from the U.S. Public Health Service and the National Science Foundation.

† Contribution 3490 from the Laboratories of Chemistry.

[1] Dulbecco, R., and M. Vogt, these PROCEEDINGS, 50, 236 (1963).

[2] Weil, R., and J. Vinograd, these PROCEEDINGS, 50, 730 (1963).

[3] Borst, P., and G. J. C. M. Ruttenburg, *Biochim. Biophys. Acta*, 114, 645 (1965).

[4] Kroon, A. M., P. Borst, E. F. J. Van Bruggen, and G. J. C. M. Ruttenburg, these PROCEEDINGS, 56, 1836 (1966).

[5] Pikó, L., A. Tyler, and J. Vinograd, *Biol. Bull.*, in press.

[6] Crawford, L. V., and P. H. Black, *Virology*, 24, 388 (1964).

[7] Crawford, L. V., *J. Mol. Biol.*, 8, 489 (1964).

[8] *Ibid.*, 13, 362 (1965).

[9] Burton, A., and R. L. Sinsheimer, *J. Mol. Biol.*, 14, 3276 (1965).

[10] Kleinschmidt, A. K., A. Burton, and R. L. Sinsheimer, *Science*, 142, 1961 (1963).

[11] Young, E. T., II, and R. L. Sinsheimer, *J. Mol. Biol.*, 10, 562 (1964).

[12] Bode, V. C., and A. D. Kaiser, *J. Mol. Biol.*, 14, 399 (1965).

[13] Play, D. S., A. Preuss, and P. H. Hofschneider, *J. Mol. Biol.*, 21, 485 (1966).

[14] Rhoades, M., and C. A. Thomas, private communication.

[15] Roth, T., and D. Helinski, private communication.

[16] David, I. B., these PROCEEDINGS, 56, 269 (1966).

[17] Nass, M. M. K., these PROCEEDINGS, 56, 1215 (1966).

[18] Hotta, Y., and A. Bassel, these PROCEEDINGS, 53, 356 (1965).

[19] Vinograd, J., J. Lebowitz, R. Radloff, R. Watson, and P. Laipis, these PROCEEDINGS, 53, 1104 (1965).

[20] Vinograd, J., and J. Lebowitz, *J. Gen. Physiol.*, 49, 103 (1966).

[21] Vinograd, J., R. Bruner, R. Kent, and J. Weigle, these PROCEEDINGS, 49, 902 (1963).

[22] M. Gellert, these PROCEEDINGS, 57, 148 (1967).

[23] Bauer, W. R., and J. Vinograd, in preparation.

[24] Crawford, L. V., and M. J. Waring, *J. Mol. Biol.*, in press.

[25] Kersten, W., H. Kersten, and W. Szybalski, *Biochemistry*, 5, 236 (1966).

[26] Waring, M. J., *Biochim. Biophys. Acta*, 114, 234 (1966).

[27] Le Pecq, J., Dissertation, University of Paris (1965).

[28] Hirt, B., these PROCEEDINGS, 55, 997 (1966).

[29] Kleinschmidt, A. K., and R. K. Zahn, *Z. Naturforsch.*, 14b, 770 (1959).

[30] LePecq, J., and C. Paoletti, *Anal. Biochem.*, 17, 100 (1966).

[31] Young, E. T., II, and R. L. Sinsheimer, private communication.

ERRATUM

In the article entitled "A Dye–Buoyant-Density Method for the Detection and Isolation of Closed Circular Duplex DNA: The Closed Circular DNA in HeLa Cells," by Roger Radloff, William Bauer, and Jerome Vinograd, which appeared in the May 1967 issue of these PROCEEDINGS (vol. 57, pp. 1514–1521), the following change should be made at the top of page 1516:

"..., and the constant density gradient is equal to approximately 0.10 [not 0.010] gm/cm^4...."

JEROME VINOGRAD

Part II

A THERMODYNAMIC THEORY FOR INTERACTING SYSTEMS AT EQUILIBRIUM IN A BUOYANT DENSITY GRADIENT: THE REACTION BETWEEN A SMALL MOLECULAR SPECIES AND A BUOYANT MACROMOLECULE

INTRODUCTION

Buoyant density centrifugation experiments[1] are normally performed in concentrated binary solvents, such as aqueous 5.8 M CsCl or 2.1 M Cs_2SO_4. Preferential interactions take place in such systems between the macrospecies and the two solvent components. The preferential solvation of CsDNA by water in a buoyant density gradient of CsCl, for example, gives rise to a buoyant complex with a specific volume of typically 0.588 ml/g as compared with the anhydrous value of 0.479 ml/g.[2] The preferential hydration may be calculated directly from the buoyant density and the partial specific volumes of anhydrous DNA and water.[3] Hearst and Vinograd[4] determined the variation of Γ, the preferential hydration parameter, with water activity in a variety of buoyant salt solutions. It was assumed in this work that the buoyant density is unaffected by the chemical nature of the anion in buoyant cesium salts. The preferential hydration calculated from the buoyant density was found to vary monotonically with the water activity. The quantitative relationship has been confirmed over part of the water activity range by Hearst.[5]

The buoyant density, θ, is an intensive thermodynamic variable which depends upon temperature, pressure, and the composition of the system. In addition, the buoyant density is sensitive to changes in structure of the macromolecule, such as occur upon denaturation of DNA and of proteins. The method is widely used to assess the base composition of DNA, and to separate DNA's which differ in base

composition, structure, or isotope content. The method is also used to separate and purify nucleic acids, proteins, and nucleoproteins such as viruses.

The addition of further chemical reagents to the three component system described above will in general give rise to chemical reactions which modify the equilibrium distributions. The addition of CsBr to buoyant CsDNA in CsCl lowers the buoyant density,[6] whereas the addition of $HgCl_2$ to buoyant CsDNA in Cs_2SO_4 raises the buoyant density by an amount which depends upon the base composition.[7] The binding of antibiotics to DNA in CsCl or in Cs_2SO_4 lowers the buoyant density.[8] Intercalating dyes, which lower the buoyant density of CsDNA in CsCl, have been used to separate closed circular DNA from nicked circular DNA.[9,10] The alkaline titration of denatured DNA increases the buoyant density,[11] and the binding of polyribonucleotides by denatured DNA increases the buoyant density by an amount which apparently depends upon the primary structure of the DNA strands.[12] Another example of polymer-polymer interactions is the joining of the sheared halves of λ DNA, which have different buoyant densities, to form hydrogen bonded whole molecules of an intermediate buoyant density.[13]

In order to understand these important, more complex systems at buoyant equilibrium it is necessary to extend the previous thermodynamic analysis. We present here a general theory for a buoyant system which contains one additional reacting component. The theory is developed in detail for the interactions of a small molecular species with a macromolecule. The buoyant density is defined in terms of the partial specific volumes and the preferential solvation and binding

parameters of the interacting components. It may be used to calculate the binding isotherm for the reagent. The buoyant density extrapolated to atmospheric pressure, which is termed here the standard buoyant density, is shown to be a thermodynamic function which characterizes the four-component system. Expressions are obtained for the concentration distributions of the free reagent and the hydrated reagent-macromolecule complex, as well as for the distribution of the free water. The concentration distribution of the solvated macrospecies is shown to be Gaussian to first order. The relationship between band width and the solvated molecular weight is derived and is found to be formally similar to the result obtained in the three-component system.[14] The effects of the fourth component upon the density gradients which characterize the system are analyzed, and procedures are developed for calculating the buoyant density by both the absolute and the marker methods. The theory is applied to the specific cases of the binding of ethidium bromide, an intercalating dye, to DNA and of the binding of mercury and silver to DNA.

The theory for reacting systems at sedimentation equilibrium in the analytical ultracentrifuge has been developed by other authors for systems having different initial and boundary conditions from those described here. In general, these analyses have been developed for experiments conducted in the presence of low salt concentrations, so that the molecular species of interest are distributed monotonically throughout the cell at equilibrium. The condition for buoyancy, that the polymer concentration distribution have an analytical maximum value within the centrifuge cell, has not been applied to these systems.

Van Holde and Rossetti[15] have developed equations to describe the association of a low molecular weight species, purine, at sedimentation equilibrium. Adams and associates[16] have examined reacting systems which involve polymer-polymer association, and have calculated equilibrium constants with the inclusion of non-ideality terms. They studied the association reactions of α-chymotrypsin and of lysozyme. Nichol and Ogston[17] developed the theory for reacting systems of the type $mA + nB \rightleftharpoons C$, where a new molecular species is formed. Steinberg and Schachman[18] analyzed the binding of small molecules to macromolecules, in particular the binding of methyl orange to bovine plasma albumin.

THEORY

(a) The Buoyant Density of the Complex

The thermodynamic theory for a four-component reacting system at equilibrium in the ultracentrifuge may be derived in a manner analogous to the treatment of Hearst and Vinograd[14] for a three-component system consisting of water, neutral salt, and neutral macromolecule, components 1, 2, and 3, respectively. The additional component, which will be considered to have a low molecular weight compared to the macromolecule and which reacts with it to form a molecular complex, will be designated neutral reagent, 4. The thermodynamic differential equations which describe the four-component system may be written[19] in terms of the chemical potentials, μ_i, and molalities, m_i.

$$M_1(1 - \bar{v}_1\rho)\omega^2 r dr = (\partial \mu_1/\partial m_1)_{m_3, m_4} dm_1 +$$

$$(\partial \mu_1/\partial m_3)_{m_1, m_4} dm_3 + (\partial \mu_1/\partial m_4)_{m_1, m_3} dm_4 \quad (1a)$$

$$M_3(1 - \bar{v}_3\rho)\omega^2 r dr = (\partial \mu_3/\partial m_1)_{m_3, m_4} dm_1 +$$

$$(\partial \mu_3/\partial m_3)_{m_1, m_4} dm_3 + (\partial \mu_3/\partial m_4)_{m_1, m_3} dm_4 \quad (1b)$$

$$M_4(1 - \bar{v}_4\rho)\omega^2 r dr = (\partial \mu_4/\partial m_1)_{m_3, m_4} dm_1 +$$

$$(\partial \mu_4/\partial m_3)_{m_1, m_4} dm_3 + (\partial \mu_4/\partial m_4)_{m_1, m_3} dm_4, \quad (1c)$$

where M_i and $\bar{v}_i$ are the molecular weight and partial specific volume of component i, ρ is the density of the solution at radial coordinate r, and ω is the angular velocity in radians/sec.

Equations (1a - 1c) may be written with Scatchard's compact notation[20]

$$M_1(1 - \bar{v}_1\rho)\omega^2 r dr = a_{11} dm_1 + a_{13} dm_3 + a_{14} dm_4 \quad (2a)$$

$$M_3(1 - \bar{v}_3\rho)\omega^2 r dr = a_{31} dm_1 + a_{33} dm_3 + a_{34} dm_4 \quad (2b)$$

$$M_4(1 - \bar{v}_4\rho)\omega^2 r dr = a_{41} dm_1 + a_{43} dm_3 + a_{44} dm_4, \quad (2c)$$

where $a_{ij} = (\partial \mu_i/\partial m_j)_{m_i, m_k}$ for i, j, k = 1, 3, 4 and i, j $\neq$ k. Since the values of the second derivatives are independent of the order of differentiation if the concentrations are expressed in molality, the cross terms in Eqs. (2a - 2c) are related by $a_{ij} = a_{ji}$ for i, j = 1, 3, 4. The preferential solvation parameters, Γ_{ij}, are defined for each pair of

components by the relationship

$$\Gamma_{ij} \equiv -(\partial\mu_i/\partial m_j)_{m_i, m_k}/(\partial\mu_i/m_i)_{m_j, m_k} \tag{3a}$$

or, in the simplified notation,

$$\Gamma_{ij} \equiv -a_{ij}/a_{ii} \tag{3b}$$

where i, j and k vary as in Eqs. (2). It may be shown with the triple product rule that

$$\Gamma_{ij} = (\partial m_i/\partial m_j)_{\mu_i, \mu_k} . \tag{4a}$$

Equation (3b) and the cross product identities for a_{ij} are combined to obtain the subscript permutation relations between the solvation parameters

$$\Gamma_{ij}a_{ii} = \Gamma_{ji}a_{jj} . \tag{4b}$$

The Eqs. (2a - 2c) describing the four-component system may now be written with the solvation parameters substituted for the cross terms, a_{ij},

$$M_1(1 - \bar{v}_1\rho)\omega^2 r dr = a_{11}dm_1 - \Gamma_{13}a_{11}dm_3 - \Gamma_{14}a_{11}dm_4 \tag{5a}$$

$$M_3(1 - \bar{v}_3\rho)\omega^2 r dr = -\Gamma_{13}a_{11}dm_1 + a_{33}dm_3 - \Gamma_{43}a_{44}dm_4 \tag{5b}$$

$$M_4(1 - \bar{v}_4\rho)\omega^2 r dr = -\Gamma_{14}a_{11}dm_1 - \Gamma_{43}a_{44}dm_3 + a_{44}dm_4 . \tag{5c}$$

In order to describe the system, we have chosen the preferential solvation parameters Γ_{13}, moles water per mole neutral polymer, Γ_{43}, moles neutral reagent per mole neutral polymer, and Γ_{14}, moles water per

mole neutral reagent. The remaining solvation parameters are determined by Eq. (4b).

The quantities dm_1 and dm_4 are eliminated from Eqs. (5) to obtain the distribution of polymer molality. Focusing attention first on Eqs. (5a) and (5c), we eliminate dm_1

$$[M_4(1 - \overline{v}_4\rho) + M_1\Gamma_{14}(1 - \overline{v}_1\rho)]\omega^2 r = \alpha \frac{dm_3}{dr} + \beta \frac{dm_4}{dr} \quad , \tag{6}$$

where $\alpha = \Gamma_{13}\Gamma_{14}a_{11} + \Gamma_{43}a_{44}$ and $\beta = a_{44} - \Gamma_{44}^2 a_{11}$. Equations (5a) and (5b) are then combined for the second elimination of dm_1

$$[M_3(1 - \overline{v}_3\rho) + M_1\Gamma_{13}(1 - \overline{v}_1\rho)]\omega^2 r = \gamma \frac{dm_3}{dr} - \alpha \frac{dm_4}{dr} \quad , \tag{7}$$

where $\gamma = a_{33} - \Gamma_{13}^2 a_{11}$. The result for the polymer distribution is obtained upon elimination of dm_4 from Eqs. (6) and (7)

$$\{M_3(1 - \overline{v}_3\rho) + M_1\Gamma_{13}(1 - \overline{v}_1\rho) + \frac{\alpha}{\beta}[M_4(1 - \overline{v}_4\rho) + M_1\Gamma_{14}(1 - \overline{v}_1\rho)]\} = (\gamma - \frac{\alpha^2}{\beta})\frac{dm_3}{dr} \quad . \tag{8}$$

The coefficients present in Eq. (8) are related by the thermodynamic identities

$$\gamma - \frac{\alpha^2}{\beta} = (\frac{\partial \mu_3}{\partial m_3})_{\mu_1, \mu_4} = a_{33} + \Gamma_{13}^2 a_{11} + \Gamma_{43}^2 a_{44} \tag{9}$$

and

$$\frac{\alpha}{\beta} = (\frac{\partial m_4}{\partial m_3})_{\mu_1, \mu_4} \, . \tag{10}$$

The polymer concentration is generally sufficiently low that the ideality assumption may be used, $(\partial \mu_3 / \partial m_3)_{\mu_1, \mu_4} = RT/m_3$. In order to examine the validity of this ideality assumption in greater detail,

the general condition for stability of the band is considered. With the above ideality assumption and the definition of γ,

$$\frac{\alpha^2}{\beta} = a_{33} - \Gamma_{13}^2 a_{11} - \frac{RT}{m_3} \quad . \tag{11}$$

The right side of Eq. (8) may then be written

$$(\gamma - \frac{\alpha^2}{\beta}) \frac{dm_3}{dr} = a_{33} \frac{dm_3}{dr} (1 - \epsilon) , \tag{12}$$

where

$$\epsilon = \frac{1}{a_{33}} (\Gamma_{13}^2 a_{11} + \alpha^2/\beta) . \tag{13}$$

The general stability condition[14] is $(1 - \epsilon) > 0$. Equations (9), (11) and (13) are combined

$$\epsilon = \frac{\Gamma_{13}^2 a_{11} + \Gamma_{43}^2 a_{44}}{\frac{RT}{m_3} + \Gamma_{13}^2 a_{11} + \Gamma_{43}^2 a_{44}} . \tag{14}$$

The assumption of the ideality condition for $(\partial \mu_3 / \partial m_3)_{\mu_1, \mu_4}$ is sufficient to assure that $\epsilon < 1$. It follows that the product $(dm_3/dr)(r - r_0) > 0$ everywhere, and a stable band will be formed around the position of the concentration maximum at r_0. The ideality assumption used above is equivalent to the requirement of independently solvated macromolecules, which is in accord with the observed gaussian shape of buoyant bands in the four-component system studied by Bauer and Vinograd.[10]

The specific solvation parameters are defined by $\Gamma'_{ij} = \Gamma_{ij}(M_i/M_j)$, where $i, j = 1, 3, 4$. The equilibrium polymer distribution, Eq. (8), with the specific solvation parameters and Eq. (9) becomes

$$M_3\{1+\Gamma'_{13}+\Gamma'_{43}(1+\Gamma'_{14})\}\{1-[\frac{\bar{v}_3+\Gamma'_{13}\bar{v}_1+\Gamma'_{43}(\bar{v}_4+\Gamma'_{14}\bar{v}_1)}{1+\Gamma'_{13}+\Gamma'_{43}(1+\Gamma'_{14})}]\rho\}\omega^2 r$$

$$= (\frac{\partial\mu_3}{\partial m_3})_{\mu_1,\mu_4}\frac{dm_3}{dr} \quad . \tag{15}$$

The polymer concentration is at a maximum at band center and $dm_3/dr = 0$. The buoyancy condition for the solvated macrospecies is

$$\rho_0 = \frac{1+\Gamma'_{13}+\Gamma'_{43}(1+\Gamma'_{14})}{\bar{v}_3+\Gamma'_{13}\bar{v}_1+\Gamma'_{43}(1+\Gamma'_{14})\bar{v}_{4,s}} \quad , \tag{16}$$

where ρ_0 is the density of the solution at band center, and $\bar{v}_{4,s} = (\bar{v}_4+\Gamma'_{14}\bar{v}_1)/(1+\Gamma'_{14})$ is the hydrated partial specific volume of the bound reagent. Equation (16) is the exact relationship for the density of the solution at band center in a four-component reacting system. If the approximation is made that $\Gamma'_{14} \ll 1$, the simpler form is obtained,

$$\rho_0 = \frac{1+\Gamma'_{13}+\Gamma'_{43}}{\bar{v}_3+\Gamma'_{13}\bar{v}_1+\Gamma'_{43}\bar{v}_4} \quad . \tag{17}$$

This approximation is especially useful in, for example, the binding of an intercalating dye to DNA. In such a case the dye moiety is placed in a non-aqueous environment, and the preferential hydration of the dye may be assumed to be very small. A further simplification of this equation is discussed in the next section.

The physical interpretation of the preferential hydration parameter, Γ_{13}, is complicated by a lack of knowledge of the structure of the aqueous layer which surrounds the macromolecular complex. This problem has been discussed by Hearst and Vinograd.[14] In the case of

the intercalation of dye between the base pairs of DNA, however, the preferential solvation of DNA by dye, Γ_{43}, may be interpreted as the binding ratio, moles dye per mole nucleotide. In this interpretation it is assumed that the binding does not involve counterion exchange, which is reasonable for either an uncharged reagent or for binding of an ionic species in a region in which binding is independent of the salt concentration. This interpretation is substantiated for the system containing DNA and ethidium bromide by the results presented elsewhere.[10]

If attention is restricted to the molecules at band center, the four-component system may be regarded as a three-component system consisting of water, salt, and a macromolecular complex containing Γ'_{43} grams of reagent bound per gram of unsolvated macromolecule. This treatment ignores all effects of the redistribution of reagent under the influence of the centrifugal field upon the band of macrospecies, which actually consists of a heterogeneous collection of molecules having constant composition at a given radial lamella. The net hydration of T4 DNA, Γ', was determined as a function of buoyant density in the three-component system by Hearst and Vinograd.[4] The preferential hydration in the four-component system is a function of the water activity, pressure, and free reagent concentration

$$d\Gamma'_{13} = \left(\frac{\partial \Gamma'_{13}}{\partial a_1}\right)_{m_4, P} da_1 + \left(\frac{\partial \Gamma'_{13}}{\partial P}\right)_{a_1, m_4} dP + \left(\frac{\partial \Gamma'_{13}}{\partial m_4}\right)_{a_1, P} dm_4. \tag{18a}$$

In many cases of interest, m_4 is small and the presence of the free reagent contributes only a second order effect to the first two terms of Eq. (18a). It may then be assumed that $(\partial \Gamma'_{13}/\partial a_1)_{m_4, P}$ and

$(\partial \Gamma'_{13}/\partial P)_{a_1, m_4}$ are independent of m_4. The coefficient in the third term of Eq. (18a) represents the change in the preferential hydration of the macromolecule at constant pressure and water activity as the amount of bound reagent is varied. In the absence of knowledge of this quantity it is assumed to be negligible and is set equal to zero. This assumption appears to be justified in the case of intercalating materials which do not grossly modify the hydrophobic character of DNA, as in the binding of ethidium bromide, silver and mercury, discussed below. The quantity $(\partial \Gamma'_{13}/\partial m_4)_{a_1, P}$ may well be significant for the binding of reagents, such as proteins or other molecules containing large organic residues, to the outside of the DNA molecule.

If the above two assumptions are adopted, Eq. (18a) may be written in the simpler form

$$d\Gamma'_{13} \approx \left(\frac{\partial \Gamma'_{13}}{\partial a_1}\right)_P da_1 + \left(\frac{\partial \Gamma'_{13}}{\partial P}\right)_{a_1} dP = d\Gamma' . \tag{18b}$$

We further introduce into Eq. (17) the symbol ν' for Γ'_{14}, which is valid under similar assumptions. Equation (17) may then be written

$$\rho_0 = \frac{1 + \Gamma' + \nu'}{\overline{v}_3 + \Gamma' \overline{v}_1 + \nu' \overline{v}_4} . \tag{19}$$

It should be stressed that the quantity ν' is a <u>net</u> binding ratio, and that the $\overline{v}_4$ which appears in Eq. (19) is an <u>effective</u> partial specific volume for the bound reagent. These quantities are equal to the actual weight binding ratio and the real partial specific volume in the case of binding reactions which consist of simple addition of neutral reagent to macrospecies. Several reaction types are possible for the binding of X^+Cl^- to

Cs^+HP^-, and these may be written

(a) $X^+Cl^- + Cs^+HP^- \rightleftharpoons Cs^+HP^- \cdot X^+Cl^-$

(b) $X^+Cl^- + Cs^+HP^- \rightleftharpoons X^+HP^- + Cs^+Cl^-$

(c) $X^+Cl^- + Cs^+HP^- \rightleftharpoons X^+Cs^+P^= + H^+Cl^-$

(d) $X^+Cl^- + OH^- + Cs^+HP^- \rightleftharpoons X^+Cs^+P^= + H_2O.$

Ethidium bromide appears to bind by mechanism (a), as is shown below. Reaction type (b) presumably occurs for any reagent, such as Mg^{++} or Mn^{++}, which binds to DNA phosphate residues. Type (c) is known to occur for binding of Hg^{++} ion to DNA in Cs_2SO_4,[7] and is applicable also to the binding of Ag^+ to DNA in Cs_2SO_4 over part of the binding range.[21] Mechanism (d) is followed in the alkaline buoyant density titration of DNA.[11]

In general, the binding of one mole of neutral reagent may displace n moles of neutral salt. If x is the molecular weight ratio of the neutral salt displaced to the neutral reagent bound, Eq. (19) may be expanded with the assumption of additive volumes to

$$\rho_0 = \frac{1 + \Gamma' + \nu' - nx\nu'}{\bar{v}_3 + \Gamma'\bar{v}_1 + \nu'\bar{v}_4 - nx\nu'\bar{v}_y}, \tag{20}$$

where $\bar{v}_y$ is the partial specific volume of the neutral species displaced. This may be written in the alternative form

$$\rho_0 = \frac{1 + \Gamma' + \nu''}{\bar{v}_3 + \Gamma'\bar{v}_1 + \nu''\bar{v}_{4,\,\mathrm{eff}}} \tag{21a}$$

where

$$\nu'' = \nu'(1 - nx) \tag{21b}$$

and $$\bar{v}_{4,\,eff} = \frac{\bar{v}_4 - nx\bar{v}_y}{1 - nx} . \qquad (21c)$$

For the binding of ethidium bromide to SV40 DNA, it has been determined experimentally that $\bar{v}_{4,\,eff} = \bar{v}_4$, and hence n = 0 for this reaction.[10] Cases are examined later (see Discussion) in which n = 1 and n = 2.

(b) The Standard Buoyant Density

The buoyant density, θ, is defined as the density of the solution at band center, corrected to atmospheric pressure with the relationship[14] $\theta = \rho_0(1 - \kappa P_0)$, where κ is the isothermal compressibility of the solution and P_0 is the pressure above atmospheric pressure at band center. The buoyant density is also a function of water activity and of the concentration of free reagent at band center, and these quantities also depend upon the pressure. The standard buoyant density, Θ', is defined as the buoyant density at 25° characteristic of a macrospecies at a specified salt and free reagent concentration in the absence of the centrifugal field.

$$\Theta' = \lim_{P \to 0} (\theta) . \qquad (22)$$

This quantity is independent of the experimental method employed for the measurements. In order to obtain the expressions for the standard buoyant density we expand about atmospheric pressure, P = 0, and set

$$\bar{v}_{3S,o} = (\bar{v}_{3S,o})_{P\to 0} + (\partial \bar{v}_{3S,o}/\partial P)_{P=0} P_o$$

$$+ (\partial \bar{v}_{3S,o}/\partial a_{1,o})_{P=0} \Delta a_{1,o} + (\partial \bar{v}_{3S,o}/\partial m_{4f,o})_{P=0} \Delta m_{4f,o} \quad (23)$$

where $(\bar{v}_{3S,o})_{P\to 0} \equiv 1/\epsilon'$ and the quantities $\Delta a_{1,o}$ and $\Delta m_{4f,o}$ represent the changes in water activity and free reagent molality at band center when the pressure is increased from zero to the pressure at band center, P_o. Since $\rho^o = \rho^o(a_1^o)$ and $\bar{v}_{3S,o} = \bar{v}_{3S,o}(a_1^o)$, we may write, at constant m_{4f}

$$\left(\frac{\partial \bar{v}_{3S,o}}{\partial a_1^o}\right)_{P=0} = -\frac{1}{\theta^2}\left(\frac{\partial \theta}{\partial a_1^o}\right)_{P=0} \quad (24a)$$

$$\frac{1}{(\bar{v}_{3S,o})_{P\to 0}}\left(\frac{\partial \bar{v}_{3S,o}}{\partial a_1^o}\right) = -\frac{1}{\theta}\left(\frac{\partial \theta}{\partial a_1^o}\right)_{P=0}. \quad (24b)$$

Hearst and Vinograd[14] have defined the apparent compressibility for the hydrated polymer in a three-component buoyant system.

$$\kappa_{3S} \equiv \frac{1}{\bar{v}_S}\left(\frac{\partial \bar{v}_S}{\partial P}\right)_{a_1^o}. \quad (25a)$$

Extending this definition to the four-component system we have, to first order,

$$\kappa_{4S} = \frac{1}{\bar{v}_{3S,o}}\left(\frac{\partial \bar{v}_{3S}}{\partial P}\right)_{a_1^o, m_{4f}} \quad (25b)$$

Combining these results at atmospheric pressure,

$$(\partial \overline{v}_{3S,0}/\partial P)_{P=0} = -\kappa_{4S}(\overline{v}_{3S,0})_{P\to 0} \cdot \tag{25c}$$

The change in the water activity distribution due to the redistribution of salt in the centrifugal field may be written, at constant m_{4f},

$$\Delta a_{1,0} = \frac{da_{1,0}}{d\rho^0}\left(\theta - \frac{1}{(\overline{v}_{3S,0})_{P\to 0}}\right) . \tag{26}$$

Similarly, the redistribution terms which arise from the free reagent may be written, at constant a_1^0,

$$(\partial \overline{v}_{3S,0}/\partial m_{4f,0})_{P=0} = -\frac{(\overline{v}_{3S,0})_{P\to 0}}{\theta}\left(\frac{\partial \theta}{\partial m_{4f,0}}\right)_P \tag{27}$$

and

$$\Delta m_{4f,0} = \frac{dm_{4f,0}}{d\rho^0}\left(\theta - \frac{1}{(\overline{v}_{3S,0})_{P\to 0}}\right) . \tag{28}$$

These results are combined to obtain the expression for the standard buoyant density.

$$\overline{v}_{3S,0} = (\overline{v}_{3S,0})_{P\to 0} - \kappa_{4S}(\overline{v}_{3S,0})_{P\to 0}\, P_0$$

$$- \frac{(\overline{v}_{3S,0})_{P\to 0}}{\theta}\left(\frac{\partial\theta}{\partial a_1^0}\right)_P \frac{da_1^0}{d\rho^0}\left(\theta - \frac{1}{(\overline{v}_{3S,0})_{P\to 0}}\right)$$

$$- \frac{(\overline{v}_{3S,0})_{P\to 0}}{\theta}\left(\frac{\partial\theta}{\partial m_{4f,0}}\right)_P \frac{dm_{4f,0}}{d\rho^0}\left(\theta - \frac{1}{(\overline{v}_{3S,0})_{P\to 0}}\right). \quad (29)$$

Equation (29) is written in a more compact form by the introduction of the parameters $\alpha_3 = \alpha_{13} + \alpha_{43}$, where

$$\alpha_{13} \equiv \left(\frac{\partial\theta}{\partial a_1^0}\right)_{P,\, m_{4f}} \frac{da_1^0}{d\rho^0} \quad (30a)$$

and

$$\alpha_{43} \equiv \left(\frac{\partial\theta}{\partial m_{4f}}\right)_{P,\, a_1^0} \frac{dm_{4f}}{d\rho^0}. \quad (30b)$$

The result is then obtained that

$$\overline{v}_{3S,0} = (\overline{v}_{3S,0})_{P\to 0}\left[1 - \kappa_{4S}P_0 - \frac{\alpha_3}{\theta}\left(\theta - (\overline{v}_{3S,0})_{P\to 0}\right)\right] \quad (31)$$

or, in terms of the buoyant densities,

$$\Theta' = \theta/[1 - \psi_4 P_0], \quad (32a)$$

where

$$\psi_4 = \frac{\kappa - \kappa_{4S}}{1 - \alpha_3}. \quad (32b)$$

The coefficient ψ_4 represents the total pressure dependence of the buoyant density in the four-component system. In the three-component system the corresponding quantity[14] is, in the present notation

$$\psi_3 = (\kappa - \kappa_{3S})/(1 - \alpha_{13}) . \qquad (32c)$$

In Eq. (32c) the notational changes are from ψ to ψ_3, α to α_{13}, and κ_S to κ_{3S}. The parameter ψ_3 was determined for T4 DNA in CsCl from a study of the pressure dependence of θ and was found to have the value 23.3×10^{-12}cgs.[22] In the presence of added reagent, ψ_4 also depends upon reagent concentration in two ways: the reagent gradient is represented in the additional term α_{43}, and the altered apparent compressibility of the macrospecies is contained in κ_{4S}. In general, the estimation of ψ_4 will require a study of the pressure dependence of θ as a function of the concentration of free reagent present in the system.

An alternate procedure is to estimate the value of ψ_4 with the aid of Eqs. (30a, b) and (32b). This calculation is carried out for the special case of binding of a reagent to DNA with independent binding sites, a situation to which the mass action law applies in a simple form. In addition, it is assumed that α_{13} and κ_{4S} are independent of the free reagent concentration at constant water activity and pressure. We then use the data of Hearst and Vinograd[4] and of Hearst, Ifft, and Vinograd[22] to estimate α_{13} from the buoyant density, θ, in the presence of dye.

The calculation of α_{43} proceeds from the formulation of Eq. (30b). Differentiating Eq. (19), we have

$$\left(\frac{\partial \theta}{\partial m_{4f}}\right)_{P,a_1^0} = \frac{\bar{v}_3 - \bar{v}_4 - \Gamma'(\bar{v}_1 - \bar{v}_4)}{(\bar{v}_3 + \Gamma'\bar{v}_1 + \nu'\bar{v}_4)^2} \left(\frac{\partial \nu'}{\partial m_{4f}}\right)_{P,a_1^0} , \qquad (33)$$

where the assumptions have been made that the anhydrous partial specific volumes are independent of the free reagent concentration, and that the pressure dependence of binding is small. It has also been assumed that $\theta \approx \rho_0$, an approximation which introduces an error of approximately 0.5% for DNA in CsCl in the analytical ultracentrifuge at 44,000 rpm. Since the above differentiation is carried out at constant water activity, it is necessary to assume further that the change in Γ' with free reagent molality is negligible at constant a_1^0. The evaluation of $(\partial \nu'/\partial m_{4f})_{a_1^0,P}$ depends upon the details of the binding interaction in the particular system under consideration. For the binding of an intercalating dye to DNA, the assumption of independent binding sites is justified over most of the reagent concentration range,[10] and the relation

$$\nu' = kc(\nu_m' - \nu') \qquad (34)$$

may be used, where k is the equilibrium constant of the binding reaction in liters/mole at a_1^0 and P, $c = Km_{4f}$ is the free reagent concentration in moles/liter, ν_m' is the maximum value attained by ν', and K is the proportionality constant between molarity and molality. Differentiating

Eq. (34), we obtain the result for the change of ν' with m_{4f} at constant a_1^0 and P

$$\left(\frac{\partial \nu'}{\partial m_{4f}}\right)_{a_1^0, P} = \frac{k}{\nu_m'} (\nu_m' - \nu')^2. \tag{35}$$

The dependence of the free reagent molality upon solution density at atmospheric pressure, $(dm_{4f}/d\rho^0)_{P=0}$, may be calculated from Eq. (42) with the further relation

$$\frac{d\ln m_{4f}}{d\rho^0} = \frac{d\ln m_{4f}}{dr} \left(\frac{d\rho^0}{dr}\right)^{-1} = \frac{\beta^0}{\omega^2 r} \frac{d\ln m_{4f}}{dr}, \tag{36a}$$

where the compositional density gradient[23] is

$$\frac{d\rho^0}{dr} = \left(\frac{1}{\beta^0}\right) \omega^2 r. \tag{36b}$$

The desired result is obtained

$$\frac{dm_{4f}}{d\rho^0} = \frac{M_{4f}(1 - \bar{v}_{4f}\, \rho^0)\beta^0 m_{4f}}{RT}. \tag{37}$$

The quantity α_{43} is obtained by combining Eqs. (33) through (37).

$$\alpha_{43} = -\frac{M_{4f}(1 - \bar{v}_{4f}\rho^0)\beta^0}{RT} \left(\frac{\nu'}{\nu_m'}\right) (\nu_m' - \nu') \left[\frac{\bar{v}_4 - \bar{v}_3 + \Gamma'(\bar{v}_4 - \bar{v}_1)}{(\bar{v}_3 + \Gamma' \bar{v}_1 + \nu' \bar{v}_4)^2}\right]. \tag{38}$$

The standard buoyant density, Θ', may then be calculated from Eqs. (32a,b), (30a), and (38). The standard buoyant density has the properties of a thermodynamic function and is fully determined by

the composition of the macromolecular complex at constant temperature and pressure. The standard buoyant density represents the buoyant density which would result from a measurement in an infinitely thin cell. Effects of the redistributions of salt and of free reagent are therefore removed from this quantity.

(c) The Distribution of Free Reagent

The total gradient in molality of the low molecular weight reagent in the presence of water and macrospecies is approximated by a first order Taylor series

$$\frac{dm_4}{dr} = \left(\frac{\partial m_4}{\partial r}\right)_{\Gamma_{41},\Gamma_{43}=0} + \Gamma_{41}\left(\frac{\partial m_1}{\partial r}\right)_{\Gamma_{43}} + \Gamma_{43}\left(\frac{\partial m_3}{\partial r}\right)_{\Gamma_{41}} . \qquad (39)$$

The gradient in molality of the free reagent is the sum of the first two terms on the right of Eq. (39) and is given by

$$\frac{dm_{4f}}{dr} = \frac{dm_4}{dr} - \Gamma_{43}\left(\frac{\partial m_3}{\partial r}\right)_{\Gamma_{41}} . \qquad (40)$$

Combination of Eqs. (6), (10), and (40) provides the solution for the free dye distribution,

$$\frac{dm_{4f}}{dr} = \frac{[M_{4f}(1 - \bar{v}_{4f}\rho) + M_1\Gamma_{14}(1 - \bar{v}_1\rho)]\omega^2 r}{a_{44} - \Gamma_{14}^2 a_{11}} . \qquad (41)$$

The presence of the macrospecies has no effect on the distribution of free dye, since Eq. (41) is the condition for equilibrium in a three-

component system consisting of neutral salt, water, and neutral reagent. If the molality of reagent is very small compared to that of water, the ideality assumption for the reagent may be introduced into Eq. (41). Introducing the specific solvation parameter into Eq. (41) we obtain

$$\frac{d\ln m_{4f}}{dr} = \frac{M_{4f,h}(1 - \bar{v}_{4f,h}\rho)\omega^2 r}{RT} , \tag{42}$$

where $M_{4f,h} = M_{4f}(1 + \Gamma_{14}')$ and $\bar{v}_{4f,h} = (\bar{v}_{4f} + \Gamma_{14}'\bar{v}_1)/(1 + \Gamma_{14}')$. Except for the omission of the reagent activity coefficient, Eq. (42) is correct without approximation for the free reagent.

The distribution of free water is given by

$$\frac{dm_{1f}}{dr} = \frac{dm_1}{dr} - \Gamma_{13}\left(\frac{\partial m_3}{\partial r}\right)_{\Gamma_{43}} . \tag{43}$$

Combining Eqs. (2a,c) and (43), with elimination of dm_4, the free water distribution is

$$\frac{dm_{1f}}{dr} = \frac{[M_{1f}(1 - \bar{v}_{1f}\rho) + M_4\Gamma_{41}(1 - \bar{v}_4\rho)]\omega^2 r}{a_{11} - \Gamma_{41}^2 a_{44}} . \tag{44}$$

The distribution of water which is not bound to the macromolecular complex is thus determined by both the water and free reagent molalities. In many cases of interest, however, the reagent concentration is low enough that $\Gamma_{41} \ll 1$, and the distribution of free water is very nearly the same as in a two-component system consisting of water and neutral salt.

The calculation of the distribution of molality of the free reagent requires integration of Eq.(42). The variables in this equation which depend upon distance are approximated by a first order Taylor series about the CsCl isoconcentration coordinate, r_e.

$$\rho = \rho_e + (d\rho/dr)(r - r_e) \tag{45a}$$

$$M_{4f,h} = M_{4f,h,e} + (dM_{4f,h}/dr)(r - r_e) \tag{45b}$$

$$\bar{v}_{4f,h} = \bar{v}_{4f,h,e} + (d\bar{v}_{4f,h}/dr)(r - r_e) . \tag{45c}$$

In the derivation to follow we employ the abbreviated notations $\delta = r - r_e$, $\rho' = (d\rho/dr)$, $\underset{\sim}{M}_4' = (dM_{4f,h}/dr)$, $\underset{\sim}{\bar{v}}_4' = (d\bar{v}_{4f,h}/dr)$, $\underset{\sim}{M}_4 = M_{4f,h,e}$, and $\underset{\sim}{\bar{v}}_4 = \bar{v}_{4f,h,e}$. Equation (42) is rewritten in terms of these variables, and

$$\frac{RT}{\omega^2}\frac{d\ln m_{4f}}{dr} = \underset{\sim}{M}_4[1 - \underset{\sim}{\bar{v}}_4\rho] + \delta[\underset{\sim}{M}_4'(1 - \underset{\sim}{\bar{v}}_4\rho_e) - \underset{\sim}{M}_4(\underset{\sim}{\bar{v}}_4\rho' + \underset{\sim}{\bar{v}}_4'\rho_e)] . \tag{46}$$

Equation (46) is in a suitable form to be integrated, with the result

$$\ln\left(\frac{m_{4f}}{m_{4f,e}}\right) = \frac{\underset{\sim}{M}_4\omega^2(r^2 - r_e^2)}{2RT}\left\{\left[1 - \underset{\sim}{\bar{v}}_4\rho_e\right] + \left[\underset{\sim}{\bar{v}}_4\rho' r_e\right] + \left[\underset{\sim}{\bar{v}}_4' r_e\rho_e\right] - \left[\frac{\underset{\sim}{M}_4'}{\underset{\sim}{M}_4} r_e(1 - \underset{\sim}{\bar{v}}_4\rho_e)\right]\right\}$$
$$- \frac{\underset{\sim}{M}_4\omega^2(r^3 - r_e^3)}{3RTr_e}\left\{\left[\underset{\sim}{\bar{v}}_4\rho' r_e\right] + \left[\underset{\sim}{\bar{v}}_4' r_e\rho_e\right] - \left[\frac{\underset{\sim}{M}_4'}{\underset{\sim}{M}_4} r_e(1 - \underset{\sim}{\bar{v}}_4\rho_e)\right]\right\} . \tag{47}$$

In the integration the quantities $\underset{\sim}{M}_4'$, $\underset{\sim}{\bar{v}}_4$, and ρ' were assumed to be constant. The first term in the first brace in Eq. (47) represents the buoyancy of the hydrated reagent in a solution of constant density. The succeeding bracketed terms in each brace represent, in order, the contributions to the reagent redistribution of the gradients of density, hydrated partial specific volume, and hydrated molecular weight. The relationships following Eq. (42) which express the solvated molecular weight and partial specific volume of the free reagent in terms of the preferential hydration, $\gamma' \equiv \Gamma_{14}'$, may be differentiated to obtain

$$\underset{\sim}{\bar{v}}_4' = \frac{\bar{v}_1 - \underset{\sim}{\bar{v}}_4}{(1+\gamma')^2}\left(\frac{d\gamma'}{dr}\right) \tag{48a}$$

and

$$\underset{\sim}{M}_4' = \underset{\sim}{M}_4\left(\frac{d\gamma'}{dr}\right) . \tag{48b}$$

Equations (48a,b) are introduced into Eq. (47), and

$$\begin{aligned}\ln\left(\frac{m_{4f}}{m_{4f,e}}\right) = {} & \frac{\underset{\sim}{M}_4\omega^2(r^2 - r_e^2)}{2RT}\left\{1 - \underset{\sim}{\bar{v}}_4\rho_e + \underset{\sim}{\bar{v}}_4\rho' r_e + \frac{(\bar{v}_1 - \underset{\sim}{\bar{v}}_4)\rho_e r_e}{(1+\gamma')^2}\left(\frac{d\gamma'}{dr}\right)\right. \\ & \left. - \frac{(1 - \underset{\sim}{\bar{v}}_4\rho_e)}{(1+\gamma)} r_e\left(\frac{d\gamma'}{dr}\right)\right\} \\ & - \frac{\underset{\sim}{M}_4\omega^2(r^3 - r_e^3)}{3RTr_e}\left\{\underset{\sim}{\bar{v}}_4\rho' r_e + \frac{(\bar{v}_1 - \underset{\sim}{\bar{v}}_4)\rho_e r_e}{(1+\gamma')^2}\left(\frac{d\gamma'}{dr}\right)\right. \\ & \left. - \frac{(1 - \underset{\sim}{\bar{v}}_4\rho_e)}{(1+\gamma')} r_e\left(\frac{d\gamma'}{dr}\right)\right\} .\end{aligned} \tag{49}$$

For the case of a free reagent with anhydrous partial specific volume

$\bar{v}_4 \approx \bar{v}_1$, the terms of Eq.(49) which involve the gradient in $\bar{v}_4$ become negligible. If the more restrictive assumption is made that $(d\gamma'/dr) \approx 0$, Eq. (49) takes on the much simpler form

$$\ln\left(\frac{m_{4f}}{m_{4f,e}}\right) = \frac{\underset{\sim}{M}_4\omega^2(r_e^2 - r_e^2)}{2RT}\left\{1 - \underset{\sim}{\bar{v}}_4\rho_e + \underset{\sim}{\bar{v}}_4\rho' r_e\right\}$$

$$- \frac{\underset{\sim}{M}_4\omega^2(r^3 - r_e^3)}{3RTr_e}\left\{\underset{\sim}{\bar{v}}_4\rho' r_e\right\} \quad . \tag{50}$$

This case, in which the density of the solution is the only distance variable, will be examined in detail. We introduce the further substitutions

$$A^2 = \frac{\underset{\sim}{M}_4\omega^2\rho'\underset{\sim}{\bar{v}}_4 r_e^3}{RT} \tag{51a}$$

$$B = \frac{1 - \underset{\sim}{\bar{v}}_4\rho_e}{\underset{\sim}{\bar{v}}_4\rho' r_e} \tag{51b}$$

and

$$X = \frac{r}{r_e} \quad . \tag{51c}$$

In addition, we use the approximation that $dm_{4f}/m_{4f} = dc/c$, where c is the free reagent concentration in moles/liter.

The free reagent distribution throughout the cell at equilibrium may be obtained in a more useful form by integrating Eq. (46) from X_0, the normalized neutral reagent isoconcentration coordinate, to X, an arbitrary normalized coordinate in the cell,

$$\ln(c/c_0) = \tfrac{1}{2}(B + 1)A^2(X^2 - X_0^2) - \tfrac{1}{3}A^2(X^3 - X_0^3). \qquad (52)$$

Equation (52) holds for either the total reagent distribution in a three-component system or for the free reagent distribution in a four-component system, provided only that $(d\gamma'/dr) \approx 0$. In the former case the quantity c_0 is equal to the initial reagent concentration, whereas in the latter case c_0 represents the total moles of free reagent divided by the total solution volume. The condition of conservation of mass is

$$c_0 (X_b^2 - X_a^2) = \int_{X_a}^{X_b} c\,dX^2 \ , \qquad (53)$$

where a and b refer to the top and bottom of the liquid column respectively. Equations (52) and (53) are then combined to obtain the iso-concentration coordinate for the free reagent. This quantity is given implicitly by the relationship

$$X_0^3 - \frac{3}{2}(B + 1)X_0^2 + \frac{3}{A^2} \ln\left[\frac{I}{X_b^2 - X_a^2}\right] = 0, \qquad (54)$$

where

$$I = \int_{X_a}^{X_b} \exp\left\{\tfrac{1}{2}(B + 1)A^2X^2 - \tfrac{1}{3}A^2X^2\right\} dX^2 \ . \qquad (55)$$

Figure (1) presents a theoretical plot of Eq. (52) for the case of the redistribution of ethidium chloride in CsCl of density 1.65 g/ml. The parameters of Eq. (52) were calculated to be A = 3.104 and B = -0.8225

Fig. 1. The redistribution of ethidium chloride at equilibrium in the analytical ultracentrifuge in $\rho = 1.65$ g./ml. CsCl, 44,000 rpm, 25°. The experimental points, o, are plotted as normalized concentrations, c/c_0. The theoretical line was calculated with Eq. (52), as described in the text.

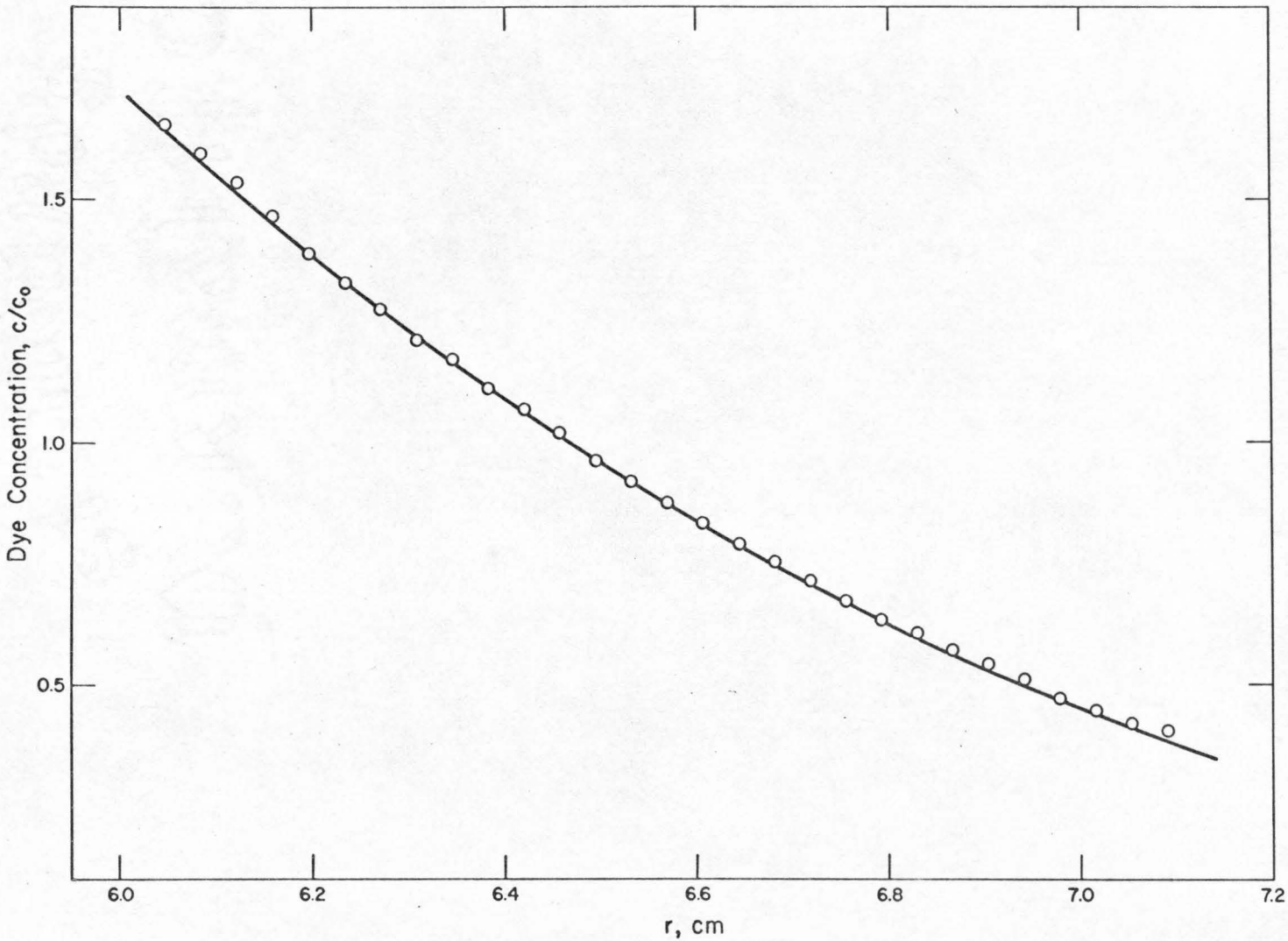
Dye Concentration, c/c₀
1.5
1.0
0.5
6.0
6.2
6.4
6.6
6.8
7.0
7.2
r, cm

with Eqs. (51a,b),and r_0 was calculated to be 6.469 cm. with Eqs. (51c), (54), and (55). The calculated curve is for 44,000 rpm, 25°, r_e = 6.601 cm., $\rho' = 0.115$ g ml^{-1} $cm.^{-1}$, $\underset{\sim}{M}_4 = M_4 = 349$, and $\bar{v}_4 = 0.975$ ml./g. The latter value was determined by a systematic variation of both γ' and $\bar{v}_4$. A computer least squares procedure was used to give the best fit to the experimental data, shown as circles on the plot. The best fit occurred at $\gamma' = 0$ and $\bar{v}_4 = 0.975$, and the curve is seen to be of the correct shape. The experimental data were obtained as described elsewhere.[10] In the event that the density gradient is very small, at a low concentration of neutral salt, or at low angular velocity, the cubic term in the distribution equations becomes negligible and Eq. (52) reduces to the well-known relationship for the redistribution in a two-component system in the absence of charge effects,

$$\ln(c/c_0) = \frac{M_{4f,h}(1 - \bar{v}_{4f,h}\rho_e)\omega^2(r^2 - r_0^2)}{2RT} . \qquad (56)$$

(d) The Width of the Buoyant Band

The distribution of the solvated macrospecies at equilibrium is given by Eq. (15). This may be rewritten with the ideality assumption, $\left(\frac{\partial \mu_3}{\partial m_3}\right)_{\mu_1, \mu_4} = \frac{RT}{m_3}$,

$$M_{3S}(1 - \bar{v}_{3S}\rho)\omega^2 r = \frac{RT \, d\ln m_3}{dr} , \qquad (57)$$

where

$$M_{3S} = M_3[1 + \Gamma_{13}' + \Gamma_{43}'(1 + \Gamma_{14}')] \qquad (58a)$$

and
$$\bar{v}_{3S} = \frac{\bar{v}_3 + \Gamma_{13}'\bar{v}_1 + \Gamma_{43}'(1 + \Gamma_{14}')\bar{v}_{4S}}{1 + \Gamma_{13}' + \Gamma_{43}'(1+\Gamma_{14}')} \quad . \tag{58b}$$

In order to obtain a first order representation of the concentration distribution of the complex, all variables are approximated by the first two terms of a Taylor series expansion around band center, r_0. In terms of the variable $\delta = r - r_0$,

$$M_{3S} = M_{3S,0} + \frac{dm_{3S}}{dr}\,\delta \tag{59a}$$

$$\bar{v}_{3S} = \bar{v}_{3S,0} + \frac{d\bar{v}_{3S}}{dr}\,\delta \tag{59b}$$

$$\rho = \rho_0 + \frac{d\rho}{dr}\,\delta \quad . \tag{59c}$$

Following Hearst and Vinograd,[14] only first order terms in δ are retained and the buoyancy condition is introduced, $1 - \bar{v}_{3S,0}\,\rho_0 = 0$. Equation (57) then becomes

$$RT\, d\ln m_3 = -M_{3S,0}\left[\bar{v}_{3S,0}\,\frac{d\rho}{dr} + \rho_0\,\frac{d\bar{v}_{3S}}{dr}\right]\delta\omega^2 r_0 d\delta \quad . \tag{60}$$

Upon integration, the same formal distribution is obtained as in the three-component system and

$$m_3 = m_{3,0}\, e^{-\delta^2/2\sigma_{3S}^2} \quad , \tag{61}$$

where

$$\sigma_{3S}^2 = \frac{RT}{M_{3S,0}\,\bar{v}_{3S,0}\left(\frac{d\rho}{dr}\right)^*_{3S}\,\omega^2 r_0} \quad , \tag{62}$$

and

$$\left(\frac{d\rho}{dr}\right)^{*}_{3S} = \frac{d\rho}{dr} + \frac{\rho_0}{\bar{v}_{3S,0}} \frac{d\bar{v}_{3S}}{dr} \tag{63}$$

is the effective density gradient for the neutral solvated macromolecule.

As in the three-component system, it is the effective density gradient which determines the width of the buoyant band. The first term which specifies this gradient is the physical density gradient. The second term takes into account the effects of the variables pressure, P, water activity, a_1^0, and free reagent molality, m_{4f}, on the polymer concentration distribution. The proper representation for the distance derivative of the partial specific volume of the complex in the four-component system is

$$\frac{d\bar{v}_{3S}}{dr} = \left(\frac{\partial \bar{v}_{3S}}{\partial P}\right)_{a_1^0, m_{4f}} \frac{dP}{dr} + \left(\frac{\partial \bar{v}_{3S}}{\partial a_1^0}\right)_{m_{4f}, P} \frac{da_1^0}{dr}$$

$$+ \left(\frac{\partial \bar{v}_{3S}}{\partial m_{4f}}\right)_{a_1^0, P} \frac{dm_{4f}}{dr} \quad . \tag{64}$$

In order to evaluate the three terms of Eq. (64), it is necessary to repeat the experiments of Hearst, Ifft, and Vinograd[22] as a function of the concentration of free reagent, as well as to measure the change in $\bar{v}_{3S}$ with free reagent concentration at constant P and a_1^0. We estimate the quantity $d\bar{v}_{3S}/dr$ by assuming that the variation of $\bar{v}_{3S}$ with water activity and pressure at constant m_{4f} is independent of reagent molality. Equation (64) may then be written in the approximate form

$$\frac{d\bar{v}_{3S}}{dr} = \left(\frac{\partial \bar{v}_{3S}}{\partial P}\right)_{a_1^0, m_{4f}=0} \frac{dP}{dr} + \left(\frac{\partial \bar{v}_{3S}}{\partial a_1^0}\right)_{P, m_{4S}=0} \frac{da_1^0}{dr}$$

$$+ \left(\frac{\partial \bar{v}_{3S}}{\partial m_{4f}}\right)_{a_1^0, P} \frac{dm_{4f}}{dr} \quad . \tag{65a}$$

The first two terms of Eq. (65a) have been evaluated by Hearst and Vinograd,[4] who showed that

$$\left(\frac{d\rho}{dr}\right)^*_{3h} = \left(\frac{\partial \bar{v}_{3S}}{\partial P}\right)_{a_1^0} \frac{dP}{dr} + \left(\frac{\partial \bar{v}_{3S}}{\partial a_1^0}\right)_{P} \frac{da_1^0}{dr} =$$

$$\left[\frac{1}{\beta^0} + \psi_3 \rho^{0\,2}\right] \left[1 - \left(\frac{\partial \theta}{\partial a_1^0}\right)_P \frac{da_1^0}{d\rho^0}\right] \omega^2 r \quad , \tag{65b}$$

where $(d\rho/dr)^*_{3h}$ is the effective density gradient in the three-component system. In order to obtain the third term of Eq. (65a) we differentiate Eq. (16) at constant pressure and water activity.

$$\left(\frac{d\bar{v}_{3S}}{m_{4f}}\right)_{a_1^0, P} = \left\{\frac{\bar{v}_4(1 + \Gamma_{13}') - \bar{v}_1(\Gamma_{13}' - \Gamma_{14}') - \bar{v}_3(1 + \Gamma_{14}')}{[1 + \Gamma_{13}' + \Gamma_{43}'(1 + \Gamma_{14}')]^2}\right\}$$

$$\times \left(\frac{\partial \Gamma_{43}'}{\partial m_{4f}}\right)_{a_1^0, P} \quad . \tag{66}$$

Assuming that Γ_{14}' is negligible and using the notation of Eq. (19), we obtain

$$\left(\frac{\partial \bar{v}_{3S}}{\partial m_{4f}}\right)_{a_1^0, P} = \left\{\frac{v_4 - v_3 + \Gamma'(v_4 - v_1)}{[1 + \Gamma' + \nu']^2}\right\} \left(\frac{\partial \nu'}{\partial m_{4f}}\right)_{a_1^0, P} \quad . \tag{67}$$

From Eq. (42) the distribution of free reagent is

$$\frac{dm_{4f}}{dr} = m_{4f} \frac{M_{4f}(1 - \bar{v}_{4f,h}\rho^0)\omega^2 r}{RT} . \tag{68}$$

Combining Eqs. (34), (35), (67), and (68), the molality conversion factor K is eliminated and the desired result is obtained,

$$\left(\frac{\partial \bar{v}_{3S}}{\partial m_{4f}}\right)_{a_1^0,P} \frac{dm_{4f}}{dr} = \frac{[\bar{v}_4 - \bar{v}_3 + \Gamma'(\bar{v}_4 - \bar{v}_1)]}{[1 + \Gamma' + \nu']^2} \left(\frac{\nu'}{\nu_m'}\right)$$

$$\times \frac{(\nu_m' - \nu')M_4(1 - \bar{v}_4\rho^0)\rho^{0^2}}{RT} \omega^2 r_0 . \tag{69}$$

The complete expression for the effective density gradient in the four-component system may then be written by combining Eqs. (65b) and (69)

$$\frac{1}{\omega^2 r_0}\left(\frac{d\rho}{dr}\right)^*_{3S} = \left[\frac{1}{\beta^0} + \psi_3\rho^{0^2}\right]\left[1 - \left(\frac{\partial\theta}{\partial a_1^0}\right)_P\left(\frac{da_1^0}{d\rho^0}\right)\right]_{m_{4f}}$$

$$+ \rho^{0^2}\left[\frac{\bar{v}_4 - \bar{v}_3 + \Gamma'(\bar{v}_4 - \bar{v}_1)}{(1 + \Gamma' + \nu')^2}\right]\left(\frac{\nu'}{\nu_m'}\right)(\nu_m' - \nu')\left[\frac{M_4(1 - \bar{v}_4\rho^0)}{RT}\right]. \tag{70}$$

Figure (2) presents a plot of the effective density gradient for the reacting system SV40 DNA II, CsCl, ethidium chloride. The solid line in Fig. (2) is the complete four-component effective density gradient given by Eq. (70). The upper dashed line represents the effective density gradient appropriate for a band centered at the indicated densities but otherwise unperturbed by the presence of reagent. This curve is given by Eq. (65b) and by the first term in Eq. (70).

Fig. 2. The effective density gradient for the reacting system SV40 DNA II, CsCl, ethidium chloride. Four component effective density gradient, Eq. (70), ____ . The contribution of the water activity and pressure gradients to the effective density gradient, Eq. (65b), -----. The contributions by the free reagent gradient to the effective density gradient, third term in Eq. (70), -·-·-·

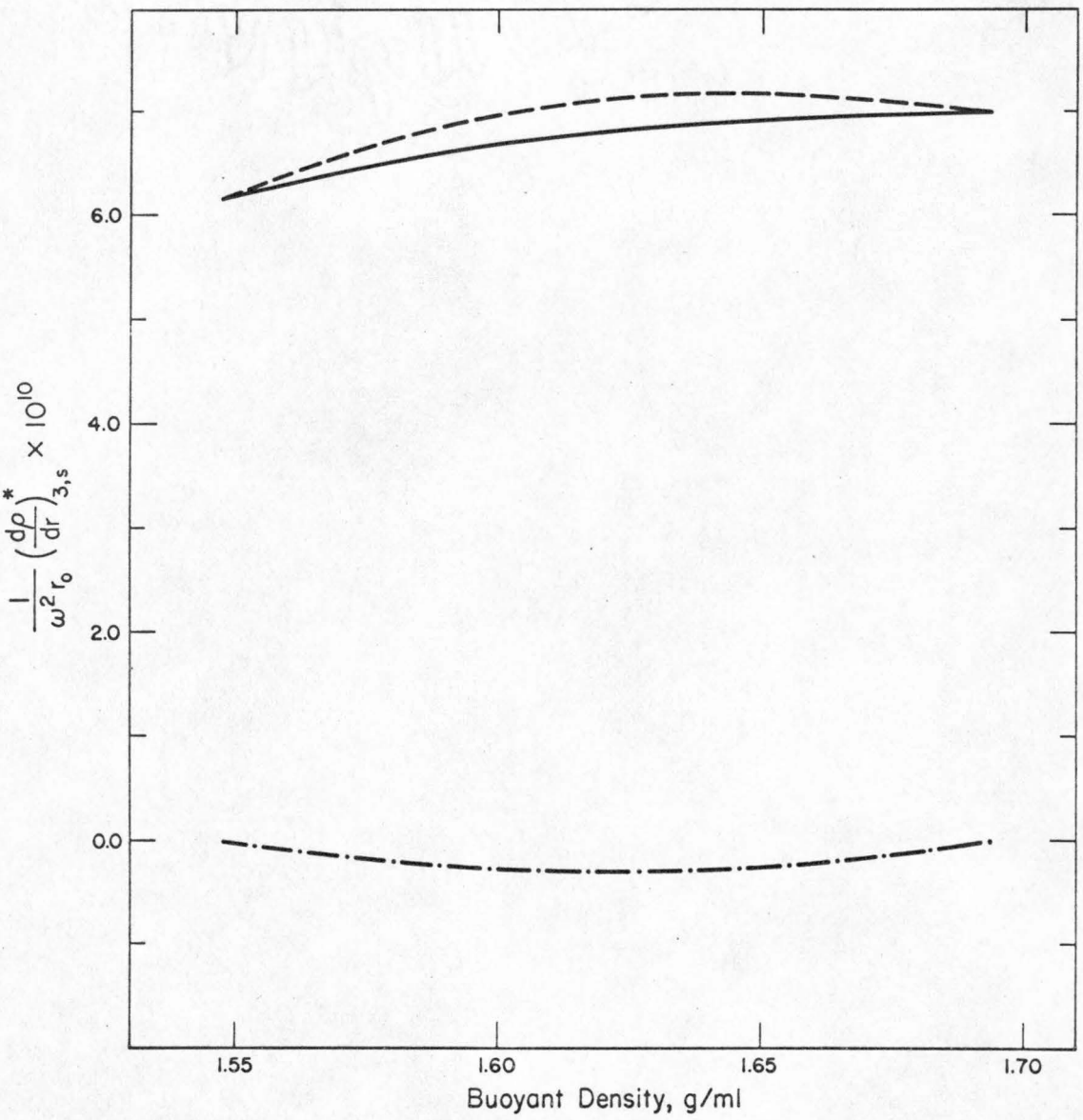
6.0
4.0
2.0
0.0
$\frac{1}{\omega^2 r_o}\left(\frac{d\rho}{dr}\right)^*_{3,s} \times 10^{10}$
1.55
1.60
1.65
1.70
Buoyant Density, g/ml

In this system the effect of the variable dye binding through the band is small, as shown by the small difference between the two upper curves. The lower curve is a plot of the second term in Eq. (70) and gives the magnitude of the perturbation caused by the variable dye binding. The experimental parameters for these calculations were taken from Bauer and Vinograd.[10]

The expression for the first order band width of a buoyant solvated macrospecies, Eq. (62), may be written

$$\sigma_{3s}^2 = \frac{RT\theta}{M_3(1 + \Gamma' + \nu')\left(\frac{d\rho}{dr}\right)^*_{3s}\omega^2 r_0} \quad . \tag{71a}$$

For the hydrated species in the absence of neutral reagent the first order band width is given by

$$\sigma_{3h}^2 = \frac{RT\theta_0}{M_3(1 + \Gamma_0')\left(\frac{d\rho}{dr}\right)^*_{3h}\omega^2 r_{00}} \quad , \tag{71b}$$

where Γ_0' is the preferential hydration of neutral macromolecule in the absence of reagent, $(d\rho/dr)^*_{3h}$ is the effective density gradient given by Eq. (65b), and r_{00} is the position of band center at $m_{4f} = 0$. Taking the ratio,

$$\frac{\sigma_{3s}}{\sigma_{3h}} = \left\{ \frac{\left(\frac{d\rho}{dr}\right)^*_{3h} r_{00}}{\left(\frac{d\rho}{dr}\right)^*_{3s} r_0} \quad \frac{(\bar{v}_3 + \Gamma_0'\bar{v}_1)}{(\bar{v}_3 + \Gamma\bar{v}_1' + \nu'\bar{v}_4)} \right\}^{\frac{1}{2}} \quad . \tag{72}$$

The quantity Γ' has been determined as a function of solution density, as shown in Appendix III of Bauer and Vinograd.[10] The solvation

parameter, ν', may also be determined from the buoyant density of the solvated polymer by a rearrangement of Eq. (19)

$$\nu' = \frac{(1 + \Gamma_0')(1 - \theta/\theta_0) - \Delta\Gamma'(\bar{v}_1\theta - 1)}{\bar{v}_4\theta - 1} , \qquad (73)$$

where $\Delta\Gamma' = \Gamma' - \Gamma_0'$ and θ_0 is the buoyant density at $m_4 = 0$. These relationships have been combined to calculate the expected field-corrected band width as a function of the buoyant density of the solvated species or, alternatively, as a function of the concentration of free reagent at band center. These results are presented in Fig. (3) for the system consisting of nicked circular SV40 DNA, CsCl, ethidium chloride and water. The band width ratio is seen to be only slightly dependent upon the level of dye binding in this system.

(e) Density Gradients and the Calculation of Buoyant Densities

The actual density of the solution at any radial position in an ultracentrifuge cell in the presence of the centrifugal field depends both upon the redistribution of the solute and upon the pressure gradient. It has been shown in the case of CsCl that the only important effect of pressure is to compress the solution without significant salt redistribution. The actual density may be calculated from the unpressured density by the relationship

$$\rho(r) = \rho^0(r)/[1 - \kappa P(r)] , \qquad (74)$$

where κ is the isothermal compressibility of the solution and P(r) is the pressure above atmospheric pressure at radial coordinate r. In

Fig. 3. Theoretical band width ratio, σ/σ_0, plotted as a function of the buoyant density for the system SV40 DNA II, CsCl, ethidium chloride. The curve was calculated with Eq. (72).

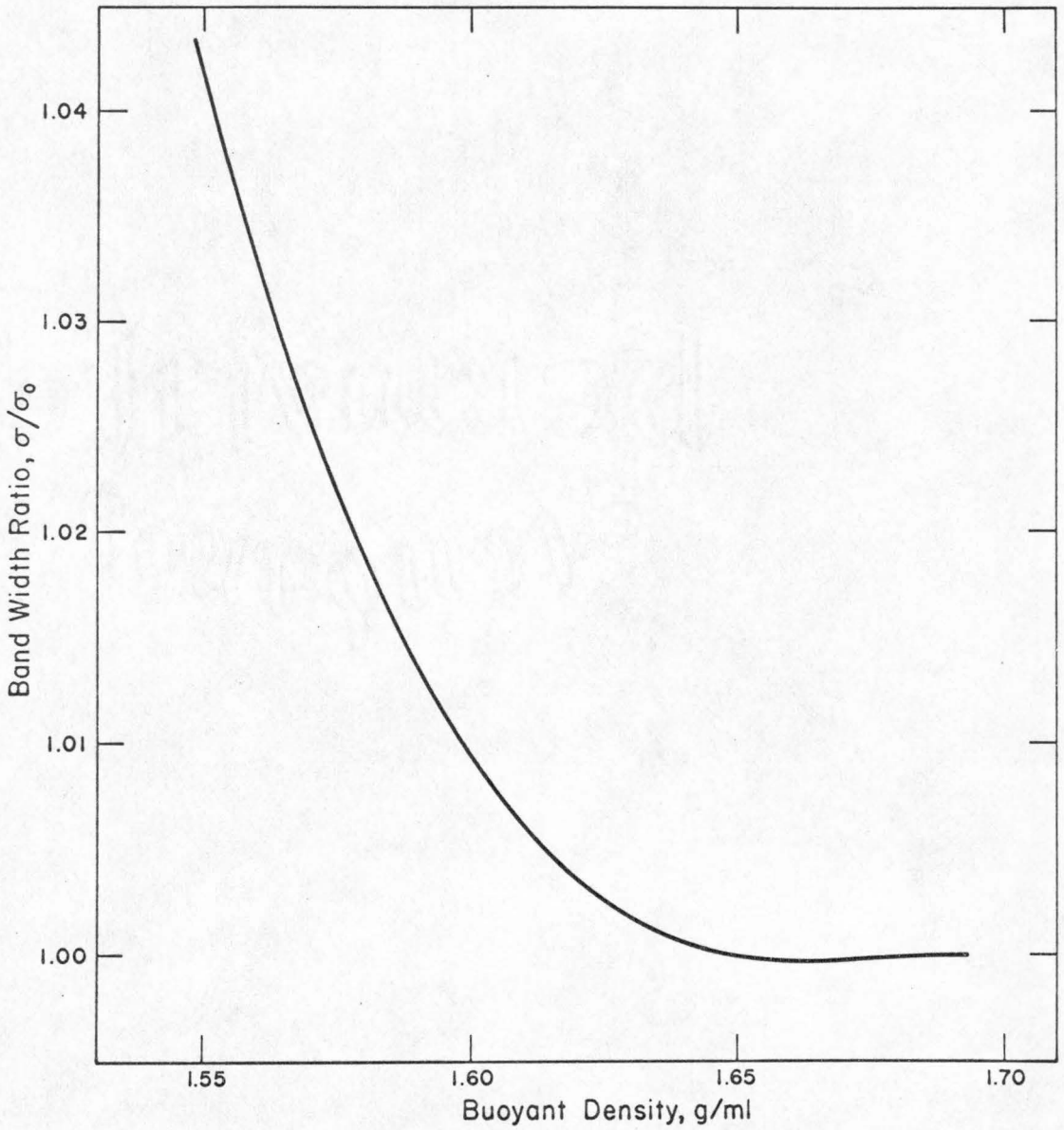
1.04
1.03
1.02
1.01
1.00
Band Width Ratio, σ/σ_0
1.55
1.60
1.65
1.70
Buoyant Density, g/ml

particular, the physical density at the salt isoconcentration coordinate, r_e, is

$$\rho_e = \rho_e^0/(1 - \kappa P_e) . \tag{75}$$

The calculation of the physical density at any other position in the cell is accomplished with the first order approximation

$$\rho(r) = \rho_e + (d\rho/dr)_{phys}(r - r_e) . \tag{76}$$

The physical density gradient, $(d\rho/dr)_{phys}$, takes into account to first order the compressional effects of the pressure gradient upon the salt redistribution and is given by

$$(d\rho/dr)_{phys} = (1/\beta^0 + \kappa\rho^{0^2})\omega^2 r . \tag{77}$$

It should be emphasized that the physical density gradient is a measurable quantity and refers directly to the actual density distribution in the cell. It is to be distinguished from the other "density gradients" discussed below, which include additional correction factors appropriate for the calculation of either the buoyant density under specified conditions or of the molecular weight. These are density gradients in the formal sense only. The physical density gradient is determined by the redistribution of the neutral salt alone, provided that the other components of the system are present in very low concentration. In other cases the term $1/\beta^0$ must be modified appropriately,and the correct value of κ must be determined. The formal representation of the physical density gradient will, however, remain unchanged.

The condition for buoyancy is that the reciprocal of the solvated

partial specific volume of the macromolecular complex be equal to the physical density of the solution at band center, $1/\overline{v}_{s,o} = \rho_o$. This density, which is a function of water activity, pressure, and free reagent concentration at band center, is related to both the buoyant density and to the standard buoyant density of the macrospecies. To obtain the buoyant density a first-order correction is made for the effects of pressure on the solution and

$$\theta = \rho_o(1 - \kappa P_o). \tag{78}$$

The standard buoyant density in the three-component system is then obtained by accounting for the redistribution of water in the centrifugal field and for the effect of pressure upon the banding position of the macrospecies.

$$\Theta' = \theta/(1 - \psi_3 P_o). \tag{79}$$

In the absence of added reagents it is the buoyant density θ at 25° which is commonly reported. Since this quantity is a function of pressure, its value depends upon the details of the centrifuge experimental conditions. In particular, θ varies with the physical location of the band in the centrifuge cell, which is determined by the choice of initial solution density, ρ_e^o, and by the angular velocity. This variability is avoided if the experimental conditions are always selected so that the buoyant band is located at the isoconcentration coordinate, r_e, for the neutral salt. We will refer to this buoyant density under specified conditions as the practical buoyant density, Θ. This quantity designates the

composition of the solution at band center at the approximately 130 atm. pressure at the rms center of a 1.1 cm. liquid column at 44,000 rpm and 25° in the analytical ultracentrifuge.[24] Although Θ does not refer to atmospheric pressure, its use eliminates first-order ambiguities arising from variable band positions. The practical buoyant density may be calculated for a band which is not located at r_e by the use of the buoyant density gradient, as discussed below. The practical buoyant density, Θ, is smaller than the standard buoyant density, Θ', by approximately 6 mg./ml. and is also smaller than the physical density at band center, ρ_0, by about 6 mg./ml. in the analytical ultracentrifuge under the conditions described above. Although the buoyant density θ depends upon the experimental conditions, the range of conditions used in the analytical ultracentrifuge is not large and the values reported in the literature have been generally consistent. In the preparative ultracentrifuge, however, the much longer liquid columns lead to a correspondingly greater pressure gradient throughout the preparative tube. Here the difference between the standard buoyant density, Θ', which is the true compositional variable, and the buoyant density, θ, may be as large as a few hundredths of a density unit.

In the four-component system, the macromolecular complex may also be regarded as a molecular species having the composition of the molecules at band center, and in equilibrium with the free reagent concentration at band center. For such a complex the <u>apparent standard buoyant density</u>, Θ'_a, is the property of interest and is given by

$$\Theta'_a = \theta/(1 - \psi_3 P_0) \quad . \tag{80}$$

Correction is here made for the redistribution of water due to the centrifugal field, but not for the redistribution of free reagent. Since no account is taken of the effect of pressure upon the binding reaction, the applicable equilibrium constant will be that appropriate to the pressure at band center. The apparent standard buoyant density may be used to calculate binding isotherms only if conditions are so selected that bands always appear at the same radial coordinate, or if the pressure dependence of the binding constant is very small. If the apparent standard buoyant density is calculated, the result must be reported as a function of the free reagent concentration at band center. Since the buoyant density is determined jointly by the initial reagent and salt concentrations, it is possible to obtain Θ_a' as a function of free reagent concentration merely by adding salt or water to the system. The apparent standard buoyant density will differ from the buoyant density and from the physical density at band center by approximately the same amounts as does the three-component standard buoyant density. If there are significant changes in the water activity distribution due to the presence of the free reagent, or if there are changes in the apparent compressibility of the solvated macrospecies with free reagent concentration, larger deviations may occur in the four-component system. In the event that the volume change in the binding reaction is large, both the buoyant density and the apparent standard buoyant density will be strongly dependent upon the radial location of the buoyant band. Consistent results will therefore not be obtained under variable experimental conditions.

The four-component standard buoyant density, Θ', includes corrections for the redistribution of free reagent in the centrifugal field, for changes in the apparent compressibility of the macromolecular complex with binding, and for the effects of pressure upon the binding equilibria. As shown earlier, Eq. (32a), this buoyant density is given by

$$\Theta' = \theta/(1 - \psi_4 P_0) \quad . \tag{81a}$$

The standard buoyant density is the appropriate thermodynamic function for the four-component system, but it is correspondingly much more difficult to determine.

As in the three-component system, an alternative procedure is to correct the buoyant density θ to the conditions which prevail at band center at 44,000 rpm, 25° in a 1.1 cm. column. In the four-component system this may be done in two ways. If full account is taken of the redistribution of the binary solvent, of the redistribution of the free reagent, and of the pressure gradient, the quantity calculated is the four-component practical buoyant density, Θ.

$$\Theta = \Theta' (1 - \psi_4 p) \quad . \tag{81b}$$

If this calculation is carried out with the correct value of ψ_4, Eq. (32b), the result will correspond to the pressure p at r_e under the standard conditions listed above. The free reagent concentration at r_e, which corresponds to the buoyant density Θ, will in general differ from the pressured initial reagent concentration, Eq. (54). The appropriate equilibrium constant will be the value at pressure p. The four-component

practical buoyant density may be calculated only when ψ_4 is known, which is not usually the case.

A simplified procedure is to take account only of the redistribution of the binary solvent and of the pressure gradient. This results in a quantity which is termed the apparent practical buoyant density, Θ_a.

$$\Theta_a = \Theta (1 - \psi_3 p) . \tag{81c}$$

The apparent practical buoyant density is calculated with the pressure coefficient ψ_3, given by Eq. (32c). The calculation of Θ_a assumes that the redistribution of the binary solvent and the pressure gradient are not affected by the presence of the reagent. The apparent practical buoyant density describes the macromolecular complex which is in equilibrium with the free reagent concentration $m_{4,0}$ at the pressure P_0 at band center.

The calculation of buoyant densities may employ either of two techniques: the absolute method or the marker method. The calculation of the buoyant density θ with the absolute method begins with measurement of the initial solution density at atmospheric pressure, ρ_e^0. The physical density at the salt isoconcentration coordinate is then given by Eq. (75), $\rho_e = \rho_e^0/(1 - \kappa P_e)$. The physical density gradient is used to calculate the actual solution density at band center with the aid of Eq. (76). For this purpose the substitution $\bar{r} = \frac{1}{2}(r_e + r_0)$ is made, and the physical density gradient is approximated as

$$\left(\frac{d\rho}{dr}\right)_p \approx \left(\frac{1}{\beta^0} + \kappa \rho_e^{0\,2}\right) \omega^2 \bar{r} . \tag{82}$$

The foregoing results are combined with Eqs. (32a) and (78) to obtain the standard buoyant density,

$$\dot{\Theta}' = \rho_e^0 \frac{(1 - \kappa P_0)}{(1 - \kappa P_e)} \left[1 + \frac{1}{\rho_e^0} \left(\frac{1}{\beta^0} + \kappa \rho_e^0\right) \omega^2 \bar{r} \Delta r\right] (1 - \psi_4 P_0)^{-1}, \quad (83)$$

where $\Delta r = r_0 - r_e$. The further approximations are introduced

$$\frac{1 - \kappa P_0}{1 - \kappa P_e} \approx 1 - \kappa(P_0 - P_e) \quad (84)$$

and

$$P_0 - P_e \approx \rho_e^0 \omega^2 \bar{r} \Delta r \ . \quad (85)$$

Equations (83)-(85) are combined to yield the result for the standard buoyant density, neglecting second order terms in Δr.

$$\Theta' = \left[\rho_e^0 + \frac{1}{\beta^0} \omega^2 \bar{r} \Delta r\right] (1 - \psi_4 P_0)^{-1} \ . \quad (86a)$$

In the three-component system, the standard buoyant density is given by a similar equation in which the quantity ψ_4 is replaced by ψ_3 and

$$\Theta' = \left[\rho_e^0 + \frac{1}{\beta^0} \omega^2 \bar{r} \Delta r\right] (1 - \psi_3 P_0)^{-1} \ . \quad (86b)$$

In the four-component system a similar equation is used for the calculation of Θ_a', the apparent standard buoyant density,

$$\Theta_a' = \left[\rho_e^0 + \frac{1}{\beta^0} \omega^2 \bar{r} \Delta r\right] (1 - \psi_3 P_0)^{-1} \ . \quad (86c)$$

The buoyant density θ, which is the pressure dependent variable, is

given by

$$\theta = \rho_e^0 + \frac{1}{\beta^0} \omega^2 \bar{r} \Delta r \quad . \tag{87}$$

In order to calculate the practical buoyant density we employ the relationship

$$\Theta = \Theta' (1 - \psi_3 p) \quad . \tag{88}$$

Combining Eqs. (86b) and (88),and again neglecting the higher order terms in Δr, we obtain

$$\Theta = \rho_e^0 + \left(\frac{1}{\beta^0} + \psi_3 \rho^{0\,2} \right) \omega^2 \bar{r} \Delta r \quad . \tag{89}$$

The formal density gradient used in Eq. (89) has been termed the <u>buoyant density gradient</u> and is given by

$$\left(\frac{d\rho}{dr} \right)_b = \left(\frac{1}{\beta^0} + \psi_3 \rho^{0\,2} \right) \omega^2 \bar{r} \quad . \tag{90a}$$

In the four-component system ψ_3 is replaced by ψ_4 and

$$\left(\frac{d\rho}{dr} \right)_b = \left(\frac{1}{\beta^0} + \psi_4 \rho^{0\,2} \right) \omega^2 \bar{r} \quad . \tag{90b}$$

A valuable procedure for the measurement of the buoyant density is to band an unknown macrospecies in the same cell with a very similar macrospecies of known but different buoyant density. If in a three-component system the standard buoyant density, Θ_1', of the marker is known, the buoyant density, θ_1, of the marker band is calculated at pressure P_{01} by Eq. (79),

$$\theta_1 = \Theta_1'(1 - \psi_3 P_{01}) \quad . \tag{91}$$

The physical density of the solution at r_{01} is then given by Eq. (78),

$$\rho_{01} = \theta_1/(1 - \kappa P_{01}) \quad . \tag{92}$$

The physical density gradient is again used to calculate the physical density at r_{02},

$$\rho_{02} = \rho_{01} + \left(\frac{1}{\beta^0} + \kappa {\rho_1^0}^2\right) \omega^2 \bar{r}_{12} \Delta r_{12} \quad , \tag{93}$$

where $\bar{r}_{12} = \frac{1}{2}(r_{01} + r_{02})$ and $\Delta r_{12} = r_{02} - r_{01}$. The standard buoyant density at r_{02} is calculated by combining Eqs. (91) - (93) to obtain the result

$$\Theta_2' = \Theta_1' \left[1 + \frac{1}{\rho_{01}^0} \left(\frac{1}{\beta^0} + \kappa {\rho_{01}^0}^2\right) \omega^2 \bar{r}_{12} \Delta r_{12}\right] \frac{(1 - \kappa P_{02})}{(1 - \kappa P_{01})} \frac{(1 - \psi_3 P_{01})}{(1 - \psi_3 P_{02})} \quad . \tag{94}$$

In addition to the approximations given in Eqs. (84) and (85), we introduce the further approximation

$$\frac{1 - \psi_3 P_{01}}{1 - \psi_3 P_{02}} \approx 1 + \psi_3 (P_{02} - P_{01}) \quad , \tag{95}$$

and the good approximation that $\rho_{01} \approx \Theta_1'$. The final result is then obtained for the standard buoyant density of the unknown macrospecies by combining Eqs. (84), (85), (94) and (95) and by neglecting terms involving $(\Delta r_{12})^2$,

$$\Theta_2' = \Theta_1' + \left(\frac{1}{\beta^0} + \psi_3 {\rho_{01}^0}^2\right) \omega^2 \bar{r}_{12} \Delta r_{12} \quad . \tag{96}$$

The calculation of the four-component standard buoyant density proceeds identically, except that ψ_4 is substituted for ψ_3. The marker method may also be used to calculate the practical buoyant density Θ_2 of an unknown species from the practical buoyant density Θ_1 of a marker band. In this case combination of Eqs. (88) and (94) leads to the immediate result

$$\Theta_2 = \Theta_1 + \left(\frac{d\rho}{dr}\right)_b \Delta r_{12}. \tag{97}$$

In the four-component system the buoyant density of the marker macrospecies must first be determined as a function of the free reagent concentration by the absolute method. This was done for crab d-AT in CsCl-ethidium chloride for low dye concentrations by Bauer and Vinograd.[10]

In the three-component system the standard buoyant density is determined by the water activity, and the density of the solution at band center, ρ_0, is equal to $1/\overline{v}_{s,0}$. Figure (4), which contains a portion of a diagram taken from Hearst and Vinograd,[4] shows the condition for the formation of a stable band in a CsCl solution. In Fig. (4) the density of CsCl solutions (I) and the buoyant density of T4 DNA measured in several salt solutions (II) are plotted as a function of water activity. The buoyant density of DNA in CsCl is uniquely determined by the intersection of the two solid curves for $\theta(a_1)$ and $\rho_0(a_1)$ for this salt. In the four-component system, the introduction of the binding reagent leads to the appearance of a family of curves, $\theta(a_1, m_4)$, which intersect the curve $\rho_0(a_1)$ at different densities.

Fig. 4. The density of CsCl solutions (I) and the buoyant density of Cs T4 DNA as determined in a variety of salt solutions (II) are plotted as a function of water activity. The solid lines were taken from Hearst and Vinograd.[4] The dashed lines represent the changes which result from the addition of a reagent with $\bar{v}_4 > 1/\theta_0$, III, and $\bar{v}_4 < 1/\theta_0$, IV.

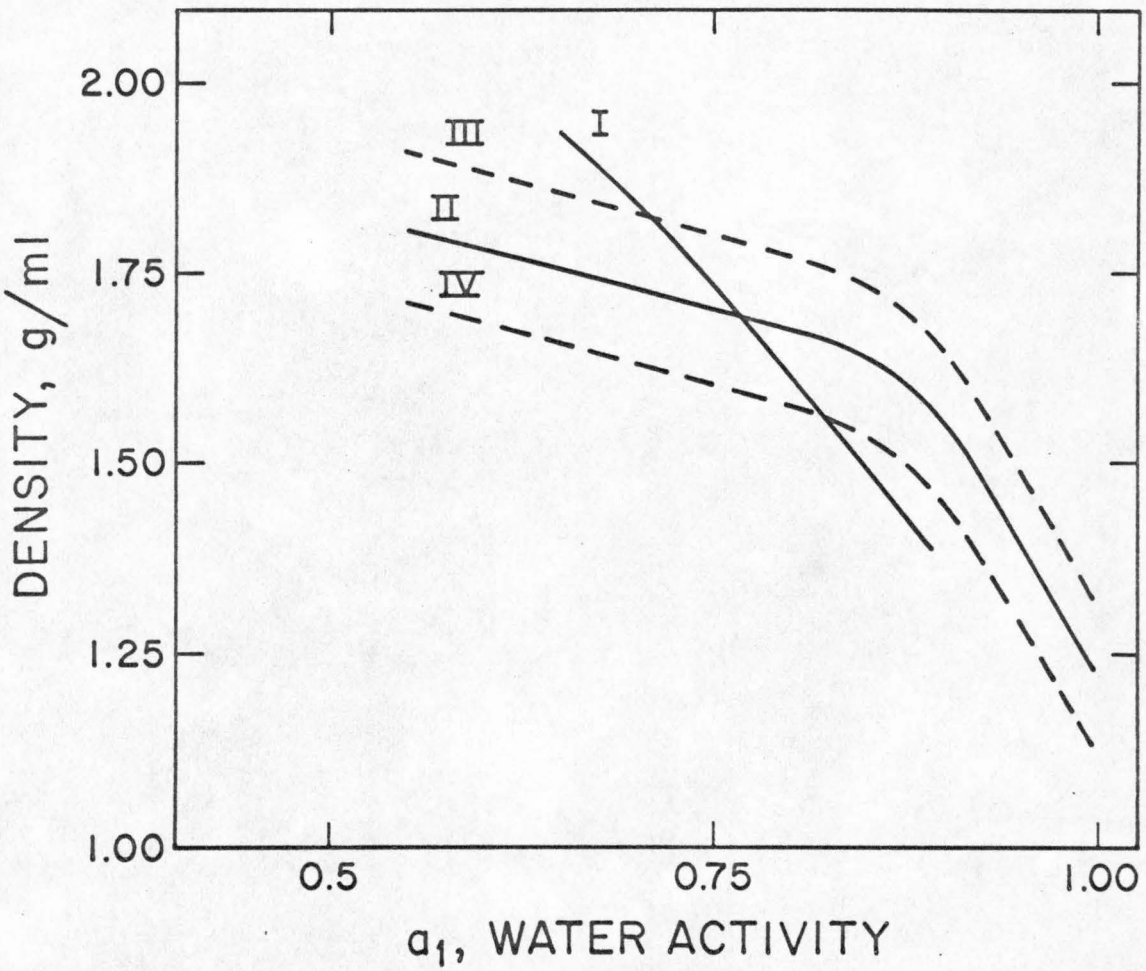
2.00
1.75
1.50
1.25
1.00
DENSITY, g/ml
III
I
II
IV
0.5
0.75
1.00
a_1, WATER ACTIVITY

TABLE 1
THE DENSITY OF THE BINARY SOLVENT

Symbol	Description	Definition	Reference Density	Density Gradient
ρ_e^0	Solution density at atmospheric pressure, P = 0.*	–	–	–
ρ_e	Pressured solution density at P_e and salt isoconcentration coordinate, r_e.	$\rho_e = \rho_e^0/(1-\kappa P_e)$ Eq. (75)	ρ_e^0	–
θ	Buoyant density.	Solution density at band center, r_0, formally corrected to $P_0 = 0$	ρ_e^0	Compositional density gradient, Eq. (36b)
ρ_0	Pressured solution density at band center, r_0.	$\rho_0 = \theta/(1-\kappa P_0)$ Eq. (78)	ρ_e	Physical density gradient, Eq. (77)

* This symbol has also been denoted ρ^0.

TABLE 2
THE BUOYANT DENSITY IN THE THREE COMPONENT SYSTEM

Symbol	Description	Definition	Reference Density	Density Gradient
Θ'	Standard buoyant density. All pressure effects extrapolated to $P_0 = 0$.	$\Theta' = \theta/(1-\psi_3 P_0)$ Eq. (79)	Marker Θ'	Buoyant density gradient, Eq. (90a)
			ρ_e^0	Compositional density gradient and definition, Eq. (86b)
Θ	Practical buoyant density. Pressure effects corrected to r_e at 44,000 rpm, 25°, 1.1 cm liquid column.	$\Theta = \Theta'(1-\psi_3 p)$ Eq. (88)	Marker Θ or ρ_e^0	Buoyant density gradient, Eq. (90a)
θ	Buoyant density. Depends upon pressure and position in the liquid column.*	–	ρ_e^0	Compositional density gradient, Eq. (36b)

* This quantity should properly be regarded as a solution parameter, as explained in the text.

TABLE 3
THE BUOYANT DENSITY IN THE FOUR COMPONENT SYSTEM

Symbol	Description	Definition	Reference Density	Density Gradient †
Θ'	Standard buoyant density. All pressure effects extrapolated to $P_0 = 0$. Equilibrium constant $k(P_0 = 0)$. Corresponds to initial free reagent concentration.	$\Theta' = \theta/(1-\psi_4 P_0)$ Eq. (81a)	Marker Θ' ρ_e^0	Buoyant density gradient, Eq. (90b) Compositional density gradient and definition, Eq. (86a)
Θ_a'	Apparent standard buoyant density. Pressure effects extrapolated to $P_0 = 0$ for components 1-3, with $\psi_4 = \psi_3$. Equilibrium constant $k(P_0)$. Function of $m_{4,0}$.	$\Theta_a' = \theta/(1-\psi_3 P_0)$ Eq. (80)	Marker Θ_a' ρ_e^0	Buoyant density gradient, Eq. (90a) Compositional density gradient and definition, Eq. (86c)
Θ	Practical buoyant density. Pressure effects corrected to r_e, 44,000 rpm, 25°, 1.1 cm liquid column. Equilibrium constant $k(p)$. Function of $m_{4,e}$.	$\Theta = \Theta'(1-\psi_4 p)$ Eq. (81b)	Marker Θ or ρ_e^0	Buoyant density gradient, Eq. (90b)

TABLE 3 (Cont'd)

Symbol	Description	Definition	Reference Density	Density Gradient †
Θ_a	Apparent practical buoyant density. Pressure effects corrected to r_e, 44,000 rpm, 25°, 1.1 cm liquid column for components 1-3, with $\psi_3 = \psi_4$. Equilibrium constant $k(P_0)$. Function of $m_{4,0}$.	$\Theta_a = \Theta'(1-\psi_3 p)$ Eq. (81c)	Marker Θ_a	Buoyant density gradient, Eq. (90a)
			ρ_e^0	Compositional density gradient and definition, Eq. (86c) with $P_0 = p$
θ	Buoyant density. Depends upon pressure, position in the liquid column and free reagent concentration.*	—	ρ_e^0	Compositional density gradient, Eq. (36b)

†At high reagent concentrations the coefficient $1/\beta^\circ$ which occurs in these density gradients may be significantly affected.

*This quantity should properly be regarded as a solution parameter, as explained in the text.

The various densities which have been defined previously and in this section are summarized in Tables I-III. In Table I the solution densities are described. It is usually assumed that these quantities are unique to the binary solvent in the ultracentrifuge and are not influenced by the presence of additional components. This may not be true for certain four-component systems, in which case the compressibility factor, κ, and the coefficient $1/\beta^0$ must be modified accordingly. Table II describes the buoyant densities which may be calculated in the three-component system, and Table III contains those appropriate for the four-component system.

The molecular weight of either the solvated macrospecies, having the composition of the molecules at band center, or of the anhydrous, unsolvated neutral macrospecies may be determined in the four-component system with the use of Eqs. (70) and (71a). The formal density gradient to be used in this case is the effective density gradient, as shown in Section (d). This quantity takes into account changes in the band width due to the gradients of water activity, free reagent molality, and pressure across a buoyant band. The unsolvated molecular weight is given by

$$M_3 = \frac{RT}{\sigma_{3S}^2 \left(\frac{d\rho}{dr}\right)^*_{3S} \omega^2 r_0 (v_3 + \Gamma' \bar{v}_1 + \nu' \bar{v}_{4S})} , \qquad (98)$$

and the solvated molecular weight is given by the corresponding expression

$$M_{3S} = \frac{RT\theta}{\sigma_{3S}^2 \left(\frac{d\rho}{dr}\right)^*_{3S} \omega^2 r_0} . \qquad (99)$$

DISCUSSION

The change in the buoyant density of a macromolecule which results from the binding of ν' grams of neutral reagent per gram of neutral dry polymer depends upon the initial buoyant density, the nature of the binary solvent, and the effective partial specific volume of the bound reagent. The addition of a reagent with $\bar{v}_{4,\mathrm{eff}} < 1/\theta_0$ increases the buoyant density, while the addition of a reagent with $\bar{v}_{4,\mathrm{eff}} > 1/\theta_0$ reduces the buoyant density. This latter is the case with the binding of the dye ethidium bromide, $\bar{v}_{4,\mathrm{eff}} = 1.02$ ml./g., to SV40 DNA, $\theta_0 = 1.6937$ g./ml. Here θ_0 is the buoyant density in the absence of added reagent.

The calculation of the change in buoyant density which results from the binding of ν' grams reagent per gram of macrospecies requires estimation of the change in net hydration of the macromolecular complex upon moving the buoyant band to a region of different water activity. The net hydration of T4 DNA in CsCl has been shown[10] to be given by

$$\Delta\Gamma'(\theta) = 0.04092 - 0.7282\eta + 4.592\eta^2 - 16.08\eta^3 + 20.56\eta^4 \quad (100a)$$

and

$$\Gamma' = \Gamma'_0 + \Delta\Gamma'(\theta) - \Delta\Gamma'(\theta_0), \quad (100b)$$

where $\eta = \theta - 1.5$. Similarly, the net hydration of T4 DNA in Cs_2SO_4 may be shown (see appendix) to satisfy the equations

$$\Delta\Gamma'(\theta) = 0.17903 - 2.63215\alpha + 14.937\alpha^2 - 57.502\alpha^3 + 136.18\alpha^4 - 139.44\alpha^5 \quad (101a)$$

and

$$\Gamma' = \Gamma'_0 + \Delta\Gamma'(\theta) - \Delta\Gamma'(\theta_0), \quad (101b)$$

where $\alpha = \theta - 1.295$. Figure (5) shows the calculated relations between $\Delta\Gamma'$ and θ for DNA in CsCl and in Cs_2SO_4.

Equation (19) may be rearranged to solve for the weight binding ratio

$$\nu' = \frac{\theta(\bar{v}_3 + \Gamma') - (1 + \Gamma')}{(1 - \bar{v}_4\theta)} \qquad (102)$$

and, with the use of Eqs. (100) or (101) above, ν' may be calculated as a function of θ for binding reagents of given $\bar{v}_4$. Figure (6a) shows the results of representative calculations for a DNA of initial buoyant density $\theta_0 = 1.700$ g./ml. in CsCl, and Fig. (6b) presents similar results for the case of a DNA of initial buoyant density $\theta_0 = 1.420$ g./ml. in Cs_2SO_4. The curves are approximately linear in the region of low $\bar{v}_4$, which corresponds to the binding of a dense reagent such as a heavy metal. The buoyant density increases with increasing reagent bound at $\bar{v}_4 < 1/\theta_0$, and decreases at $\bar{v}_4 > 1/\theta_0$. In this latter region the buoyant density is not a linear function of ν', even at relatively high values of $\bar{v}_4$.

Figure (7) presents an experimental curve taken from Bauer and Vinograd[10] for θ vs. ν for the binding of ethidium chloride to SV40 DNA II. The values of ν calculated from the buoyant density measurements were used to determine the binding isotherm, employing the experimentally measured $\bar{v}_{4,\text{eff}} = 1.02$ ml./g. The binding constant in 5.8 M CsCl and the maximum number of available sites were calculated from the isotherm.[25] The buoyant density method is comparable to dialysis equilibrium, but with the distinct advantages that much

Fig. 5. The change in preferential hydration for a DNA of $\theta_0 = 1.6$ as a function of buoyant density, based upon the data of Hearst and Vinograd[4] for T4 DNA. a. Binary solvent CsCl-H_2O. The theoretical curve was plotted according to Eqs. (100a,b). b. Binary solvent Cs_2SO_4-H_2O. The theoretical curve was plotted according to Eqs. (101a,b).

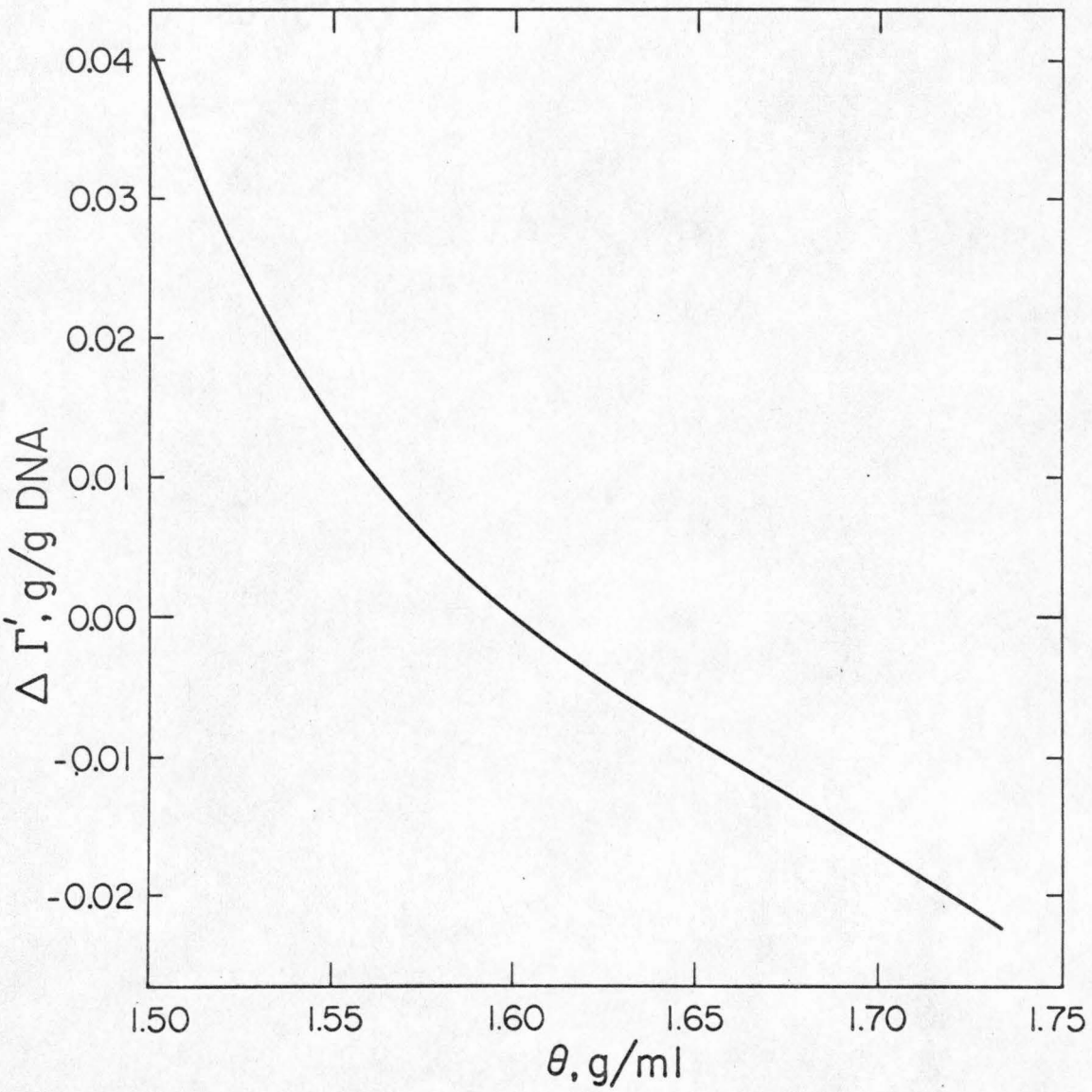
0.04
0.03
0.02
0.01
0.00
-0.01
-0.02
Δ Γ', g/g DNA
1.50
1.55
1.60
1.65
1.70
1.75
θ, g/ml

a

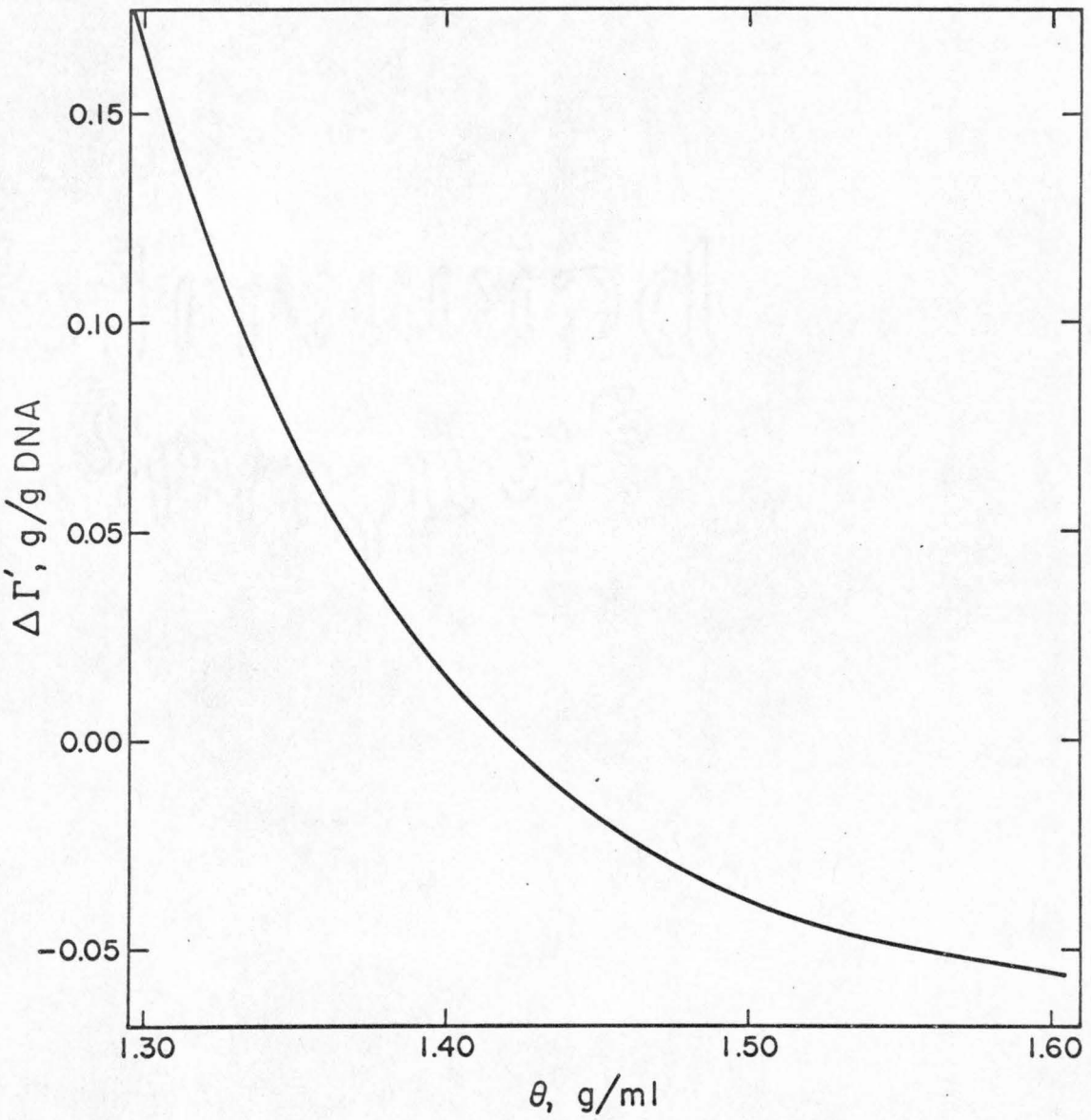

b

Fig. 6. The buoyant density of DNA in a four-component system as a function of the binding parameter ν' for representative values of $\bar{v}_4$, calculated with Eq. (102). a. Binary solvent CsCl-H_2O. The theoretical curves were plotted for a DNA of $\theta_0 = 1.70$ and the net hydration was calculated with Eqs. (100a,b). b. Binary solvent Cs_2SO_4-H_2O. The theoretical curves were plotted for a DNA of $\theta_0 = 1.42$ and the net hydration was calculated with Eqs. (101a,b).

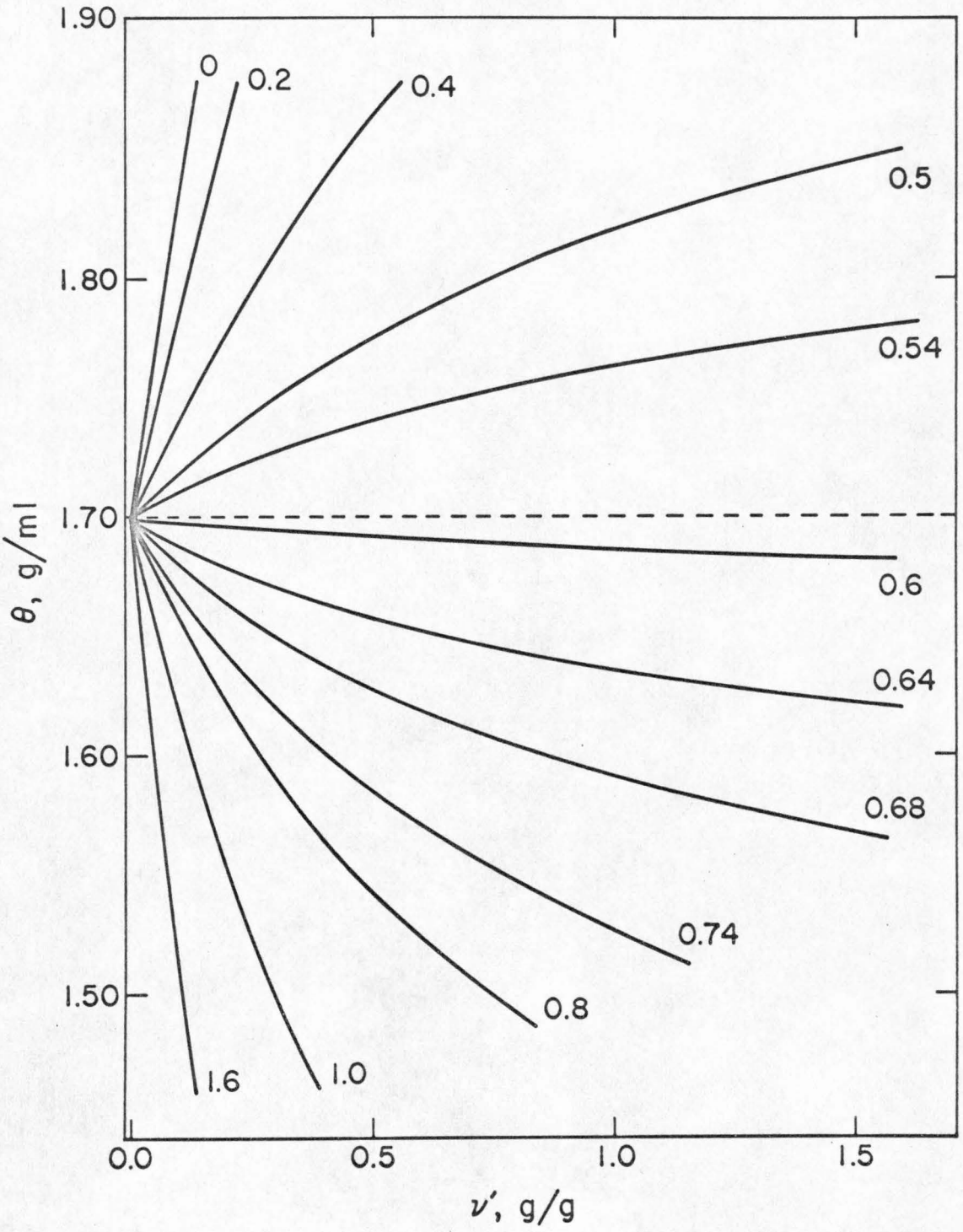
1.90
1.80
1.70
1.60
1.50
θ, g/ml
0
0.2
0.4
0.5
0.54
0.6
0.64
0.68
0.74
0.8
1.0
1.6
0.0
0.5
1.0
1.5
ν', g/g

a

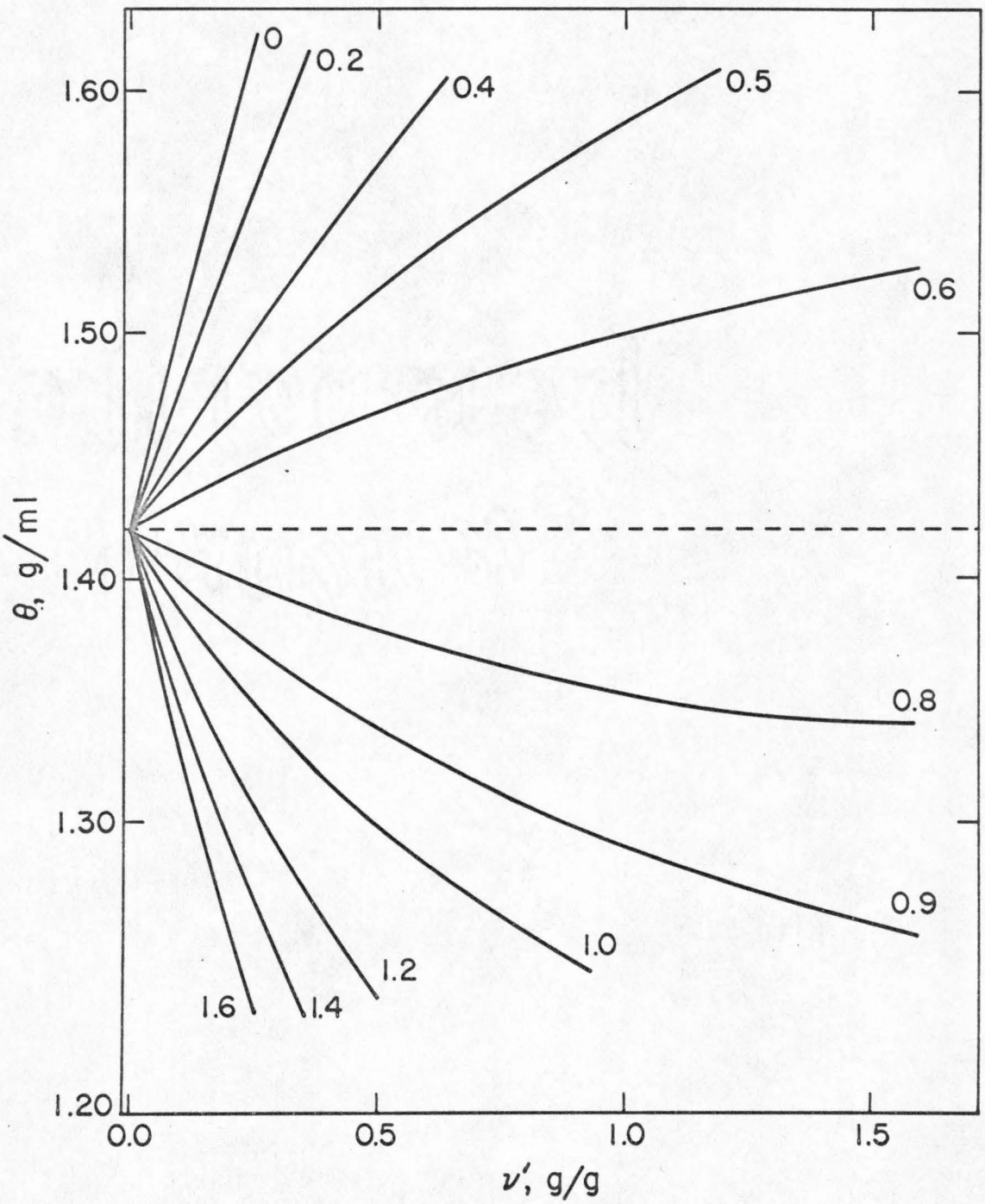
0
0.2
0.4
0.5
0.6
0.8
0.9
1.0
1.2
1.4
1.6
1.60
1.50
1.40
1.30
1.20
0.0
0.5
1.0
1.5
θ, g/ml
ν', g/g

b

Fig. 7. The buoyant density of the complex formed between SV40 DNA II and ethidium chloride in CsCl as a function of ν, the moles ethidium chloride bound per mole Cs nucleotide. The experimental data were obtained as described elsewhere.[10]

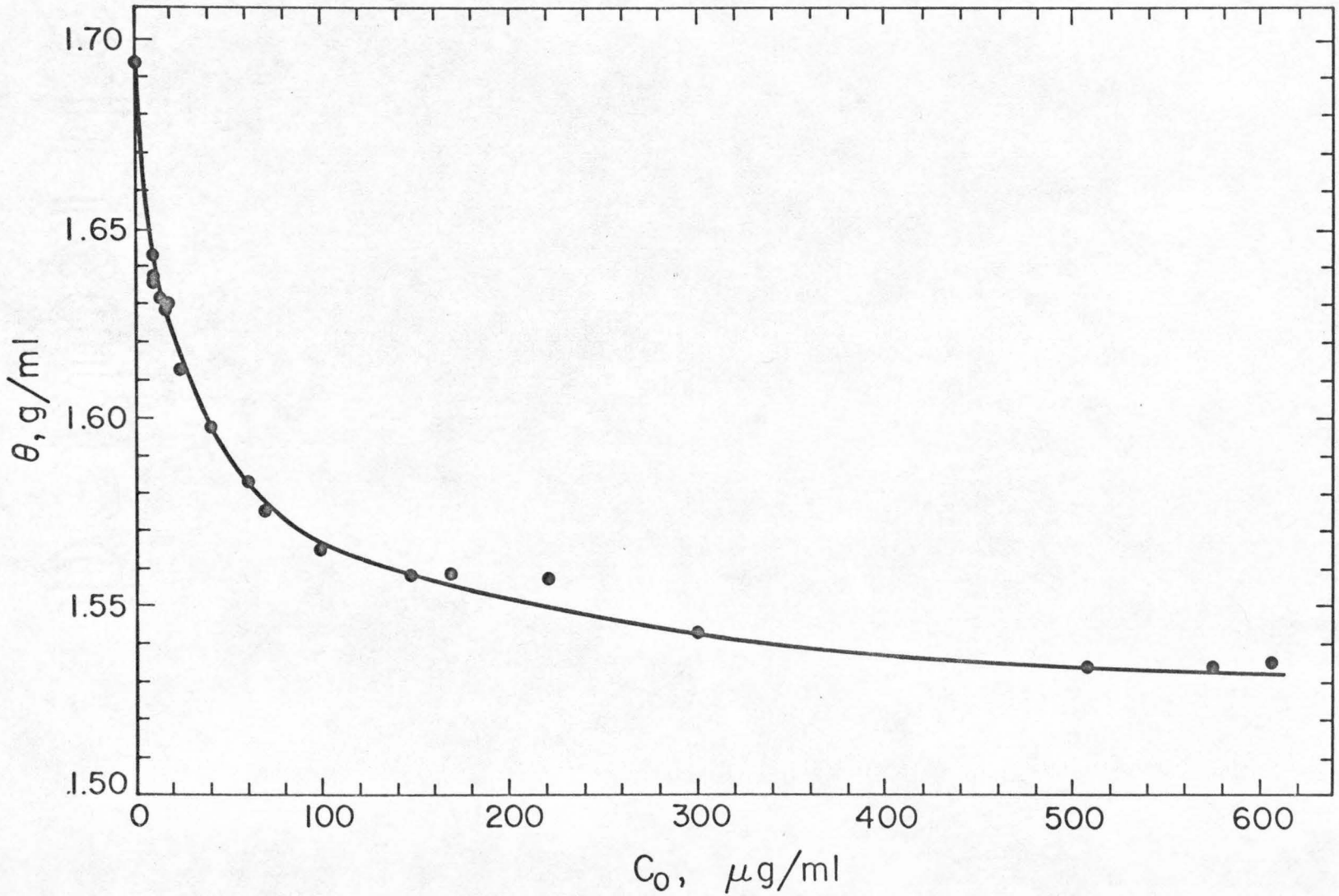
1.70
1.65
1.60
1.55
1.50
θ, g/ml
0
100
200
300
400
500
600
C0, μg/ml

smaller amounts of material are required and that nonoverlapping macromolecular impurities do not interfere. The method has the disadvantage that its use is restricted to buoyant binary solvents.

In order to test the theoretical predictions further, Eqs. (101) and (102) were applied to the binding of mercuric ion by both E. Coli and T4 DNA's in Cs_2SO_4, a case which has been studied experimentally by Nandi, Wang, and Davidson.[7] The results of the theoretical calculations are presented in Fig. (8), where θ is plotted as a function of $\nu = \nu'(M_3/M_4)$, where we take $M_3 = 440$ for Cs E. Coli DNA or $M_3 = 477$ for Cs T4 DNA, and $M_4 = 296.7$ for $HgSO_4$. The reciprocal of the crystal density of mercuric sulphate, 0.16 ml./g., was used as an estimate of $\bar{v}_4$. The binding of mercury to DNA appears to follow a stoichiometry, in terms of the neutral components selected here, similar to reaction type (c) listed in Section (a) above.

$$Hg^{++}SO_4^{=} + 2Cs^{+}H^{+}P^{=} \rightleftharpoons Cs^{+}Hg^{++}P_2^{=} + H_2^{+}SO_4^{=} \ .$$

Two protons are eliminated for every mercuric ion bound by the DNA, and Eq. (21a) applies with $x = 0.331$ and $n = 1$. We use the reciprocal of the density of sulfuric acid, 0.543 ml./g., as an estimate of $\bar{v}_y$. Because of the large difference in molecular weight between H_2SO_4 and $HgSO_4$, the calculation is insensitive to the choice of the value for $\bar{v}_y$. The experimental points in Fig. (8) were taken from Nandi, Wang, and Davidson.[7] The theoretical lines are seen to be in substantial agreement with the experimental data.

The binding of silver to DNA has been studied by Jensen and

Fig. 8. The four component reacting system Cs_2SO_4, H_2O, Cs DNA, and $HgSO_4$. The experimental data were taken from Nandi, Wang, and Davidson[7] and the theoretical curves were calculated with Eqs. (101a,b) and (102) as described in the text. ⊙, ——— T4 DNA. O, ---- E. Coli DNA.

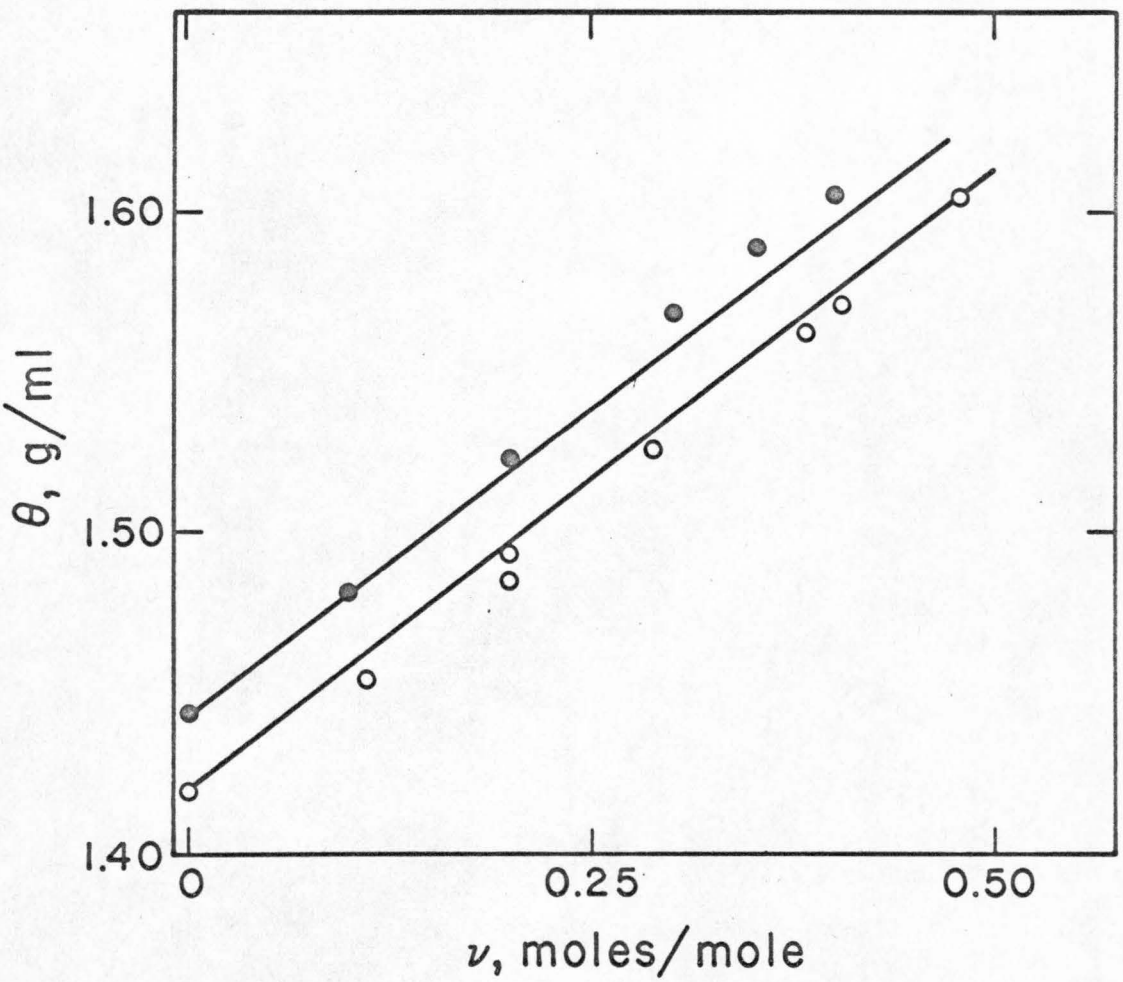
1.60
1.50
1.40
θ, g/ml
0
0.25
0.50
ν, moles/mole

Davidson,[21] who have presented experimental plots of θ as a function of ν, moles silver bound per mole Cs nucleotide. The points in Fig. (9) represent experimental results at both pH 5.6 and pH 8. The theoretical curve which fits the data at pH 5.6 was calculated with the assumption that the binding stoichiometry is similar to type (c) given in Section (a),

$$Ag_2^+SO_4^= + 2Cs^+H^+P^= \rightleftharpoons 2Cs^+Ag^+P^= + H_2^+SO_4^= .$$

The molecular weight of Ag_2SO_4 is 311.82, x = 0.315 and n = 1.

At pH 8 the experimental points are significantly higher than at pH 5.6. This requires either that the binding of silver is accompanied by an incorporation of cesium ions into the complex, or that the complex becomes significantly more hydrophobic and loses preferentially solvated water. If it is assumed that an additional proton is expelled per silver ion bound, the reaction stoichiometry will be of the modified type (c) given in Section (a),

$$Ag_2^+SO_4^= + Cs_2^+SO_4^= + 2Cs^+H^+P^= \rightleftharpoons Cs_2^+P^= \cdot Ag^+Cs^+P^= + 2H_2^+SO_4^= ,$$

and one additional cesium ion is bound per silver ion. The additional cesium ion is incorporated in order to maintain an electrically neutral species. Stoichiometrically, the addition of one equilivent of Ag_2SO_4 is accompanied by the addition of one equilivent of Cs_2SO_4 and by the loss of two equivalents of H_2SO_4. In order to account for these effects Eq. (21c) must be modified so that

$$\bar{v}_{eff} = \frac{\bar{v}_4 + x'\bar{v}_2 - 2x\bar{v}_y}{1 + x' - 2x} \qquad (103a)$$

Fig. 9. The four component reacting system Cs_2SO_4, H_2O, Cs DNA, and Ag_2SO_4. The experimental data were taken from Jensen and Davidson[21] and the theoretical curves were calculated with Eqs. (101a,b) and (102) as described in the text. O, —— Binding at pH 8.0. ⊙, —— Binding at pH 5.6.

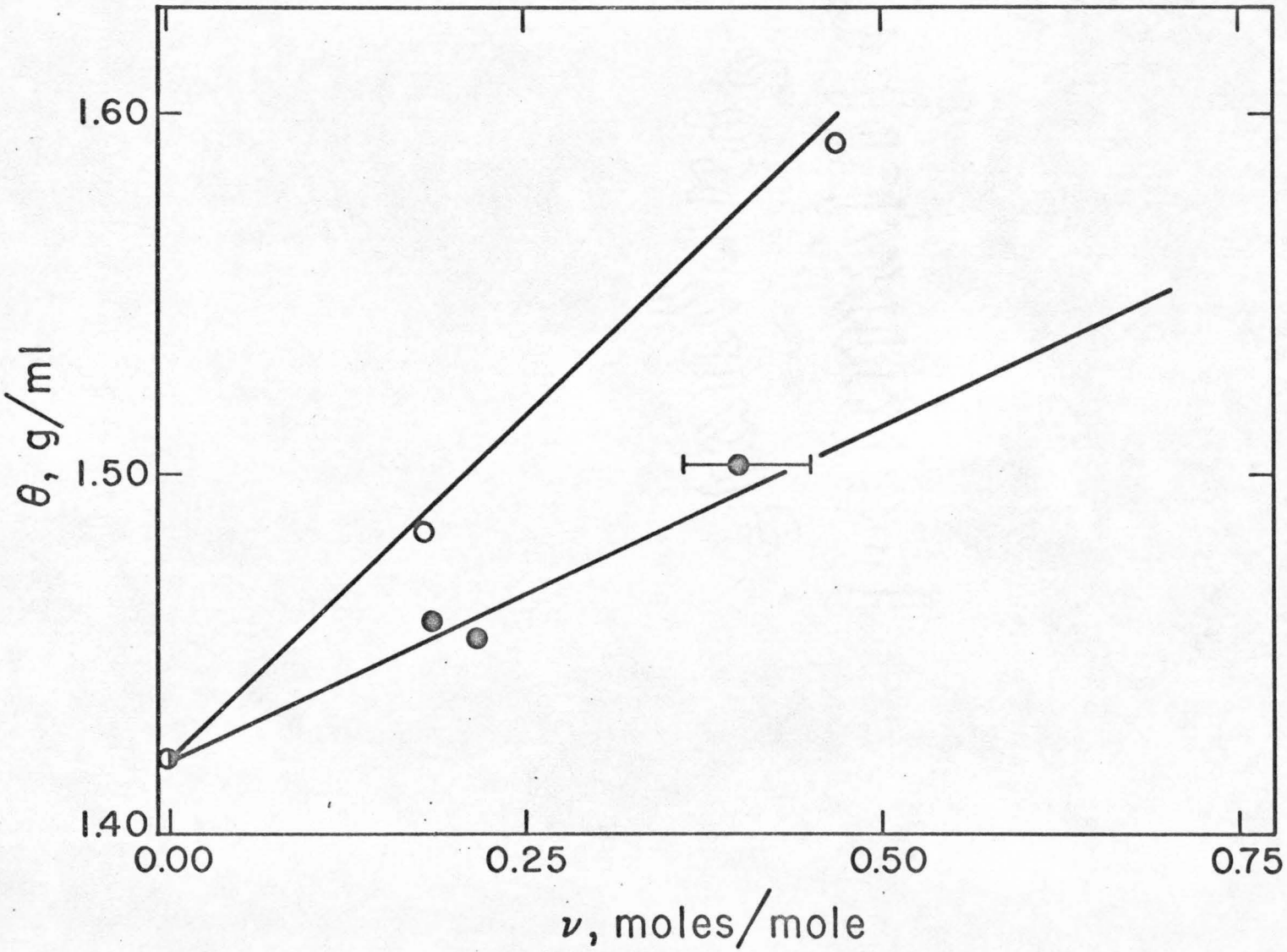
1.60
1.50
1.40
θ, g/ml
0.00
0.25
0.50
0.75
ν, moles/mole

and

$$\nu'' = \nu'(1 + x' - 2x) \quad , \tag{103b}$$

where x′ is the molecular weight ratio M_2/M_4. The molecular weight of Cs_2SO_4 is 361.9, X′ = 1.161 and $\bar{v}_2$ = 0.236 ml./g., the reciprocal of the crystal density. The theoretical result for the variation of θ with ν is also plotted in Fig. (9) and is seen to agree well with the experimental data at pH 8. The mechanism of silver binding to DNA proposed earlier[21] does not lead to the stoichiometric relationships which had to be assumed here in order to reproduce the experimental results. If the results of the silver and mercury additions are compared, it is seen that the experimental curves of θ versus ν differ by only 20-25% at pH 8. Since the mercuric ion is approximately twice as massive as the silver ion, this result is not readily understandable on the basis of addition of silver ion alone.

Another possible binding stoichiometry is indicated by reaction type (b) given in Section (a),

$$Ag_2^+SO_4^= + 2Cs^+H^+P^= \rightleftharpoons 2Ag^+H^+P^= + Cs_2^+SO_4^= \quad .$$

The net result of this reaction would be the replacement of a cesium ion by a silver ion, which would be expected to cause a slight net decrease in the buoyant density.

The change in buoyant density with the amount of reagent bound may be approximated over a limited range of ν' by

$$\theta = \theta_0 + \left(\frac{d\theta}{d\nu'}\right) \nu' \quad . \tag{104}$$

Differentiating Eq. (19), the derivative in Eq. (104) is obtained as

$$\frac{d\theta}{d\nu'} = \left\{\frac{1 - \bar{\nu}_4\left(\frac{1 + \Gamma'}{\bar{\nu}_3 + \Gamma'\bar{\nu}_1}\right)}{\bar{\nu}_3 + \Gamma'\bar{\nu}_1}\right\}\left\{1 - \frac{\bar{\nu}_4\nu'}{\bar{\nu}_3 + \Gamma'\bar{\nu}_1}\right\}^2 . \qquad (105)$$

In the case that $\nu' \ll 1$, $\Gamma' \approx \Gamma'_0$. This result may be further approximated to obtain the simple form

$$\frac{d\theta}{d\nu'} = \frac{1 - \bar{\nu}_4\theta_0}{\bar{\nu}_3 + \Gamma'_0\bar{\nu}_1} . \qquad (106)$$

In the event that the reaction stoichiometry is more complex, $\bar{\nu}_4$ is to be replaced by $\bar{\nu}_{4,\,\mathrm{eff}}$, Eq. (21c) or (103a), in Eq. (106). For higher values of ν', Eq. (105) predicts that the absolute value of the slope always decreases, which is consistent with the exact results obtained by combining Eq. (102) with either Eq. (100) or (101), as shown in Fig. (6).

APPENDIX

The calculation of $\Delta\Gamma'(\theta)$ for Cs_2SO_4 solutions proceeds in a manner identical to that described in Bauer and Vinograd,[10] Appendix III. For this purpose it was necessary to recalculate the quantities β^0 and $da_1/d\rho^0$. The data for β^0 in Cs_2SO_4 solutions was obtained from Ludlum and Warner[26] and was fitted to a fourth degree polynomial in the variable $x = \theta - 1.26$.

$$\beta(\rho) \times 10^{-7} = 81.674 - 159.41x + 398.97x^2 - 46.809x^3 - 417.78x^4. \quad (107)$$

The variation of solution density with water activity for Cs_2SO_4 solutions was calculated from data given in the International Critical Tables.[27] The result for the first derivative is expressed in terms of the variable $y = \theta - 1.25$.

$$\frac{da_1^0}{d\rho^0} = -0.20034 + 1.6636y - 13.967y^2 + 44.666y^3 - 52.574y^4. \quad (108)$$

REFERENCES

1. MESELSON, M., F. W. STAHL & J. VINOGRAD. 1957. Proc. Nat. Acad. Sci. 43: 581.
2. HEARST, J. E. 1962. J. Mol. Biol. 4: 415.
3. WILLIAMS, J. W., K. E. VAN HOLDE, R. L. BALDWIN & H. FUJITA. 1958. Chem. Revs. 58: 728.
4. HEARST, J. E. & J. VINOGRAD. 1961. Proc. Nat. Acad. Sci. 47: 1005.
5. HEARST, J. E. 1965. Biopolymers. 3: 57.
6. HEARST, J. E. & J. VINOGRAD. 1961. Proc. Nat. Acad. Sci. 47: 825.
7. NANDI, U.S., J. C. WANG & N. DAVIDSON. 1965. Biochemistry. 4: 1687.
8. KIRSTEN, W., H. KIRSTEN & W. SZYBALSKI. 1966. Biochemistry. 5: 236.
9. RADLOFF, R., W. BAUER & J. VINOGRAD. 1967. Proc. Nat. Acad. Sci. 5: 1514.
10. BAUER, W. & J. VINOGRAD. J. Mol. Biol. in press.
11. VINOGRAD, J., J. MORRIS, N. DAVIDSON & W. F. DOVE, JR. 1963. Proc. Nat. Acad. Sci. 49: 12.
12. KUBINSKI, H., Z. OPARA-KUBINSKA & W. SZYBALSKI. 1966. J. Mol. Biol. 20: 313.
13. HERSHEY, A. D. & E. BURGI. 1965. Proc. Nat. Acad. Sci. 53: 325.

14. HEARST, J. E. & J. VINOGRAD. 1961. Proc. Nat. Acad. Sci. 47: 999.

15. VAN HOLDE, K. E. & G. P. ROSSETTI. 1967. Biochemistry. 6: 2189.

16. ADAMS, E. T. 1967. Biochemistry. 6: 1864.

17. NICHOL, L. W. & A. G. OGSTON. 1965. J. Phys. Chem. 69:4365.

18. STEINBERG, I. Z. & H. K. SCHACHMAN. 1966. Biochemistry. 5: 12.

19. GOLDBERG, R. J. 1953. J. Phys. Chem. 57: 194.

20. SCATCHARD, G. 1949. Ann. N.Y. Acad. Sci. 51: 660.

21. JENSEN, R. H. & N. DAVIDSON. 1966. Biopolymers. 4: 17.

22. HEARST, J. E., J. B. IFFT & J. VINOGRAD. 1961. Proc. Nat. Acad. Sci. 47: 1015.

23. IFFT, J. B., D. VOET & J. VINOGRAD. 1961. J. Phys. Chem. 65: 1138.

24. VINOGRAD, J. 1963. Methods in Enzymology. Vol. VI. S. P. Colowick and N. O. Kaplan, Eds. Academic Press, Inc., N.Y.; 854.

25. BAUER, W. & J. VINOGRAD. 1967. Manuscript in preparation.

26. LUDLUM, D. B. & R. C. WARNER. 1965. J. Biol. Chem. 240: 2961.

27. International Critical Tables. 1933. McGraw-Hill Book Co., Inc., N.Y.

PROPOSITION I

ABSTRACT

A model is developed for the structure of nucleohistone analogs in solution. Experiments are proposed to test the predictions of the model.

The binding of unbranched hydrocarbon derivatives to DNA is important for understanding both the regulation of gene expression and the chemical properties of nucleic acids in solution. Several of these compounds, such as spermine and cadaverine, occur as intracellular DNA complexes. Other compounds, such as poly-L-lysine and cetyltrimethylammonium bromide (CETAB), are of interest as analogs for the more complex binding found in nucleohistones. Detailed knowledge of the binding mechanism for the latter compounds is expected to contribute significantly to the understanding of what occurs in similar reactions in the cell.

One of the characteristic parameters of the linear organic binding reagents is the number of residues contained in the chain. It is proposed that the binding of the long-chain and short-chain reagents may be explained by different mechanisms, and that only the long-chain compounds are appropriately considered to be nucleohistone analogs. It is further proposed that the long-chain reagents bind principally through hydrophobic interactions, and that consequently the DNA duplex in solution is partially relaxed. By contrast, the binding of the short-chain ligands depends primarily upon charge neutralization and no appreciable unwinding of the helix results.

Representative short-chain binding agents, all less than approximately twelve residues in length, include the diterminal diamines (1), the terminal monoamines (2), and the short polyamines spermine (3) and spermidine (3, 4). No change in the DNA spectrum is observed

upon binding by these reagents, and the melting profile is always monotonic. The midpoint of the thermal transition (T_m) is either raised by a small amount, 3-5° (1), or is slightly lowered (2).

The long-chain binding agents are represented by protamine (5), CETAB (6), and the cationic polypeptides poly-L-lysine (7, 8), poly-L-ornithine, poly-L-arginine, and poly-L-homoarginine (8). The results obtained in studies with these compounds differ in several important respects from those cited above for short-chain ligands. First, melting profiles are generally biphasic. The low temperature transition, at T_m, corresponds to the melting of unbound DNA and the higher transition, at T'_m corresponds to the melting of the complex. These two melting temperatures differ typically by 40°. Second, the ratio of the absorbance change at T_m to that at T'_m decreases linearly with the amount of reagent bound. Third, a DNA hyperchromicity accompanies addition at room temperature. This hyperchromicity increases linearly with the amount of bound reagent, reaching a maximum value of approximately 20% at saturation. Fourth, the higher melting temperature, T'_m, decreases more upon the addition of methanol than does the lower melting temperatue, T_m. Fifth, the binding is extremely strong at low ionic strength, and has been described as "irreversible" (3).

Recent work concerning the stability of the helical form of DNA in nonaqueous solvents (9) has emphasized the importance of hydrophobic interactions. The results of a study by Sinanõglu and Abdulnar (10) of the solvent denaturation of DNA show that the free energy change

in the helix–coil transition may be divided into four parts, of which the significant term for solvent denaturation is $\Delta G(c)$, the difference between the free energy required to create a "cavity" around the helix and two cavities around the coils in a given solvent. They show that $\Delta G(c)$ varies at $\gamma \Delta A$, where γ is the surface tension of water (considered as a macroscopic phase) around a base pair, and ΔA is the difference in surface area between the cavities surrounding a helical base pair and two bases in the coil form. The effect of a nonaqueous solvent is to lower γ.

It is proposed that a similar effect arises in the case of the binding of long-chain compounds to DNA, and that the chains act like a local nonaqueous solvent. The introduction of the hydrocarbon chains into the helical grooves causes a reduction of the surface tension of the cavity surrounding the bases, resulting in relaxation of the duplex helix and partial denaturation. This prediction may be tested experimentally with the use of closed circular DNA. In the presence of increasing concentrations of a reagent which unwinds the duplex, the sedimentation coefficient of closed circular DNA first decreases, then passes through a dip region, and later increases (11, 12). It is anticipated that this characteristic behavior will be observed upon the binding of poly-L-lysine, a representative long-chain reagent. The sedimentation coefficient of closed circular DNA is expected to remain unchanged, or to decrease slightly, in the presence of the short-chain molecule spermine.

The characteristic differences in binding properties between the

long- and short-chain reagents may be most readily understood in terms of their relative tendencies to form micelles in solution. The ability of hydrocarbons and their derivatives, either charged or uncharged, to form micelles is a function of the length of the hydrocarbon chain. Micelle formation is not observed for hydrocarbons of chain length less than twelve. Above this threshold value the critical micelle concentration (that concentration required for the first formation of micelles) decreases linearly with increasing chain length (13). The formation of hydrophobic bonds is a concerted process, and the inability of short-chain hydrocarbons to form micelles indicates that the free energy gained by the exclusion of the hydrocarbon moieties from water is more than compensated by the loss of entropy associated with the more ordered form of the micelle.

It is proposed that the different behavior exhibited by the long- and short-chain compounds upon binding to DNA is of a similar origin. This prediction may be examined with the use of compounds in which the hydrocarbon chain length is varied in a systematic way. Such a series is represented by compounds of the type $CH_3(CH_2)_n N^+(CH_3)_3$, in which n may range from zero to twenty or greater. It is predicted that the special properties listed above which are associated with long-chain reagents will diminish with n, and that a threshold value of about n = 12 will be observed. These experiments should include both the measurement of any spectral changes in DNA which occur upon reagent addition, and the determination of the melting profile of the complex at a constant low ionic strength.

The binding of CETAB, which contains one charge per sixteen carbon atoms, is similar (6) to that of poly-L-ornithine (8), which has one charge per five carbon atoms. This result emphasizes the relatively greater importance of the hydrophobic contribution to the binding, and suggests that long-chain neutral compounds should bind to DNA. It may be, however, that at least one positive charge per ligand is necessary to assist in the orientation of the molecule in the DNA groove. This question may be resolved by a study of the binding of dimethyl acetylhexadecanal, a long-chain neutral compound which is sufficiently soluble in water. The model predicts that short-chain uncharged compounds will not bind to DNA. This may be tested with the water-soluble compounds octanediol and 2, 4, 6-heptanetrione.

Other characteristics of the melting of complexes formed between DNA and the long-chain ligands may be understood in terms of the model presented here. The high cooperativity of the binding reaction may be due to the relatively greater ease of inserting a helix-unwinding reagent into a region of the helix adjacent to a partially unwound region. The effect of added methanol, which reduces the melting temperature of the complex more than that of the uncomplexed DNA (8) may be understood on the basis of hydrophobic interactions. The free energy gained by transferring a hydrophobic reagent from water to the DNA groove decreases in the presence of a nonaqueous solvent. This effect is not readily comprehensible in terms of electrostatic interactions alone.

Further evidence for the above interpretations is obtained from electrophoretic experiments on DNA complexes with long- and short-chain ligands. Liquori et al. (4) found that the mobility of a DNA-spermidine complex, an example of a short-chain interaction, is decreased markedly relative to that of the native DNA. The mobility of the complex with poly-L-lysine (7), on the other hand, is about 79% of the value in the absence of reagent. This indicates that the cationic groups of poly-L-lysine are much less closely associated with the DNA phosphates than are the cationic groups of spermidine. Such a result is expected if in the former case the main interaction is hydrophobic bonding, with consequent partial unwinding of the helix. The DNA B form has been shown (4) to provide a good matrix for charge neutralization in the case of spermidine. A relaxation of the helix upon the binding of poly-L-lysine will bring about a relatively greater charge separation, allowing the cationic charges of the reagent to be partially shielded by outside anions.

The mechanism of the binding of the histones to DNA in solution is not yet known (14). The related experiments of Wilkins and coworkers (5, 15) on the structure of the nucleoprotamines indicate that these ligands probably bind along the narrow groove of the DNA helix. The experiments also showed that the DNA B form is maintained in the complex at 95% relative humidity and in the semicrystalline state, in contrast to the conclusions presented here for the structure of the complex in solution. Four mechanisms are presently recognized for the binding of various reagents to DNA: intercalation, as with the

acridines at low concentration; ion pair formation, as with Mg^{++}; nonspecific outside binding, as with the acridines at high concentration; and the insertion of residues into the DNA helical grooves. In the case of the nucleohistones, it would appear reasonable that the binding in solution is, at least in large part, of this latter type. If so, it should be anticipated that a major portion of the binding affinity is due to hydrophobic interactions, and that the pitch of the nucleohistone molecule in aqueous solution is greater than that of the B form of DNA.

REFERENCES

1. Mahler, R. H. and B. D. Mehrotra, Biochim. Biophys. Acta, 68, 211 (1963).
2. Venner, H., C. Zimmer, and S. Schröder, Biochim. Biophys. Acta, 76, 312 (1963).
3. Mandel, M., J. Mol. Biol., 5, 435 (1962).
4. Liquori, A. M., L. Costantino, V. Crescenzi, V. Elia, E. Giglio, R. Puliti, M. De Santis Savino, and V. Vitagliano, J. Mol. Biol., 24, 113 (1967).
5. Feughelman, M., R. Langridge, W. E. Seeds, A. R. Stokes, H. R. Wilson, C. W. Hooper, M. H. F. Wilkins, R. K. Barkley, and L. D. Hamilton, Nature, 175, 834 (1955).
6. Bauer, W. and J. Vinograd, unpublished observations.
7. Tsuboi, M., K. Matsuo, and P. O. P. Ts'o, J. Mol. Biol., 15, 256 (1966).
8. Olins, D. E., A. L. Olins, and P. H. von Hippel, J. Mol. Biol., 24, 157 (1967).
9. Herskovits, T. T., S. J. Singer, and E. P. Geiduschek, Arch. Biochem. Biophys., 94, 99 (1961).
10. Sinanŏglu, O. and S. Abdulnar, Symposium on Molecular Mechanisms in Photobiology, Wakulla Springs, Fla. (Feb., 1964).
11. Bauer, W. and J. Vinograd, J. Mol. Biol., in press.

12. Crawford, L. V. and M. J. Waring, J. Mol. Biol., 25, 23 (1967).

13. Shinoda, K., Colloidal Surfactants (Academic Press: New York), 1 (1963).

14. Wilkins, M. H. F. and G. Zubay, J. Mol. Biol., 7, 756 (1963).

15. Wilkins, M. H. F., Cold Spr. Harb. Symp. Quant. Biol., 21, 75 (1956).

PROPOSITION II

ABSTRACT

It is proposed that the interaction of cardiac glycosides with erythrocyte ATPases be studied by NMR spectroscopy. The suggested experiments are relevant to an understanding of the sodium pump.

Recent investigations of the movement of alkali cations against an electrical gradient in human erythrocytes (the "sodium pump") have established that this process is correlated with the degradation of ATP[†] to ADP and inorganic phosphate (1, 2). It has been suggested (3) that ATPase activity is directly related to the functioning of the sodium pump. Dunham and Glynn (2) have demonstrated, however, that part of the ATPase activity of erythrocyte "ghosts" (4) occurs in the absence of sodium and potassium and is therefore independent of active ion transport. This has been confirmed by the separation of two ATPases, possessing the required specificities, from human erythrocyte membranes (5).

An important part of the evidence linking ATPase activity to the sodium pump rests upon the joint inhibition of these two functions by the cardiac glycosides, such as digoxin and ouabain. This latter compound has the structure

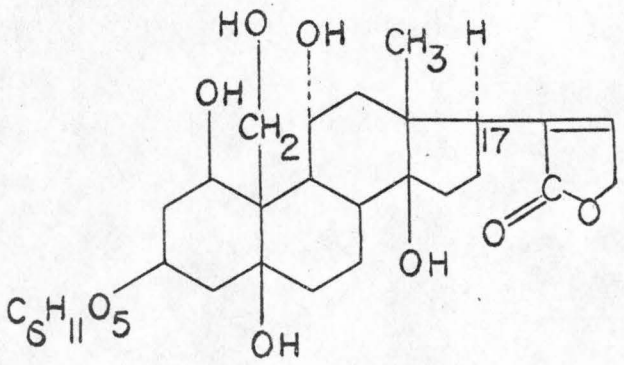

[†]Abbreviations used: ATP, adenosine triphosphate. ADP, adenosene diphosphate. ATPase, adenosine triphosphatase. ppm, parts per million. NMR, nuclear magnetic resonance.

It has been established (3) that at least three structural properties are necessary for the inhibition to take place. The lactone must be unsaturated and must be linked to a steroid ring system; and the configuration at C_{17} must be that shown above.

A causal relationship between inhibition of a membrane-associated ATPase fraction and blockage of the sodium pump has not yet been demonstrated, nor has it been shown that the cardiac glycosides act directly on the hydrolytic enzyme. It is proposed here that the NMR of ouabain be investigated in the presence and in the absence of various membrane fractions, including the recently isolated (5) ATPase activities. These experiments are expected to provide information concerning the specificity of the reaction with ouabain as well as to indicate which portion of the ouabain molecule is primarily responsible for the interaction. Comparison with the NMR spectrum of the reagent bound to the fragmented erythrocyte membrane and to the erythrocyte ghost might be expected to indicate whether or not a similar binding mechanism pertains in vivo.

The technique of NMR spectroscopy has been refined to the extent that it is now possible to study the binding of small molecules to macromolecules at sufficiently low concentrations. Jardetzky, for example has employed NMR to characterize the binding of penicillin G and oxytetracycline to albumin (7), and Hollis has studied the interaction of a variety of substrates with alcohol dehydrogenases (8). In these cases the NMR spectrum of the protein generally consists of a few broad peaks and constitutes a background for the measurement of

the high resolution proton NMR spectrum of the much smaller binding agent. When the small molecule is bound its characteristic lines broaden due to the restricted rate of molecular, mainly rotational, motion. A shift in the peak position (chemical shift) may also be observed. If the various spectral peaks have been previously identified with protons at particular locations within the molecule, a differential broadening upon binding may often be used to indicate which portion of the molecule is most intimately connected with the macrospecies.

The high resolution NMR spectrum of ouabain has not been reported, but the gross features of the spectrum may be estimated from a consideration of simpler analogs. 2-Butenoic acid-8-lactone has three resonance peaks, at 4.92, 6.15, and 7.63 ppm (9). The lactone is linked to the steroidal residue in ouabain through the α-C residue, and the 6.15 ppm resonance would be lacking in this compound. A comparison of a variety of steroid derivatives (9, 10) indicates that all resonance peaks are clustered in the region 0.7-2.5 ppm, and a variety of substituents introduces only small chemical shifts (10). The third major group in ouabain is a $C_6H_{11}O_6$ residue. The NMR peaks of β-methyl arabinoside, a representative six-carbon sugar, lie between 3.4 and 4.8 ppm (9). If large chemical shifts do not result from the binding interactions, the three principal rotational groups of ouabain should therefore give rise to three distinct groups of NMR peaks: the lactone at 7-8 ppm, the steroid at 0-2.5 ppm, and the sugar at 3-5 ppm.

In view of the above considerations, NMR seems to be especially appropriate for the study of the inhibitory effects of ouabain upon membrane ATPase activity in relation to the sodium pump. If the method is successful, a variety of subsequent experiments are indicated. Some examples are:

(1) The ATPase inhibition is overcome by potassium at low concentrations of ouabain (2). The NMR spectrum of ouabain in the presence of ATPase should be studied as a function of potassium concentration, in order to determine if the expected line broadening is reversed.

(2) Other ATPases, such as the one recently isolated from the streptococcus cell membrane (11), consist of as many as five subunits. If this proves to be the case for the erythrocyte ATPases, NMR could be used to determine whether one or more of these subunits is specific for ouabain binding.

(3) A variety of other cardiac glycosides are known, some of which (Scillaren A and cymarin) are active inhibitors, and others (Hexahydroscillaren A and 17α-cymarin) are inactive (2). These could be studied by NMR to determine the correlation between activity and extent and type of interaction with the enzyme fractions.

The erythrocytes from some species (for example, rat and rabbit) do not appear to contain membrane-bound ATPase activity (12). A correlation between the sodium pump and ATP degradation has, however, been demonstrated in a variety of other tissues from several organisms (6). In the human erythrocyte only about 10^3 molecules of ouabain

per cell are required for complete inhibition of the pump. It is hoped that the experiments proposed here will help to determine whether or not this interaction takes place at the site of membrane-bound ATPase molecules.

REFERENCES

1. Post, R. L., C. R. Merritt, C. R. Kinsolving, and C. D. Albright, J. Biol. Chem., 235, 1796 (1960).
2. Dunham, E. T. and I. M. Glynn, J. Physiol., 156, 274 (1961).
3. Glynn, I. M., J. Physiol., 136, 148 (1957).
4. Whittam, R., Biochem. J., 84, 110 (1962).
5. Nakao, T., K. Nagano, K. Adachi, and M. Nakao, Biochem. Biophys. Res. Comm., 13, 444 (1963).
6. Baker, R. F., Endeavour, 25, 166 (1966).
7. Jardetzky, O., Advan. Chem. Phys., 7, 499 (1964).
8. Hollis, D. P., Biochemistry, 6, 2080 (1967).
9. NMR Spectra Catalog, comp. by N. S. Bhacca, D. P. Hollis, L. F. Johnson, E. A. Pier, and J. N. Shoolery, The National Press (1963).
10. Zürcher, R. F., Helv. Chim. Acta, 44, 1380 (1961).
11. Abrams, A. and C. Baron, Biochemistry, 6, 225 (1967).
12. Duggen, D. E., J. E. Baer, and R. M. Noll, Naturwissenschaften, 52, 264 (1965).

PROPOSITION III

ABSTRACT

A new method is presented for the estimation of superhelix density in closed circular DNA, based upon the restricted binding of dye caused by the superhelical turns.

The superhelix density of covalently closed circular duplex DNA may be measured by means of three alternative methods. These include the alkaline buoyant density titration, which has been used for polyoma DNA (1); the sedimentation velocity-dye titration with ethidium bromide, which has been applied to both polyoma (2) and SV 40 (3) DNAs; and the buoyant density shift resulting from ethidium bromide binding, for SV 40 DNA (3). The latter two are only partially independent, both relying upon knowledge of the angle of unwinding upon dye intercalation, ϕ, as estimated by Fuller and Waring (4).

All three methods involve a series of experiments in the analytical ultracentrifuge to determine a titration or binding curve. This procedure is not only time-consuming but often presents serious problems of stability of the closed circular DNA over the period of the experiments. The alkaline titration may not be used with certain DNAs which are unstable at high pH, such as sea urchin mitochondrial DNA (5). The dye-buoyant density method is experimentally difficult in the low binding region because only small changes in buoyant density are involved, although it may be used to determine the binding isotherm and the free energy of superhelix formation (6). The dye-sedimentation velocity method has the advantage that it may be used at low salt concentration, although several micrograms of DNA are required. For both dye methods it is necessary to measure the free dye concentration.

An alternative method for the determination of superhelix

density is presented here which involves a single experiment in either the analytical or preparative ultracentrifuge, and which does not require measurement of the free dye concentration. This method is based upon the observation that the difference in buoyant density, $\Delta\theta = \theta_1 - \theta_2$, between closed circular (I) and nicked circular (II) SV 40 DNAs becomes constant at very high dye levels (3). The saturation buoyant density difference has been attributed to the positive free energy of superhelix formation. This quantity increases with the increasing superhelix density which accompanies intercalative dye binding, eventually exceeding the negative free energy change due to the binding reaction (6). No further binding to DNA I is possible, although binding to DNA II continues until all available sites are occupied. For SV 40 DNA I intercalative binding stops at a mole ratio of ethidium bound to DNA nucleotide of $\nu = 0.20$ (3).

The superhelix density, σ, is an intensive quantity equal to the number of superhelical turns per ten base pairs. It is assumed in the derivations to follow that the free energy of superhelix formation per mole base pair depends only upon σ and not upon the length of the DNA molecule. The value of the superhelix density at saturation with ethidium chloride at 25° in cesium chloride will therefore be the same for all closed circular DNAs. A decrease in the initial superhelix density, σ_0, of the native closed circular DNA is consequently expected to reduce the saturation buoyant density difference between DNAs I and II, while an increase in the number of native turns will reduce this quantity. The magnitude of the saturation buoyant density

difference between the closed and nicked circular DNAs in ethidium bromide may be used as a measure of the superhelix density of the closed molecule in the absence of dye.

The superhelix density may be calculated with the relation (3)

$$\sigma = \sigma_0 + (\frac{10\phi}{\pi})\nu, \tag{1a}$$

and at saturating dye concentrations

$$\sigma_S = \sigma_0 + (\frac{10\phi}{\pi})\nu_S \ . \tag{1b}$$

In the derivations to follow all symbols containing a superscript * refer to a closed circular duplex DNA of unknown superhelix density, and the corresponding symbols without superscripts refer to SV 40 DNA. The basic assumption discussed above is that $\sigma_S = \sigma_S{}^*$. Combining eqs. (1a, b), the result is

$$\sigma_0{}^* - \sigma_0 = (\frac{10\phi M_4}{\pi M_3})(\nu_S{}' - \nu_S{}'^*), \tag{2}$$

where ν' is the weight binding ratio in grams of ethidium bromide per gram of cesium nucleotide, M_3 is the Cs nucleotide molecular weight and M_4 is the molecular weight of ethidium chloride.

The buoyant density difference between closed circular (1) and nicked circular (2) DNAs at a dye concentration sufficiently high to saturate all primary or intercalative binding sites is approximately (3)

$$\bar{v}_4(\theta_1 - \theta_2) = \frac{a + \nu_1'}{b + \nu_1'} - \frac{a + \nu_2'}{b + \nu_2'} \quad , \tag{3}$$

where $a = 1 + \bar{\Gamma}'$ and $b = (\bar{v}_3 + \bar{\Gamma}'\bar{v}_1)/\bar{v}_4$. The average net hydration, $\bar{\Gamma}' = (\Gamma_1' + \Gamma_2')/2$, has been used for each component, an approximation which leads to only a small error. The quantities $\bar{v}_1$, $\bar{v}_3$, and $\bar{v}_4$ are the partial specific volumes of water, anhydrous Cs DNA, and bound ethidium chloride. Equation (3) is rewritten

$$\bar{v}_4 \Delta\theta = \frac{a}{b}\left[\frac{1 + \nu_1'/a}{1 + \nu_1'/b} - \frac{1 + \nu_2'/a}{1 + \nu_2'/b}\right] \quad . \tag{4}$$

Introducing the approximation

$$\left(1 + \nu_i'/b\right)^{-1} = 1 - \nu_i'/b + (\nu_i'/b)^2/2, \quad i = 1, 2, \tag{5}$$

and neglecting terms in $\nu_i'^3$,

$$\bar{v}_4 \Delta\theta = \frac{a}{b}\left[\left(\frac{1}{b} - \frac{1}{a}\right)(\nu_2' - \nu_1') + \frac{1}{b}\left(\frac{1}{2b} - \frac{1}{a}\right)(\nu_2'^2 - \nu_1'^2)\right] . \tag{6a}$$

Equations (3)-(6a) apply also to the DNA of unknown superhelix density, and

$$\bar{v}_4 \Delta\theta^* = \frac{a^*}{b^*}\left[\left(\frac{1}{b^*} - \frac{1}{a^*}\right)(\nu_2'^* - \nu_1'^*) + \frac{1}{b}\left(\frac{1}{2b} - \frac{1}{a}\right)(\nu_2'^{*2} - \nu_1'^{*2})\right] . \tag{6b}$$

Letting $\Delta\nu' = \nu_2' - \nu_1'$ and $\bar{\nu}' = (\nu_2' + \nu_1')/2$, eqs. (6a, b) are combined to obtain the result

$$\frac{\Delta\theta^*}{\Delta\theta} = \left(\frac{b}{b^*}\right)^2 \left(\frac{a^* - b^*}{a - b}\right) \frac{\Delta\nu'^*}{\Delta\nu'} \left[1 + \frac{1}{b^*}\left(\frac{a^* - 2b^*}{a^* - b^*}\right)\bar{\nu}'^* - \frac{1}{b}\left(\frac{a - 2b}{a - b}\right)\bar{\nu}'\right] \tag{7}$$

where the approximation has also been used that

$$\left[1 + \frac{1}{b}\left(\frac{a - 2b}{a - b}\right)\bar{\nu}'\right]^{-1} \approx 1 - \frac{1}{b}\left(\frac{a - 2b}{a - b}\right)\nu'.$$

Since the difference between the last two terms in the bracket of eq. (7) is less than 0.01, the result may be written to a good approximation

$$\frac{\Delta\theta^*}{\Delta\theta} = \left(\frac{b}{b^*}\right)^2 \left(\frac{a^* - b^*}{a - b}\right) \frac{\Delta\nu'^*}{\Delta\nu'} \tag{8a}$$

or, in different notation,

$$\frac{\Delta\theta^*}{\Delta\theta} = f\left(\frac{\nu_1'^* - \nu_2'^*}{\nu_1' - \nu_2'}\right), \tag{8b}$$

where $f = (b/b^*)^2 [(a^* - b^*)/(a - b)]$. We use the fact that at saturation $\nu_2' = \nu_2'^*$ and rearrange eq. (8b) to obtain, at saturating dye concentration,

$$\nu_1'^* - \nu_1' = (\nu_2' - \nu_1')\left(1 - \frac{1}{f}\frac{\Delta\theta^*}{\Delta\theta}\right). \tag{9}$$

The number of superhelical turns present in the molecule is given by $\tau = \beta^0 \sigma$, where β^0 is a normalization factor numerically equal to one-tenth the number of base pairs. Equations (2) and (9) are combined to give the result

$$\tau_0^* = \tau^0 \frac{\beta^{0*}}{\beta^0} - \left(\frac{10\phi\beta^{0*} M_4 \Delta\nu'}{\pi M_3}\right)\left(1 - \frac{1}{f}\frac{\Delta\theta^*}{\Delta\theta}\right). \qquad (10)$$

The factor f may be calculated from the definitions of a and b given previously.

$$f = \left(\frac{\bar{v}_3 + \Gamma'\bar{v}_1}{\bar{v}_3 + \Gamma'^*\bar{v}_1}\right)^2 \left[\frac{\bar{v}_3 - \bar{v}_4 + \Gamma'^* (\bar{v}_1 - \bar{v}_4)}{\bar{v}_3 - \bar{v}_4 + \Gamma' (\bar{v}_1 - \bar{v}_4)}\right] \qquad (11a)$$

Since $\bar{v}_1 \approx \bar{v}_4$ (3), eq. (11a) is approximated by

$$f = \left(\frac{\bar{v}_3 + \Gamma'\bar{v}_1}{\bar{v}_3 + \Gamma'^*\bar{v}_1}\right)^2 . \qquad (11b)$$

The change in preferential hydration upon moving a buoyant band to a different position in the density gradient as a result of dye binding, $\Delta\Gamma'$, is small and of comparable magnitude for all DNA species (3). The preferential hydrations of the native DNAs in the absence of dye may therefore be used in eq. (11b), and

$$f = \left(\frac{\bar{v}_3 + \Gamma_0'\bar{v}_1}{\bar{v}_3 + \Gamma_0'^*\bar{v}_1}\right)^2 . \qquad (11c)$$

The relationship between θ_0 and Γ_0' is given by Hearst and Vinograd (7),

$$\theta_0 = \frac{1 + \Gamma_0'}{\bar{v}_3 + \Gamma_0'\bar{v}_1} \qquad (12)$$

and combining with eq. (11c),

$$f = \left(\frac{\theta_0 \bar{v}_1 - 1}{\theta_0 * \bar{v}_1 - 1} \right)^2 \quad . \tag{13}$$

In this equation the buoyant density of SV 40 DNA is $\theta_0 = 1.6937$ (3) and we take $\bar{v}_1 = 1$ (7). The factor f expresses the effect of varying initial buoyant density (base composition) upon the buoyant separation at saturating dye concentrations, and it is generally close to unity. At $\theta_0 = 1.67$, $f = 0.924$, and at $\theta_0 = 1.73$, $f = 1.107$.

Equations (10) and (12) may be put in numerical form with the values $\Delta\nu' = 0.0885$ (3), $\phi = \pi/15$ (4), $\beta^0 = 480$, and $\tau_0 = -12.7$ (3).

$$- \frac{\tau_0 *}{\beta^0 *} = 0.0724 - 0.0459 \frac{1}{f} \frac{\Delta\theta *}{\Delta\theta} \tag{14}$$

$$f = \frac{0.4812}{(\theta_0 * - 1)^2} \quad . \tag{15}$$

The quantity $\Delta\theta$ in eq. (14) refers to the buoyant density difference between DNAs I and II measured at the same high dye concentration. In an actual experiment, the free dye concentration, c_2, in equilibrium with DNA II will be greater than that concentration, c_1, in equilibrium with DNA I. Because the amount of secondary binding increases with the dye concentration (4), the observed buoyant density difference, $\Delta\theta_{obs}$, will be greater than $\Delta\theta$. For SV 40 DNA it has been shown (3) that $\Delta\theta = 0.039$ g/ml and $\Delta\theta_{obs} = 0.048$ g/ml at dye

concentrations greater than 200 μg/ml. It is shown in the appendix that, to a good approximation,

$$\frac{\Delta\theta^*}{\Delta\theta} \approx \frac{\Delta\theta^*_{obs}}{\Delta\theta_{obs}} \quad . \tag{16}$$

It is therefore sufficient to compare the experimentally observed buoyant density separation at saturating dye concentrations with that of SV 40 DNAs I and II in order to calculate the initial superhelix density.

It has been shown elsewhere (8) that less than 0.1 μg of DNA may be detected visually in a preparative gradient tube containing ethidium bromide. The tube is illuminated at 365 mμ and the fluorescence of the bound dye, at 540 mμ, is approximately a factor of 100 greater than that of the free dye background (9). The method described here is therefore suitable for use with very small amounts of unlabeled closed circular DNA, and the only measurement necessary is the separation between the closed and nicked circular DNA species.

In order to test the method, it is proposed that the superhelix density of intercellular λ DNA be estimated both by the procedure detailed here and by the dye-sedimentation velocity method at 3.1 M CsCl, and the results compared. The use of a DNA approximately ten times the size of SV 40 will provide the strongest test of the assumption that $\sigma_s = \sigma_s^*$. The buoyant density separation between λ DNAs I and II has already been determined at a dye concentration of

100 μg/ml (8). From this data and eq. (14) it may be calculated that for intracellular λ DNA I, $\sigma_0 = -0.035$, a value approximately 35% greater than for SV 40 DNA I. The dye concentration in this case was, however, probably somewhat less than saturation. If the method proves satisfactory for λ DNA, it may be used for all other DNAs in the range $3\text{-}33 \times 10^6$ Daltons.

APPENDIX

The variation of the buoyant density with the amount of secondary binding has been shown to be approximately linear for ethidium bromide binding to SV 40 DNAs I and II (3). In terms of the free dye concentration, c, the change in buoyant density due to secondary binding is

$$\theta_1 = \theta_{1S} - K(c_1 - c_{sat}) \tag{A1}$$

and

$$\theta_2 = \theta_{2S} - K(c_2 - c_{sat}) \tag{A2}$$

where θ_S is the buoyant density at high dye concentration in the absence of secondary binding and $K = -\lim_{c \to \infty} (d\theta/dc)$. Then $\Delta\theta_{obs} = \theta_2 - \theta_1$, and $\Delta\theta = \theta_{2S} - \theta_{1S}$, and the differences are related by

$$\Delta\theta = \Delta\theta_{obs} - K\Delta c \tag{A3}$$

and

$$\Delta\theta^* = \Delta\theta^*_{obs} - K\Delta c^* . \tag{A4}$$

These equations are combined to obtain

$$\frac{\Delta\theta^*}{\Delta\theta} = \frac{\Delta\theta^*_{obs}}{\Delta\theta_{obs}} \left[\frac{1 - K\Delta c^*/\Delta\theta^*_{obs}}{1 - K\Delta c/\Delta\theta} \right] . \tag{A5}$$

From the data for SV 40 DNA given by Bauer and Vinograd (3) it is estimated that $K = 2 \times 10^{-5}$ g/μg and $\Delta c/\Delta\theta = 6 \times 10^3$ μg/g. Equation (A5) may therefore be approximated

$$\frac{\Delta\theta^*}{\Delta\theta} = \frac{\Delta\theta^*_{obs}}{\Delta\theta_{obs}} \left[1 - K\left(\frac{\Delta c}{\Delta\theta^*_{obs}} - \frac{\Delta c}{\Delta\theta_{obs}} \right) \right] \quad . \qquad \text{(A6)}$$

In the high dye region the difference term in the bracket in eq. (A6) is very close to zero and, to a good approximation,

$$\frac{\Delta\theta^*}{\Delta\theta} = \frac{\Delta\theta^*_{obs}}{\Delta\theta_{obs}} \quad . \qquad \text{(A7)}$$

REFERENCES

1. Vinograd, J., J. Lebowitz, and R. Watson, J. Mol. Biol., in press.
2. Crawford, L. V. and M. J. Waring, J. Mol. Biol., 25, 23 (1967).
3. Bauer, W. and J. Vinograd, J. Mol. Biol., in press.
4. Fuller, W. and M. J. Waring, Berichte der Bunsengesellschaft, 68, 805 (1964).
5. Pikó, L., J. Vinograd, D. Blair, and A. Tyler, manuscript in preparation.
6. Bauer, W. and J. Vinograd, manuscript in preparation.
7. Hearst, J. E. and J. Vinograd, Proc. Nat. Acad. Sci., 47, 1005 (1961).
8. Radloff, R., W. Bauer, and J. Vinograd, Proc. Nat. Acad. Sci., 57, 1514 (1967).
9. Le Pecq, J.-B. and C. Paoletti, J. Mol. Biol., 27, 87 (1967).

PROPOSITION IV

ABSTRACT

An electrostatic model is proposed to explain the broadening of the DNA melting profile at low ionic strength. The results are used to predict the effects of nonaqueous solvents.

Dove and Davidson (1), in the course of a study of the effect of variation of salt concentration on the thermal denaturation of DNA, found that the breadth of the transition curve increases with decreasing ionic strength. They explained this trend qualitatively in terms of Zimm's equilibrium statistical mechanical theory of DNA denaturation (2), pointing out that broadening can result both from a "direct" increase in the stacking parameter, σ_0, and from an increased contribution from intramolecular compositional heterogeneity at low ionic strength.

It was also shown in this investigation that the midpoint of the thermal denaturation curve, T_m, increases linearly with the logarithm of the ionic strength. Attempts have since been made (3, 4) to explain this result in terms of the appropriate thermodynamic functions describing the transition. It is proposed to extend this approach to express the observed variation in transition sharpness in terms of the same functions. The calculations will apply to the case of denaturation without strand separation, and electrostatic interactions will be considered the only variables affecting the transition breadth. The simple model chosen to represent DNA in solution will be a charged rod, and the results are expected to indicate the influence of changes in ionic strength in altering the transition breadth in the absence of further assumptions concerning the cooperativeness of the transition.

In general, the free energy change accompanying the transition helix $\rightleftharpoons$ coil may be written

$$\Delta G^{o}_{tr} = \Delta G^{o}_{h} + \Delta G^{o}_{hp} + \Delta G^{o}_{el} \quad . \tag{1}$$

Here ΔG^{o}_{tr} is the total free energy change without strand separation, ΔG^{o}_{h} is the free energy change involved in breaking the hydrogen bonds of the paired bases, ΔG^{o}_{hp} is the free energy change resulting from the disruption of hydrophobic bonds, and ΔG^{o}_{el} is the difference in electrostatic free energy between the helix and the random coil. Following Kotin (3), eq. (1) is written in the simpler form

$$\Delta G^{o}_{tr} = \Delta G^{o}_{0} + \Delta G^{o}_{el} , \tag{2}$$

where ΔG^{o}_{0} is the free energy change of the transition per mole of base pair at very high ionic strength. The electrostatic contribution is equal to $Ne\psi$, and eq. (2) becomes

$$\Delta G^{o}_{tr} = \Delta G^{o}_{0} + Ne\psi \tag{3}$$

Here N is Avagadro's number, e is the charge on the phosphate group, and ψ is the electrostatic potential at a phosphate group which results from all charged phosphates on the other chain. It can be shown (5) that, to a good approximation,

$$\frac{Ne\psi}{RT} = C_1 + C_2\, pNa, \tag{4}$$

where C_1 and C_2 are constants independent of temperature, the approximate values of which are known, and pNa is the negative logarithm of the free sodium ion concentration, taken equal to the ionic strength.

Letting ΔH_0^0 and ΔS_0^0 be the standard enthalpy and entropy of the transition at high ionic strength, it then follows that

$$\Delta G_{tr}^0 = \Delta H_0^0 - T\Delta S_0^0 + RT(C_1 + C_2\, pNa). \qquad (5)$$

The quantity α is defined as the fraction of base pairs in the coil form at any temperature and $\alpha = N_c'/N'$, where N_c' is the number of base pairs in the coil form, and N' is the total number of base pairs. The standard free energies of formation of the helix base pair and of two adjoining but nonpaired bases in the coil, respectively, are G_{hel}^0 and G_c^0, and $\Delta G_{tr}^0 = G_{hel}^0 - G_c^0$.

$$\alpha = N_c'/N' = \frac{\exp(G_c^0/RT)}{\exp(G_c^0/RT) + \exp(G_{hel}^0/RT)}$$

$$\alpha = \frac{1}{1 + \exp(\Delta G_{tr}^0/RT)} \quad . \qquad (6)$$

This result indicates that the thermal melting curve has the form of a simple hyperbolic tangent (6). The sharpness of the transition, s, is defined as the slope of a plot of α vs temperature, evaluated at $T = T_m$.

$$s \equiv \left(\frac{d\alpha}{dT}\right)_{T_m} . \qquad (7)$$

Differentiating eq. (6), and using the fact that $\Delta G_{tr}^0 = 0$ at $T = T_m$,

$$s = -\frac{1}{4RT_m}\left(\frac{d\Delta G^{o}_{tr}}{dT}\right)_{T_m} . \qquad (8)$$

Using eq. (5) for ΔG^{o}_{tr} and differentiating,

$$\left(\frac{d\Delta G^{o}_{tr}}{dT}\right)_{T_m} = \left(\frac{d\Delta H^{o}_{0}}{dT}\right)_{T_m} - T_m\left(\frac{d\Delta S^{o}_{0}}{dT}\right)_{T_m} + RT_m\left(\frac{d\,pNa}{dT}\right)_{T_m}$$

$$-\Delta S^{o}_{0} + R(C_1 + C_2\,pNa). \qquad (9)$$

Since the sodium ion concentration is the independent variable in this treatment, its temperature variation may be set equal to zero. Assuming that the temperature variations of ΔH^{o}_{0} and ΔS^{o}_{0} are small (4), these quantities may also be neglected. These approximations may lead to error in the estimation of the absolute transition breadth, as noted below. The expression of eq. (9) becomes approximately

$$\left(\frac{d\Delta G^{o}_{tr}}{dT}\right)_{T_m} = -\Delta S^{o}_{0} + R(C_1 + C_2\,pNa). \qquad (10)$$

Substituting eq. (10) into eq. (8),

$$s = \frac{1}{4RT_m}\left[\Delta S^{o}_{0} - R(C_1 + C_2\,pNa)\right] . \qquad (11)$$

Since C_1 and C_2 are both positive (5), this preliminary result indicates, as found by Dove and Davidson, that the transition breadth should increase (s decreases) as the ionic strength is lowered. However, T_m also contains a term involving the ionic strength. As derived by

Kotin (3),

$$T_m = \frac{T_m^0}{1 + (R/\Delta S_0^0)(C_1 + C_2 pNa)} . \qquad (12)$$

Here T_m^0 is the transition temperature in the absence of electrostatic interactions, and ΔS_0^0 is taken as positive for the transition helix $\rightleftharpoons$ coil as written.

Substituting eq. (12) into eq. (11) and simplifying, the result is obtained

$$s = K_1 - K_2\, pNa - K_3 (pNa)^2, \qquad (13)$$

where

$$K_1 = \frac{\Delta S_0^0}{4RT_m^0} - \frac{C_1 R}{4\Delta S_0^0 T_m^0} , \qquad (13a)$$

$$K_2 = \frac{RC_1 C_2}{2\Delta S_0^0 T_m^0} , \quad \text{and} \qquad (13b)$$

$$K_3 = \frac{RC_2^2}{4\Delta S_0^0 T_m^0} . \qquad (13c)$$

Here the ratio $K_2/K_3 = 2C_1/C_2 = 1$ (3). Equation (13) is rewritten in the form

$$s = K_1 - K_2 (pNa + p^2 Na) . \qquad (14)$$

Because of the approximations used in deriving eq. (10), the final result may be more appropriately expressed in terms of the fractional change expected in s for a given change in the ionic strength. An ionic strength of 0.1 M is chosen as a reference state, for which the slope is denoted s′, and eq. (14) is written for both the reference state and for an arbitrary ionic strength. The resultant fractional change in s is approximately given by eq. (15), for the case that $K_2/K_1 \ll 1$.

$$\frac{s - s'}{s'} = \frac{K_2}{K_1} (pNa - 1)(pNa + 2) \qquad (15)$$

Dove and Davidson's σ_T, the transition breadth, is inversely related to s; hence, the transition breadth clearly increases as pNa increases, and the functional relationship is that shown in eq. (15). K_1 and K_2 may be estimated by employing the proper values for ΔS_0^0, C_1 and C_2 in equations (13a) and (13b). Using the estimate $\Delta S_0^0 = 20$ entropy units, it follows that $K_2/K_1 = 0.01$ and the approximation used for eq. (15) is justified. The transition breadth is expected to increase by about 30% as the ionic strength is decreased from 0.1 M to 10^{-5} M. Although the value of σ_T for the transition in 0.1 M NaCl is not listed by Dove and Davidson (1), it may be estimated from their Fig. 1 as approximately 2°. At an ionic strength of 4.1×10^{-4} M, which corresponds to pNa = 3.4, the value of σ_T is 4.2°. This change in ionic strength results in an increase of about 50% in $1/\sigma_T$, which may be used as an estimate of the increase in s. The prediction from eq. (15)

for this change in ionic strength is about 15%. The assumption of a simple electrostatic model, combined with classical thermodynamic considerations, accounts for at least one-third of the observed broadening in aqueous solution.

Qualitatively, the broadening of the transition predicted by the model employed in this analysis results from a decrease in the linear charge density of the DNA molecule, regarded as a rod, upon relaxation of the helical structure of the duplex. This contribution to σ_T should arise regardless of increases in either Zimm's stacking parameter, σ_0, or of changes in the factor $(j + 1)^{-3/2}$, which is a term expressing the entropy change in combining j unbonded bases at the ends of a double stranded molecule into a ring containing j units and located in the interior of the molecule. If an increase in σ_T is to be interpreted as an increase in the cooperativeness of the transition, the change must exceed the amount predicted by the electrostatic model.

An alternate approach to the calculation for the charged rod is to use Hill's (7) expression for the electrostatic free energy of a charged cylinder, in which the charge is spread uniformly over the surface. This approach is complicated, however, by the necessity of knowing the local dielectric constant of the medium surrounding the molecule as well as its temperature variation.

The model can also be used to predict the change in σ_T arising from changes in the linear charge density of the DNA molecule in the presence of nonaqueous solvent components. Here ΔS_0^0

increases, due to a smaller $-\Delta S_0^0$ contribution from changes in the water structure upon denaturation. This suggests that the rod-like effects should be relatively greater in pure water than in the non-aqueous medium. In particular, the dependence of s upon ionic strength should be less in nonaqueous solvents, since K_2/K_1 varies as the inverse square of ΔS_0^0. Equations (13) and (14) also predict that s should increase (σ_T decreases) in the presence of a non-ionic, nonaqueous solvent.

Inspection of the melting profiles of DNA in methanol studied by Herskovits, Singer, and Geiduschek (8) shows the expected decrease in σ_T compared to the aqueous system at constant ionic strength. In the same study it was also found that electrostatic interactions are generally much less important in the nonaqueous solvents. Although no specific data could be found relating σ_T to pNa in the nonaqueous media, the second prediction would appear to be followed as well. More experimental evidence is needed, however, in order to fully check this prediction.

REFERENCES

1. Dove, Jr. and N. Davidson, J. Mol. Biol., 5, 467 (1962).
2. Zimm, B., J. Chem. Phys., 33, 1349 (1960).
3. Kotin, L., J. Mol. Biol., 7, 309 (1963).
4. Walker, I. O., Biochim. Biophys. Acta, 88, 407 (1964).
5. Kotin, L. and M. Nagasawa, J. Chem. Phys., 36, 873 (1962)
6. Schellman, J. A., Compt. rend. trav. lab. Carlsberg, Sér. chim., 29, 230 (1955).
7. Hill, T. L., Arch. Biochem. Biophys., 57, 229 (1955).
8. Herskovits, T. T., S. J. Singer, and E. P. Geiduschek, Arch. Biochem. Biophys., 94, 99 (1961).

PROPOSITION V

ABSTRACT

A potential error exists when the ultracentrifuge absorption optical system is used to measure the concentration profile of a macrospecies in the presence of a redistributing, light-absorbing reagent. Equations are derived to define the error in band width and position, and magnitudes are estimated for some typical cases. Experimental conditions may be chosen so as to minimize both errors.

The use of the absorption optical system of the analytical ultracentrifuge to measure the concentration profile of a macrospecies in density gradient sedimentation may be complicated by the presence of a light-absorbing reagent. If the reagent itself redistributes in the centifugal field, as is commonly the case, two types of measurement error may arise. The position of the peak maximum may undergo an apparent shift, and the apparent standard deviation of a Gaussian band may differ from the true standard deviation. Two special cases will be analyzed here, the first in which the observed profile of absorbance contains contributions from both macrospecies and bound reagent, and the second in which only the absorbance profile of bound reagent is measured. The binding of ethidium bromide to SV40 DNA II will be used as an example.[1]

If it is assumed that the contributions of the macrospecies and reagent to the absorbance, A, are additive, the net absorbance may be written in terms of the molar extinction coefficients of CsDNA, ϵ_3, and of ethidium bromide, ϵ_4.

$$A = k\, m_3 (\epsilon_3 + \nu \epsilon_4) \tag{1}$$

where m_3 is the molality of CsDNA nucleotide, ν is the binding ratio in moles ethidium bromide per mole CsDNA nucleotide, and k is a constant accounting for the conversion from molality to molarity and for the optical path. Equation (1) may be written in logarithmic form for an arbitrary radial co-ordinate and for the position of true band center, denoted with a subscript zero, and the results combined.

$$\ln(m_3/m_{3,0}) = \ln(A/A_0) - \ln(1 + \frac{\epsilon_4}{\epsilon_3}\nu) + \ln(1 + \frac{\epsilon_4}{\epsilon_3}\nu_0). \tag{2a}$$

For small values of the second and third terms,

$$\ln(m_3/m_{3,0}) \approx \ln(A/A_0) + \frac{\epsilon_4}{\epsilon_3} \frac{(\nu - \nu_0)}{(1 + \frac{\epsilon_4}{\epsilon_3} \nu_0)} \qquad (2b)$$

The DNA concentration distribution is Gaussian to first order,[2] and

$$\sigma^2 \ln(m_3/m_{3,0}) = -\tfrac{1}{2}(r - r_0)^2 \quad . \qquad (3a)$$

The observed absorbance profile may be described by a similar equation to a good approximation.

$$\sigma_a^2 \ln(A/A_0) = -\tfrac{1}{2}(r - r_0)^2 \quad . \qquad (3b)$$

In Eqs. (3a, b) σ is the correct Gaussian standard deviation for the macromolecular complex and σ_a is the apparent standard deviation for the observed absorbance distribution. The quantity σ_a is calculated from measurements at $r = r_\sigma$, which is defined by the condition $\ln(A/A_0) = -\frac{1}{2}$. Combining this condition with Eqs. (2b) and (3a, b) gives the result

$$\frac{\sigma^2}{\sigma_a^2} = 1 + 2 \frac{\epsilon_4}{\epsilon_3} \frac{(\nu_\sigma - \nu_0)}{(1 + \frac{\epsilon_4}{\epsilon_3} \nu_0)} \quad , \qquad (4a)$$

or, approximately,

$$\frac{\sigma}{\sigma_a} = 1 + \frac{\epsilon_4}{\epsilon_3} \frac{(\nu_\sigma - \nu_0)}{(1 + \frac{\epsilon_4}{\epsilon_3} \nu_0)} \quad . \qquad (4b)$$

In order to estimate $\nu_\sigma - \nu_0$ for a typical case, this difference is expanded in a first order Taylor series and

$$\nu_\sigma - \nu_0 = (\frac{d\nu}{dr}) (r_\sigma - r_0). \qquad (5)$$

The Scatchard equation[3] may be used for this purpose if it is assumed that the binding sites are independent.

$$\nu = \frac{\nu_m K c}{1 + K c} \tag{6}$$

In Eq. (6) K is the equilibrium constant, 1.7×10^4 liters/mole[4], c is the free reagent concentration in moles/liter, and $\nu_m = 0.2$ is the maximum value of ν.[5] The differentiated form of Eq. (6) is

$$\frac{d\nu}{dr} = \frac{\nu}{1 + Kc} \frac{d \ln c}{dr} \quad . \tag{7}$$

The free reagent concentration distribution is given by[6]

$$\ln(c/c_0) = \tfrac{1}{2}(\beta + 1)\, \alpha^2 (r^2 - r_0^{\,2}) - \tfrac{1}{3} \frac{\alpha^2}{r_e} (r^3 - r_0^{\,3}) \ , \tag{8a}$$

where

$$\alpha^2 = \frac{M_4 \omega^2 (\frac{d\rho}{dr})\, \bar{v}_4 r_e}{RT} \tag{8b}$$

$$\beta = \frac{1 - \bar{v}_4 \rho_e}{\bar{v}_4 (\frac{d\rho}{dr})\, r_e} \tag{8c}$$

and r_e is the CsCl isoconcentration coordinate.

Equation (8a) is differentiated and combined with Eq. (7),

$$\frac{d\nu}{dr} = \frac{\nu \alpha^2 r (\beta + 1 - r/r_e)}{1 + Kc} \tag{9}$$

At $r_\sigma - r_0 = \pm \sigma$, Eq. (4b) then becomes

$$\frac{\sigma}{\sigma_a} = 1 \pm \frac{\nu\alpha^2 \, r(\beta + 1 - \frac{r}{r_e}) \, \sigma \, \epsilon_4/\epsilon_3}{(1 + Kc)\,(1 + \frac{\epsilon_4}{\epsilon_3}\,\nu_0)} \tag{10a}$$

or approximately, for a band near the center of the cell,

$$\frac{\sigma}{\sigma_a} \approx 1 \pm \frac{\alpha^2 \beta r_0 \; \sigma(\epsilon_4/\epsilon_3)\, \nu_m Kc_0}{(1+Kc_0)\,[\,1 + Kc_0\,(1+\epsilon_4/\epsilon_3\,\nu_m)\,]} \; . \tag{10b}$$

In Eqs. (10) the positive sign refers to the case $r_\sigma > r_0$, and the negative sign to the case $r_\sigma < r_0$. If a wave length is chosen at which only the bound reagent is observed spectrally, $\epsilon_3 = 0$ and Eq. (10b) becomes

$$\frac{\sigma}{\sigma_a} = 1 \pm \frac{\alpha^2 \beta r_0 \sigma}{1 + Kc_0} \; . \tag{10c}$$

We take

$$\alpha^2 \beta r_0 \sigma = \frac{M_4 \omega^2 (1 - \bar{v}_4 \rho_e)\, r_0 \sigma}{RT} = -0.08 \tag{11}$$

for ethidium bromide binding to SV40 DNA, where the following values have been chosen for the parameters: $M_4 = 349$, $\bar{v}_4 = 1.02$ ml/g,[1] $\rho_e = 1.65$ g/ml, $r_0 = 6.5$ cm, $\sigma = 0.03$ cm, $R = 8.317 \times 10^7$ ergs mole^{-1} deg^{-1}, $T = 298°$, $K = 0.05$ ml/μg,[4] and 44,000 rpm. Figure (1) presents a plot of the calculated percentage error in σ^2, $\mp 100 \times (1 - \frac{\sigma^2}{\sigma_a^2})$,

Fig. 1. The percentage error in σ^2 for the reacting system SV 40 DNA II, CsCl, ethidium chloride plotted as a function of the free dye concentration at band center. The curves were calculated for extinction coefficient ratios ϵ_4/ϵ_3 of 2.5, 10, 1000, and ∞ in order from lowest to highest. The curve for $\epsilon_4/\epsilon_3 = 2.5$ corresponds to 265.4 mμ and the curve for $\epsilon_4/\epsilon_3 = \infty$ corresponds to 521 mμ.

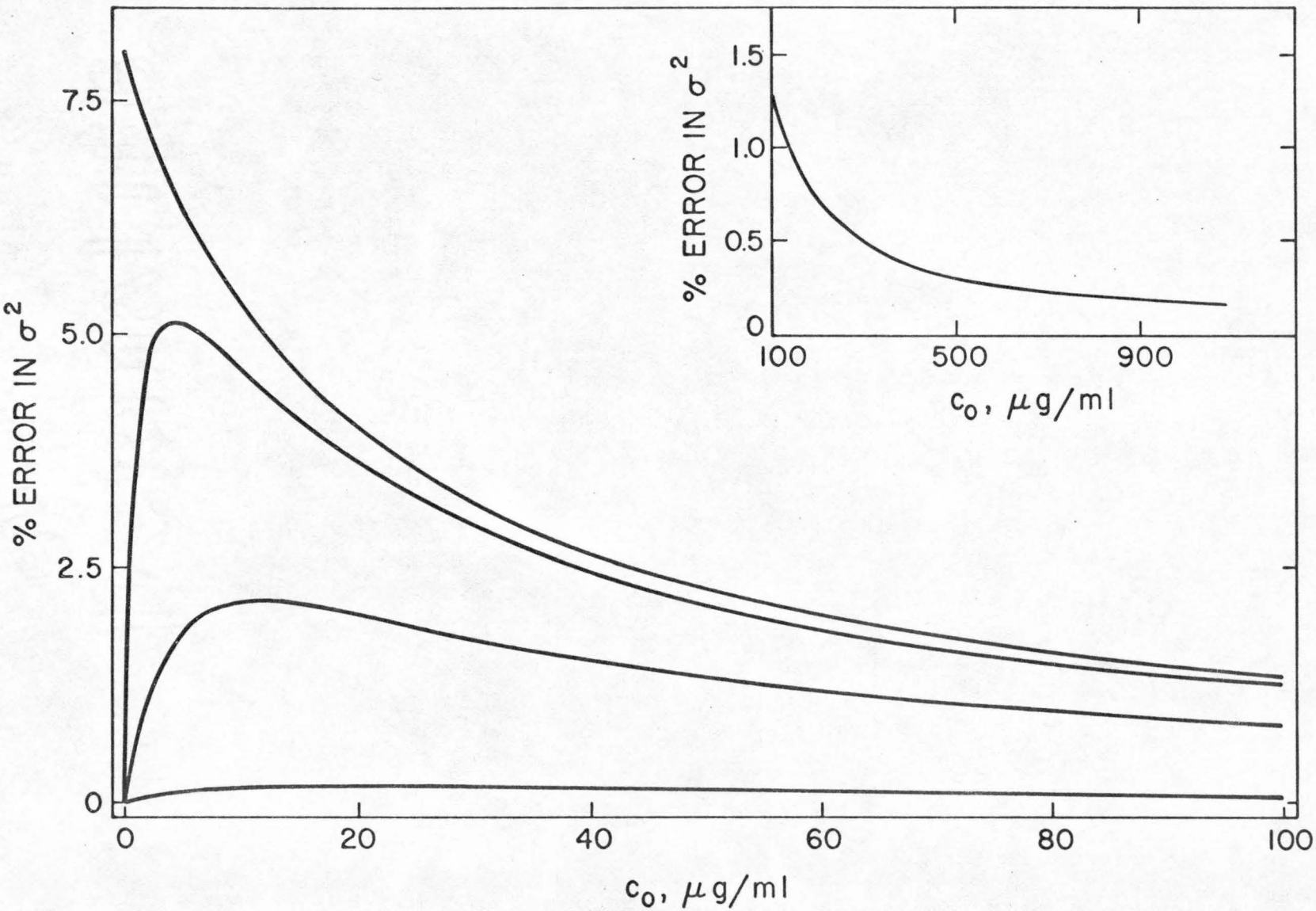
% ERROR IN σ^2
7.5
5.0
2.5
0
0
20
40
60
80
100
c_0, μg/ml
% ERROR IN σ^2
1.5
1.0
0.5
0
100
500
900
c_0, μg/ml

for four cases. At 265.4 mμ, ϵ_3 = 6580 liters/mole, ϵ_4 = 15,930 liters/mole and ϵ_4/ϵ_3 = 2.5. At 521 mμ ϵ_3 = 0, and the ratio of extinction coefficients does not influence the result. Two intermediate cases are also shown in Fig. (1) for ϵ_4/ϵ_3 = 10 and for ϵ_4/ϵ_3 = 100. At 265.4 mμ, the lower curve, the error in σ^2 is always very small, regardless of the dye concentrations greater than 100 μg/ml, which is the range of usefulness of this wavelength.

The concentration of dye at which the error is maximum is also a function of ϵ_4/ϵ_3. Differentiating Eq. (10b) and setting the result equal to zero, the concentration at the maximum error is

$$c_{max} = \frac{1}{K\sqrt{1 + \frac{\epsilon_4}{\epsilon_3}\nu_m}} \quad . \tag{12}$$

Figure (2) presents a plot of C_{max} and of the percent error in σ^2 at c_{max} as a function of ϵ_4/ϵ_3.

The error in the location of the true concentration maximum is found by differentiating Eq. (1) and setting $dA/dr = 0$.

$$\frac{d \ln m_3}{dr} = - \frac{d \ln (\epsilon_3/\epsilon_4 + \nu)}{dr} \quad . \tag{13}$$

We combine this result with Eqs. (6) and (7), to obtain

$$\frac{d \ln (\epsilon_3/\epsilon_4 + \nu)}{dr} = \frac{(d \ln c/dr)}{(1 + Kc)\,(1 + \epsilon_3/\epsilon_4\,\nu)} \quad . \tag{14}$$

Fig. 2. The maximum percentage error in σ^2 and the free dye concentration giving rise to the maximum error, c_{max}, plotted as a function of the extinction coefficient ratio ϵ_4/ϵ_3 for the reacting system SV40 DNA II, CsCl, ethidium chloride.

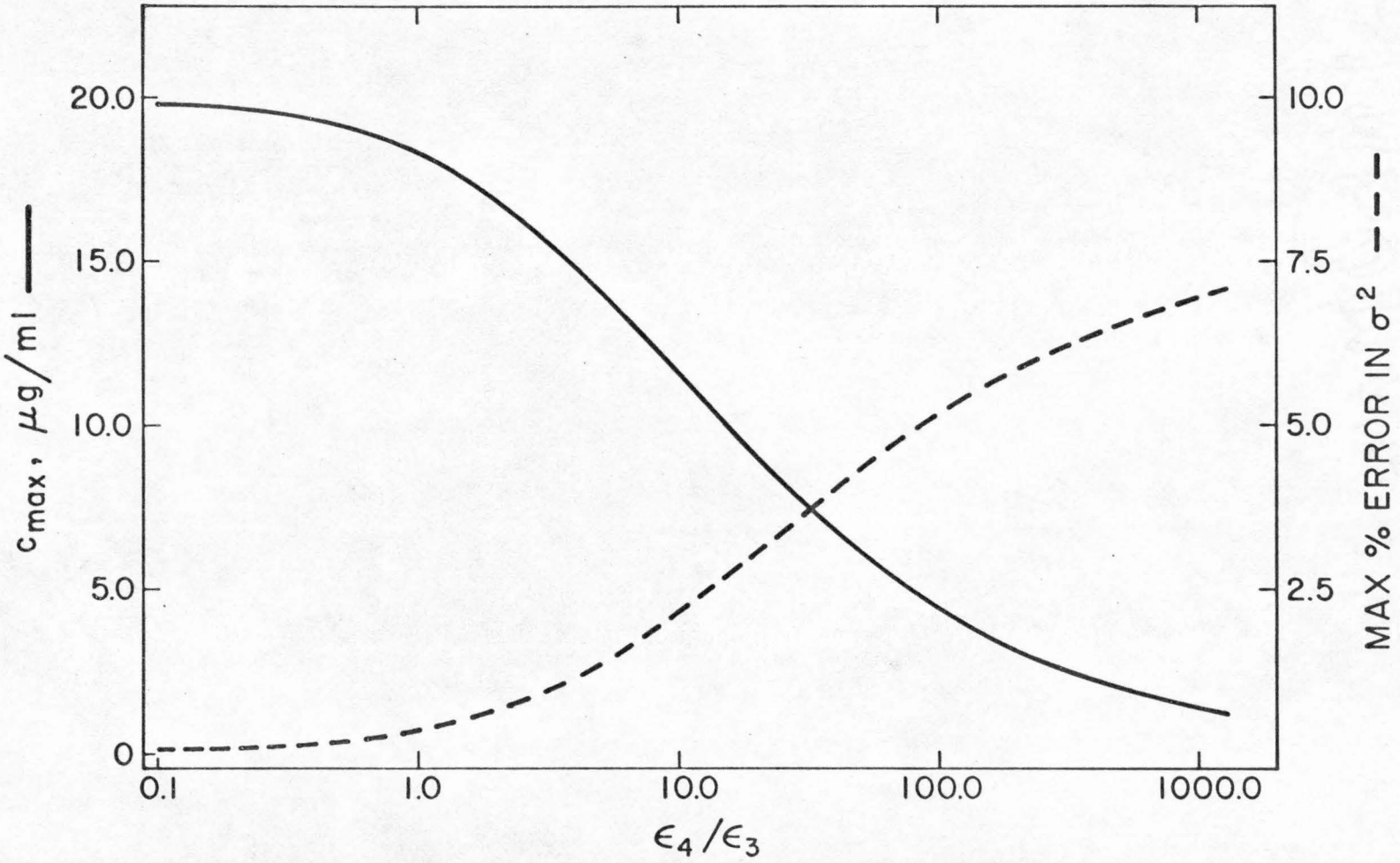
20.0
15.0
10.0
5.0
0
c_{max}, μg/ml
10.0
7.5
5.0
2.5
MAX % ERROR IN σ^2
0.1
1.0
10.0
100.0
1000.0
ϵ_4/ϵ_3

Equation (3a) is next differentiated with respect to r and substituted in Eq. (13) to obtain the coordinate r_0 at which the maximum polymer concentration occurs, relative to the coordinate r_{0a} of the maximum in the observed absorbance profile.

$$r_0 = r_{0a} - \sigma^2 \left[\frac{d \ln (\epsilon_4/\epsilon_3 + \nu)}{dr} \right]_{r = r_{0a}} . \tag{15}$$

This result is combined with Eq. (14) and the differentiated form of Eq. (8a) to give

$$r_0 = r_{0a} \left\{ 1 - \frac{\sigma^2 \alpha^2 \beta (\epsilon_4/\epsilon_3) \nu_m Kc_0}{(1 + Kc_0)\,[1 + Kc_0 (1 + \nu_m \epsilon_4/\epsilon_3)]} \right\} \tag{16a}$$

As $\epsilon_3 \rightarrow 0$, Eq. (16a) becomes

$$r_0 = r_{0a} \left[1 - \frac{\sigma^2 \alpha^2 \beta}{1 + Kc_0} \right] . \tag{16b}$$

The error in r_0 is greatest at $c_0 = 0$, where the percentage error in r_0 is 0.1%. At a dye concentration of 100 μg/ml the error in r_0 is reduced to 0.004%. It is concluded that no significant error in the location of the band maximum occurs regardless of the wavelength chosen to measure the polymer concentration distribution.

Other reagents may differ from ethidium chloride both in binding properties and in extent of the concentration redistribution in the centrifugal field. For a reagent which binds with $\nu_m \neq 0.2$ the maximum

errors encountered in the measurement of both r_0 and σ will not be affected, as shown by Eqs. (10c) and (16b). The effect of a different reagent concentration redistribution is to change the numerical values calculated here by a factor proportional to the product $M_4(1 - v_4\rho_e)$. Reagents for which either the molecular weight or the buoyance factor is greater than in the case of ethidium chloride will therefore introduce correspondingly greater errors into the measurement of both σ and r_0. The magnitude of the errors for any particular reagent may be calculated with Eqs. (10) and (16).

REFERENCES

1. Bauer, W., and J. Vinograd, J. Mol. Biol., in press.
2. Hearst, J. E., and J. Vinograd, Proc. Natl. Acad. Sci., 47, 999 (1961).
3. Scatchard, G., Ann. N.Y. Acad. Sci., 51, 660 (1949).
4. Bauer, W., and J. Vinograd, manuscript in preparation.
5. Le Pecq, J.-B., Thesis, Faculté des Sciences, Paris (1965).
6. Bauer, W., and J. Vinograd, paper to be presented at Conference on Advances in Ultracentrifugal Analysis February 15-17, 1968; and to be published in Ann. N.Y. Acad. Sci.